

Cellular and Tissue Responses to Implant Materials:
Development of a Novel Organ Culture Model

Theresa Leung *B.D.S., M.Sc., F.D.S. R.C.S.(Edin.)*

Thesis submitted for the degree of Doctor of Philosophy

Department of Prosthetic Dentistry

Eastman Dental Institute

University of London 1998



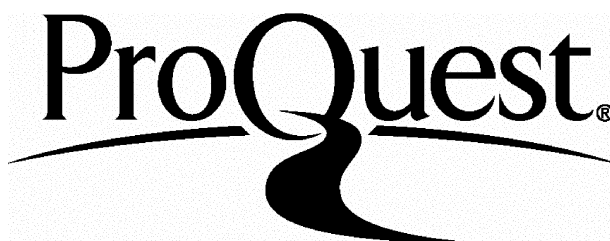
ProQuest Number: U642122

All rights reserved

INFORMATION TO ALL USERS

The quality of this reproduction is dependent upon the quality of the copy submitted.

In the unlikely event that the author did not send a complete manuscript and there are missing pages, these will be noted. Also, if material had to be removed, a note will indicate the deletion.



ProQuest U642122

Published by ProQuest LLC(2015). Copyright of the Dissertation is held by the Author.

All rights reserved.

This work is protected against unauthorized copying under Title 17, United States Code.
Microform Edition © ProQuest LLC.

ProQuest LLC
789 East Eisenhower Parkway
P.O. Box 1346
Ann Arbor, MI 48106-1346

Abstract

The development and use of endosseous implants in dentistry have increased worldwide since the introduction of the concept of “osseointegration”. This concept of a direct bone-to-metal interface, according to Brånemark, consists of a highly differentiated tissue making a direct structural and functional connection between ordered living bone and the surface of an implant. Much of the research supporting this concept was based on *in vivo* animal studies and clinical results from human patients. *In vitro* models are increasingly being used to examine the short-term behaviour and function of connective tissue cells on implant surfaces. The first section of this thesis presents an examination of the dynamic behaviour of fibroblast cells cultured *in vitro*, using time-lapse video micrography, to evaluate initial attachment and spreading. It is acknowledged that *in vitro* culturing of isolated cells on the biomaterials may not represent all the characteristics of tissue responses around dental implants *in vivo* since the structural organization of connective tissue is lost in these systems. The main aim of the work presented in this thesis was to develop a new organ culture model for studying bone-biomaterial interactions. This model is based on grafting bone explants onto the chorioallantoic membrane (CAM) of chick eggs. The model was characterised to provide a test bed for the assessment of early bone-biomaterial interactions. The stages of development of the early bone-implant interface were studied using commercially pure titanium and a glass ceramic material, Apoceram. Light microscopy, histochemical, ultrastructural and immunocytochemical examinations were carried out. The feasibility of using the model for studying the effects of basic fibroblast growth factor on bone healing around the implants was assessed and the role of the CAM graft model as a bridge between *in vitro* and *in vivo* methods of studying bone-implant interactions examined.

Contents

1. Literature Review	1
1.1 Introduction	1
1.2 Testing of implant materials	2
1.2.1 In vitro tests	3
1.2.1.1 Cytotoxicity tests	3
1.2.1.2 Mutagenicity	4
1.2.1.3 Haemocompatibility	4
1.2.2 In vivo animal tests	4
1.2.2.1 Systemic acute toxicity	4
1.2.2.2 Short-term implantation	5
1.2.2.3 Long-term implantation	5
1.2.2.4 Sensitisation	5
1.2.2.5 Neoplastic potential	5
1.3 Experimental models for studying bone-biomaterial interactions in vitro	7
1.3.1 Introduction	7
1.3.2 Background on bone culture systems	10
1.3.2.1 Bone as an organ	10
1.3.2.2 Bone as a tissue	10
1.3.2.3 Bone organ and tissue culture	12
1.3.2.4 Bone cell culture	14
1.3.2.5 Bone cell lines	16
1.3.2.6 Bone formation in cell cultures	17
1.3.2.7 Culture conditions	18
1.3.3 Investigations on the interactions of bone cells with various implant materials	20
1.3.4 Choice of model	22
1.3.4.1 Tissue and organ cultures	22
1.3.4.2 Primary or passaged normal bone cells	23
1.3.4.3 Human osteoblasts	24
1.3.4.4 Permanent cell lines	25
1.3.5 Measurable events on implant surfaces	26
1.3.6 Mechanism of cell-substratum adhesion	27
1.3.7 Cell attachment assays	29
1.3.7.1 Bone RGD proteins and cellular responses	30
1.3.7.2 Cytoskeletal Organisation	30
1.3.7.3 Integrin-mediated adhesion	31
1.3.8 Cell growth/proliferation	32
1.3.9 Functional activity and phenotypic expression	33
1.3.10 Mineralisation of the extracellular matrix	35
1.3.11 Ultrastructure of bone cells cultures on implant materials <i>in vitro</i>	35
1.3.12 Monoclonal bodies against osteoblastic cells	36
1.3.13 Regulation of cellular function	36
1.3.14 Resorption of implant materials in vitro	37
1.3.15 Inflammatory and immunological response	39
1.3.16 In vitro models representing soft tissue responses	40
1.3.17 Aspects of implant surface characteristics investigated using in vitro models	41
1.4 Do in vitro cultures reflect the in vivo situation?	42
1.5 Experimental models for studying bone-biomaterial interactions in vivo	44
1.5.1 Choice of <i>in vivo</i> models	45

1.5.2 Diffusion chamber studies	45
1.5.3 Implantation into bone <i>in vivo</i>	47
1.5.4 Techniques for assessing bone responses to implants <i>in vivo</i>	49
1.5.4.1 Radiography and microradiography	49
1.5.4.2 Mechanical tests	50
1.5.4.3 Ground sections for light microscopy	50
1.5.4.4 Histomorphometric methods	50
1.5.4.5 Tracer methods	52
1.5.4.6 Scanning Electron Microscopy	53
1.5.4.7 Transmission electron microscopy	54
1.5.4.8 Ultrastructural features	55
1.5.4.9 Enzyme histochemistry and immunocytochemical methods	57
1.5.5 Scope of <i>in vivo</i> experimentation	59
1.5.6 Phases of healing following <i>in vivo</i> implantation	59
1.5.7 The early bone-implant interface	61
 1.6 Statement of the problem	 62
 2. Dynamic recording of short-term cell behaviour on an implant surface	 65
2.1 Introduction	65
2.2 Materials and methods	66
2.2.1 Substratum preparation	66
2.2.2 Cell culture	67
2.2.3 Video microscopy	68
2.2.4 Scanning electron microscopy (SEM)	68
2.3 Results	68
2.3.1 Attachment and cell morphology	68
2.3.2 Changes in cell phenotypes	69
2.3.3 Cell Ruffling Activity	73
2.4 Discussion	78
 3. Bone tissue/organ culture on the chorioallantoic membrane	 81
3.1 Introduction	81
3.2 Aim and objectives	83
3.3 Materials and methods	84
3.3.1 Preparation of host eggs	84
3.3.2 Preparation of cell cultures for grafting	85
3.3.3 Preparation of bone tissue for grafting	86
3.3.4 Grafting the bone tissue/organ	86
3.3.5 Implant materials	86
3.3.5.1 Apoceram	87
3.3.6 Preparation of the implants	87
3.3.7 Insertion of implants into the chick bone tissues	88
3.3.8 Retrieval of the grafts	89
3.3.9 Fixation and embedding of specimens	89
3.3.10 Location of implants and preparation of sections for light microscopy	89
3.3.11 Photomicrography	90
3.3.12 Serial grafting	90
3.4 Results	91

3.4.1 MG63 and human mandibular bone cells	91
3.4.2 Calvaria, mandibles and femurs	92
3.4.2.1 <i>Survival rates of the bone grafts</i>	93
3.4.2.2 <i>Serial grafts</i>	98
3.4.3 Histology of grafts containing implants	99
3.4.3.1 <i>Calvarial grafts with implants</i>	100
3.4.3.2 <i>Mandibular grafts with implants</i>	100
3.4.3.3 <i>Femoral grafts with implants</i>	100
3.5 <i>Discussion</i>	104
3.5.1 Culture of bone cells on the CAM	104
3.5.2 Bone organ culture on CAM	104
3.5.3 Choice of model for studying bone-implant interactions	106
3.5.4 Chick vs. Man	107
4. The bone-implant interface in the femoral graft model	108
4.1 <i>Introduction</i>	108
4.1.1 Aims and objectives	109
4.2 <i>Materials and methods</i>	109
4.2.1 Histology	109
4.2.2 Histomorphometric analysis	110
4.2.3 Von Kossa staining	111
4.2.4 Alkaline phosphatase and tartrate resistant acid phosphatase	111
4.2.5 Tetracycline labelling	112
4.2.6 Immunohistochemistry of bone matrix proteins	113
4.2.7 Ultrastructure of the bone-implant interface	114
4.3 <i>Results</i>	115
4.3.1 Chronological development of the bone-implant interface	115
4.3.2 Percentage of bone-implant contact	128
4.3.3 Histochemical and immunohistochemical staining	132
4.3.3.1 <i>Von Kossa staining for mineralised bone tissue</i>	132
4.3.3.2 <i>Alkaline phosphatase staining</i>	134
4.3.3.3 <i>Tartrate resistant acid phosphatase</i>	135
4.3.3.4 <i>Tetracycline labelling</i>	137
4.3.3.5 <i>Immunohistochemistry of bone matrix proteins</i>	139
4.3.4 Ultrastructure of the bone implant interface	141
4.3.4.1 <i>Apoceram</i>	141
4.3.4.2 <i>Titanium</i>	142
4.4 <i>Discussion</i>	148
4.4.1 The sequence of events following implantation and grafting	148
4.4.2 Cells contributing to the healing response	149
4.4.2.1 <i>Multinucleated giant cells</i>	150
4.4.3 Immunohistochemistry and enzyme histochemistry	152
4.4.4 Bone formation around the implant	154
4.4.5 Ultrastructure of the bone-implant interface	157
4.4.6 Does the model mimic bone healing <i>in vivo</i> ?	158
4.4.6.1 <i>Immunological capacity of the host chick embryo</i>	161
4.4.6.2 <i>Avian vs mammalian bone</i>	161
4.4.7 How does the model compare with bone organ culture <i>in vitro</i> ?	161
4.5 <i>The main findings:</i>	162

5. Bone response to local release of basic fibroblast growth factor in the CAM graft model	163
5.1 Introduction	163
5.1.1 Aim and objective	163
5.1.2 Bone growth factors implicated in bone repair	164
5.1.2.1 Basic fibroblast growth factor	164
5.2 Materials and Methods	167
5.2.1 Preparation of implants loaded with bFGF	167
5.2.2 Insertion of implants and grafting	167
5.2.3 Histology & histochemistry	167
5.3 Results	168
5.4 Discussion	177
5.4.1 The mode of delivery of the growth factor	179
5.4.2 The time factor	180
5.5 Conclusion	180
6. General Discussion	182
6.1 <i>The advantages and limitations of the CAM graft system</i>	183
6.2 <i>In vitro vs. in vivo approaches to implant testing: where does the CAM graft model fit in?</i>	185
Acknowledgements	189
References	190
Appendix I	214
Appendix II	219
Appendix III	221
Appendix IV	224

List of figures

Figure 2.1	a. SEM of a round 3T3 fibroblast on Apoceram. Surface blebs can be seen. Cytoplasmic extensions appear on the periphery as the cell begins to spread. b. The leading edge of this apparently elongating cell shows layers of ruffling lamellipodia. c. SEM of a polarised and flattened 3T3 fibroblast. Inset. The large arrow indicates the most likely direction of migration of this fibroblast. Lamellipodia are seen extending from its leading edge (small arrows). d. The fibroblasts are well spread. Long thin filopodia appear to bridge some cells.	70
Figure 2.2	Distribution of behavioural phenotypes with time on tissue culture polystyrene	71
Figure 2.3	Distribution of behavioural phenotypes with time on Apoceram	72
Figure 2.4	Tracings of cells seen through the phase-contrast microscope, recorded by the time-lapse video at 15, 30 min, 1, 2 and 3h. a. Progression from a rounded morphology to a spread cell which later exhibits crawling. b. This cell has spread and remained stationary with little ruffling activity. c. Constant ruffling of a large proportion of the cell margin was observed on this cell throughout the recording period.	73
Figure 2.5	Left: The margin of this fibroblast has three ruffling sites (asterisks); the remainder of the cell margin appears quiescent. Right: A transparent overlay was placed on a 'freeze frame' image of a similar cell on the video monitor. The cell was divided into 18 sectors. Border ruffling was observed in sectors 6, 7, 8, 12 and 18. This cell scored 5 out of 18.	74
Figure 2.6	Proportion of cell margin ruffling (n/18) versus number of ruffling sites for cells cultured for 1 hour on tissue culture polystyrene	75
Figure 2.7	Proportion of cell margin ruffling (n/18) versus number of ruffling sites for cells cultured for 1 hour on Apoceram	75
Figure 2.8	Proportion of cell margin ruffling (n/18) versus number of ruffling sites for cells cultured for 2 hours on tissue culture polystyrene	76
Figure 2.9	Proportion of cell margin ruffling (n/18) versus number of ruffling sites for cells cultured for 2 hours on Apoceram	76
Figure 2.10	Proportion of cell margin ruffling (n/18) versus number of ruffling sites for cells cultured for 3 hours on tissue culture polystyrene	77
Figure 2.11	Proportion of cell margin ruffling (n/18) versus number of ruffling sites for cells cultured for 3 hours on Apoceram	77
Figure 3.1	Cross-section of developing chick egg with 10 day embryo (from Hamburger, 1973)	81
Figure 3.2	View of chorioallantoic membrane (CAM) in a developing chick egg incubated for 9 days. The capillary network of the transparent CAM is seen overlying the yellow yolk sac. Original magnification x20	84
Figure 3.3	MG63 cells grafted on the CAM (left & right). The cells remained as clumps on the surface of the CAM without being enveloped by the epithelium (e) or invaded by blood vessels within the mesenchymal tissue (m). Stain: H&E	91
Figure 3.4	Human mandibular bone cells grafted on CAM (mbc). Left: The cells settled as a clump on the CAM (c). Right: The grafted cells enveloped by the CAM, showing fibroblast-like morphology (f). Necrotic cells were found at the centre of the graft (nc). Stain: H&E.	92
Figure 3.5	Graft of calvarium from 9-day old donor (containing an Apoceram implant) cultured for 7 days. Part of the implant was situated outside the calvarial tissue. Original magnification x16	97
Figure 3.6	Graft of a half mandible from 9-day old donor (containing an Apoceram implant) cultured for 7 days. Original magnification x9	97
Figure 3.7	A well-integrated femur cultured for 9 days. Its length was 19mm. Original magnification x6	97
Figure 3.8	A femoral graft which had failed to be enveloped by the CAM. The bone appears necrotic. Original magnification x6	97
Figure 3.9	One epiphyseal end of this femur had become necrotic during the culture period and was enclosed in a fluid-filled vesicle. Original magnification x6	98
Figure 3.10	Examples of SEM images of the side view of pieces of titanium retrieved after sectioning. The surface facing (a) was produced by the 'good' diamond knife for producing 1-2µm sections. (b) is the edge in contact with the resin embedded tissue. (c) was produced by the	

- old diamond knife used for rough trimming. The curvature of the titanium is evident in both pictures (original magnification x4980) 99
- Figure 3.11 The titanium implant (i) had been displaced from the folded calvarial bone (ca) during the culture period and became located within the mesenchymal tissue of the CAM (c) 101
- Figure 3.12 Mesenchymal cells (m) from the calvarial bone tissue (ca) migrating towards the surface of this titanium implant (i), their morphology resembles fibroblasts rather than osteoblasts (o) seen on the surface of the calvarial bone. 101
- Figure 3.13 The implant (i) in this mandibular section was placed in the interstitial connective tissue (ct) between the Meckel's cartilage (mc) and the associated membrane bone (mb); it is covered by a layer of fibroblast-like cells. 102
- Figure 3.14 The implant (i) was inserted within the membrane bone (b) in this mandibular graft. Its is surrounded by marrow tissue with many large blood capillaries (m). The Meckel's cartilage is at the top left corner . 102
- Figure 3.15 A femoral graft which received an Apoceram implant showing new bone formation on the implant surface (nb). The thickness of bone on the implant surface varies, on one side consisting of a very thin seam (arrow); implant space (i); 9 day graft. 103
- Figure 3.16 A femoral graft which received a titanium implant. Bone formation parallel to the surface of the implant within the central marrow cavity (m). Direct bone-implant contact (b); implant space (i); 9 day graft. 103
- Figure 4.1 Cross section of a femur containing an Apoceram implant one day after grafting on the CAM. The implant was inserted via the wound (w) made through the thickness of the bone collar. Part of the CAM on which the graft lay is seen at the top right (c). Periosteum (p). 116
- Figure 4.2 Day 1 after grafting. Apoceram. Blood cells accumulated adjacent to the implant (arrow). Osteocytes at the centre of the graft became necrotic, some empty lacunae can be seen (l). There is degeneration of the marrow tissue between the trabeculae. 117
- Figure 4.3 Day 2. Titanium. The marrow spaces are filled with cell debris. There are many macrophages with cytoplasmic vacuoles (arrows) 118
- Figure 4.4 Day 3 after grafting. Titanium. m - mesenchymal cells, bv - blood vessel, o - osteoblasts, * - new osteoid, arrow - macrophage. 119
- Figure 4.5 Day 3 after grafting. Apoceram. Blood vessels (bv) are clearly visible in the central marrow cavity. Osteoblasts (*) repopulate the surface of an existing bone trabeculum close to the implant surface and lay down new matrix. 120
- Figure 4.6 Day 3 after grafting. Apoceram. Cell proliferation and migration are the key features at regions near the end of the implant (i). Osteoid formation (*) has resumed at the surface of the existing bone trabeculae. o = osteoblasts. 120
- Figure 4.7 Day 5 after grafting. Apoceram. Osteoid (*) being laid down on the surface of the implant. A bone trabeculum (t) from the endosteal region extends down the side of the implant. A thin seam of new bone is formed on the marrow-facing surface of this implant (arrow). 121
- Figure 4.8 Day 5 after grafting. Particles of Apoceram (a) are attached to the newly formed osteoid (*). The osteogenic cells, some of which lie directly on the implant surface (arrow), become trapped within the matrix. 122
- Figure 4.9 Day 5 after grafting. Titanium. A new T-shaped strut of bone is being formed (nb). Osteoblasts (o) line the surface of the new bone which is separated from the implant surface by marrow tissue (m) in which a blood vessel with a pericyte (p) can be seen. Adjacent to this pocket of marrow are flattened cells (f) trapped between the osteoid and the implant surface (i). 122
- Figure 4.10 Day 7 Apoceram. Multinucleated giant cells on the surface of the implant (i), in close proximity to a region of new bone formation (nb). bv = blood vessel. fc = fat cell. 123
- Figure 4.11 Day 9. Apoceram implant across the central marrow cavity. Mineralised bone (mb) in direct contact with implant surface. 125
- Figure 4.12 Day 9. Apoceram. A thin seam of bone has been laid down on the implant surface. The distribution of mineralised bone matrix (mb) and osteoid (os) suggests that the osteoblasts (o) secreted the matrix directly on the implant. The earlier formed matrix becomes mineralised first, new osteoid is deposited as the osteoblasts move away from the implant surface. 125
- Figure 4.13 Day 9. Titanium. Mineralised bone tissue forming direct contact with the implant surface with an intervening basophilic line (b). At the junction between mineralised bone, implant and marrow, an osteoclast (oc) can be seen with its base against the bone surface. 126

Figure 4.14 Day 9. Titanium. Magnified view of field shown in Fig. 4.13. The basophilic line can be seen clearly at a higher magnification.	126
Figure 4.15 Chronological development of the bone-implant interface	127
Figure 4.16 Summary of the means and standard errors of percentage of implant perimeter in contact with bone and osteoid. Titanium: Ti. Apoceram glass ceramic :GC.	132
Figure 4.17 Von Kossa staining. Titanium implant. Calcified bone is stained dark brown. Toluidine blue counterstain.	133
Figure 4.18 Von Kossa staining. Apoceram. Mineralised bone forming direct contact with particles of the glass ceramic attached to the interface.	133
Figure 4.19 Alkaline phosphatase distribution. Titanium implant. 7 days after grafting. Haematoxylin counterstain.	134
Figure 4.20 Apoceram at 7 days after grafting. Many alkaline phosphatase positive cells are present on the surface of the implant. Haematoxylin counterstain.	135
Figure 4.21 Apoceram 5 days. Intense staining for TRAP is present in a multinucleated giant cell (mgc) on the surface of the implant and osteoclasts (oc) on the bone trabeculae. The endosteal bone surface and the implant surface also showed positive staining.	136
Figure 4.22 Titanium at 5 days. Positive staining for acid phosphatase is found mostly on the endosteal surfaces and in osteoclasts and some mononuclear cells in the marrow.	136
Figure 4.23 Day 7. Titanium. The mineralisation front on the bone trabeculae. Original magnification: x200	137
Figure 4.24 7 days after grafting. A thin line of fluorescent material lies against the surface of this Apoceram implant. Original magnification: x400	137
Figure 4.25 Day 9. Apoceram. Tetracycline fluorescence located between the osteoid and mineralised bone at the mineralisation front. Original magnification: x200	138
Figure 4.26 Day 9. Titanium. Tetracycline fluorescence located between the osteoid and mineralised bone at the mineralisation front. Original magnification: x200	138
Figure 4.27 Negative control, pre-immune rabbit serum used instead of primary antibody. The section is clear at the end of the staining procedures.	139
Figure 4.28 Staining for type I collagen (LF67). Left: Day 7. Titanium. No counterstaining. (m) central marrow cavity. Right: Day 7. Apoceram. Counterstained with toluidine blue.	140
Figure 4.29 Staining for osteonectin (LF 8) Left: Day 7. Titanium. No counterstaining. Right: Day 7. Apoceram. Counterstained with toluidine blue.	140
Figure 4.30 An osteoblast (o) on the surface of Apoceram (gc) is being surrounded by mineralised matrix (mm). Two osteocytes with cell processes (cp) can be seen within the bone matrix. Collagen fibres in cross-section can be seen at the top of the field. Field width: 25µm	143
Figure 4.31 The osteoid and mineralised matrix surrounding this osteoblast on Apoceram (gc) can be differentiated by the different levels of electron density. Collagen fibres are visible within the osteoid (os) but not discernable where they are more heavily mineralised (mm). Matrix vesicles are present in the cytoplasm of this bone forming cell (arrow). Field width: 25µm	143
Figure 4.32 Apoceram. Collagen fibres at different orientation surrounding a lacuna containing the cell process of an osteoblast. Osteoid in direct apposition against the glass ceramic (gc) particles. #collagen fibres in longitudinal section. *collagen fibres in cross-section. Field width: 14µm	143
Figure 4.33 Apoceram. The presence of ceramic particles (gc) at the top of the field reflects the preservation of the interface. The implant surface is covered by several elongated cells showing signs of degeneration. Field width: 14µm	144
Figure 4.34 Part of a multinucleated giant cell on the surface of Apoceram (gc). Two nuclei (n) are visible with many electron dense lysosomal granules in the cytoplasm (*). m - mineralised matrix. Field width: 17.5µm	144
Figure 4.35 Part of a multinucleated giant cell attached to the surface of an Apoceram implant (gc). Arrows: lysosomal granules. Field width: 8.75µm	144
Figure 4.36 Dense mineralised matrix (mm) making direct contact with Apoceram. The arrows indicate a continuous layer of the glass ceramic remaining attached to the mineralised matrix following sectioning. Field width: 35µm	145
Figure 4.37 Apoceram (gc). Needle-like mineral aggregates (s) amongst the collagen fibres. The glass ceramic is continuous with amorphous globular deposits (g), collagen fibres (c) with characteristic banding intermingle with the mineral deposits. Field width: 1.75µm	145

- Figure 4.38 Apoceram (gc). Fused globular mineral deposits continuous with the glass ceramic particles. Isolated spheres of mineral (arrow) interspersed among banded collagen fibres (f) on a background of thin fibrillar material. Field width: 1.75µm 145
- Figure 4.39 Apoceram. A less dense fibrillar zone (f) is present between the mineralised matrix and the glass ceramic particles (gc). Spherical mineral deposits are present along the edge of the calcified collagen matrix (mc). Field width: 3.5µm 146
- Figure 4.40 Titanium. A continuous electron dense line at the metal interface with the tissue (arrows). Collagen fibres within a band of osteoid surround the cytoplasm and part of the nucleus (n) of this osteoblast on the implant surface. A small area of mineralised matrix (m) can be seen at the bottom right of the field. Field width: 7µm 146
- Figure 4.41 Titanium. Mitochondria (m) and rough endoplasmic reticulum (r) in the cytoplasm surrounding the nucleus (n) of this osteoblast surrounded by osteoid (os) at the interface. i - implant space. Field width: 8.75µm 146
- Figure 4.42 Titanium. Electron dense secretory granules (sg) within the cytoplasm of a secretory cell depositing collagen (c). mm- mineralised matrix. Arrows - interface. Field width: 7µm 147
- Figure 4.43 Titanium. A layer of loose fibrils with a reticular appearance (f) lies between the titanium surface and collagen fibres (c) on the surface of the mineralised matrix (mm). Arrows - electron dense line at the interface. Field width: 2.6µm 147
- Figure 4.44 Titanium. Unmineralised layer with thin fibrils (f) between the titanium surface (arrow) and collagen fibres (c) overlying the mineralised matrix (m). Field width: 2.6µm 147
- Figure 5.1 Cross-section of femur from the control group at day 9. The wound created for the insertion of the agarose bead has healed completely. The bead is surrounded by mineralised bone (arrow) and marrow tissue (*). Toluidine blue stain. 170
- Figure 5.2 Cross-section of femur from test group at day 9. There is a localised increase in cell density around the bead (*). Further away, the thickness of the osteoid (os) layer is increased. The central marrow cavity (mc) is filled with new bone trabeculae. 170
- Figure 5.3 Femur from the control group at day 7. Osteoid (*) and new bone (arrow) formation around the agarose bead. 171
- Figure 5.4 Femur from the control group at day 9. This bead is almost completely surrounded by mineralised bone (arrows). 171
- Figure 5.5 Test group at day 7, there is a massive increase in cell density(*) around the bead and thick layers of osteoid (arrows) further away. 172
- Figure 5.6 Test group at day 9, the increased cell density(*) and osteoid thickness (arrows) are still apparent. 172
- Figure 5.7 Control group at day 7. The cells surrounding this bead stain positively for alkaline phosphatase (in red). Counterstain haematoxylin. 173
- Figure 5.8 Test group at day 7. Alkaline phosphatase staining is conspicuously absent in the cells (*) around the bead up to 5 cell diameters away from its surface. 173

List of tables

Table 1.1	Bone organ culture studies	13
Table 1.2	In vitro model systems for studying bone-biomaterial interactions	21
Table 1.3	In vivo models for studying bone-biomaterial interactions	47
Table 1.4	In vivo studies of tissue response to endosseous implants	59
Table 2.1	Composition of Apoceram CP31	67
Table 3.1	Composition of Apoceram CP1	87
Table 3.2	Number and types of grafts made	92
Table 3.3	Grafts of limb rudiments, mandibles, calvaria and femurs without implants	93
Table 3.4	Calvarial grafts containing implants	94
Table 3.5	Mandibular grafts (mandible halves) containing implants	95
Table 3.6	Grafts of 12 day embryonic femur containing implants	96
Table 3.7	Femoral grafts of different donor age without implants	96
Table 4.1	Grafts of femur with implants on CAM	115
Table 4.2	Day 1 Titanium	129
Table 4.3	Day 1 Apoceram	129
Table 4.4	Day 2 Titanium	129
Table 4.5	Day 2 Apoceram	129
Table 4.6	Day 3 Titanium	130
Table 4.7	Day 3 Apoceram	130
Table 4.8	Day 5 Titanium	130
Table 4.9	Day 5 Apoceram	130
Table 4.10	Day 7 Titanium	131
Table 4.11	Day 7 Apoceram	131
Table 4.12	Day 9 Titanium	131
Table 4.13	Day 9 Apoceram	131
Table 5.1	Growth factors implicated in bone repair	164
Table 5.2	Grafts of femur implanted with carrier beads	168
Table 5.3	Day 6 after grafting femurs containing agarose beads on CAM	174
Table 5.4	Day 7 after grafting femurs containing agarose beads on CAM	175
Table 5.5	Day 9 after grafting femurs containing agarose beads on CAM	176

1. Literature Review

1.1 Introduction

The most recent Adult Dental Health Survey (1988) (Office of Population Censuses and Surveys, 1991) revealed that 21% of the UK population over the age of 16 are edentulous. Whilst conventional prostheses provide satisfactory service in the majority of cases, there are many who are unable to use their dentures successfully (Harrison et al., 1992). The use of endosseous dental implants provides the opportunity to rehabilitate such individuals (Adell et al., 1990; Albrektsson, 1988).

Today, the goal of the treatment with endosseous dental implants is to achieve osseointegration, which is defined as a direct structural and functional connection between ordered, living bone and the surface of a load-carrying implant (Brånemark, 1983). A precise histologic definition of osseointegration is difficult since the interface morphology of clinically asymptomatic and rigidly fixed implants can show great variation along the interface of the same specimen, as well as varying between different materials and possibly also between different designs of implants. Osseointegration is clearly not an all-or-nothing concept. The direct contact with bone means the absence of a fibrous layer but the level of resolution of the direct contact and what is meant by a functional connection has yet to be resolved. [Note: Lalor and Revell (1993) stated that a layer of fibrous tissue usually develops between bone and a prosthetic implant regardless of whether it is cemented or uncemented. This comment holds true for many orthopaedic implants but should not be regarded as the norm for endosseous dental implants *ad modum* Brånemark.]

There is also controversy as to what osseointegration really represents. Sennerby (1991) felt that bone being in direct contact with implants reflects a normal bone healing which is 'correct' from a biological point of view. Stanford and Keller (1991) took the view that a direct bone contact at the histological level or osseointegration is not the result of an advantageous tissue response but rather the lack of a negative local or systemic response. Researchers working on 'bioactive' materials, such as Hench who

invented Bioglass, thought that ‘an ideal implant material must have a dynamic surface chemistry that **induces** histological changes at the implant interface which normally occur if the implant were not present’ (Hench & Ethridge, 1982), implying that the implant material ought to positively influence the healing process. A bioactive material is regarded as one which is designed to induce specific biological activity, for instance, surface chemical reactions leading to bonding of the implant with bone.

From the point of view of the assessment of biological safety, artificial materials intended for implantation into bone are usually tested at four different levels prior to clinical evaluation:

1. Evaluation of the material and its constituents for cytotoxic effects.
2. Short and long term animal implantation studies.
3. Histological and morphometric investigation of the implant bed and interface.
4. Biomechanical evaluation of the interface.

(Gross et al, 1986)

In vivo implantation studies are a necessary prerequisite to clinical evaluation of biomaterials, since they allow assessment of the gross histological response to a material. However, they do not allow the investigation of the response of different, isolated cell populations to a material. Alternatives to *in vivo* implantation as a means of studying the interaction of bone cells and bone substitute materials do exist. *In vitro* techniques provide scope for the observation of the behaviour of an isolated cell population on artificial substrata. Modified *in vivo* implantation techniques are also available, in which an isolated cell population or tissues can be maintained in an *in vivo* environment. All of these techniques have the potential to provide powerful tools for the detailed examination of the formation of the living/non-living interface between cells and biomaterials.

1.2 Testing of implant materials

Apart from strength requirements, the selection of biomaterials suitable for use as dental implants is based on the concept of biocompatibility which is defined as the ability of a material to perform with an appropriate host response in a specific application

(Williams, 1987). It has to be remembered that the biocompatibility of a material may differ according to its end-use application. Factors such as the duration and frequency of exposure, the amount of local as well as systemic biological activity imply that biological reactions that are detrimental to the success of a material in one implant application may have little or no bearing on the successful use of the material for a different application. This is reflected in the International Standards Organisation (ISO) guideline document 'Biological Testing of Medical Devices' (International Standards Organisation, 1991). It categorises the devices by: 1. the nature of their contact with the body (surface contacting/ external communicating/ implant devices). 2. the duration of their interaction with the body (limited exposure < 24hrs, prolonged exposure >24hrs and < 30 days, permanent contact >30 days).

The interaction duration and contact type between the device and tissues affect the selection of the test to assess device biocompatibility. Dental implants would come under the category of external communicating devices in permanent contact with bone and soft tissue. The procedures for testing of implant materials and devices would encompass *in vitro* tests, *in vivo* implantation in animals and clinical monitoring of implants. The following biological tests are recommended by the ISO for the evaluation of implants for surgery (ISO/TR 9966, 1989):

1.2.1 In vitro tests

1.2.1.1 Cytotoxicity tests

These tests demonstrate the potential toxicity of extractable or diffusible components of implant materials to cloned and/or differentiated cells in culture either by direct contact with or by exposure with extracts. A number of parameters are being used for assessing the cytotoxic effects of materials on cells: the permeability of the membrane to dyes, radioactive markers and intracellular proteins where cell membrane integrity usually indicates cell viability. The physical form of the material, whether it is in bulk or particulate form, or as soluble products, could affect the degree of cytotoxicity observed (Rae, 1986).

The cell types most widely employed in cytotoxicity studies are epithelial cells and fibroblasts, mainly as well-characterised, established cell lines in monolayer culture. The advantages of such a system are that a large number of results can be obtained very quickly and cheaply compared to animal studies; the system is very sensitive to toxic substances and quantification of the toxic response is possible; isolated cell types can be investigated and the response of living cells observed directly. Finally it is the only practical way to experiment with human derived cells. However, the static conditions employed in culture and the lack of systemic detoxification processes (present in the liver and kidney, for example) may result in oversensitivity to toxic substances; complex reactions such as tumour formation or those requiring an intact blood and nerve supply are impossible to mimic in culture and thus care must be exercised in extrapolating results from such studies to clinical situations (Rae, 1986).

1.2.1.2 Mutagenicity

These tests involve the application of mammalian or non-mammalian cell culture techniques for the determination of gene mutations, changes in chromosome structure and number and other DNA or genotoxicities.

1.2.1.3 Haemocompatibility

Areas of blood compatibility which may be studied include haemolysis, thrombosis, effect on formed blood elements, effect on haemostasis and effect on the complement system.

1.2.2 In vivo animal tests

1.2.2.1 Systemic acute toxicity

This is a test intended to determine the biological response of the test animal (usually mouse) to a single-dose intravenous or intra-peritoneal injection of an extract of a sample of the implant material.

1.2.2.2 Short-term implantation

This is a test for evaluating the reaction of living tissues at both macroscopic and microscopic levels to materials which are surgically implanted in appropriate tissue sites in animals for between 7 days and 30 days. It is carried out as a short-term *in vivo* screening of materials, usually in non-specific soft tissue sites such as muscle or the subcutaneous space.

1.2.2.3 Long-term implantation

The objective of long-term implantation is to evaluate the reaction of living tissues to implants at both macroscopic and microscopic levels for periods of 6 months to 2 years. The test is conducted, where possible, in tissues which are appropriate to the end-use of the implanted device.

1.2.2.4 Sensitisation

This is a test to estimate the potential for sensitisation either through direct contact or through diffusion of components of the implants.

1.2.2.5 Neoplastic potential

These tests are intended to determine the neoplastic potential of samples from either single or multiple exposures over a period of the total life of the test animal (usually the rat). It is well known that the neoplastic response varies significantly between species and strains. The frequency of implant-induced malignancy in human beings can only be determined by long-term clinical follow-up in human beings.

The above approaches to testing of implant materials provide the means to identify potential adverse effects. Clinical evaluation remains the ultimate test for all materials and implant systems. However, the sequence of events leading to implant survival or failure at cellular and biochemical levels is not yet well-understood. To examine the influence of various host and material factors we require techniques to observe and detect changes with greater specificity than what can be achieved with clinical or histological examination of successful or failed implants. It is also notable

that the *in vitro* cell culture tests described above are limited to screening procedures prior to *in vivo* testing. Pizzoferrato et al. (1994) made a distinction between cytotoxicity tests from response tests. The former highlight and quantify the cells which have died or have undergone regressive phenomena after contact with a material, the latter deal with specific cell/tissue functions that reflect interactions relevant to the clinical application of the material. Harmand et al (1986) were of the opinion that detailed investigation of the behaviour of cells at an interface was essential for accurately assessing the biocompatibility of a material but that existing cytotoxicity tests, with their poorly differentiated established cell lines, were unsuitable for this purpose. To address the problem, they proposed the introduction of *in vitro* studies utilising differentiated cells typical of the tissues encountered *in vivo*. They approached the issue of defining the biocompatibility of a bone biomaterial by formulating four criteria which could be applied to any tissue/material combination:

1. Basal biocompatibility, relating to general cell functions such as proliferation and cell membrane integrity and assessed by accepted cytotoxicity parameters.
2. Specific biocompatibility, relating to differentiated cell structures and functions.
3. Stimulation of phenotypic expression specific to particular cell types.
4. Integration of the material by cell and extracellular matrix attachment due to physicochemical characteristics of the material.

In essence, the drive is towards a better understanding of the cell reactions and material characteristics responsible for bone responses to biomaterials. The development of new materials as well as the attainment of any influence or even control over bone formation around an implant depend on the identification of the mechanisms underlying tissue-implant interactions and the regulatory processes. Dental implants are located in the unique environment of the oral cavity and are in contact with different media, cells and tissues: saliva, crevicular fluid and other contents of the oral cavity; the mucosal or soft tissue interface; and bone. This literature review will examine the methods currently available for studying cell and tissue responses to biomaterials relevant to dental implantology, with a focus on bone-biomaterial interactions, and explore the capabilities and limitations of various models and techniques.

1.3 Experimental models for studying bone-biomaterial interactions *in vitro*

1.3.1 Introduction

Over the last ten years, there has been growing support for the use of *in vitro* methods for examining biological responses to implant materials. Economic considerations, and changes in social attitudes towards animal experimentation are two factors amongst the many which encourage the use of cell/tissue techniques. The use of *in vitro* cell cultures reduce the need for whole animal work and present other advantages. The animal's physiology represents a network of interrelated systems making it difficult to examine the specific interactions of various cell types with the implant materials. The cell/tissue culture model, with its restricted number of variables would allow direct observation of the cell-biomaterial interaction. The microenvironment of the culture systems can be consistently produced and maintained and additional variables can be added under controlled conditions.

The advantages of using *in vitro* systems have been expounded by Rae (1986) and Davies (1990):

1. It can give very quick results, but results obtained quickly are likely to be confined to those which represent acute toxic reactions.
2. Tissue culture test systems can be extremely sensitive to toxic materials.
3. It is the only practical way to investigate and experiment on human tissue.
4. The quantitative measurement of toxicity is a possibility
5. A large number of controlled experiments are possible at a cost much lower than comparable investigations using experimental animals.
6. Single cell types can be investigated.
7. Living cells can be studied directly.

There are however several drawbacks in this approach to biocompatibility testing:

1. Caution must be exercised in extrapolating directly to the clinical situation.
2. Some investigations are impossible to reproduce *in vitro*.

3. It is unsuitable for the investigation of complex tissue responses where the integrity of the blood supply is required.

While *in vivo* methods involve the implantation of the material into a complex environment of blood, tissue fluid and heterogeneous cell populations, *in vitro* experimental studies address problems related to specific cellular interactions at the biomaterial interface as well as interactions at the molecular level.

In vitro culture permits three types of studies: the organ, the tissue and cell culture. An organ culture is one in which a whole organ, often from an embryo, is explanted and cultured *in vitro*. Organ culture preserves both parenchymal and stromal components of the organ, as well as their connections and functions. When a small fragment of tissue (e.g. epithelium) retaining its histological and biochemical differentiation, is cultured *in vitro*, this is regarded as a tissue culture. As with organ cultures, they cannot be propagated and generally incur greater experimental variation between replicates.

Cell cultures are achieved through enzymatic or mechanical disaggregation of a piece of tissue or by spontaneous migration from an explant, often of foetal or embryonic tissues. The major advantage is their ability to be propagated and divided into replicates; they can be characterised and preserved by freezing. Cell cultures derived from embryonic tissues will survive and grow more easily than those derived from adult tissues.

A fresh isolate of cells which is cultured *in vitro* is called a “primary culture” until cells are subcultured or passaged. Primary cell cultures are generally heterogeneous, with a low fraction of growing cells, but they contain a variety of cell types which are representative of the tissue. The subculture allows the propagation of the culture, which is now called a “cell line”: It appears to be more uniform, but specialised cells and functions can be lost. The greatest advantage of a cell line is the availability of a large amount of homogeneous material to be used for long periods of time.

After several passages a cell line may die (finite cell line) or be induced to transform into an established or continuous cell line. Most of the continuous cell lines originate from neoplastic tissues, but several continuous cell lines are derived from normal embryonic tissue (e.g. 3T3 fibroblasts). The transformation into a continuous cell line is usually accompanied by morphological alterations, such as decreased cell size, reduced adherence, higher nucleus:cytoplasm ratio, by an increased growth rate, by a reduction in serum requirements and by changes in chromosome number (Pizzoferrato et al., 1994). Cell culture models tend to examine the response of single cell types. Also complex local and systemic regulatory elements present *in vivo* cannot be completely reproduced. The response of transformed cells to test materials may be unrepresentative of a “normal” cell response. Despite these drawbacks, cell culture models can still provide useful information in isolating specific components of the biological response to materials (Boyan et al., 1996). In addition to simple cell viability tests, *in vitro* methods have been applied to study defined cellular processes including the rate of cell attachment, cytoskeletal organisation, changes in cell morphology, cell spreading and motility, growth and proliferation of cells, as well as the synthesis and release of a variety of cell factors, including the products of extracellular matrix synthesis. An increasing range of techniques is available for specific biochemical, histochemical as well as genetic analysis of cell functions specific to the cell types relevant to particular implant applications.

Davies (1990) has summarised succinctly the reasons for using *in vitro* methods for exploring bone-biomaterial interactions:

1. There is a need to examine the reaction of specific cell types on and adjacent to the surface of the biomaterial.
2. Examination of individual cellular reactions to biomaterials is necessary to understand the complexities of the environment *in vivo*. What is observed *in vitro* is a simplified part of the complex mechanisms *in vivo*.
3. It is only by developing assays *in vitro* that the creation of an interface can be examined in a “controlled” environment and under the same conditions.
4. The development of reliable testing methods *in vitro* will reduce the need for testing *in vivo* - this will not only reduce the number of animal experiments

necessary to achieve detailed understanding of biointeractions but will also reduce the time scale of experimental methods employed for such testing regimes.

5. Since materials which are destined for human implantation should, ideally, be tested with human cells rather than animal cells, it is only by developing methods *in vitro* that there is a chance that these methods may be adapted for use with human cells.

1.3.2 Background on bone culture systems

Bone cells and tissues form the basis of the majority of *in vitro* investigations into biological responses to dental implant materials. A review of the key features of bone at different levels of organisation as well as the methods for culturing bone *in vitro* is therefore appropriate at this stage.

1.3.2.1 Bone as an organ

Anatomically, there are two types of bones in the skeleton, flat bones (cranial bones, mandible, ileum) and long bones (tibia, femur) which derive from intramembranous and endochondral ossification respectively. The outer layer of bone is formed by dense cortical bone serving mainly the mechanical and protective function and the inner layer is made of cancellous or trabecular bone serving principally the metabolic function, although also having a structural role. Marrow, blood vessels and connective tissue occupy the medullary cavity within the metaphysis of the long bone as well as forming over 70% of the volume of trabecular bone. The external and internal bone surfaces are lined with osteogenic cells organised in layers: the periosteum and endosteum.

1.3.2.2 Bone as a tissue

At a microscopic level, bone can be seen to be composed of a relatively small number of cells and an abundance of extracellular matrix. There are three types of bone cells: osteoblasts, osteocytes and osteoclasts.

The osteoblast originates from a local mesenchymal stem cell (bone marrow stromal stem cell or connective tissue mesenchymal stem cell). These precursors proliferate and differentiate into pre-osteoblasts, then become mature osteoblasts which are seen as clusters of cuboidal cells lining the bone surface. At the light microscope level, the osteoblast is characterised by a round nucleus at the base of the cell and a strongly basophilic cytoplasm. At the ultrastructural level, notable features are a well developed rough endoplasmic reticulum and a prominent Golgi complex. Cytoplasmic processes on the secreting side extend into the unmineralised matrix (osteoid) and are in contact with osteocytes.

Osteoblasts are responsible for the production of the proteins of bone matrix, including Type I collagen, osteocalcin and osteonectin. They secrete the growth factors that are stored in the bone matrix, such as transforming growth factor β (TGF- β), bone morphogenetic proteins (BMPs), platelet derived growth factor (PDGF), insulin-like growth factors (IGFs) and fibroblast growth factors (FGFs) (Hauschka, 1990). Osteoblasts are capable of mineralising newly formed matrix. Their plasma membranes are characteristically rich in alkaline phosphatase and have been shown to have receptors for parathyroid hormone (PTH).

When bone matrix is deposited and calcified around an osteoblast, the cell will eventually be embedded in a lacuna and becomes an osteocyte. It has numerous cell processes in contact with those from other osteocytes and/or cells lining the bone surface. Ultrastructurally, a young osteocyte resembles an osteoblast but has a smaller volume and fewer organelles.

The osteoclast is a large multinucleated cell usually found in contact with a calcified bone surface and within a lacuna (Howship's lacuna) formed as a result of its resorptive activity. They arise from haematopoietic mononuclear cells in the bone marrow. Mononuclear osteoclast precursors can circulate in the blood, proliferate at endosteal bone surfaces and fuse to form multi-nucleated cells. At the light microscopy level, the cell has a foamy cytoplasm with many vacuoles and between 4-20 nuclei. The contact zone with bone is characterised by a ruffled border and dense patches on either

side forming the sealing zone. Ultrastructurally, osteoclasts have abundant Golgi complexes, mitochondria and transport vesicles. Deep foldings of the plasma membrane facing the bone matrix form the ruffled border. Lysosomal enzymes are actively secreted via the ruffled border into the extracellular bone resorbing compartment.

Bone matrix is formed by collagen fibres (type I collagen, 90% of total bone proteins), non-collagenous proteins and a ground substance composed of glycoproteins and proteoglycans. The orientation of collagen fibres alternates from layer to layer in adult bone to give it a lamellar structure. During histogenesis and fracture healing, collagen fibres are randomly oriented, giving rise to woven bone. The inorganic component of bone is mainly in the form of hydroxyapatite crystals which are found on the collagen fibres, within them and in the ground substance.

1.3.2.3 Bone organ and tissue culture

Historically, the chick limb organ culture model (Fell, 1928) provided the first insights into the conditions for the *in vitro* support of bone and cartilage development. Organ culture was used in early investigations of the developmental, metabolic and endocrinological processes in bone (Gaillard et al., 1979). The most commonly used bones in organ cultures are: the calvarium and the long bone. Foetal or neonatal chick, mouse or rat bones are explanted and cultured at the surface of the medium. The explants are supported by filters that are held onto metal screens, a technique originated by Trowell (1954).

The calvarium has a relatively simple cellular composition and is easy to dissect and handle. Apart from being a popular source of tissue for the enzymatic isolation of bone cells, calvarial explants in organ culture have also been extensively used in bone formation and resorption studies. The cellular composition of the calvarium is less complicated than that of the long bone rudiment and thought to be more suitable for metabolic studies. Long bones, on the other hand, are more suitable for studying the formation, activity and interrelation between the various tissues responsible for bone formation, modelling and remodelling (Nijweide & Burger, 1990). Some examples of the factors studied using these two model systems are shown in Table 1.1.

Table 1.1 **Bone organ culture studies**

Factors studied	Reference
Metabolic effects e.g pH on resorption	Bushinsky et al. (1993)
Parathyroid hormone	Pilbeam et al. (1993); de la Piedra et al. (1993)
Thyroid hormone	Lakatos & Stern (1992)
Vit D	Sato et al. (1993)
Cytokines and growth factors associated with resorption	Bertolini et al. (1994); Bertolini & Strassmann (1991); Canalis et al. (1991); Simmons & Raisz (1991)
Differentiation of chondrocytes	Roach (1992)
Mechanical stress	Lozupone et al. (1993); Klein-Nulend et al. (1993); Burger et al. (1991)
Effects of reduced gravity	Klement & Spooner (1993); Yamaguchi et al. (1991)

Calvarial explants are used equally often for bone formation and resorption studies. Long bone cultures are mainly used for resorption experiments. In long-term organ culture of long bones, the osteogenic precursors from the periosteum and endosteum differentiate into osteoblasts which synthesise matrix that subsequently mineralise but only at a slow rate. Roach (1994) felt that this was an advantage in that the regions of osteoid are much wider than *in vivo*, making it easier to study the spatial distribution of non-collagenous proteins relative to the mineralisation front. Neither the calvarium nor the long bone organ culture system has been successfully used for studying bone repair.

Apart from the calvarium and long bone, periosteal tissue has also been used as a model to study osteogenesis. Fell (1932) was again the first to use this model. Periosteal tissue dissected from 6-10 day old chick embryonic limb bones formed bone when cultured *in vitro*. Osteoblasts could be recognised in the explants after 2-4 days in culture. Osteoid matrix was present around day 7 and calcifications around day 12. Nijweide (1975) used a double layer technique where the periosteum of 17-18 day old foetal chick calvaria was folded with the osteogenic layer inside. Newly differentiated osteoblasts formed osteoid within 2-6 days. When the explant was cultured with the

addition of 5-10mM β -glycerophosphate, the osteoid calcified (Tenenbaum and Heersche, 1982).

Within this system, the process of *de novo* bone formation can be examined separate from interfering resorption. The tissue offers the three dimensional structure needed for a regular bone formation pattern which is often missing in cell cultures. It forms a link between organ and cell culture and was thought to be appropriate for the study of the initiation of osteoblast differentiation and osteogenesis *in vitro* (Nijweide & Burger, 1990).

1.3.2.4 Bone cell culture

Peck et al. (1964) treated bones from the calvaria of foetal and neonatal rats with collagenase. The result was the digestion of the uncalcified matrix and the release of bone cells which remained viable and proliferated in culture. The isolated cells were a mixed population consisting of many different cell types. By using sequential enzyme digestion, mouse calvariae can produce subpopulations rich in osteoblasts (Wong & Cohn, 1974). Early in the digestion process, cells with osteoclast characteristics were released, cells from later digestions presented osteoblast-like characteristics and exhibited properties that include parathyroid hormone responsiveness, as demonstrated by an increase in cyclic adenosine monophosphate (cAMP), and synthesis of bone-related proteins.

Non-enzymatic isolation techniques have also been widely used. Jones and Boyde (1979) noted that endocranial osteoblasts migrated readily from the bone surface onto various materials e.g. glass and dentine. Ecarot-Charrier et al. (1983) made use of this feature and placed glass fragments on the endocranial surface of neonatal mouse calvarial after removal of the periosteum. Osteoblasts migrated on the glass and from the glass onto culture dishes. Beresford et al. (1983) dissected trabecular fragments from human bone biopsies, cut and washed the fragments to remove marrow cells, then cultured the bone particles. Endosteal cell outgrowths eventually became confluent and were passaged for further studies. Robey & Termine (1985) used a similar technique but

treated the bone fragments with collagenase to remove marrow and loosely adhering cells prior to seeding the fragments in culture.

Osteoblast-like model culture systems have been established for several species, including: mouse (Scott et al., 1980; Sudo et al., 1983; Ecarot-Charrier et al., 1988), rat (Martin et al., 1976; Bhargava et al., 1988; Bellows et al. 1986; Owen et al., 1990), chicken (Gerstenfeld et al., 1987, 1988), calf (Whitson et al., 1984; Ibaraki et al. 1992), human (Fogh and Trempe, 1975; Gallagher et al., 1983; Beresford et al., 1984; Rodan et al. 1987a; Robey and Termine, 1985).

Potentially osteogenic cells are also present in bone marrow. Marrow stromal cells form a heterogeneous mixture of cell lineages which can differentiate into many different cells types (Locklin et al., 1995). In a long-term (1 year) murine bone marrow culture, Hauser et al. (1995) made positive identification of fibroblastoid, endothelial, macrophage and fat-containing cells using immunocytochemistry. The proportions of these different cell types changed with time. Attempts have been made to direct the path of differentiation towards osteogenic expression. Maniatopoulos et al. (1988) was the first to report that when rat marrow cells, obtained from the femur, were grown in the presence of ascorbic acid, β -GP and 10^{-8} M dexamethasone, osteoprogenitor cells within the population divide and differentiated to form bone nodules. Human marrow has also been shown to have osteogenic potential. Vilamitjanaamedee et al. (1993) reported the isolation of osteogenic precursors from human bone marrow stromal cells by cloning and successive subculturing. The cloned cells produced type I collagen, synthesised osteocalcin and osteonectin, responded to Vit D₃ by increasing osteocalcin synthesis and to PTH by increasing cAMP synthesis. After the third successive subculture in the absence of β -GP, the cells formed clusters which expressed high AP activity and positive von Kossa staining.

Primary osteoblastic cell populations are heterogeneous at any time due to differences in maturation or differentiation state between the individual cells or to the existence of different subpopulations of cells in one culture (Aubin et al., 1993; Liu et al., 1994). Culture of isolated bone cells can also result in the alteration of phenotypic

expression. Dedifferentiation of mature cells or overgrowth by immature cells can lead to decreased expression of osteoblastic features with subculturing.

1.3.2.5 Bone cell lines

Permanent or immortal cell lines derived either from osteosarcoma tumours, or from bone cell clones selected from primary cultures, have been utilised to address questions related to factors that influence the expression of the osteoblast phenotype and recently to study the regulation of genes encoding osteoblast phenotype markers (Rodan & Noda, 1991). They have the following advantages:

1. A large number of cells is available for biochemical studies and extraction/purification of cellular products.
2. The cell populations are homogeneous compared to primary cell cultures.
3. Cloning techniques permit selection of cells expressing varying degrees of osteoblastic characteristics.

Many of the osteosarcoma-derived osteoblastic cell lines have retained the principal properties exhibited by osteoblasts *in vivo*. There are unique differences between clones and they are known to react differently in culture to bone cells in organ culture. For example, Vit D₃ stimulates collagen synthesis by MC3T3 cells while inhibiting collagen synthesis in foetal bone tissue. Similarly, collagen synthesis in ROS17/2.8 cells is not affected by prostaglandin or epidermal growth factor while these factors affect cultured bone tissue (Heersche & Aubin, 1990). It is not known if these clones represent osteoblastic phenotypes present in bone or are aberrations induced by culture.

The choice of an experimental model of bone-forming cells depends on the problem to be studied. Freshly isolated and/or primary cultures allow studies of developmental stages, differentiation and cellular interactions among subpopulations of osteogenic cells. Markers established by these studies may permit and/or confirm the classification of transformed clones into several developmental stages. Transformed cloned cell lines on the other hand can produce large amounts of homogenous material for large scale studies and biochemical tests.

Nijweide et al (1982) stated that osteoblasts could be characterised *in vitro* by the following parameters:

1. Possession of a typical morphology.
2. Possession of a high level of membrane-specific alkaline phosphatase activity.
3. Respond to stimulation by PTH with an increase in intracellular cyclic AMP (cAMP).
4. Ability to form a bone (Type I collagen) matrix.
5. Ability to mineralise that matrix.

1.3.2.6 Bone formation in cell cultures

Prior to the removal of the bone cells from their matrix, individual cells may be relatively easily identified by their position, morphology, histochemistry and hormonal responses. Once removed from the matrix, the cells lose their characteristic position and morphology. Isolation procedures and culture conditions currently employed in published reports produce varying degrees of expression of osteoblastic phenotype. Osteoblast-like cells seeded in culture would attach to the substratum, spread and proliferate. After a period of proliferation, extracellular matrix is formed. There is increased expression of collagen type I and fibronectin mRNA. Extracellular matrix maturation begins with the increased expression of alkaline phosphatase. Finally, the matrix mineralises, coinciding with the expression of osteocalcin and osteopontin mRNA (Lian & Stein, 1992). During the culture, discrete multi-layered areas of cells become visible (nodules) (Beresford et al., 1993). In the presence of ascorbic acid and β -glycerophosphate (β -GP), the nodules become mineralised and stain with von Kossa's reagent and alizarin red and are positive for alkaline phosphatase. Ascorbic acid is involved in collagen synthesis and β -GP acts as a source of organic phosphate for the mineralisation of the matrix. The central region of the mineralising nodule is covered by a continuous layer of cuboidal cells resembling osteoblasts. Immediately adjacent to the osteoblast layer is a seam of unmineralised matrix which contains collagen fibrils. Further into the nodule, there are 200-300nm diameter vesicles thought to be the initial site of mineral deposition. In the more heavily mineralised portions of the nodule, poorly crystalline hydroxyapatite is closely associated with the collagen fibrils. Cells

resembling osteocytes are found embedded within the mineralised and unmineralised portions of the nodule matrix. This structure is said to resemble woven bone (Bhargava et al., 1988). Immunochemical and biochemical assessment has revealed the presence of collagen type I, III, V, osteonectin, osteopontin, bone sialoprotein, decorin, biglycan and osteocalcin in the matrix of the nodules (Beresford et al., 1993).

The time-course of this sequence is dependent on medium components, seeding density, the species and whether primary or secondary cultures are used (Aronow et al., 1990). Osteoblasts tend to lose some of their specific characteristics *in vitro* especially when cultured as a monolayer. Unambiguous identification of osteoblasts removed from their natural matrix and maintained in a culture system, is complex, since they share many characteristics with other cell types (Bellows et al, 1986). The typical morphology of osteoblasts is usually resumed when multilayers are formed. There is some evidence for the requirement of a specific three-dimensional arrangement of the cells in order to achieve osteoblast phenotypic expression *in vitro* (Nijweide et al, 1982).

1.3.2.7 Culture conditions

An advantage of working *in vitro* is that the environment can be controlled to a greater or lesser degree. The physicochemical environment for example can be controlled very precisely, although the physiological environment often still requires the addition of serum and is therefore undefined. Important factors in the maintenance of tissues *in vitro* are that the three dimensional geometry of the tissues is usually disrupted, with the loss of specific cell interactions and the opportunity for the cells to become mobile and proliferate. In addition, the culture environment lacks nervous and endocrine control and as such, cell metabolism may be more constant but less representative of the cell type *in vivo* (Freshney, 1987).

The question of differentiation *in vitro* was discussed by Freshney (1987). It was suggested that in culture, multi-potent stem cells would reach an equilibrium with undifferentiated but committed precursor cells and mature differentiated cells and that the equilibrium would shift according to the environmental conditions. It was thought that maintenance of cells at low density and high serum levels promoted cell proliferation and

discouraged differentiation - this is presumably the situation in the maintenance of established cell lines. On the other hand, maintenance of cells at high density with low serum levels and the appropriate hormones would inhibit proliferation and encourage differentiation. Therefore, it is important to select carefully the conditions for the maintenance of differentiated osteoblasts *in vitro*.

Several media supplements have been found to be important in maintaining the osteoblastic phenotype. Ascorbate promotes differentiation in animal bone cell culture systems *in vitro* (Aronow et al., 1990). Glucocorticoids promote osteogenic differentiation in relatively undifferentiated cell populations and stimulate alkaline phosphatase in human bone cells but are inhibitory to matrix synthesis (Beresford et al., 1993; Beresford et al., 1994). Dexamethasone is an absolute requirement for *in vitro* matrix nodule formation and mineralisation by rat marrow-derived stromal cells and enhances nodule development in calvaria-derived cells (Maniatopoulos et al., 1988; Bellows et al., 1987).

Mineralisation by calvarial cells has been found to depend on the cell density in culture (Tenenbaum & Heersche, 1986; Maniatopoulos et al., 1988; Zimmermann et al., 1991). In sparsely seeded monolayer cultures of rat calvarial cells, only the rarely occurring stem cells form mineralised foci after the development of a cell cluster by repeated cell divisions (Bellows & Aubin 1989). Osteoblast-like cells do not appear to be capable of calcification until the cultures become multi-layered.

Models which are transitions between tissue cultures and the use of isolated bone cells have been used to address the issue of cell density and differentiation. Casser-Bette et al. (1990) commented that demonstration of osteogenic potential *in vitro* is hampered by the problem that cells *in vivo* build up a three-dimensional structure prior to terminal differentiation, and this is hard to reproduce in conventional cell culture systems. They reported on the use of a matrix of collagen to provide a three-dimensional network for the formation of bone-like tissue by the clonal cell line MC3T3-E1.

Zimmermann et al. (1991) described an “organoid” system for studying mineralisation *in vitro*. Cells released from enzymatic digestion of foetal rat calvaria were collected and cultured on a membrane filter held at the medium/air interface. Within this arrangement, different cell types segregate, form organoid structures and differentiate. The first mineralised structures appeared after 4-6 days. Mineralisation took place in media with and without β -GP but occurred earlier and to a greater extent in the presence of β -GP. Different patterns of mineralisation could be found. During the culture period, mineralisation of the collagen fibrils was observed, further mineralisation occurred by apposition of a calcifying matrix on previously mineralised structures. Necrotic cells as well as extracellular vesicles were also detected close to areas of mineralisation. The authors concluded that in this “organoid” culture system, calvarial osteoblasts evolve all the different types of mineralisation that occur *in vivo* only at different sites or at different stages of the mineralisation process. They assumed that the conditions in the organoid culture: a high cell density and the separation from the medium by a membrane, favour differentiation.

1.3.3 Investigations on the interactions of bone cells with various implant materials

In addition to simple cell viability tests for cells grown on various implant materials, *in vitro* methods have been applied to study the rate of cell attachment, changes in cell morphology, cell spreading and motility, growth and proliferation of bone-forming cells. There exists a range of biochemical and histochemical techniques for the analysis of cell functions specific to the cell types relevant to endosseous implant applications. The drive towards a huge array of different assays is fuelled by the realisation that a cascade of events takes place when biological tissues come into contact with non-viable materials. Virtually all of the bone culture models discussed so far have been used for assessing biological responses to implant materials. A survey of the source of cells/tissues used in some of the recent reports on bone-biomaterial interactions *in vitro* is shown on the next page. (Table 1.2)

Table 1.2 *In vitro model systems for studying bone-biomaterial interactions*

	Reference
Tissue/organ culture	
Embryonic chick tibia	Anselme et al. (1994)
Neonatal rat calvaria	Davies (1990)
	Shelton et al. (1988)
	Brook et al. (1992)
Neonatal rat calvarial envelope	Davies (1990)
Rabbit calvaria	Courteney-Harris et al. (1995)
Human trabeculae - iliac crest	Anselme et al. (1994)
Primary cell culture from	
Chick embryonic calvaria	Groessner-Schreiber & Tuan (1992)
Foetal rat calvaria	Sautier et al. (1994a, 1994b)
	Vrouwenvelder et al. (1993)
	Qu et al. (1996)
Neonatal rat calvaria	Stanford et al. (1994)
	Bowers et al. (1992)
	Bouvier et al. (1994)
	Attawia et al. (1995)
	Chesmel et al. (1995)
Neonatal rat periosteum (calvarium)	Sammons et al. (1994)
Rat bone marrow	Davies et al. (1990)
	Ozawa & Kasugai (1996)
	Hulshoff et al. (1995)
Rabbit calvaria	Courteney-Harris et al. (1995)
Foetal bovine mandible	Yliheikkilä et al. (1995,1996)
Bovine bone	Meyer et al. (1993)
Human trabeculae - hip	Sinha et al. (1994)
Finite cell lines from	
Neonatal rat calvaria	Puleo et al. (1991); Puleo & Bizios (1992); Puleo et al. (1993)
	Healy et al. (1996) passage 2-4
	Cheung & Haak (1989)
Rabbit calvaria	Malik et al. (1992)
Human bone trabeculae - iliac crest	Doglioli & Scortecci (1991)
maxilla & mandible	Riccio et al. (1994)
embryo	Gregoire et al. (1990) passage 5-10
site unknown	Zambonin & Grano (1995) passage 1
	Howlett et al. (1994)
	Doherty et al. (1994)
Permanent Cell lines	
<i>Normal</i>	
MC3T3-E1 (mouse, calvaria)	Itakura et al. (1988)
	Bagambisa & Joos (1990)
	Alliot-Licht et al. (1991)
	Schneider & Burridge (1994)
	Cooper et al. (1993)
	Morrison et al. (1995)
rat calvarial osteoblasts	
<i>Osteosarcoma</i>	
UMR-106 (rat)	Ferguson et al. (1991)
	Hunter et al. (1995)
MG63 (human)	Granchi et al. (1995)
	Martin et al. (1995)
ROS17/2.8	Alliot-Licht et al. (1991)
SAOS-2 (human)	Benbassat et al. (1994)
	Gronowicz & McCarthy (1996)

1.3.4 Choice of model

1.3.4.1 Tissue and organ cultures

Primary bone tissue/organ cultures were used in place of isolated bone cells in many *in vitro* experiments on biomaterials. The advantage is the maintenance of the structural relationship of the bone cells and the bone matrix. Neonatal rat calvarial explants are the most commonly used model .

- ***Calvarial explants***

Davies et al. (1987) described the technique which is a modification of the method by Jones & Boyde (1979) for the observation of osteoblast migration over glass fragments. The material being studied was placed on the endocranial surface of a square piece of neonatal rat parietal bone stripped of the periosteum. Osteoblasts migrate from the bone surface to colonise the material. This was followed by new tissue formation by the migrated cells. One argument for using such a culture model is the relatively rapid production of an extracellular collagen matrix (Courteney-Harris et al., 1995). The young age of the animal favours rapid migration of cells onto the implant but rapid colonisation may be offset by a lack of differentiation and the calvaria may not have sufficient physical strength to support the weight of the material without damage.

- ***Calvarial envelope systems***

A further modification of the calvarial explant is the envelope technique which involves partial elevation of the endocranial periosteum to accommodate the test material in the envelope formed by the bone and the periosteal layer. The periosteal cell population includes fibroblasts, undifferentiated mesenchymal cells, and osteoprogenitor cells. This system may be used to observe the effects which the test material may have on the behaviour of these cells, with an osteogenic population covering the endocranial surface of the bone. The system is also useful for materials less dense than the culture medium and which would otherwise float, or for high solubility materials whose dissolution products would otherwise be rapidly dispersed in the volume of the culture medium. Supplementation of the medium with ascorbic acid and β -glycerophosphate is essential for collagen formation and its subsequent mineralisation within these cultures.

- ***Organotypic culture***

Anselme et al. (1994) introduced an organotypic culture as follows: Human trabecular bone from the iliac crest and chick femur fragments were layered over a buffered agar medium with nutrients. A piece of tissue culture plastic or stainless steel was deposited on each tissue explant. The culture was maintained for 14 days. Cells grew preferentially along the materials' surfaces. They examined parameters including: cell morphology, alkaline phosphatase activity, immunolabelling of various bone associated proteins and cell growth as measured by surface area, cell number/explant, adhesion, density. Positive staining for alkaline phosphatase was detected after 10 days of incubation. Human cell layers labelled positively for type I procollagen, type I collagen, fibronectin, osteopontin. Negative results were found with type II collagen, type III collagen, type III procollagen, bone sialoprotein, osteocalcin. Chick cell layers stained positive for type I collagen, type III collagen, fibronectin and negative for type II collagen. The authors concluded that the model allows the production of osteoblastic cells with the characteristics of immature osteoblasts.

In general, tissue and organ cultures can provide a picture of the organisation of the bone cells, the formation and mineralisation of new bone matrix in relation to implant surfaces by means of morphological, histochemical, immunohistochemical and ultrastructural examinations.

1.3.4.2 Primary or passaged normal bone cells

Using isolated primary or passaged normal bone cells for examining bone-biomaterial *in vitro* has advantages compared to organ or tissue culture systems. Quantitative assessments using biochemical or immuno- assays are much easier to perform. There is the possibility of using human cells. On the other hand, it may be more time-consuming, requiring a long time (weeks in the case of human cells) for the cultures to be established.

Foetal or neonatal rat calvarial cells and the rat marrow cell culture developed by Maniatiopoulous et al. (1988) have been the most extensively used. Morphological

characteristics, differentiation of the osteoblastic cells and the formation of a matrix on titanium (Davies et al., 1990; Groessner-Schreiber & Tuan, 1992), titanium alloy, alumina (Malik et al., 1992), hydroxyapatite (Garvey & Bizios, 1994), bioactive glass-ceramic (Sautier et al., 1994a), bioactive glass (Vrouwenvelder et al., 1994) have been demonstrated by separate studies. Other species from which osteoblast-like cells were harvested for culturing on implant materials are chick (Groessner-Schreiber & Tuan, 1992), rabbit (Cheung & Haak, 1989; Courteney-Harris et al., 1995) and calf (Meyer et al., 1993; Yliheikkilä et al., 1995).

Obtaining large numbers of cells from primary cultures without repeated passaging can be a challenge. When Yliheikkilä et al. (1995) grew foetal bovine mandibular osteoblasts on titanium alloy, a small number of cells were seeded on each metal disk but they maintained low levels of ascorbic acid, calcium and phosphate early in the culture to maximise proliferation and added the supplements when the cells were confluent to steer the cultures toward multilayering, matrix elaboration and mineralisation.

1.3.4.3 Human osteoblasts

Most of the earlier *in vitro* studies of bone cell responses to biomaterials involved animal-derived cells. Reports of the interaction of human osteoblasts with artificial materials began to emerge in the biomaterials literature in the last few years as the culturing of human bone cells became better established, and cells derived from human trabecular bone and marrow from different skeletal sites have been shown to express osteoblast-like characteristics (Beresford et al., 1984; Gowen et al., 1990; Ernsts et al., 1989; Chenu et al., 1990). Results from experiments using human derived bone cells may be more relevant to the clinical situation. However, human osteoblasts are difficult to establish because of their slow proliferation rate. Most cultures are established from young individuals. The cells also become senescent after a relatively short time. A more significant feature is their heterogeneity. Differentiated human osteoblasts do not have all the phenotypical parameters expressed simultaneously, but can change according to cell cycle and the level of differentiation (Fedarko et al., 1990).

Despite these difficulties, the following sources of bone cells have been used for *in vitro* studies of implant materials: alveolar bone from patients undergoing endodontic surgery (Naji & Harmand, 1991), cancellous and cortical bone from maxillae and mandibles (Doglioli & Scortecchi, 1991), human embryonic bone (Riccio et al., 1994), trabecular bone from young patients undergoing surgery (Howlett et al., 1994; Zambonin & Grano, 1995; Gregoire et al., 1990), patients undergoing hip arthroplasty (Sinha et al., 1994) and cancellous bone biopsies (Labat et al., 1995).

Howlett et al. (1994) reflected that functional expression of osteoblastic markers including alkaline phosphatase and type I collagen was observed in only 30% of the human bone cells used in their experiments due to the cultures having a mixed population of cells arising from the explant culture method. Alkaline phosphatase activity was displayed in about 70% of the cells used by Gregoire et al. (1990). Zambonin and Grano (1996) described the cells used in their study as having different degrees of alkaline phosphatase activity from weak to very intense, low basal cAMP level which was not increased by PTH and high osteocalcin levels increased by VitD₃. These observations highlight the non-uniformity of human-derived bone cells even though they have been regarded as populations of well differentiated osteoblasts in all the examples cited.

1.3.4.4 Permanent cell lines

Clonal osteogenic cell lines, on the other hand, would provide greater homogeneity. They are convenient to maintain and are usually well characterised. Hence, they have been the basis of many *in vitro* experiments on bone biomaterials.

Itakura et al. (1988) suggested the use of the mouse clonal MC3T3-E1 cell line developed by Sudo and co-workers (1983) for testing the effects of various implant materials on bone cell growth, differentiation and calcification. This cell line derived from normal calvarial cells has since been used on studies involving hydroxyapatite (Bagambisa & Joos, 1990; Sun et al., 1994; Alliot-Licht et al., 1991), tricalcium phosphate (Gregoire et al., 1990); platinum-plated titanium (Itakura et al., 1989); aluminium oxide (Itakura et al., 1988); titanium (Ferguson et al., 1991; Cooper et al.,

1993). Osteosarcoma cell lines including ROS17/2.8 (Alliot-Licht et al., 1991), MG63 (Martin et al., 1995; Granchi et al., 1995), SAOS-2 (Benbassat et al., 1994; Gronowicz & McCarthy, 1996), UMR-106 (Ferguson et al., 1991; Hunter et al., 1995) have also been tested on biomaterials for orthopaedic use.

Research groups which favour primary cultures or culture of normal cells with limited lifespan have argued that transformed cell lines are inappropriate for studying bone-biomaterial interactions on the basis that cloned osteoblast-like cells react differently than bone cells in tissue or organ culture (Davies, 1990). When interpreting the results of experiments involving transformed cell lines, it is useful to consider that not all cell lines express all of the properties of osteoblasts *in vivo*. For instance, the UMR 106 line does not express osteocalcin and only certain cell lines e.g. ROS 17/2.8, SAOS-2 are competent to develop mineralised matrix under the appropriate conditions. Expression of osteoblastic activities is low at low cell density and increases as cells reach confluence. Also, genes encoding osteoblast-specific proteins that are expressed sequentially and independently during normal bone cell differentiation are expressed concomitantly following transformation. Furthermore, the relationship between growth and differentiation is deregulated in transformed cells.

1.3.5 Measurable events on implant surfaces

The study of cell interaction with prosthetic surfaces can involve measurement of at least six kinds of events:

1. Attachment of fibronectin and other substances affecting cell adhesion to biomaterials.
2. Initial cell attachment.
3. Cell spreading.
4. Cell growth on the surface or in the interstices of the material.
5. Cell differentiation and expression of the phenotype.
6. Post-implantation losses and changes in phenotype due to *in vivo* stresses.

The attachment, growth and differentiation of cells together with the formation of extracellular matrix, its organisation and mineralisation (in the case of bone-forming

cells) on implant materials have been regarded as a representation of the early implant-tissue interface. The cell-attachment properties of a material are closely linked to how attachment proteins bind to the material in a bioactive form. The density and active or inactive conformation of the bound proteins influence initial cell adhesion to the artificial substrata and in turn affect cell spreading, and growth on the surface.

1.3.6 Mechanism of cell-substratum adhesion

Protein attachment precedes cellular interaction with the substratum. Cell adhesion to a substrate includes the steps of serum-protein adsorption, cell contact, attachment and spreading (Vogler and Bussian, 1987). For a cell inoculum attaching to a substrate from a static fluid, there is a brief lag phase followed by a rapid increase in attached-cell numbers, then a declining rate of attachment to a plateau or equilibrium-adherence level. Cell spreading begins well after initial contact, continuing during and after the first hour of attachment, while adhesion patches and plaques form with progressive adherence to the substrate. By contrast, steps prior to spreading occur over a shorter time period. Protein adsorption is nearly spontaneous, depositing from serum a 2-5 nm layer within the first minute of contact. Cells in suspension can gravitate to within 5-8 nm of a substrate in less than 5 minutes, although maximal attachment seldom occurs in this time frame. Rather there is a time-dependent cellular interaction with adsorbed proteins, probably involving both microextensions of the cell surface that break electrostatic barriers and cell-membrane receptors specifically directed towards various adsorbed factors (Sharefkin and Watkins, 1986). Thus, cell contact and adhesion is a time-dependent phenomenon.

The primary step in cell-substrate interactions is the rapid and differential adsorption of proteins from the media to form a substrate more enriched in some proteins than others. However, the significance of these differences is not so well understood. Differences in the adsorbed protein layer on different substrates might affect cell behaviour in a variety of ways. The simplest theory is the 'composition' mechanism, whereby increased amounts of adsorption of a protein for which the cell has an affinity cause that cell to interact more strongly with the substrate. An alternative theory is that

the 'state' or conformation of the adsorbed protein is more important than its amount in affecting cell attachment (Grinnell & Feld, 1981).

Cell attachment to surfaces begins with protrusion of ruffled edges or lamellipodia, followed by cellular spreading. Initial attachment, spreading, and flattening are active, energy-requiring processes. Cell flattening and spreading appear to be necessary, though not sufficient, events for later DNA synthesis and cell division. Most eukaryotic cells have networks of 70Å diameter microfilaments containing the contractile protein actin, which functions together with myosin-like proteins to cause cell movement and shape changes. Attachment and spreading on plane substrata involves the dynamic reorganisation of three filamentous structures: microtubules, microfilaments and intermediate filaments (Ireland et al., 1987). Several types of cell-substratum adhesion have been described, including focal contacts, close contacts and extracellular matrix contacts (Puleo & Bizios, 1992). Of particular interest is the interaction between the cytoskeleton and a number of adhesive glycoproteins in the extracellular matrix. Fibronectin and vitronectin are the two most well studied. They play an important role in linking the cells to surfaces, inducing cell spreading, and possibly regulating later cell growth and phenotype expression (Alberts et al., 1989). These proteins can attach in an active form to plastic surfaces, to collagen and to the fibrin strands of fresh clots. They enhance attachment of cell types as diverse as fibroblasts, osteoblasts, endothelial cells to collagenous matrices or plastic surfaces (Howlett et al., 1994). They do so by binding to transmembrane glycoprotein receptors which are in turn attached to the cytoskeleton (Yamada et al., 1985). These and other matrix receptors including some that bind collagen and laminin belong to the family of transmembrane glycoproteins called integrins. They are heterodimers with α and β chains and recognise the arginine-glycine-aspartic acid (RGD) tripeptide sequence in the matrix components they bind. The integrins link the extracellular matrix to the cytoskeleton and provide a mechanism by which matrix proteins can influence cellular activities via changes in cell shape or morphology (Sauc et al., 1991).

In bone matrix there are multiple glycoproteins that contain the integrin-binding RGD sequence: fibronectin (FN), thrombospondin (TSP), osteopontin (OPN), bone sialoprotein (BSP), type I collagen (COL I), and vitronectin (VN). Grzesik & Robey

(1994) localised TSP, FN, VN, and several integrins within developing human long bone using immunohistochemical methods. They went on to assess the effect of all bone RGD proteins on the adhesion of human osteoblastic cells. Thrombospondin, fibronectin, and vitronectin showed distinct localisation patterns within bone tissue. TSP was found mainly in osteoid and the periosteum; VN appeared to be present mainly in mature bone matrix. FN was present in the periosteum as well as within both mature and immature bone matrix. Using a panel of anti-integrin antibodies, it was found that bone cells *in vivo* and *in vitro* express α_4 , α_v , $\alpha_5\beta_1$, $\alpha_v\beta_3$, and β_3/β_5 integrins, and these receptors were expressed on all bone cells at different stages of maturation with quantitative rather than qualitative variations, with the exception of α_4 , which was expressed mainly by osteoblasts. Cell attachment assays performed using primary human bone cells under serum-free conditions revealed that COL I, TSP, VN, FN, OPN, and BSP promoted bone cell attachment in a dose-dependent manner and were equivalent in action when used in equimolar concentrations. In the presence of GRGDS peptide in the medium, the adhesion to BSP, OPN, and VN was almost completely blocked and attachment to FN, COLL I, and TSP was only slightly reduced. These results suggest that human bone cells may use RGD-independent mechanisms for attachment to the latter glycoproteins.

1.3.7 Cell attachment assays

Many different cell types may potentially attach to the surface of dental implants. In the absence of infection, the desired goal is to achieve a stable interface with adjacent bone and the connective tissue. Although it is not clear that bone cells are actually attaching to the surfaces of endosseous implants *in vivo*, many research groups have used cell attachment studies to explore the primary interaction between implant surfaces and osteoblast-like cells.

Measurement of cell attachment is usually carried out by means of counting at different time intervals either the number of cells not attached to the material surfaces or dissociating the attached cells from the substrata and resuspending them for counting. Cell number can also be assessed by radioisotope labelling and scintillation counting of labelled cells.

1.3.7.1 Bone RGD proteins and cellular responses

Howlett et al. (1994) investigated the contribution that serum fibronectin (Fn) or vitronectin (Vn) make to the attachment and spreading of cells cultured from explanted human bone (bone-derived cells) during the first 90 min of culture on metallic and ceramic surfaces. The requirement for Fn or Vn for attachment and spreading of bone-derived cells onto stainless steel 316 (SS), titanium (Ti) and alumina (Al_2O_3) and to polyethyleneterephthalate (PET) was directly tested by selective removal of Fn or Vn from the serum prior to addition to the culture medium. Attachment and spreading of bone-derived cells onto SS, Ti and Al_2O_3 surfaces were reduced by 73-83% when the cells were seeded in medium containing serum from which the Vn had been removed. Cell attachment and spreading on these surfaces when seeded in medium containing Fn-depleted serum (which contained Vn) were not reduced to the same extent as in the medium containing Vn-depleted serum. The bone-derived cells failed to attach to the surfaces to the same extent when seeded in medium containing serum depleted of both Vn and Fn. The results show that for human bone-derived cells, the attachment and spreading of cells onto SS, Ti and Al_2O_3 as well as PET during the first 90 min of a cell culture attachment assay are a function of adsorption of serum Vn onto the surface.

1.3.7.2 Cytoskeletal Organisation

Sinha et al. (1994) hypothesised that the nature of cell substratum attachment may determine subsequent cellular behaviour and in the context of bone-implant interfaces, may be a predictor of bone growth on clinically relevant surfaces of varying chemical composition and topography. Apart from measuring the number of cells attached to a variety of metal surfaces, they examined other characteristics including cell spreading, cytoskeletal organisation and focal contact formation. Different patterns of actin filament distribution were found and focal contact areas varied between cells grown on different materials.

An alternative assay for cell attachment was proposed by Hunter et al. (1995). They assessed fibroblast and osteoblast attachment on a variety of metals and polymers for orthopaedic use by indirect immunofluorescent labelling of vinculin, a component of

the cell's focal adhesion plaque. The degree of cell attachment was quantified on the materials by determining the mean number of adhesion plaques and using an image analysis system to determine the mean total area of plaques per cell. Fibroblasts and osteoblasts responded differently to the materials tested. Scanning electron microscope (SEM) observations of cells on the materials correlated with the morphometric data. Cells with the greatest number and area of adhesion plaques were well spread and flattened whilst those with the least number of adhesion plaques were more rounded and less spread.

1.3.7.3 Integrin-mediated adhesion

The question of whether integrins are involved in the attachment of osteoblasts to implant materials has been addressed only recently. Sinha & Tuan (1996) found that the integrin subunits, α_2 , α_3 , α_4 , α_5 , α_v , α_6 , β_1 and β_3 , were expressed by primary human osteoblasts cultured on polystyrene coated with various extracellular molecules. However, α_5 and α_6 were notably absent in cells attached to the orthopaedic metal alloys. Also, α_3 was not present on rough TiAlV, polished CoCr, or rough CoCr, and β_3 was not expressed by cells on rough CoCr. The ability of cells to adhere to and receive messages from the extracellular matrix may also be influenced by the substratum. These differences in integrin expression may underlie previously observed differences in degree of cell attachment to these metals.

Gronowicz & McCarthy (1996) looked into the details of how the human osteoblast-like cell line SAOS-2 adhere to orthopaedic implant materials. To determine if integrins were involved in cell attachment to implant materials, the peptide GRGDSP (Gly-Arg-Gly-Asp-Ser-Pro), which blocks integrin receptors through the Arg-Gly-Asp sequence, was added to the cells in serum-free medium. This peptide inhibited cell adhesion on the metal alloys. Inhibition of protein synthesis and enzymatic removal of surface proteins did not affect the ability of Arg-Gly-Asp peptides to inhibit cell attachment to the implant materials. These results suggest that integrins are able to bind directly to metals. Western blot analysis of integrin proteins revealed different levels of many integrin subunits, depending on the substrate to which cells attached. To determine specifically which integrins may be involved in adhesion, antibodies to integrins were

added. An antibody to the fibronectin receptor, $\alpha_5\beta_1$, significantly inhibited binding of cells to the metals but the antibody to vitronectin receptor, $\alpha_v\beta_3/\beta_5$, did not alter cell adhesion. The conclusion was that osteoblast-like cells appear to be capable of attaching directly to implant materials through integrins. The type of substrate determines which integrins are expressed by osteoblasts.

1.3.8 Cell growth/proliferation

Cell growth or proliferation on biomaterials can be assessed by a variety of methods: 1. dissociating the cells and counting cell numbers at different time intervals (Hulshoff et al., 1995) 2. indirect cell number assay by measuring metabolic enzyme activity (Ong et al., 1995). 3. measuring [^3H]-thymidine incorporation in the cultures (Zambonin and Grano, 1995). 4. measuring DNA and protein content in cell lysates (Itakura et al., 1988; Vrouwenvelder et al., 1994; Ozawa & Kasugai, 1996)

Flow cytometry has added to the sophistication of cell proliferation studies. Granchi et al. (1995) tested extracts from five different orthopaedic cements at different time intervals on MG63 osteoblast-like cells and evaluated cell cycle phases at 24, 48 and 72 hours using flow cytometry. They reasoned that bone-forming processes are correlated with the proliferation and cell cycle phases of bone cells. Therefore, inhibition of cell proliferation by a biomaterial can be studied in conjunction with cell cycle phases to evaluate the toxicity of the material. Cellular DNA content and the percentage of cells in S phase were assessed. The bone cements inhibited the proliferation of the osteoblast-like cells with different degrees depending on the time interval between cement setting and extract preparation (an inverse relationship was observed). The damage did not selectively hit a specific phase of the cell cycle and did not seem to be irreversible as the cells maintained their proliferation capability.

In addition to the quantitative techniques described above, many studies utilised scanning electron microscopy to illustrate the morphology of the cells and the arrangement of the matrix on the biomaterials (Doherty et al., 1994; Begley et al., 1993). The group led by Davies was one of the first to report on the morphology of osteogenic cells and their extracellular matrix on titanium (Davies et al., 1990). Vrouwenvelder et

al. (1992) found differences in the morphology of foetal rat osteoblasts cultured on bioactive glass and non-reactive glasses. Non-reactive glass cultures showed flattened cells with almost no dorsal ruffles. Bioactive glass cultures showed compact cells with dorsal ruffles and filopodia resulting in the formation of a denser cell layer. Many biomaterials intended to promote bone regeneration have porous structures which make visualisation of cells growing within the three-dimensional structure difficult. Attawia et al. (1995) reported the use of immunofluorescence and confocal laser scanning microscopy to characterise bone cells growing within an opaque polymer-ceramic matrix. Fluorescence-labelled monoclonal antibody to osteocalcin, a non-collagenous bone protein, allowed the visualisation of cells expressing osteoblast phenotype within the porous material.

1.3.9 Functional activity and phenotypic expression

The functional activity of osteoblast-like cells cultured on biomaterials can be detected in terms of their alkaline phosphatase activity, the synthesis of collagen and other bone matrix proteins (Vrouwenvelde et al., 1994).

Alkaline phosphatase can be demonstrated histochemically within the culture or its level in cell lysates assessed by colorimetric methods using *p*-nitrophenyl phosphate as a substrate (Itakura et al., 1988; Ozawa & Kasugai, 1996). Expressing alkaline phosphatase activity per unit protein or DNA would give an indication of the level of cellular activity independent of cell numbers or proliferation.

Quantitation of cAMP in cultures incubated with and without parathyroid hormone using radio-immunoassay is another confirmation of osteoblast-like character of the cells growing on the materials (Cheung & Haak, 1989).

Protein levels may be measured by pulsing the cells with [³H]-proline, followed by enzymatic digestion of the cells, extraction and separation of the collagenous and non-collagenous proteins and measuring the radioactivity of the extracts using a liquid scintillation counter (Puleo et al., 1991; Zamboni & Grano, 1995). Commercially

available radioimmunoassay kits are available for measurement of non-collagenous proteins such as osteocalcin (Grégoire et al., 1990; Zambonin & Grano, 1995).

Alternatively, the levels of the various bone matrix proteins have been assessed by separating cell proteins in lysates using SDS-PAGE. Employing immunolabelling and Western blot techniques, Sammons et al. (1994) have reported on the levels of collagen Type I and osteopontin produced by neonatal rat calvarial cells cultured on hydroxyapatite. They found a high rate of synthesis of alkaline phosphatase, collagen and osteopontin up to 10 days in culture followed by a decline and then a new peak of synthesis at 17 days. The cell number had been increasing up to day 15. The late peak of synthesis was attributed to the onset of mineralisation of the extracellular matrix which followed the cessation of cell proliferation.

There are many comparative studies examining different implant materials. Osteoblasts cultured on titanium-doped bioactive glass were found to have significantly higher proliferation and osteoblast expression compared with standard 45S5 glass. Iron-, fluorine- or boron- containing glass demonstrated lower proliferation and osteoblast expression compared with the standard glass (Vrouwenvelder et al., 1994). When the same 45S5 glass was compared earlier with hydroxyapatite, Ti-6Al-4V, and stainless steel, it had the highest osteoblast proliferation rate, DNA content, alkaline phosphatase (AP) content as well as AP/DNA ratio (Vrouwenvelder et al., 1993). Itakura et al. (1988) reported that MC3T3-E1 cells had significantly lower cell growth and differentiation when cultured on silver-palladium compared to titanium and single crystal aluminium oxide. Ozawa & Kasugai (1996) found little difference in DNA content in rat bone marrow cells between hydroxyapatite (HA), titanium (Ti) and an apatite; wollastonite containing glass-ceramic (GC) but higher AP activity on HA and GC than on Ti. It is almost impossible to collate results from different reports given that different osteoblast-like cells were seeded at different densities and cultured under different conditions. This is in addition to variables such as different surface preparation and sterilisation regimes for the biomaterials.

It is also by no means certain that the material with the best primary attachment characteristics is that on which the cells differentiate the most. Puleo et al. (1991) found significantly slower and lower cell adhesion and growth on hydroxyapatite compared with stainless steel, Ti-6Al-4V and CoCrMo but collagen synthesis was similar on all the materials tested. Meyer et al. (1993) cultured primary bovine osteoblasts on three different biomaterials, ionomeric cement (IC), tri-calcium phosphate poly-L-lactic acid composite foil (TCP) and poly-L-lactate-polycitric acid composite foil (PLA). The cells which grew on the materials produced all typical bone matrix proteins and were osteoblast-like as shown by immuno-staining. Analysis of the cell attachment kinetics revealed significant differences within the first 7 hours between the various materials. The highest rate of cell attachment was found on the IC surface, followed by the TCP and then the PLA surface. However, quantitative analysis of non-collagenous protein matrix production and DNA content per cell showed a different ranking for the three materials: PLA > IC > TCP.

1.3.10 Mineralisation of the extracellular matrix

The group led by Davies reported that when rodent calvaria-derived cells were densely seeded onto titanium discs and grown in the presence of ascorbic acid and β -glycerophosphate, mineralising nodules formed with the elaboration of a collagenous matrix at the implant surface and there were CaPO_4 globular accretions similar to morphologies from *in vivo* analysis (Davies et al., 1990; de Bruijn et al., 1995; Lowenberg et al., 1991; Orr et al., 1992). On the other hand, Yliheikkilä et al. (1996) in a study on long-term multi-layer cultures of primary foetal bovine osteoblasts found that matrix elaboration was only present above two to three layers of confluent cells. Mineralisation of the matrix did not occur at the interface region. Their result was similar to those presented by Garvey and Bizios (1994) using rat calvarial osteoblast cultures grown on HA and those of Bouvier et al. (1994) using rat calvaria-released cells grown on cpTi and Ti-6Al-4V surfaces.

1.3.11 Ultrastructure of bone cells cultures on implant materials *in vitro*

Davies et al. (1990) used a freeze fracture technique to separate Epon embedded rat bone marrow cells growing on titanium disks for sectioning. TEM examination

showed globular mineralisation of the collagen matrix in three week old cultures. The interfacial zone had two layers, a 'bonding' zone containing few collagen fibres and a ruthenium red positive (proteoglycan rich) layer containing more densely packed collagen.

De Bruijn et al. (1992) described the ultrastructure of rat bone marrow cells and matrix on plasma-sprayed hydroxyapatite (HA). Initially, the deposition of a globular, afibrillar matrix was observed. This was followed by the integration of collagen fibres in this matrix and their subsequent mineralisation. At the bone-HA interface, an electron-dense layer with a thickness of 20-60 nm was regularly present, which contained both organic and inorganic material and was rich in glycosaminoglycans. Parts of the interface also had an amorphous zone which was free of collagen fibres and had an average thickness of 0.7-0.8 microns. It was frequently seen interposed between the electron-dense layer and the hydroxyapatite. They felt that this was similar to the lamina limitans-like structure described *in vivo*. In a subsequent report they found that different levels of crystallinity of HA gave rise to different interfacial features (De Bruijn et al., 1993).

1.3.12 Monoclonal bodies against osteoblastic cells

With the development of monoclonal antibodies against osteoblasts at different stages of differentiation, it is possible to identify osteoblasts definitively without relying only on the measurement of cell products which typifies the phenotype (Aubin & Turksen, 1996). Vrouwenvelder et al. (1994) used a specific monoclonal antibody (E11) against a cell membrane associated antigen as an exclusive marker for osteoblast expression in rat calvarial cells. Using indirect immunofluorescence to locate the E11 antibody, they demonstrated the distribution of the osteoblast marker over monolayer and clusters of cells with varying cell morphology growing on bioactive glasses.

1.3.13 Regulation of cellular function

Developments in molecular biology make possible subcellular investigations of cell-biomaterial interactions. Assessments of the level and time-course of the expression of genes which ultimately determine cell phenotype may reveal the mechanisms by

which biomaterials influence cell function. The pattern and steady-state levels of mRNAs for matrix associated products can be related to the pattern and rates of protein or enzyme synthesis. Lian & Stein (1992) have shown a temporal sequence of gene expression during cell proliferation, extracellular matrix maturation and mineralisation in bone cell cultures. Since gene products are the ultimate determinants of cell phenotype, the hope is that these cellular and molecular processes studied *in vitro* can be correlated with events that occur *in vivo* after implant surgery.

The expression of mRNA for bone related proteins produced by osteoblast-like cells growing on biomaterials may be identified by hybridizing Northern blots of total cellular RNA with radiolabelled cDNA probes for the proteins (Ohgushi et al., 1993). Densitometric assessments provide a measure of the levels of specific mRNA relative to control cultures, for instance, on tissue culture polystyrene (Puleo et al., 1991; Ozawa & Kasugai, 1996).

Puleo et al. (1993) used polymerase chain reaction to demonstrate the expression of genes for the bone-related proteins, osteocalcin, osteonectin and osteopontin by neonatal rat calvarial osteoblasts. In addition, Northern blotting was used to demonstrate the expression of mRNAs encoding osteopontin and osteonectin during culture of osteoblasts on Ti-6Al-4V and hydroxyapatite over a five week period. It has to be noted that the expression of an mRNA does not necessary mean that the encoded protein would be found in the extracellular matrix. Multiple control mechanisms at the transcriptional and post-transcriptional levels determine whether the gene transcript becomes translated into a protein and whether the protein is eventually secreted into the matrix. Further comparative evaluation of extracellular levels of the bone-related proteins and levels of their respective mRNAs would help to build up a clearer picture of the mechanisms of cellular responses to biomaterials.

1.3.14 Resorption of implant materials in vitro

Most of the *in vitro* assessments on the bone-implant interface focus on the bone-forming cells. It is equally important to consider the reactions of cells capable of resorbing the implants. The materials subjected to investigations tend to be those known

or designed to be resorbable such as Plaster of Paris, tricalcium phosphate, and hydroxyapatite (Sidqui et al., 1995; Gomi et al., 1993; de Bruijn et al., 1994).

The major bone resorbing cells is the osteoclast. Monocytes and macrophages have also been shown to degrade devitalised bone. Osteoclasts are relatively inaccessible cells, but *in vitro* techniques are now available for isolating pre-formed osteoclasts from chicks, rodents, and baboons and for formation of osteoclasts from marrow precursors (Roodman et al., 1985; Zamboni Zallone et al., 1982). Osteoclasts can be removed from the endosteal side of growing rat or rabbit femurs and tibiae by curetting the bone surface. Pipetting the released fragments and incubating the cell suspension results in a mixed culture containing adherent osteoclasts. The number of cells obtained is low and the life-span of the culture is very short (< 1day). Medullary bone of laying hens fed with a hypocalcaemic diet has been used to provide relatively large numbers of osteoclasts. Osteoclasts formation can also be induced in bone marrow populations *in vitro*. Another source of osteoclasts is human osteoclastomas.

Markers for osteoclastic activity include tartrate resistant acid phosphatase and reactivity with antibodies against vitronectin receptor. Calcitonin will inhibit their activity whilst parathyroid hormone will increase acidification of these cultures (Szulczewski et al., 1993). Unambiguous identification of osteoclasts is difficult as they share many characteristics with multinucleated cells formed by the fusion of macrophages. Blottiere et al. (1995) suggested the use of a monoblastic cell line U937 which forms multinucleated giant cells following stimulation with Vit D₃ for the testing of biodegradation of calcium phosphate ceramics.

There is evidence of resorption of synthetic hydroxyapatite, tricalcium phosphate, biphasic ceramics combining the two materials as well as natural calcium carbonate by osteoclasts *in vitro* (Gomi et al., 1993; de Bruijn et al., 1994; Soueidan et al., 1995; Guillemin et al., 1995). Gomi et al. (1993) reported small tartrate-resistant acid phosphatase positive cells creating resorption pits morphologically similar to those in natural bone tissue and multi-nucleate giant cells caused erosion of the ceramic surface without pit formation. Substrates with greater surface roughness were associated with a

higher number of tartrate-resistant acid phosphatase positive cells and multinucleated cells. The ability of multinucleated cells in bone marrow cultures to resorb synthetic calcium phosphates gives rise to the potential for using these ceramics as culture substrata instead of bone slices in osteoclast resorption assays (Davies et al., 1993).

To test the hypothesis of whether bone matrix constituents would affect cell-mediated resorption of artificial materials, De Bruijn et al. (1994) first cultured osteogenic cells on tricalcium phosphate and hydroxyapatite until a bone-like matrix was formed on the surfaces and then introduced an osteoclastic cell culture to the materials. A potentiation effect was found whereby resorption of the mineralised extracellular matrix was followed by degradation of the underlying tricalcium phosphate.

1.3.15 Inflammatory and immunological response

There is extensive work in orthopaedic literature on the failure of orthopaedic joint prostheses due to osteolysis. This destructive process is believed to be the result of the phagocytosis of implant wear debris by peri-prosthetic and synovial macrophages and the release of inflammatory mediators (Kim et al., 1994). Wear debris is not a feature of endosseous dental implants although degradation of coatings has given rise to some concern (Albrektsson & Sennerby, 1991; Wataha, 1996). One *in vitro* method of investigating the role of macrophages in mediating bone resorption is to use a medium conditioned by macrophages interacting with implant materials in bone resorption assays using bone organ cultures (Murray & Rushton, 1992; Glant & Jacobs, 1994). Collagenase, Prostaglandin E₂ (PGE₂), interleukin-1 (IL-1), tumour necrosis factor (TNF), interleukin-6 (IL-6) have been implicated as mediators with a stimulatory effect on resorption (Haynes et al., 1993). The form in which the material is presented may be significant in such studies. Particulate rather than bulk materials would be more appropriate for investigations on the effect of wear particles.

It has to be remembered that the act of insertion of an implant into bone evokes an immediate inflammatory response due to the inevitable tissue trauma. Cells involved in this reaction are the granulocytes, followed by the monocytes and macrophages. These cells, together with other inflammatory mediators such as complement fragments,

contribute to a complex cascade of activities which can ultimately affect the recruitment, and differentiation of bone-forming cells which are the effectors of the bone healing process. The effect of metal ions and particulates, as well as some calcium phosphate materials on neutrophils, macrophages and complement activation have been examined *in vitro* (Remes & Williams, 1992). The concern that some patients may develop T-lymphocyte-mediated immune response or type IV hypersensitivity reaction to ions or particulates released from implants has also prompted lymphocyte activation and proliferation tests (Pizzoferrato et al., 1994).

1.3.16 In vitro models representing soft tissue responses

In addition to the nature of the bone-implant interface associated with osseointegration, the transgingival portion of endosseous dental implants has also received some attention (Guy et al., 1993). Epithelial cells and fibroblasts, often from human gingivae, have been cultured either as dissociated cells or as tissue explants on implant materials for the assessment of cell attachment, migration and proliferation.

Quantitative as well as qualitative approaches have been used for such assays. A typical quantitative assay is an experiment by Jansen et al. (1991a) using rat dermal fibroblasts cultured on titanium and carbon coated coverslips. Cell attachment was quantified by measuring the percentage of unattached cells relative to number of seeded cells at different time intervals. Cell proliferation was determined by detaching all the cells by trypsinisation after initial attachment has taken place and counting them. This approach is typical of many assays studying cell growth on implant surfaces e.g. Berstein et al. (1992); Niederauer et al. (1994). Indirect quantification of cell numbers can be performed by radiolabeling cells with tritiated thymidine and counting by liquid scintillation (Guy et al., 1993). Instead of removing the cells from the material surfaces for evaluation, some researchers relied on scanning electron micrographs for assessment of cell numbers. Burchard et al. (1991) in a study on the effects of chlorhexidine and stannous fluoride on human gingival fibroblast attachment to different implant surfaces, counted the number of cells visible in non-overlapping fields of 1.0mm² on the materials following 24 hours incubation.

The extent of migration is a characteristic often assessed in epithelial and fibroblast cultures on artificial materials. Jansen et al. (1991) devised a 'fence' technique where a cell suspension was allowed to settle within a ring placed on the artificial substratum. The ring was then removed to allow outward migration of the cells. The area of cell coverage was measured after three days to assess the extent of cell migration onto the implant surfaces. Warocquierclerout et al. (1995) have found that precious (Au, Pd, Ag) and non-precious (Ni-Cr) dental alloys, Ti and Cu showed different effects on human gingival epithelial cell proliferation and migration. Cells grown on Pd and Au exhibited a high migration potential, whereas Au-Pd and Ti allowed efficient cell proliferation but restricted migration. Reduced migration and proliferation was found on Ag. The toxicity of Cu and Ni-Cr prevented cell migration.

The roles of fibronectin and other cell attachment proteins in the attachment of fibroblasts on implant surfaces *in vitro* have been the subject of several studies. Steiz et al. (1982) reported that precoating bioglass with fibronectin reduces the time required for fibroblasts spreading on bioglass but in a similar study involving commercially pure titanium, non-porous hydroxyapatite, and porous hydroxyapatite, Guy et al. (1993) found that pre-coating with fibronectin did not produce any increase in the number of cells attached to titanium or hydroxyapatite. Abiko et al. (1993) recorded the fibronectin tracks deposited by human gingival fibroblasts moving on smooth and grooved titanium surfaces and found that fibronectin production was more abundant in cells cultured in fibronectin-depleted medium.

1.3.17 Aspects of implant surface characteristics investigated using in vitro models

Implant materials of many different bulk chemical compositions have been studied using *in vitro* methods. Much effort has also been made to clarify the effects of surface properties such as surface roughness and topography on cell responses to implant materials. The main concern is that processes during the preparation of an implant can affect its surface properties and these, in turn, influence cell responses. (Kasemo & Lausmaa, 1988).

The alignment of various cells types in response to topographical features within their culture environment is a well documented phenomenon (Dunn, 1982; Wood & Thorogood, 1987; Meyle et al., 1995). With bone replacements, there are queries as to whether the materials should be roughened and perhaps even finished with aligned surface striae to orient any connective tissue cells that should attach to them. Micromarks on the surface, introduced perhaps in polishing or surface fabrication, may subsequently play a role in cell behaviour on such substrata. Various attempts have been made to make use of topographic features to influence tissue reaction around implant materials. The scale of features ranged from macroscopic pores of several hundred microns to ordered grooves of a few microns' width. Brunette et al. (1983) developed the use of a silicon mask-etching technique to prepare surfaces with micro-grooves. They evaluated the behaviour *in vitro* of fibroblasts and epithelial cells (Brunette, 1986a; Brunette, 1986b; Chehroudi et al., 1989; Chehroudi et al., 1990; Oakley & Brunette, 1993) and more recently reported on osteoblasts growing on such grooved surfaces (Qu et al., 1996).

Surface preparations which result in no distinct orientation of feature but resemble more closely the manufacturing processes received wider attention, as did sterilisation regimes for implants. The processes which have been explored using *in vitro* cell culture studies include: manufacturing e.g. machining, porous coating, plasma-spraying (Naji and Harmand, 1990); special treatment e.g. electropolish, sandblast, acid-pickling, ion implantation (Könönen et al., 1992; Bowers et al., 1992; Hormia et al., 1991; Hormia & Könönen, 1994); sterilisation e.g. autoclave, Ar plasma cleaning, UV-ozone cleaning, irradiation (Jansen et al., 1989; Michaels et al., 1991; Stanford et al., 1994).

1.4 Do *in vitro* cultures reflect the *in vivo* situation?

The problems of developing *in vitro* models for tissue-biomaterials interactions lie in the need to identify significant *in vivo* biological reactions for which simulation assays can be devised and designing *in vitro* assays which are relatively simple to perform and which produce consistent results among laboratories (Hanks et al., 1996).

The question of whether the state of maturation of osteoblast-like cells has any effect on the result of *in vitro* investigations of bone-biomaterial interactions has been addressed by a group in San Antonio, Texas (Windeler et al., 1991). A series of cultures was performed, involving a variety of bone cell lines and bone explants (ROS 17/2.8, UMR-106, SAOS-2, MC3T3-E1, MG-63, foetal baboon bone explants) growing on a wide range of materials sputter-coated on glass coverslips or polystyrene culture dishes (aluminium oxide, titanium, titanium dioxide, zirconium, zirconium dioxide, and two calcium phosphate ceramics). Assays of cell number, total protein, alkaline phosphatase in lysates and media and type I collagen were carried out. Significant differences in performance were observed for each osteoblast-material combination. Under identical culture conditions, no two of the transformed cell lines demonstrated the same performance on similar coated surfaces, nor did any of the lines duplicate the performance of normal primate cells. The group believed that the six cell lines represent different stages of differentiation of the osteoblast. It was suggested that MC-3T3 and MG-63 represent early undifferentiated or pre-osteoblast cells, whereas UMR-106 and SAOS-2 may represent the mature phenotype. The tissue explant from foetal baboons was a mixture of bone cells and not a pure osteoblast culture. On the basis of this extensive study and many others covering a range of different sources of bone cells, it is clear that interpretation of *in vitro* findings is a not a straightforward task.

Another area of contention is whether bone cells come into direct contact with implant surfaces *in vivo*. Yliheikkilä et al. (1995) took the view that most of the *in vitro* studies have focused on the interactions of osteoblasts with implant materials suggesting that the direct interaction of osteoblasts with implant surfaces is one determinant of osseointegration. Yet the published histology of the implant-bone interface indicates that there is an apposition of mineralised matrix and that few cells lie directly against the implant surface. They acknowledged that the situation *in vivo* is quite different from that created *in vitro* when bone-forming cells are initially attached to the culture surface. This leads to the question of whether osseointegration should be interpreted as bone formation towards implant surfaces or on implant surfaces (Cooper et al., 1993). The few studies of the early interface between bone and titanium in rat and rabbit tibia *in vivo* suggest that bone formed towards the implant (Sennerby, 1991; Clokie & Warshawsky, 1995).

Schwartz & Boyan (1994) reflected on this early interface and stated that differentiated osteoblasts or chondrocytes rarely come into contact with a material prior to its modification by biological fluids, immune cells and less differentiated mesenchymal cells *in vivo*. This was a major reason for their preference of an *in vivo* rat marrow ablation model of endosteal wound healing to detect whether the ability of osteoblasts to synthesise and calcify their extracellular matrix is affected by the local presence of the material. However, they did not reject the need for *in vitro* studies since it is the only way of isolating the specific components of the biological responses to materials (Boyan et al., 1996). They suggested that the first cells which interface with a material *in vivo* would be wound-healing cells, generally of mesenchymal origin. These pluripotential cells may differentiate into osteoblasts, chondrocytes, fibroblasts and fat cells. Which of the differentiation pathways they pursue would be dependant on the local and systemic factors present at the implant site.

Since the primary response to implant surgery is a local inflammatory reaction, and there is much work in the literature on how inflammatory cells and cytokines affect bone formation and resorption *in vitro*, it would be interesting to see investigations which make a link between how implant materials or implant surface preparations affect inflammatory cells which take part in the early local response and the subsequent effect on bone cells growing on these surfaces.

1.5 Experimental models for studying bone-biomaterial interactions *in vivo*

In vitro models are, in general, static and do not take into account the dynamics of implants *in vivo*. Also cell culture systems *in vitro* are mainly influenced by autocrine or paracrine factors and are not subject to systemically superimposed regulation.

Many factors such as the anatomical position of the material, size and geometry of the implants, and mechanical loads are important considerations *in vivo* but cannot be adequately studied *in vitro*. The application of *in vitro* results to reflect the behaviour of

a composite tissue such as bone is hampered by the fact that cell culture studies tend to focus on a single cell type. The growing trend of using primary human bone cells for experiments on implant materials also poses a challenge in that these cells do not always form bone *in vitro*.

1.5.1 Choice of *in vivo* models

There have been attempts to bring the bone-implant interface created *in vitro* a step closer to *in vivo* conditions. Modified *in vivo* implantation techniques are available in which an isolated cell population can be maintained in an *in vivo* environment.

1.5.2 Diffusion chamber studies

The diffusion chamber system has been used extensively to study the osteogenic capacities of freshly isolated bone marrow cell suspensions and cultured marrow cells from a variety of experimental animal species (Review by Owen, 1970). The diffusion chamber is constructed using membrane filters of known pore size, supported by Perspex rings and containing target cells. The chambers are implanted into the host, their purpose being to prevent direct cell contact between host and target cells whilst the target cells were maintained by the diffusion of essential nutrients and metabolites across the filter. This system allows the direct study of the cellular potentials for differentiation as host tissues are excluded. The tissue formed, although avascular, resembles osseous tissue by both light and electron microscopic examination. Furthermore temporal expression of extracellular matrix and cellular components during the generation of tissue in the diffusion chamber is similar to that observed in the process of osteogenesis occurring in normal embryonic and adult development (Ashton et al., 1980).

Tarrant & Davies (1987) placed various artificial bone substitute materials into a primary rat osteoblast culture until the materials were colonised by the cells and transferred the combination into diffusion chambers to be further maintained *in vivo* in rats. They argued that such a system would avoid the problems associated with long term *in vitro* maintenance of primary bone cell populations and at the same time allow the examination of single cell types on the substrates by excluding host cell participation. However, the matrix formed within the chambers was poorly organised and showed little

calcification. This was attributed to the low seeding density since the particles of bone substitute materials only carry a small number of cells relative to the size of the chambers.

Human bone marrow cells cultured in diffusion chambers have also repeatedly failed to form bone. Bab et al (1988) failed to observe bone formation from adult donors. Davies (1987) found no bone when culturing fresh marrow from 5-yr old. Neither did Ashton et al. (1985) when they cultured fibroblasts from composite pieces of bone and marrow from children and young adults inoculated in diffusion chambers. However, bone formation was consistently observed in ceramic carriers filled with marrow-derived cells which were grafted subcutaneously *in vivo*. Haynesworth et al. (1995) obtained bone marrow from donors of various ages, first cultured them to increase cell numbers and introduced subcultures into either diffusion chambers (implanted intra-peritoneally in nude mice) or ceramic carriers (implanted subcutaneously in nude mice). The marrow derived cells failed to form bone or cartilage in diffusion chambers whereas bone but not cartilage was formed within the ceramic carriers.

Gundle et al. (1995) in experiments similar to those above cultured human osteoprogenitor cell populations derived from trabecular bone explants or marrow suspensions of three patients in the absence or continuous presence of dexamethasone. The cells were impregnated into porous hydroxyapatite ceramics before subcutaneous implantation or placed within diffusion chambers for intraperitoneal implantation in athymic mice. All subcutaneous implants of cells in ceramics showed morphological evidence for the formation of bone tissue. In the diffusion chambers, it was found that both marrow and bone-derived fibroblastic cells cultured in the absence of dexamethasone generally produced fibrous tissue. When cultured in the continuous presence of dexamethasone, these cell populations produced similar osteogenic tissues with active osteoblasts, wide osteoid seams and mineralised tissue, with cartilage toward the interior of the chamber. The authors therefore refuted the claim by Haynesworth and co-workers that the diffusion chamber is an inappropriate system for demonstrating the differentiation potential of human osteogenic cell populations. They felt that by using

cultured cells instead of fresh marrow, the number of osteoprogenitor cells may be increased.

It would seem that within diffusion chambers the access of mesenchymal cells to growth and nutrient factors supplied by the vasculature or direct interaction with vascular cells are limited. Further investigations into the optimisation of the pre-implantation culture conditions and chamber configuration is needed before the system can form a significant bridge between *in vitro* experiments and *in vivo* implantation for examining bone-biomaterial interactions.

1.5.3 Implantation into bone in vivo

Early work on implants placed in bone was centered on histological examination of the tissues around the implants. One experimental approach was to insert implants into readily accessible anatomical sites such as the diaphyseal portion of the tibia in animals ranging from rats to sheep. Other researchers placed more emphasis on mimicking the clinical situation by choosing anatomical sites reflecting where implants were to be placed clinically. In the case of dental implants, this usually involves the extraction of teeth to create edentulous saddles in the jaws, into which implants, sometimes identical in size and shape to those used clinically, are placed. These studies tend to involve animals higher in the phylogenetic tree: dogs, pigs and primates (Table 1.3).

Table 1.3 *In vivo models for studying bone-biomaterial interactions*

Animal	Site	Reference
Rat	Tibia Femurs Cranium Subcutaneous tissue	Amir et al. (1989) Turner et al. (1989) Cabrini et al. (1993) Nakano (1991) Stevenson et al. (1994) van den Bos et al. (1995) Hosny & Sharawy (1985) Arvidson et al. (1991)
Rabbit	Iliac crest Mandible Tibia Femur Face Cranium	Hobkirk (1981) Hobkirk (1981) Albrektsson et al. (1985) Shimazaki & Mooney (1985) Burr et al. (1993) Kitsugi et al. (1995) Heikkila et al. (1993) Li (1993) Papagelopoulos et al. (1993) Tisdell et al. (1994) Goldberg et al. (1995) Wennerberg et al. (1996b) Ivanoff et al. (1997) Toriumi et al. (1991) Kleinschmidt et al. (1993)
Dog	Mandible Femoral condyles Femur Ileum Ulna Hip	Hollinger & Schmitz (1987); Pilliar et al. (1991b) Ohno et al. (1991) Lin et al. (1992) Weinlaender et al. (1992) Parr et al. (1992) Nelson et al. (1993) Soballe et al. (1991) Nimb et al. (1995) Bagambisa et al. (1993) Hetherington et al. (1995) Dalton & Cook (1995) Lew et al. (1994) Grundel et al. (1991) Szivek et al. (1994) Dowd et al. (1995)
Sheep	Tibia	Haider et al. (1993) Hur�� et al. (1996)
Pig	Edentulous jaws	Hale et al. (1991)
Monkeys	Extraction sockets Mandible	Anneroth et al. (1985) Ohta (1993) Akagawa et al. (1990)

The choice of animal species may affect the experimental outcome as the rate of bone apposition and speed of repair is known to differ between species (Simmons & Grynpas, 1990). Also, osteoblastic activity and the rate of bone turnover decreases with age at all locations. The age of the animals used for *in vivo* implantation experiments would therefore influence speed of the healing response (Simmons & Grynpas, 1990). Murai et al. (1996) placed identical titanium implants in young and mature rats and, not unexpectedly, found that the amount of bone formed along the implant in young rats was greater than in mature rats at 28 days after implantation.

Variability in the physiology of animals, even within the same species and age group, is inevitable. Spivak et al. (1990) attempted to overcome this difficulty by designing an implantable chamber containing multiple channels which can be lined by different materials with different surface textures to measure intramedullary bone ingrowth. A range of materials could then be tested in nearly identical conditions. Implants in the form of a titanium bone harvest chamber, as used by Brånemark for bone regeneration studies, have been used to contain biomaterials, for example, bone cement (Albrektsson, 1984a) and hydroxyapatite (Wang et al., 1994), to examine the process of bone regeneration in the presence of these materials.

The healing process can also be affected by the surgical technique used for inserting the implants and the initial stability of the implants following placement. Excessive heat generation during the cutting or drilling of bone as well as excessive motion during the early phases of healing can lead to the formation of a fibrous interface.

1.5.4 Techniques for assessing bone responses to implants in vivo

Following short and long term implantation, the implant, interface and surrounding tissues may be evaluated by a variety of techniques:

1.5.4.1 Radiography and microradiography

Radiography is generally applied in a clinical setting. It is valuable for an overall estimation of bone-implant interactions but the maximal resolution capacity, even of

controlled microradiographs, is in the order of 0.1mm. True tissue reactions are beyond the scope of radiography. Qualitative microradiography has been used to measure the amount of bone formed within bone harvest chambers in experiments on bone regeneration (Kalebo & Jacobsson, 1988).

1.5.4.2 Mechanical tests

The fixation of implants within bone has been assessed using a variety of mechanical tests. Modes of testing included push or pull out tests, tensile tests and removal torque measurements (Wennerberg et al., 1996c). The results of these tests are subject to the influence of many variables such as implant geometry, surface topography (Wennerberg et al., 1996c), surface chemistry (Larsson et al., 1996), initial fit (Carlsson et al., 1988; Maxian et al., 1994), and implant site, in addition to the type of implant material studied.

1.5.4.3 Ground sections for light microscopy

Materials for dental and orthopaedic implants including metals, ceramics and polymer or composites of the above have greater hardness than soft tissues. Resins are routinely used as embedding media to preserve the structural integrity of hard tissues and for holding implants in place during specimen preparation. The technique published by Donath and Breuner (1982) is widely adopted for producing ground sections for light microscopic examination of the bone-implant interface. It has been shown descriptively that bone can directly interface titanium implants (Hansson et al., 1983; Brånemark, 1983; Sisk et al., 1992), titanium alloy implants (Lum & Beirne, 1986; Lum et al., 1988), titanium plasma-sprayed implants (Listgarten et al., 1992; Schroeder et al., 1981), porous titanium implants (Pilliar et al., 1991a; Keller et al., 1987), hydroxyapatite-coated titanium implants (Cook et al., 1987; de Lange & Donath, 1989), titanium blade implants (Steflik et al., 1992b), and single crystal ceramic implants (Akagawa et al., 1986).

1.5.4.4 Histomorphometric methods

Histomorphometry involves microscopic measurements of histologic sections. Measurement of structurally visible or displayed objects or features is performed by

using eye-piece micrometers and eye-piece graticules or grids, with a specific geometry or pattern, covering the visible field of measurements. By point or linear intercept counting of microscopic structures falling on a grid pattern, i.e. relative values of area, perimeter or boundaries and the number of selected features may be obtained. The advantage is the opportunity to obtain qualitative and quantitative analyses of a section. In recent years, advances in computerised image analysis systems have meant a progress in morphometrical techniques. Computer-based systems, with video cameras as scanning devices, generate images converted into digital values in array of picture elements (pixels) and allow the assessment of area, intercept, perimeter, size and density values automatically or semi-automatically with suitable software. (Revell, 1983). However, the method can be limited by the ability to discriminate between structures, by section thickness and projection errors, by the method of calibration. Counting is performed on two-dimensional data. Sample handling, fixation, staining and sectioning are factors that must be properly controlled.

The parameter most commonly used for assessing the bone-implant interface is the percentage of the perimeter of an implant in contact with mineralised bone in longitudinal ground sections observed with light microscopy (Weinlaender et al., 1992; Cabrini et al., 1993; Lew et al., 1994; Hetherington et al., 1995; Nimb et al., 1995; Huré et al., 1996; Wennerberg et al., 1996a; Ivanoff et al., 1997). Such measurements still rely on the human observer to distinguish between what is and is not direct contact between implant and bone. In addition to measurement of bone contact lengths, the area of bone formed within the threaded portions of endosseous implants was routinely measured by the Gothenburg group led by Albrektsson (Johansson et al., 1990; Gottlander & Albrektsson, 1991; Wennerberg et al., 1996c). Members of the group have looked into technical factors which could affect the outcome of histomorphometrical quantifications of the bone-implant interface in ground sections. Section thickness and cutting directions were investigated (Johansson and Morberg, 1995a, 1995b). They concluded that sections over 30µm thick could result in overestimation of the bony contact. In their rabbit tibia model, 25% more contact lengths were found when the implants were cut in the longitudinal direction of the tibia than those cut in the transverse direction. This was thought to be due to the variation in the mode of loading of transcortical implants in the

rabbit femur model. Barzilay et al. (1996) compared the use of decalcified thin sections (4µm) and ground sections (30 - 150µm) and found no significant differences between the two histologic techniques in the bone:implant interface ratio which either technique provided.

The type of implant material may also have an effect on the measurement procedure. Evans et al. (1996) have found that interpretation of the percentage of bone-implant contact was more difficult when evaluating HA-coated implants as compared to titanium implants since they sometimes experienced difficulty in distinguishing the HA-bone interface. Also to be considered is the site of implantation. Percentage figures of bone-implant contact are likely to be higher for implants or parts of implants residing in cortical rather than cancellous bone (Hipp & Brunski, 1987). Johansson et al. (1990) chose to measure bone-implant contact of threaded implants where they cross the cortical region of the tibia in their rabbit model for the reason that there was no cancellous bone in the marrow cavity where part of the implants were sited.

1.5.4.5 Tracer methods

Newly formed bone may be labelled with the aid of a tracer. The tracer may be detected in the light microscope due to fluorescing properties or with the aid of a radiation detector due to radioactivity.

• *Fluorochrome labelling*

Tetracyclines, alizarins, calceins, hematoporphyrins and xylenol orange are examples of non-radioactive, *in vivo* tracers of bone formation, where tetracyclines are the most frequently and widely used bone markers. They have common properties such as binding to calcium during mineralisation or demineralisation of bone and they fluoresce under UV-illumination. Tetracyclines bind to mineral in two ways, firstly, to the bone surface mineral front at the time of peak blood level in a reversible manner and secondly by trapping of new mineral deposited after the peak blood perfusion. The fluorochromes, usually tetracyclines, may be administered in sequences at regular time intervals yielding bands of labelled new bone or continuously during the the healing

period. Polyfluorochrome labelling may also be performed, by administering different tracers in specific schedules. Goldberg et al. (1995) used fluorochrome uptake to demonstrate the remodeling of bone on the surface of grit-blasted titanium implants in rabbit femurs. Haider et al. (1993) compared external and internal drill cooling methods for the preparation of holes to receive implants. By means of polyfluorochrome sequential labeling, they found that patterns of new bone formation in cortical and cancellous bone differed according to the cooling method used.

- ***Radionuclide labelling***

Radioisotope labelling has been used in qualitative and quantitative studies of bone healing. The detector systems generally used in the analysis of bone repair are photographic emulsions. Organic matrix formation may be studied by tritiated amino acids, as ^3H -glycine or ^3H -proline in collagen synthesis analysis and ^{35}S -sulphate in proteoglycan or ground substance formation. Proliferative cell activity in fracture repair may be assessed by ^3H -thymidine, labelling DNA synthesis.

An elegant study by Clokie & Warshawsky (1995) employed ^3H -proline labelling to reveal the pattern of new bone formation during six weeks following the implantation of titanium implants in rat tibia. Radiolabelled new bone was deposited only on previously existing bone and extended towards the available space, leading to the suggestion that titanium does not influence the direction of bone growth in threaded implants but provides an inert template around which normal bone healing takes place.

1.5.4.6 Scanning Electron Microscopy

Scanning electron microscopy (SEM) is a useful tool for observing the topography of implant surfaces either before or after implantation (Boyde, 1991). It is extensively used in secondary electron imaging mode for visualisation of the morphology of cells and extracellular matrix on implant materials. Boyde (1991) has warned against artefacts which are liable to occur at the junction between tissue and implants because of their differential shrinkages during specimen preparation. In fact, mechanical separation by fracturing is often necessary to expose the implant-tissue interface.

Back-scattered electron (BSE) images can help to distinguish bone with different mineral densities in addition to offering topographical contrast. When the surface of the material is absolutely flat, or has been embedded, cut and polished flat, and viewed normally to the electron beam, the BSE image would be density-dependent. Nanci et al. (1994) have used this method to examine resin embedded sections of the bone adjacent to screw-shaped titanium implants in rat tibia and to visualise the distribution of silver-enhanced protein A-gold immunolabels for a series of bone matrix proteins in such sections.

1.5.4.7 Transmission electron microscopy

A major problem of preparing specimens for ultrastructural examination of the bone-implant interface is the hardness of the tissue itself and that of the implant material. This is especially true in the preparation of thin sections for ultrastructural studies. Many published protocols involved removal of the implants from the bone prior to or after embedding. The techniques used to overcome the problem of sectioning hard implants are:

- ***Decalcification of the bone and ‘careful’ removal of the implant***, the remaining bone tissue was then embedded and sectioned. (Barzilay et al., 1996; Murai et al., 1996).

- ***Fracturing the implant from the bone*** (with or without decalcification) following embedding in resin. Nanci et al. (1994) softened the embedding resin by heating the specimen in an oven at 125°C, the block was then prised apart at a score-line made along the middle of the implant. Using this approach, the screw generally remained attached to one of the fractured faces.

- ***Cryofracture***. Steflik et al. (1994) cut 1mm thick sections of the fixed, undecalcified, resin embedded specimens and placed them into liquid nitrogen followed by immediate immersion into boiling water to separate the implant from the bone.

•**Electrodissolution.** Bjursten et al. (1990) embedded implants and their surrounding tissue in plastic and removed the bulk of the metal by electrochemical dissolution (electropolishing) to facilitate preparation of ultrathin sections for TEM. Garvey & Bizios (1995) removed the metal substrates using an electrolytic dissolution technique and a 7% NaCl solution. Ericson et al. (1991) found that the electropolishing method induced serious artefacts to sections of the bone-titanium interface in the form of demineralisation of the interface zone and infiltration of Ti ions.

•**Coating plastic substrate with a metal film.** Several research groups have coated plastic implants with titanium and investigated the ultrastructural interface between bone and titanium (Listgarten et al., 1992; Linder et al., 1983; Qu et al., 1996). This technique has the advantage that the sections contain an intact interface between the tissue and the thin titanium coating layer. There is however, uncertainty as to whether the surface properties of such a film can represent those of solid titanium implants used clinically.

1.5.4.8 Ultrastructural features

The bone-titanium interface at the electron microscope level has been described by many investigators in models ranging from rat femur, rabbit tibia to dog mandible. Linder et al. (1983) and Albrektsson and Hansson (1986) reported that bone made contact with the titanium directly and that an amorphous layer 20-40nm thick was present between the mineralised bone and titanium or between the collagen fibres in the unmineralised matrix and the titanium. Steflik et al. (1992a) found that the interface varies from a densely mineralised matrix to zones of unmineralised tissue. TEM showed that much of the implant surface was apposed directly by highly mineralised bone. They described mineralised thick collagen fibre matrix close to the implant surface separated from the implant by a mineralised fine fibrillar zone. In some areas a 20nm electron dense deposit separated the implant from the mineralised thick matrix. Many unmineralised areas were observed. Fibroblastic cells and osteoblasts were found at these locations. A layer of amorphous material of low electron density was also described. This 100-300nm afibrillar layer separated the calcified bone from the implant surface. They thought that these observations were consistent with early work by Linder

et al. (1983) as well as Albrektsson & Hansson (1986) although the dimensions of the amorphous afibrillar layer differed between studies. Linder et al. (1983) reported a 20 to 50nm gap between the closest collagen fibres and the oxide surface of titanium (120 - 250nm coating on polycarbonate in this study) and further characterised this layer as consisting of a hyaluronidase and chondroitinase sensitive material - proteoglycans. Albrektsson & Hansson (1986) made a similar conclusion about the 20-40nm amorphous layer found in their model. On the other hand, Sennerby et al. (1992) described the amorphous layer situated between the mineralised bone and titanium implants as being 100-200nm thick. In addition, they reported that in some areas mineralised bone reached close to the implant surface and formed a dense osmiophilic lamina limitans-like line. This layer was about 100nm wide and was often in continuity with the lamina limitans lining those osteocyte lacunae or canaliculi which reached the implant surface. It was thought to be an accretion of organic material at sites where calcification starts or ends. A study by Nanci et al. (1994) indicated that this 'lamina limitans' contains osteopontin and α_5 -glycoprotein. However, they did not describe any amorphous layer. They reported an electron dense layer separating unmineralised collagen or mineralised bone matrix from the implant surface; cement lines in the bone surrounding the implant; bone immediately adjacent to the electron dense areas at the interface; and patches of organic material with a granular or reticular appearance found throughout the mineralised bone matrix. Studies by Listgarten et al. (1992) and Chehroudi et al. (1992) also did not find any electron dense deposit between the collagen fibre matrix of the bone and the implant.

Sennerby (1991) tried to attribute the difference in thickness of the amorphous zone to differences in surface and bulk properties between the coated plastic plugs used in the early studies and the solid titanium used in his. However, the titanium used by Linder et al. (1983) was solid. Murai et al. (1996) proposed a different explanation: different animal species. They went further to say that the difference in the bone-titanium interface between the above studies may be due to the nature of the bone where titanium was inserted. In their investigation, as well as those of Linder et al. (1983), and Sennerby et al. (1992), the implants were inserted in the tibiae. Where titanium made contact with the bone marrow of the tibial metaphyses, the bone formed made direct contact with the implant via an amorphous zone. On the other hand, Listgarten et al.

(1992) inserted titanium into the compact bone of the mandible which direct contact with the titanium via a collagen fibril layer.

1.5.4.9 Enzyme histochemistry and immunocytochemical methods

Morphological techniques for studying the nature of the bone-implant interface can be complemented by histochemical and immunohistochemical examination of the expression of enzymes associated with bone formation and bone resorption as well as various bone matrix components in the tissues adjacent to implants.

- ***Technical considerations***

The presence of hard implants in calcified bone tissue poses specific problems in the immunodetection of bone-forming cells in peri-implant tissues. Previously published techniques for immunocytochemical detection of bone cells capable of producing matrix proteins were either performed on frozen sections or involved fixation of the specimens followed by decalcification. They were then processed and embedded in paraffin for immunodetection of the proteins. Such methods are often not applicable to bone tissues containing hard implants. Hillman et al. (1991) described the use of a light cured embedding resin (Technovit 7200 VLC) for the localisation of enzymes and antigens in the soft and hard tissues around implants at the light microscopic level.

According to Muda et al. (1992) most methyl methacrylate based embedding protocols, which are widely used in bone histology, are not generally suited for enzyme cytochemistry although some enzymes like acid phosphatase, can be successfully demonstrated when highly abundant. Conversely, glycol methacrylate based protocols offer excellent preservation of both morphology and most enzyme activities but are generally unsatisfactory as standard protocols for immunocytochemical studies. They proposed a protocol which combined freeze-drying of tissues and low-temperature embedding in glycol methacrylate to permit combined enzyme cytochemistry and immunostaining on the same tissue block. Alkaline phosphatase, tartrate-resistant acid phosphatase, collagen types I, and III and laminin were demonstrated on foetal rat bone rudiments.

- ***Alkaline phosphatase and acid phosphatase***

There are two main enzymatic activities which are searched for when studying the histochemical characteristics of bone: alkaline and acid phosphatase. Alkaline phosphatase is produced by osteoblasts and is involved in the mineralisation process. Two forms of acid phosphatase are present in bone. One of the two isoenzymes is resistant to tartrate inhibition and particularly abundant in osteoclasts. Piatelli et al. (1995) described the distribution of alkaline phosphatase (ALP) and acid phosphatase (ACP) in the tissues adjacent to smooth screw-shaped threaded titanium implants in rabbit tibia. Positive staining for ALP was found in osteoblasts surrounding islands of soft tissue or woven bone near the implant surface during the first three weeks after implantation, corresponding to new bone formation originating from the periosteal and endosteal surfaces. Few cells with weak staining for ACP were detected up to two months. A later increase in ACP activity was noted and attributed to the bone remodelling process.

- ***Bone matrix proteins***

Nanci et al. (1994) performed extensive immunocytochemical characterisations of the bone-titanium interface using the protein A-gold immunolabelling technique. Transmission electron microscopy and scanning electron microscopy in backscattered mode were used to observe the labelling. A panel of antibodies was used to identify non-collagenous bone proteins including: osteopontin, osteocalcin, α_2 HS-glycoprotein, albumin and fibronectin. Part of the implant surface was covered with a layer rich in osteopontin and α_2 HS-glycoprotein. Osteonectin, fibronectin and albumin show no preferential accumulation at the bone implant interface.

The future direction of histological examination of tissues around implants is heading towards the demonstration of genetic expression. The distribution of mRNA for specific proteins within the matrix formed on the biomaterials has been visualised using *in situ* hybridisation. Casser-Bette et al. (1990) have applied the technique to detect osteocalcin mRNA in frozen sections of MC3T3-E1 within a three dimensional collagen matrix. Zhou et al. (1994) used a titanium chamber to harvest bone for examination

using *in situ* hybridisation to show the temporal and spatial expression of mRNA for procollagen, alkaline phosphatase, osteopontin, and bone Gla protein during bone regeneration *in vivo*. A further technical breakthrough is needed before this technique can be extended to specimens in which the implant and hard-tissue interface is preserved.

1.5.5 Scope of *in vivo* experimentation

The factors which determine tissue responses to endosseous implants include implant material composition, implant design characteristics, implant surface characteristics, the surgical technique, state of the host bed and loading. All of these factors have been examined to a greater or lesser extent in whole animal models and it is outside the scope of this literature review to present details of the findings. The table below provides some useful references.

Table 1.4 *In vivo studies of tissue response to endosseous implants*

Factors studied	References
Implant composition metallic: Ti sputter-coated Ta, Nb, Ti Zr calcium phosphates and hydroxyapatite bioactive glass and glass ceramics	Albrektsson & Hansson (1986) Albrektsson (1984b) Johansson et al. (1990) Albrektsson et al. (1985) Nimb et al. (1995) Tisdell et al. (1994) Szivek et al. (1994) Nelson et al. (1993) Burr et al. (1993) Nimb et al. (1995) Heikkila et al. (1993) Nakano (1991) Soballe et al. (1991)
Implant design	Ivanoff et al. (1997) Steflik et al. (1996) Parr et al. (1992) Pilliar et al. (1991b)
Implant surface characteristics	Wennerberg et al. (1996b) Huré et al. (1996) Hartwig et al. (1995) Goldberg et al. (1995)
Surgical technique	Barzilay et al. (1996) Lundgren et al. (1996) Haider et al. (1993) Moy et al. (1993) Frodel et al. (1993) Akagawa et al. (1990)
Loading conditions	Evans et al. (1996) Akagawa et al. (1986)

1.5.6 Phases of healing following *in vivo* implantation

The surgical procedures to create space for implant insertion involve mechanical and possibly thermal damage to intercellular substances, cells and vessels. Secondary effects are caused by impaired circulation, exudation and haemorrhage (Gross et al., 1988). The exact distance over which such damage will occur is not known precisely and probably depends on the particulars of the anatomical site, animal model, implantation technique, etc. The time course of events has been described in three stages:

The first stage of reaction comprises the formation of a haematoma and a circulatory change due to the liberation of a cascade of chemical products, which, functioning as mediators, act on vessels and surviving cells and attract cells from the blood and surrounding tissue. There will also be local changes in pH and oxygen tension (Hench & Ethridge, 1982). Inflammatory mediators as well as growth factors capable of stimulating cells involved in subsequent healing are released.

The second stage is characterised by organisation tissue, regeneration and repair. There is formation of new local connective tissue, new capillaries, new supportive cells. The duration and the number of the processes involved are related to the amount of damage and the geometry of the implantation site. Primary immobilisation of the implant will exclude repeated mechanical damage. The function of cells in the implantation bed and the extracellular products can be affected by the soluble chemical products (ions) and soluble or insoluble particles derived from the implant as well as by the biomechanical influence of the implant itself. The interfaces of bone in animal experimental models with different implant materials have included soft tissue with few inflammatory cells, marrow, non-mineralised bone (osteoid tissue) and bone (woven bone, lamellar bone).

The third stage comprises wound maturation via remodelling which is an ongoing process in bone and is affected by the transfer of strain via the interface between implant and tissue.

1.5.7 The early bone-implant interface

Gross et al. (1991) commented that the early phase up to 1 week post-operatively has not been sufficiently investigated by research groups working in the field of glass ceramics and other implant materials. In one of their studies, in which the behaviour of the blood clot and the subsequent cellular reaction were reported in a combined scanning electron microscopy, light microscopy and histochemical (acid phosphatase) investigation, it was found that the first cells colonising the surface of bone-bonding and non-bonding glass ceramics were macrophages. These macrophages were said to settle for a longer time on the surface of the non-bonding glass ceramic than on the bone-bonding glass ceramic. The cause of the macrophages disappearing from the surface was not clear. After the macrophages had disappeared from the bone-bonding glass-ceramic, bone-forming cells appeared and developed extracellular matrix, matrix vesicles, leading to the primary mineralisation of bone.

Sennerby (1991) described the histology of the early bone-titanium implant interface in a rabbit femur model. Prior to the establishment of contact of mineralised bone with the implant surface a variety of cell types was observed at the surface of the implant during the first two weeks after implantation. Red blood cells and macrophages were present in the small gap between the implant and the cut bone surface. Multinucleated giant cells (MGC) feature prominently in the description of cells found on the implant surface. The nature of a large number of cells with large rounded nuclei, prominent nucleoli and extensive cytoplasm, designated as mesenchymal cells, was not established. Two weeks after implantation, remodelling of the old bone in the cortex area was observed. Blood cells and bone fragments had disappeared from the space between the implant and the cut bone. MGCs were still present. Newly formed woven bone, or acellular fibrous tissue occupied the space. In the endosteal area, newly formed trabecular bone was observed.

1.6 Statement of the problem

With the proven clinical success of endosseous dental implants (Albrektsson & Sennerby, 1991), one could almost argue that there is no need for further basic science studies on the issue of osseointegration. However, when current clinical practice is examined further, there are two areas of great interest to the clinician who wants to extend the application of dental implants and optimise the treatment process. The first is the widely accepted guideline of leaving implants buried and/or unloaded for three months in the mandible and six months in the maxilla to permit healing. The question often asked is: Is there a way of accelerating the process of osseointegration? The second area of concern is in patients whose bone quality is poor and fixtures are more likely to fail to integrate at an early stage. The question here is: Is there a way of promoting new bone formation around implants? Both questions concern the early stages leading up to the formation of direct contact between bone and the implant interface but the majority of *in vivo* experimental work on dental implants focus on the outcome at several weeks or months after implant surgery. There is also some controversy over whether bone forms on implants or towards implants and whether some materials play a permissive role in the healing process with others inducing the formation of new bone on their surface.

In vivo animal work is well suited to empirical studies for measuring the outcome of different or new treatment protocols using models which are analogous to the clinical situation but it is less often used for unravelling the biological processes underlying the bone healing response to implant surgery. The difficulty lies in the complexity of the physiology of *in vivo* systems and the interactions between different cellular and molecular elements. At the other end of the scale, *in vitro* models have capitalised on the advances in cell and molecular biology and permit studies of individual cell types under more controlled environments. However, we require answers to the questions of which cells take part and what roles they play in the healing process, before meaningful and clinically relevant *in vitro* assays can be made. Cell culture studies have also by default, sidestepped the relationship and interactions between different cell types involved in the healing process.

The initial events leading up to the formation of tissue-implant interface have not been closely studied. The original aim of the research presented in this thesis was to look into the dynamic behaviour of cells as they first come into contact with implant surfaces. Chapter 2 in this thesis describes a time-lapse video experiment recording the progressive, dynamic changes in the morphology of a fibroblast cell line as cell attachment took place on a glass-ceramic material.

Subsequent to the first set of experiments, it was felt that the early tissue-implant interactions involve a range of cell types and that a wide gap exists between what can be studied *in vitro* using cell and tissue cultures versus *in vivo* implantation experiments. In particular, implants placed in bone are interacting with a complex tissue involving not just the bone forming cells but many other cellular elements as well as the bone matrix. The normal structural organisation of its matrix is virtually lost in *in vitro* cell culture systems. Moreover, when bone is wounded, as in the preparation of a bone site for implants or following a fracture, it reacts as an organ in which the vascular, marrow, periosteal and bone tissues all contribute to the healing process. The premise was that if all these elements could be brought together in a culture system that mimics the *in vivo* response of bone to implant insertion, it may bridge part of the gap between *in vitro* cell and tissue cultures and *in vivo* studies for examining early bone responses to implant materials. Having reviewed the literature, it seems that *in vitro* cultivation of bone is limited by the absence of vascularisation. Bone organ cultures *in vitro* have slow rates of bone formation and *in vivo* diffusion chamber studies where implant materials were placed in the chambers with potentially bone-forming cells have inconsistent results in terms of actual bone formation. Effort was therefore directed towards the characterisation of a bone organ culture technique based on grafting bone on the chorioallantoic membrane of developing chick eggs, in which a blood supply to the bone in culture was rapidly established. The assessment of this model is reported in Chapter 3. The CAM graft technique was then applied in conjunction with the insertion of implant materials into the bone being cultured. The materials chosen for evaluating the model were commercially pure titanium, generally thought to be inert, and a glass-ceramic, thought to be 'bioactive'. The general hypothesis is that a difference exists in the healing response to the two materials within the new culture model. In Chapter 4, the healing

response within the bone graft containing implant materials at different time intervals are described and a quantitative evaluation of bone formation around the implants, together with histochemical, immunohistochemical and ultrastructural examination of the tissues surrounding the implants are presented.

Chapter 5 is a report on a set of experiments performed to assess the suitability of the CAM bone organ culture model for assessing growth factor effects on the healing response to implants. The result of localised delivery of basic fibroblast growth factor, one of the many growth factors present in bone which may contribute to bone wound healing, on the tissues within CAM cultured chick embryonic femurs, is presented and discussed.

The final chapter provides a general appraisal of this new bone organ culture model in terms of its advantages and drawbacks. Its role is discussed in the context of the experimental strategies for the evaluation of bone-biomaterial interactions and suggestions for future work are made.

2. Dynamic recording of short-term cell behaviour on an implant surface

2.1 Introduction

Biocompatibility testing *in vitro* often involves the detection of cell damage and death, i.e. cytotoxicity (Doillon and Cameron, 1990; Haustveit et al., 1984; Johnson et al., 1985; Rae, 1986). Indeed, the International Standards Organization's (1989) recommendation on test methods to assess biocompatibility of implants for bone and joint surgery includes cytotoxicity and mutagenicity tests. Whilst such screening is useful to detect overt adverse effects of a test material, other less dramatic expressions of incompatibility may be overlooked. The sequence of events during the interaction of cells with implant surfaces include:

1. Attachment of fibronectin and other substances affecting cell adhesion to biomaterials.
2. Initial cell attachment.
3. Cell spreading.
4. Cell growth on the surface or in the interstices of the material.
5. Cell differentiation and expression of the phenotype.
6. Post-implantation losses and changes in phenotype due to *in vivo* stresses.

The rate of growth, proliferation and differentiation of cells on a material may be dependent on successful initial attachment and spreading of the cells on the surface of the substratum. In this respect, the initial and short-term responses of cells to an implant material *in vitro* may provide valuable indicators of the long-term biocompatibility *in vivo*.

Although *in vitro* morphological responses of various cell types to different implant materials have been widely reported, such analyses are based almost without exception on fixed specimens examined by various combinations of light microscopy, scanning and transmission electron microscopy (Sharefkin and Watkins, 1986; Naji and Harmand, 1991; Jansen et al., 1991; Könönen et al., 1992; Revel et al., 1974).

This chapter describes a dynamic analysis of early behaviour of fibroblasts cultured on a glass-ceramic material using time-lapse video microscopy (TLV). Time-lapse video recording offers a number of advantages over analysis of fixed preparations. *Firstly*, it permits the continuous observation of a population of living cells exposed to the substratum, in contrast to observation of a fixed and stained preparation which at best is simply a 'freeze-frame' record. *Secondly*, it allows qualitative assessment of changes in the morphology and behaviour of individual cells. *Thirdly*, quantitative assessment of such changes in relation to time and the total population under observation can be made. This method of analysis can provide unique insights into the initial and dynamic interactions between connective tissue cells and a potential implant material and, as such, provides a valuable means of assessing biocompatibility before embarking on longer and more expensive testing strategies.

The experiment involved a common murine fibroblastic cell line and, using a combination of TLV and scanning electron microscopy, the behaviour of dispersed cells upon initial contact and attachment to a substratum consisting of a potential implant material was monitored. This has been facilitated by the inherent semi-transparency of the material selected, which permits visualisation of the living cells. A sequence of cell phenotypes can be distinguished, each reflecting the behavioural activity of the cell *at that time*. Morphometric analysis of cells populations as they pass through this sequence has been used to assess the short-term cellular response to the substratum.

2.2 Materials and methods

2.2.1 Substratum preparation

The substratum employed for this study was a translucent glass-ceramic material, one of a group called Apoceram, developed at Imperial College, University of London, for bioengineering applications (Rawlings, 1993). Glass-ceramics are polycrystalline fine-grained materials formed when glasses of suitable composition are subjected to a carefully controlled heat-treatment regime and thereby undergo controlled crystallisation. For this experiment, a cast and heat-treated form of Apoceram with CP31 composition was used (Table 2.1). Its phase proportions are: Apatite 44.3%, Wollastonite 39.9%,

Residual glass 15.8%). Transcortical implantation of Apoceram in rabbit tibiae produced interfacial shear strengths in push-out tests comparable to those of commercially pure titanium (Wolfe, 1990).

Component	Normalised Mass % CP31
Na ₂ O	2.78
MgO	10.12
CaO	34.27
Al ₂ O ₃	10.12
SiO ₂	25.60
P ₂ O ₅	14.45
CaF ₂	2.65

Table 2.1 *Composition of Apoceram CP31*

0.5mm thick sections of Apoceram were cut from a cast block using a precision wire saw (Laser Technology, California, U.S.A.). These were then serially ground with four grades of silicon carbide coated paper (P240, 400, 800, 1200) and polished with 5µm and then 1µm diamond compound (Hyprez 5 star; Engis Ltd., Kent, U.K.) on a Metaserv rotary polishing machine (Buehler Ltd., Coventry, U.K.). The samples were soaked overnight in a 1:10 aqueous dilution of 7X detergent (ICN Flow, Irvine, Scotland) and rinsed in running tap water for two hours. This was followed by ultrasonic cleaning for 3-5 minutes in deionised water, a 30 minutes wash in 70% ethanol, after which the samples were heat-sterilised in an autoclave.

2.2.2 Cell culture

3T3 fibroblasts were maintained in alpha modification of Eagle's minimal essential medium (αMEM, ICN Flow, U.K.) + 10% foetal bovine serum (FBS, ICN Flow, U.K.) + Penicillin(50U/ml)/Streptomycin(50µg/ml) (Gibco Ltd., U.K.). When confluence was reached, the cells were dissociated from the culture flask by incubation with 0.05%(w/v) trypsin- 0.02%(w/v) EDTA (Gibco Ltd., U.K.) at 37°C for 4 minutes. The dissociated cells were washed, centrifuged and resuspended in αMEM + 10% FBS. Concentration of the cell suspension was calculated using a haemocytometer (Improved Neubauer) and adjusted to 1.5×10^5 /ml. 5ml of the suspension was added to a 25cm² standard treated polystyrene tissue culture flask (Grenier Labortechnik, Germany) containing the glass-ceramic

specimen. 5ml of the cells suspension was put in a separate, empty flask. Tissue culture polystyrene (TCP), the material of the flask acted as a control substratum.

2.2.3 Video microscopy

The cell cultures were viewed using an Olympus IMT-2 inverted phase contrast microscope fitted with a high resolution (330TVLines) charge coupled device (CCD) colour video camera (JVC model TK-870U). Time-lapse video recordings were made at 2 second intervals using a VHS recorder (JVC model BR-9000 UEK). Three-hour recordings of cells plated onto the glass-ceramic material and the control tissue culture polystyrene and maintained at 37°C, were taken separately and repeated twice. The size of each field examined was 57µm by 45µm. The average cell number per field analysed was 15 (range 10-20).

2.2.4 Scanning electron microscopy (SEM)

Specimens for SEM were fixed in 2% glutaraldehyde in 0.1M sodium cacodylate buffer, pH 7.2, followed by 1% osmium cacodylate in 0.1M cacodylate buffer. The specimens were then dehydrated through a graded series of acetone, critical point dried with CO₂ and gold sputter-coated for examination in an Hitachi S800 field emission scanning electron microscope.

2.3 Results

2.3.1 Attachment and cell morphology

From the TLV recordings, a highly invariant sequence of events could be defined. On sedimentation onto the substratum from suspension, cells exhibited many bleb-like protrusions which were constantly in motion (the intensity of blebbing varied from cell to cell). At the point at which attachment to the substratum occurred, blebbing largely ceased and, upon withdrawal of the blebs, the cell acquired a 'smoother' profile. Initial attachment was followed by a spreading stage during which extension of the cytoplasm along the substratum proceeded with a concomitant flattening of the central mass. The margin of the

spreading cell was invariably active. It was characterised by filopodia and lamellipodia being extended and withdrawn, giving rise to the appearance of ruffles. Typically, spreading took place in a radially symmetrical fashion but where a distinct leading edge became established, then the cell became polarised, both in its spreading and in its subsequent locomotion. Upon polarisation, the degree and rate of ruffling became reduced at non-motile regions of the cell margin. This general pattern of cell behaviour was observable in cell populations cultured on both Apoceram and TCP, although with important quantitative differences.

2.3.2 Changes in cell phenotypes

A number of behavioural phenotypes was defined which, in sequence, exemplify the changes in morphology displayed by a cell as it attaches and adheres to a substratum. High resolution images of key phenotypes, generated by SEM, are shown in Fig. 2.1. The major phenotypes are:

- a)* the onset of visible activity
- b)* blebbing of the cell surface (Fig. 2.1a)
- c)* border ruffling (Fig. 2.1b)
- d)* polarisation, defined as the cell being 50% longer in its longest dimension than in its broadest dimension (Fig. 2.1c)
- e)* onset of crawling (Fig. 2.1c inset)
- f)* cell appearing well-spread and stable (Fig. 2.1d)

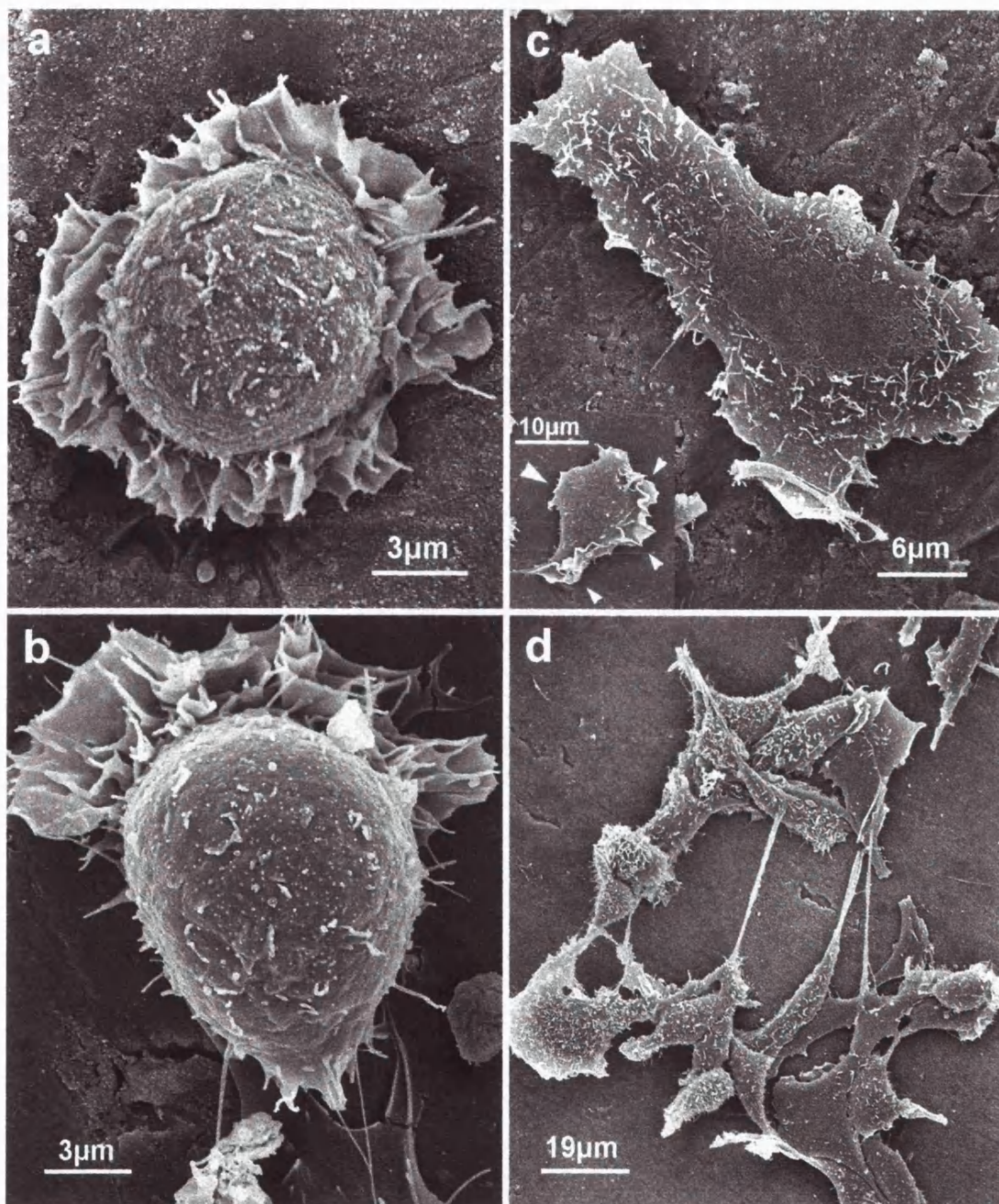


Figure 2.1 a. SEM of a round 3T3 fibroblast on Apoceram. Surface blebs can be seen. Cytoplasmic extensions appear on the periphery as the cell begins to spread. b. The leading edge of this apparently elongating cell shows layers of ruffling lamellipodia. c. SEM of a polarised and flattened 3T3 fibroblast. Inset. The large arrow indicates the most likely direction of migration of this fibroblast. Lamellipodia are seen extending from its leading edge (small arrows). d. The fibroblasts are well spread. Long thin filopodia appear to bridge some cells.

From the TLV recordings, the position of every cell within a recording field was mapped. Each cell was followed through the duration of the recording in order to categorise the state of the cell, according to phenotype, at 15 minute intervals. The collated results for each of the cell populations (i.e. on TCP and on Apoceram) are presented in Figures 2.2 and 2.3.

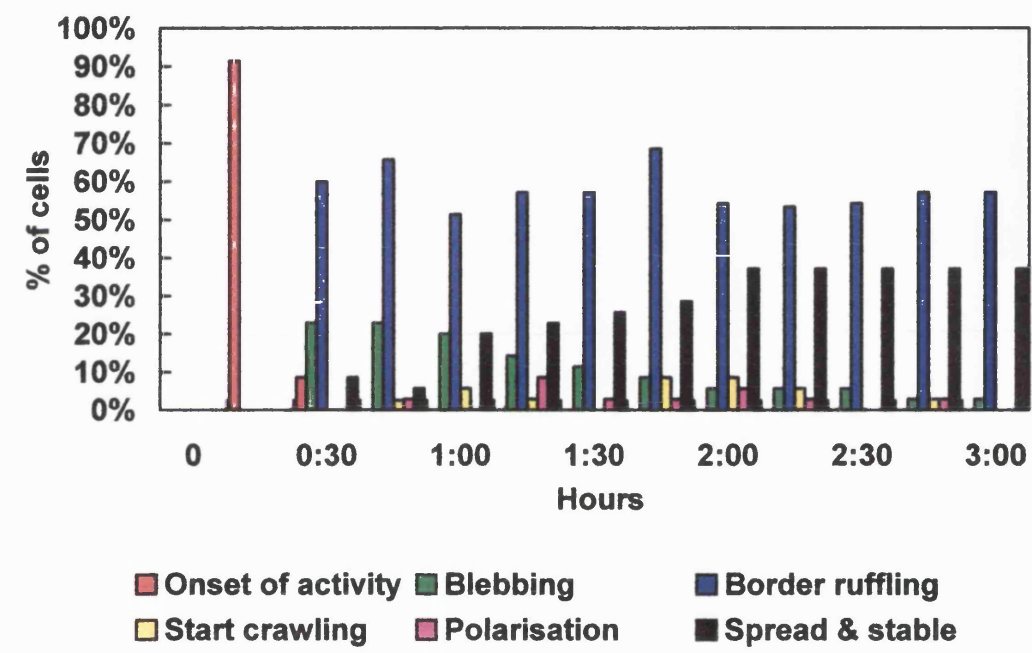


Figure 2.2 Distribution of behavioural phenotypes with time on tissue culture polystyrene

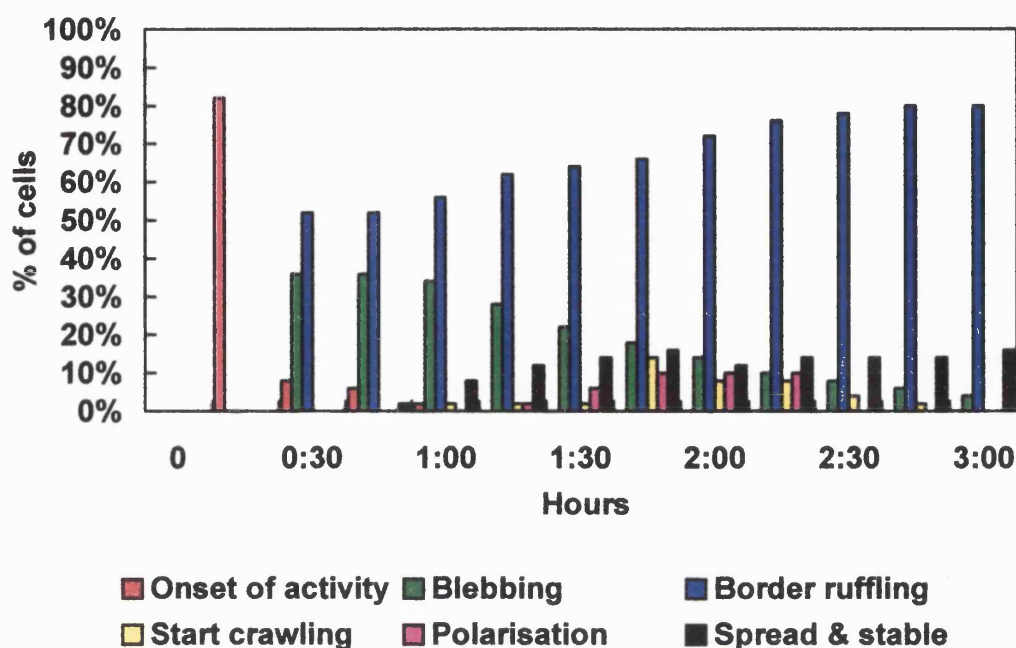


Figure 2.3 *Distribution of behavioural phenotypes with time on Apoceram*

Figures 2.2 and 2.3 reveal that on both substrata at 15 minutes post-plating, the majority of the cells are just contacting the substratum having sedimented out of suspension. In marked contrast, in both populations at 30 minutes, the majority of cells either display surface blebbing or have moved on to display ruffling. Subsequently, although both populations show the same progression, they do so at different rates. Thus, on TCP, the first spread and stable cells are seen at 30 minutes and both polarised and locomotory phenotypes are first observed at 45 minutes. On Apoceram, blebbing continues for longer, such that even at 1 hour 45 minutes, almost 20% of the cells display this phenotype (TCP controls, less than 10%). On the glass-ceramic, the first 'spread and stable' cells are only distinguishable at 45 minutes, the first locomotory cells at 1 hour and the first polarised cells at 1 hour 45 minutes. Clearly, there is a relative retardation of the behaviour pattern of the cells upon the glass-ceramic substratum. A further picture emerges from detailed analysis of the activity of the cell margin.

Even within the relatively short time window employed in this study a progression in behaviour can be seen. Figure 2.4 shows examples of tracings of cells obtained from individual frames on the video recordings at 15, 30 minutes, 1, 2 and 3 hours.

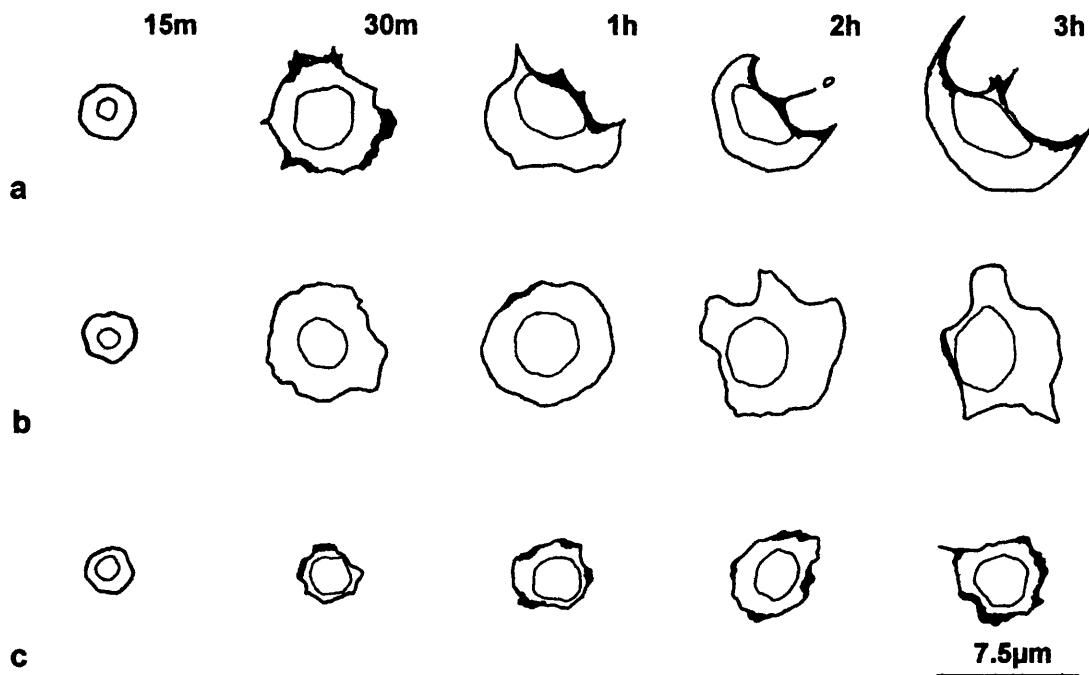


Figure 2.4 Tracings of cells seen through the phase-contrast microscope, recorded by the time-lapse video at 15, 30 min, 1, 2 and 3h. *a. Progression from a rounded morphology to a spread cell which later exhibits crawling. b. This cell has spread and remained stationary with little ruffling activity. c. Constant ruffling of a large proportion of the cell margin was observed on this cell throughout the recording period.*

2.3.3 Cell Ruffling Activity

The activity of the cell margin will reflect the functional state of the cytoplasm at that point, in terms of adherence to the substratum. Well-spread and flattened margins reflect stable cell/substratum adhesions whereas ruffled margins indicate unstable cell/substratum adhesions and reflect movement of the cytoplasm at that point on the margin. Marginal ruffling can therefore be a sensitive indicator of cell/substratum

interactions. To investigate this further, from the TLV recordings, cells were individually analysed for margin activity at 1, 2 and 3 hours post-plating using a method according to Bell (1978). The margins of selected cells were proportionately scored as being 'ruffled' (i.e. non-adherent and motile) or 'quiescent' (i.e. adherent, non-motile). Ruffled and quiescent sites are typically illustrated, using SEM, in Fig. 2.5. Using a transparent overlay on the monitor screen, the margin of a cell was divided into eighteen sectors each of which was individually scored and then summed on a per cell basis (Fig. 2.5). The resultant data were plotted as scatter diagrams (Figs. 2.6 to 2.11).

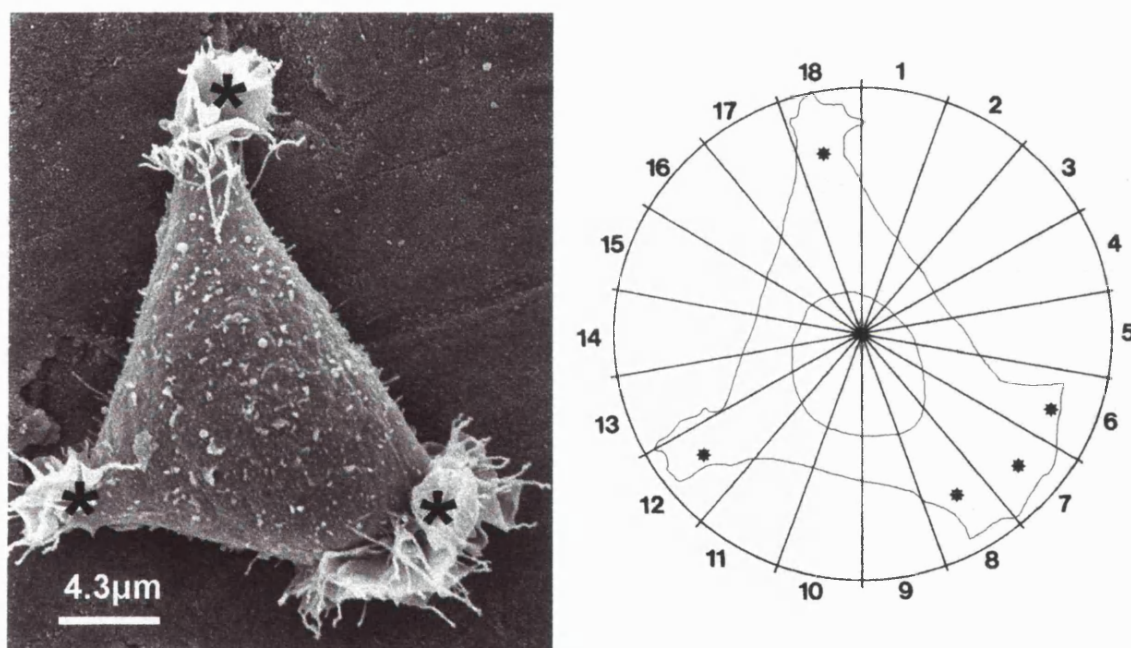


Figure 2.5 *Left: The margin of this fibroblast has three ruffling sites (asterisks); the remainder of the cell margin appears quiescent. Right: A transparent overlay was placed on a 'freeze frame' image of a similar cell on the video monitor. The cell was divided into 18 sectors. Border ruffling was observed in sectors 6, 7, 8, 12 and 18. This cell scored 5 out of 18.*

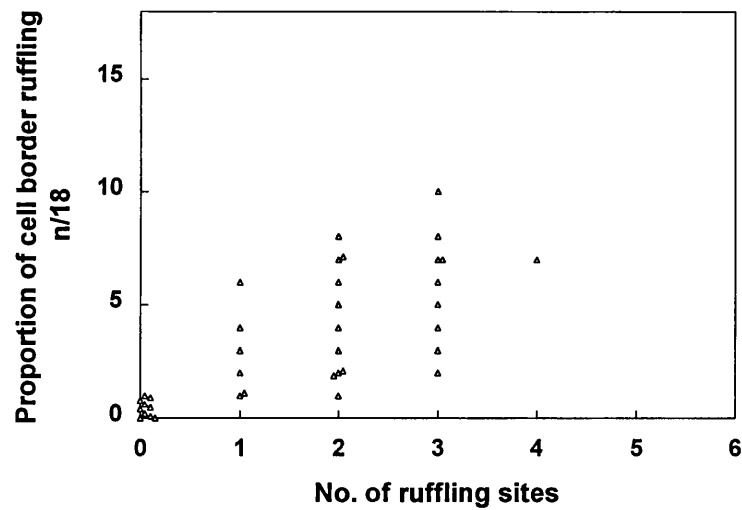


Figure 2.6 Proportion of cell margin ruffling (n/18) versus number of ruffling sites for cells cultured for 1 hour on tissue culture polystyrene

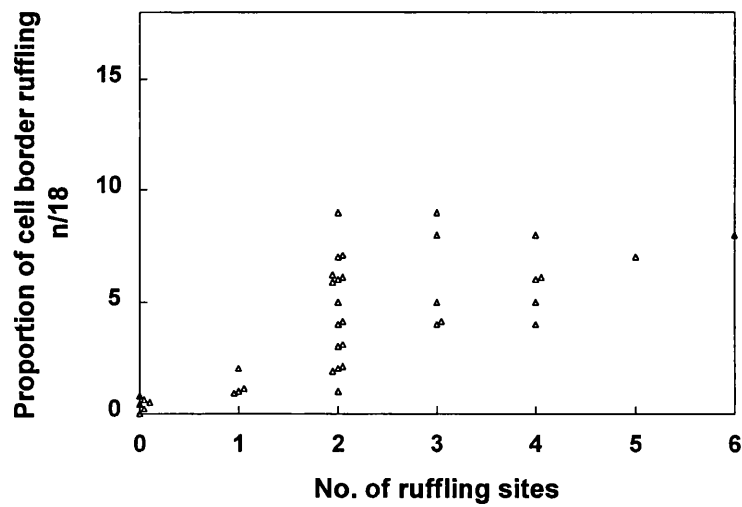


Figure 2.7 Proportion of cell margin ruffling (n/18) versus number of ruffling sites for cells cultured for 1 hour on Apoceram

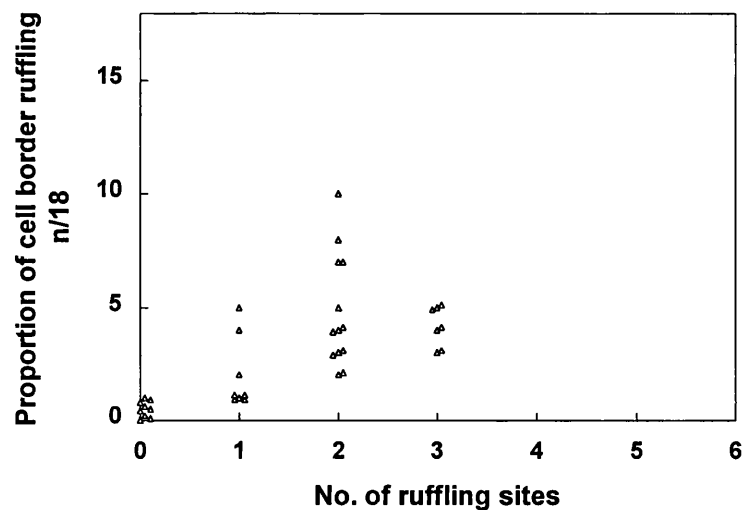


Figure 2.8 Proportion of cell margin ruffling (n/18) versus number of ruffling sites for cells cultured for 2 hours on tissue culture polystyrene

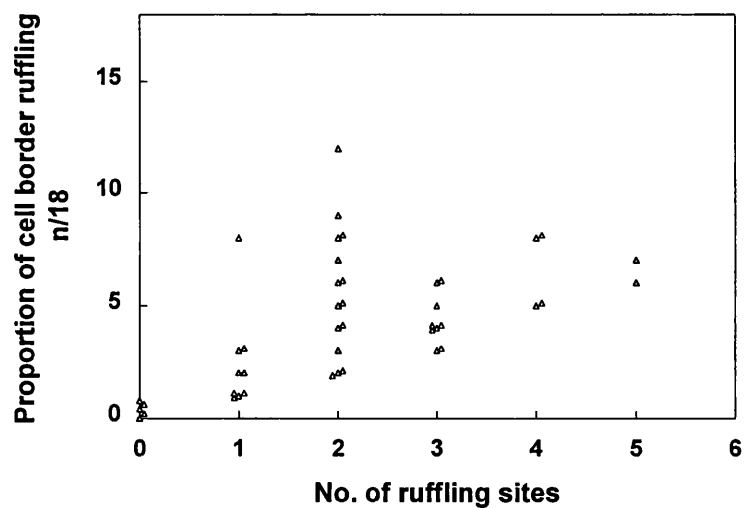


Figure 2.9 Proportion of cell margin ruffling (n/18) versus number of ruffling sites for cells cultured for 2 hours on Apoceram

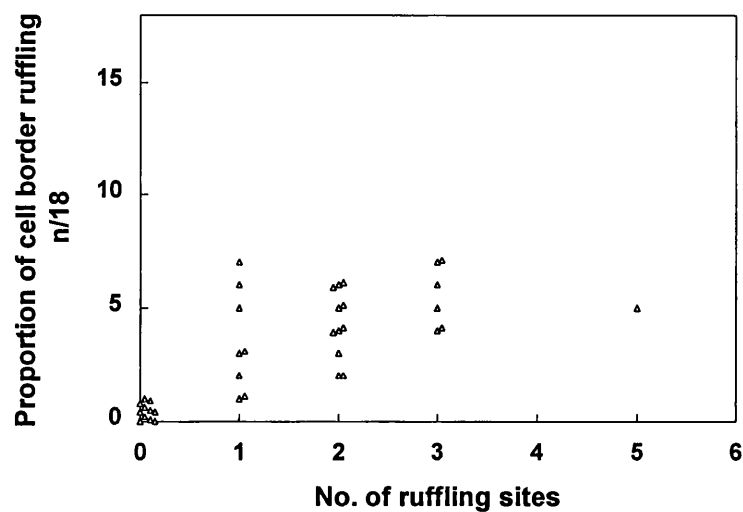


Figure 2.10 Proportion of cell margin ruffling (n/18) versus number of ruffling sites for cells cultured for 3 hours on tissue culture polystyrene

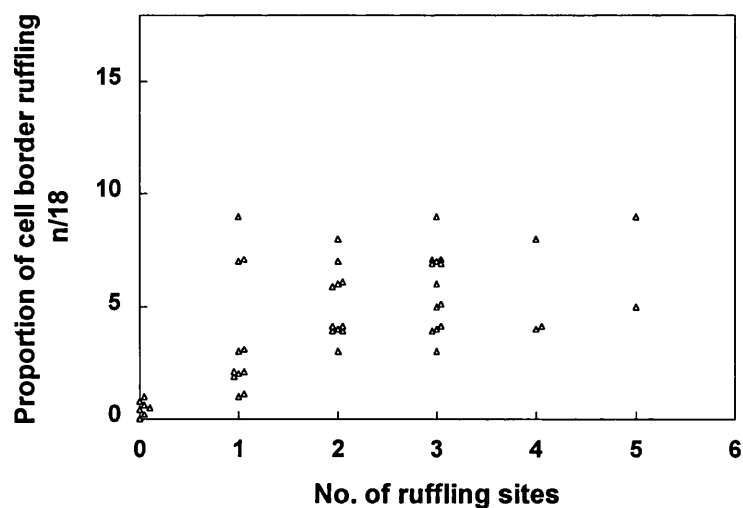


Figure 2.11 Proportion of cell margin ruffling (n/18) versus number of ruffling sites for cells cultured for 3 hours on Apoceram

It emerges from this analysis that for all three time intervals studied that the 3T3 cells on Apoceram displayed, on a per cell basis, a higher number of ruffling sites with means of 1.69, 2.09, 2.00, at 1, 2 and 3 hours respectively. In contrast, the cells on TCP displayed a lower number of ruffling sites, with means of 1.59, 1.49, 1.38 at the equivalent time intervals, and with smaller upper limits to the distribution ranges. The average number of segments of ruffling cell margin, out of 18 segments per cell at 1, 2 and 3 hours was 3.17, 4.16, 4.26 for Apoceram and 3.32, 2.89 and 3.05 for TCP. In other words, over the period analysed, cells on the glass-ceramic are likely to be less adherent and less capable of locomotion (through an inability to maintain tractional purchase) than their counterparts on TCP.

2.4 Discussion

The results of this study show that 3T3 fibroblast plated onto tissue culture polystyrene and the glass-ceramic material, Apoceram, exhibited similar morphological changes but with differences in the timing of the typical behavioural response to contact and adhesion to the substratum in question. A higher proportion of cells on TCP appeared well-spread and flattened at the end of the recording indicating the formation of stable adhesive contacts. The border ruffling represents the activity of lamellipodia and cell processes extending from the spreading cells. Those lamellipodia that fail to attach firmly to the substratum, because of weak cell-to-substratum adhesions would be pulled backward by the cortical tension to produce a "ruffle" (Abercrombie et al., 1970). Ruffling activity was significantly more widespread on the Apoceram and this is interpreted as poor or weak cell-to-substratum adhesion as compared to that displayed by cells on the TCP.

The adhesion of cells in suspension to an artificial substratum involves the adsorption of serum proteins to the substratum (Revel, 1973), contact of rounded cells with the substratum followed by attachment and spreading of the cells. Three morphological stages have been described by Taylor (1961):

Stage 1. Spherical or irregular cells with no processes attached to the substratum.

- Stage 2. Flattening cells with attached processes, retaining an elevated cytoplasmic mass.
- Stage 3. Spread cells, nuclei flattened.

A similar progression from rounded to spread morphologies has been observed in this study. However, assessment of the rate of progression through the sequence of behavioural phenotypes, and of marginal activity, provides a more sensitive view of cell response during the process of attachment and spreading on the substratum. Such activity can be influenced by range of factors such as surface energy, surface charge, wettability, in a protein-free medium (Baier et al., 1984; Weiss and Blumenson, 1967). Moreover, in the presence of serum, similar factors would affect the affinity of the substratum for adhesion proteins such as fibronectin, and thereby modify the rate of attachment (Grinnell and Feld, 1981). The conformation of these proteins when they are adsorbed to the substratum may also influence their binding activity with cell surface receptors (Yamada et al., 1985). Additionally, surface preparation during either manufacturing or sterilisation can produce different adsorption properties on the same material (Kasemo and Lausmaa, 1988). Seitz et al. (1982) reported that in serum-free culture, coating of Bioglass (U. of Florida, Gainesville, U.S.A.) with fibronectin had no apparent effect on the initial adhesion of rounded fibroblasts but the rate of spreading was more rapid and the final morphology of the cells were more flattened. Tissue culture polystyrene is known to have enhanced fibronectin binding properties (Bentley and Klebe, 1985) and, although these variables have not been explored within this system, fibronectin from the serum will have been similarly bound in our assays.

The procedures described in this chapter whereby analysis of the dynamic train of events following initial cell/substratum interactions can be carried out, provide a very sensitive means of exploring the short-term attachment of cells on artificial materials with implantation potential. Phenomena emerge from such analyses which are not easily recognisable in the assessment of fixed and stained preparations on *in vitro* assays. Cell division is dependent on cell shape and anchorage (Ireland et al., 1987), possibly coupled to the changes in the organisation of the cytoskeleton when a cell attaches via transmembrane receptors to proteins which are in the extracellular matrix or adsorbed onto artificial

substrata. Following the completion and publication of the work described in this chapter (Appendix I), many new reports on the either cell attachment and/or growth and differentiation on implant materials *in vitro* have appeared in recent biomaterials and implant literature, as evident in the literature review. Yet so far, very few of these have explored the association between the very early phenomena of cell attachment and spreading, and later cell proliferative rates or phenotypic expression on implant materials to the actual processes in the initial development of the tissue-implant interface *in vivo*.

3. Bone tissue/organ culture on the chorioallantoic membrane

3.1 Introduction

The use of tissue and organ cultures to follow processes of differentiation and morphogenesis is limited by the absence of vascularisation under conditions of *in vitro* cultivation. Bone is especially dependent upon adequate vascularisation if it is not to undergo necrosis. A variety of *in vivo* grafting and transplantation procedures are available that overcome this limitation. One useful alternative method is the grafting of tissues or whole organs to the chorioallantoic membrane (CAM) of the embryonic chick.

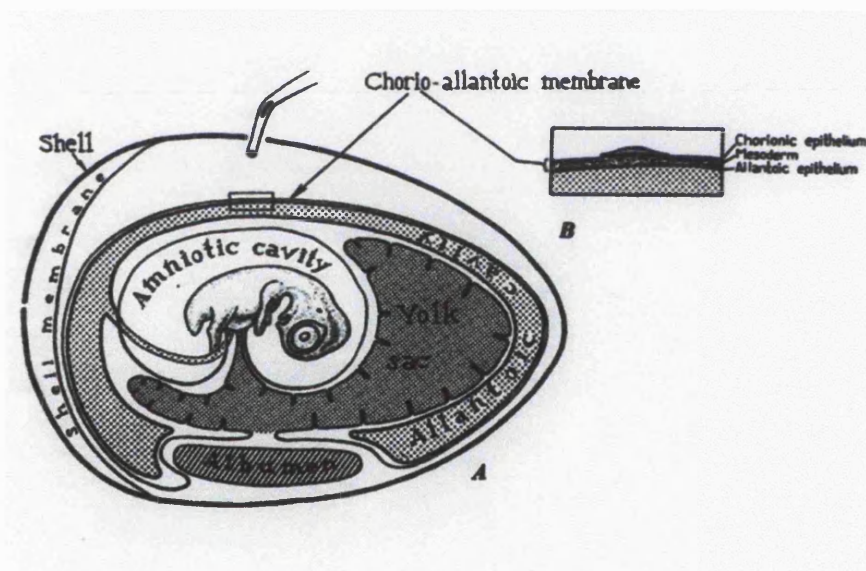


Figure 3.1 Cross-section of developing chick egg with 10 day embryo (from Hamburger, 1973)

The technique of using the chick chorioallantoic membrane (CAM) for the cultivation of isolated organs, tissues was developed by Willier in the 1920's (Hamburger, 1973). The chorioallantoic membrane is formed by the fusion of the chorion and allantois at the 6th day of incubation. It lies close to the egg shell underneath the egg membrane. (Figure 1). The CAM consists of a layer of mesodermal tissue covered by epithelium on both sides. At the outer surface (close to the egg shell) the epithelium is the chorionic epithelium and at the inner surface the epithelium is the

allantoic epithelium. The mesodermal layer is well-vascularised by the 8th day of incubation. Because of its extensive blood supply, the CAM has proven to be a valuable site for the cultivation of isolated organs and tissues, and also tumours and viruses (New, 1966). Grafts placed on the membrane become invaded by allantoic blood capillaries and continue to grow.

This culture method has been extensively used in the study of self-differentiating capacities of isolated parts of the young embryo (Murray, 1936). Grafting embryonic tissues on the CAM is a method that allows the development of normal morphology and histogenesis of the tissue (Hall, 1978). It is relatively rapid and inexpensive. Eggs are readily available, so the method does not require maintenance of large colonies of laboratory animals. The eggs provide a pre-sterilized environment in which there is sufficient space so that during an 8- to 10-day period, tissue growth to lengths of the order of 2 cm can be accommodated. Tissues are normally grafted onto the CAMs of eggs incubated for between 8 and 10 days. Eighteen days of incubation represents the age at which the closing down of the chorioallantoic vasculature preparatory to hatching commences, which makes 10 days the maximum duration of life as a graft in that host. According to Hall (1978), mammalian tissues have to be recovered earlier since rejection mechanisms develop within the embryonic chick at around 15 or 16 days of incubation. Until that age, mammalian tissues survive very well. Non-mammalian tissues can be left on the CAM until 18 days of incubation of the host. Hall (1972) also suggested that the grafts can be regrafted from host to host and in this way be maintained for several weeks. Relatively large and complex structures, such as whole limbs can be grown by this method compared to what is possible using *in vitro* organ cultures.

The CAM itself has been used for testing the irritant effect of topically applied skin preparations and other chemicals in place of the Draize eye test in rabbits. (McCormick et al., 1984; Lawrence et al., 1986; Pape & Hoppe, 1991). The vascularity of the CAM also made it a popular model for studying angiogenesis. The system has the advantage of allowing many samples to be screened for angiogenetic activity in an inexpensive way (Vu et al., 1985).

In recent years, the CAM has been utilised to examine giant cells/ osteoclast recruitment and function. Devitalised mineralised human bone particles (Groessner-Schreiber et al., 1992), hydroxyapatite and non-resorbable materials such as Sepharose beads, mica and methacrylate (Webber et al., 1990) placed directly on the CAM resulted in recruitment and differentiation of osteoclast precursors from the haemopoietic system of the host chick.

There are several reports on using the CAM model to study fracture healing. Monro (1988) examined the growth of the chick femur in ova, and its growth and repair *in vitro* and on the chorioallantoic membrane. He concluded that it was possible to mimic different fracture repair patterns and examine how they progressed. Takahashi et al. (1991) performed transverse osteotomies at the mid-shaft region of embryonic chick femurs and cultured the bone on the CAM of host eggs. The grafts were harvested from 1 to 9 days after the transplant. Histologic examination showed that repair progressed rapidly. The fracture gap was invaded by blood vessels and fibrous ingrowth. Ossification followed and the repair process was completed by day 9. Bale & Andrew (1994) grafted fractured femurs from 12-18 days old chick embryos and neonatal chicks on the CAM of 9 days old host chick eggs. They reported that there was no callus response and minimal inflammatory response to fracture. Granulation tissue was not seen at the site. The bones appeared to repair by subperiosteal bone formation to bridge the fracture gap. The authors postulated that the graft was a chimera with the osteoblasts derived from donor bone and the osteoclast and marrow component derived from the host.

3.2 Aim and objectives

This exploratory study made use of the CAM as a vascularised culture bed for bone cells, tissues and bone as an organ with the aim of establishing a system for studying bone-biomaterial interactions.

The objectives were to establish protocols for the grafting of bone cells and tissue/organ on the chorioallantoic membrane of developing chick eggs and to evaluate

different bone tissues for examining bone-implant interactions using the CAM as a culture environment. The experiments involved: i. Grafting bone cells from an established cell line and from human mandibular bone; bone tissue/organ from the developing chick embryo including the calvaria, the mandible, and the femur on the CAM. ii. Grafting combinations of implant materials and bone tissue on the CAM iii. Testing the feasibility of serial grafting in order to extend the culture period.

3.3 Materials and methods

3.3.1 Preparation of host eggs



Figure 3.2 *View of chorioallantoic membrane (CAM) in a developing chick egg incubated for 9 days. The capillary network of the transparent CAM is seen overlying the yellow yolk sac. Original magnification x20*

Fertile eggs of the common fowl (*Gallus domesticus*) were used. The eggs were incubated at 37°C and 70% relative humidity (in a humidified, forced-air incubator) for 8 days (counting the day the eggs were placed into the incubator as day 0). Each egg was taken in turn out of the incubator and its surface was swabbed with 70% Industrial Methylated Spirit (IMS) for disinfection. The host egg was rested horizontally on a silicone elastomer support. A square window with sides approximately 1cm long was cut in the eggshell using a diamond cutting disk and a straight dental handpiece. Overlapping cuts were made to ensure that the corners of the square were complete. Care was taken during cutting to avoid puncturing the underlying shell membrane. The changing resistance of the shell indicated when the shell membrane had been reached. Then a pinhole was made in the shell at the blunt end of the egg to puncture the air space. This lowered the embryo, reduced the chances of damage to the chorioallantoic

membrane (CAM) and created space for the graft. The shell window was gently levered upwards with a pair of sterile Watchmaker's forceps No2 (A.Dumont and Fils, Switzerland), working around its sides until it was separated from the shell membrane. The shell should remain intact at this stage and there should be no rupture of blood vessels in the underlying CAM. A small slit in the shell membrane was made using Watchmaker's forceps No5 to facilitate its detachment from the underlying CAM (Figure 2). Again, care was taken in order not to rupture the CAM or to drop dust from the eggshell onto the CAM. Adhesive tape (3M, U.K.) was used to seal the window. The tape was used sparingly as the embryo required free shell surface for gaseous exchange. Finally, the eggs were returned to the incubator with the windows facing upwards.

3.3.2 Preparation of cell cultures for grafting

A human osteosarcoma cell line, MG63, was maintained in alpha modification of Eagle's minimal essential medium (α MEM, ICN Flow, U.K.) + 10% foetal bovine serum (FBS, ICN Flow, U.K.) + Penicillin(50U/ml)/Streptomycin(50 μ g/ml) (Gibco Ltd., U.K.). When confluence was reached, the cells were dissociated from the culture flask by incubation with 0.05%(w/v) trypsin- 0.02%(w/v) EDTA (Gibco Ltd., U.K.) at 37°C for 4 minutes. The dissociated cells were washed, centrifuged. The cell pellet was divided into three portions with a sharp scalpel and transferred in 0.2ml α MEM onto the CAM of a host egg.

Fragments of mandibular bone removed during third molar surgery of adult patients were collected and washed in Eagle's minimal essential medium (α MEM, ICN Flow, U.K.) Penicillin(50U/ml)/Streptomycin(50 μ g/ml) (Gibco Ltd., U.K.). The fragments were minced and placed in the bottom of 25cm² tissue culture flasks with 10ml of Eagle's minimal essential medium (α MEM, ICN Flow, U.K.) + 10% foetal bovine serum (FBS, ICN Flow, U.K.) + Penicillin(50U/ml)/Streptomycin(50 μ g/ml) (Gibco Ltd., U.K.). When cell outgrowth from the bone fragments reached confluence, the cultures were passaged. Second passage cultures of mandibular bone cells derived from three patients were used for the experiments.

3.3.3 Preparation of bone tissue for grafting

As a source of donor bone tissue, chick embryos at different stages of development were used. The incubation was timed such that the donor eggs and the host eggs achieved the required stages of development on the day the grafting was carried out. The tissues to be grafted were dissected out under sterile conditions. The procedure was as follows: A fertilised chick egg which has been incubated for the required period was taken out of the incubator and placed, with blunt end on top, in a plastic bowl. The egg shell was cut open and the egg membrane trimmed away. The CAM was cut with a pair of scissors, and the chick embryo was separated from the yolk sac and the amniotic membrane. The spinal cord of the embryo was then severed at the neck using the scissors. (The embryos were killed by decapitation, according to Home Office Guidelines). The mandible, parietal bones or femurs of each embryo were dissected out in a sterile petri-dish filled with sterile phosphate buffered saline (PBS). Under a dissecting microscope (magnification x7) (Olympus Optical Co. Ltd., London, UK), the bones were dissected from the skin and the muscles, retaining the periosteum. After dissection, the bones were transferred to a new petri-dish filled with PBS.

3.3.4 Grafting the bone tissue/organ

A host egg in which a window had been prepared was taken out of the incubator and the adhesive tape was removed. The donor tissue was removed from the petri-dish using a spatula and placed on the CAM of the host egg. The adhesive tape was used again to seal the window and the egg was placed in the incubator. From this point onwards, the eggs were kept with the window facing upwards and the turning mechanism in the egg incubator was switched off to stop rotation.

The above procedure was repeated until all grafts had been made. The host eggs were kept in the incubator for 6-10 days.

3.3.5 Implant materials

The implant materials used for this study were commercially pure titanium (Goodfellow, Cambridge, U.K.) and the glass-ceramic Apoceram. Titanium was chosen

as a representative inert implant material and Apoceram selected for its surface reactivity (Rawlings, 1993).

3.3.5.1 Apoceram

This material was provided in hot-pressed form for the project by the Department of Materials at Imperial College, University of London, using the composition known as CP1. The parent glass batch compositions are listed in Table 3.1. The glass-ceramic had been prepared by melting dried powders of the raw materials followed by quenching to produce amorphous glass particles used as a material for sintering and crystallisation. This glass frit was milled to produce the ground powder for the production of the hot-pressed samples. Hot-pressing is analogous to pressing and sintering except that pressure and temperature are applied simultaneously.

Milled glass powders of CP1 composition yielding a particle size distribution smaller than 20µm with an approximate mean size of 10µm had been processed at 3.45MPa at a holding temperature of 1000°C for one hour.

Component	Normalised Mass %
	CP1
Na ₂ O	4.47
CaO	28.62
Al ₂ O ₃	6.45
SiO ₂	50.65
P ₂ O ₅	7.04
CaF ₂	2.77

Table 3.1 *Composition of Apoceram CP1*

3.3.6 Preparation of the implants

0.5mm thick sections of Apoceram, composition CP1, were cut from a rectangular block using a precision wire saw (Laser Technology, California, U.S.A.). These were then serially ground with four grades of silicon carbide coated paper (P240, 400, 800, 1200) to thickness of 0.15 to 0.2mm and polished with 5µm and then 1µm diamond compound

(Hyprez 5 star; Engis Ltd., Kent, U.K.) on a Metaserv rotary polishing machine (Buehler Ltd., Coventry, U.K.). The resulting slices were then fractured to produce smaller, roughly rectangular pieces. The samples were soaked overnight in a 1:10 aqueous dilution of 7X detergent (ICN Flow, Irvine, Scotland) and rinsed in running tap water for two hours. This was followed by ultrasonic cleaning for 3-5 minutes in deionised water, a 30 minute wash in 70% ethanol, after which the samples were heat-sterilised in an autoclave. The titanium implants were cut into 0.6mm by 0.8mm rectangular pieces from a 0.15mm thick sheet of commercially pure titanium. They were then cleaned and sterilised in the same way as the Apoceram implants.

3.3.7 Insertion of implants into the chick bone tissues

In this set of preliminary experiments, an implant was inserted into the mesenchymal tissue between the Meckel's cartilage and the membrane bone in the posterior lateral part of one half of day 6, 8 and 9 embryonic mandibles. The implants were also placed within the membrane bone in day 12 mandibles. Embryonic parietal bones (age 8 and 9 days) were trimmed into pieces, approximately 4mm by 4mm, using miniature scissors designed for ophthalmic surgery. An implant was placed on the endocranial surface of the bone following the separation of the periosteum and the soft membrane bone was folded over the implant. Chick embryonic femurs (age 12, 14, 16 days) had implants inserted into the diaphyses using the following method: At the midshaft of each femur a cut was made through the periosteum into the trabecular bone under the dissecting microscope using a sterile 26 gauge needle (Microlance 3, Beckton Dickinson, Dublin, Ireland). The wound was made parallel with the long axis of the diaphysis. With a pair of No 5 Watchmaker's forceps, an implant was inserted into the wound which was then closed with gentle pressure. The implant was fully buried in the femur. One femur from each donor received a titanium implant and the contralateral femur received an Apoceram implant. The bones with the implants were placed on the CAM of host eggs which had been incubated for 9 days and were harvested 6 to 10 days after implantation.

3.3.8 Retrieval of the grafts

To retrieve the grafts cultured on the CAM, the eggs were taken out of the incubator and the sealing tape was removed from the windows. The grafts were always near or below the window area. They would appear as discernible organised structures retaining the normal morphology of the bone. If the grafts were not near the window area, the remainder of the CAM was searched. The CAM was cut around the graft with scissors, and the CAM with the attached graft transferred to a petri-dish filled with PBS. Immediately after retrieval of the grafts, the host chick embryos were decapitated (according to Home Office guidelines). The grafts were examined under the dissecting microscope at x7 magnification prior to being transferred to a fixative solution.

3.3.9 Fixation and embedding of specimens

Grafts involving bone cells were fixed overnight in 10% neutral buffered formalin, processed and embedded in paraffin. Grafts involving bone tissue were fixed overnight in 10% neutral buffered formalin and prepared for embedding in methylmethacrylate resin.

After fixation, the epiphyses of the femoral grafts were trimmed off with a sharp scalpel to assist dehydration and infiltration. The femurs, calvaria and mandibles were dehydrated in a graded series of ethanol and then infiltrated in LR White Resin (Monomethylmethacrylate resin) [LR White resin, London Resin Company Ltd, Reading, Berkshire, England]. Embedding was carried out at 4°C in gelatin capsules (Agar Scientific Ltd, Essex, U.K.) [see Appendix II].

3.3.10 Location of implants and preparation of sections for light microscopy

The LR White blocks were allowed to set for at least 24 hours at 4°C. The implants within the resin-embedded tissues were located visually, using the dissecting microscope and a strong fibre optic light source. The resin block was roughly trimmed with a metal file and razor blades and oriented to produce a block face perpendicular to the longest edge of the implants, and, for the femoral specimens, at right angles to the long axis of the diaphysis. Further trimming with a glass knife on an ultramicrotome

(Ultracut E, Reichert Jung, Austria) produced a smooth block face without exposing the hard implant surface.

Conventional ground section techniques were not feasible for the specimens owing to the small size of the tissues and implants. The specimens containing implants were trimmed by cutting thick sections with an old diamond knife (Diatome 45°, Diatome, U.K.) with a clearance angle of 3°. Then 1-1.5µm thick sections were produced at approximately 50µm intervals using another diamond knife (Histoknife, Diatome, U.K.) with its boat filled with distilled water. The sections were lifted onto drops of distilled water on a glass slide and then dried on a hot plate. The sections were stained with 1 % toluidine blue plus 1% borax for light microscopy.

3.3.11 Photomicrography

The stained sections were mounted using Histomount or DPX mounting resin and observed using an Olympus BH2 light microscope. In the early stages of the project, the sections were recorded using 35mm colour transparencies (Ektachrome 64T, Kodak, UK). Subsequently, all light microscopic images were captured electronically. The original mounted sections were recorded using a Kontron ProgRes digital camera attached to the light microscope. Version 2.0 of the associated software was used for image acquisition and the files were stored in JPEG format for handling via Adobe Photoshop v.3.0 or 4.0. The sections were scanned at a resolution of 1024 x 774 pixels. Contrast and brightness levels were adjusted during scanning. The images were cropped or rotated for presentation without further editing.

3.3.12 Serial grafting

To assess whether it was possible to extend the culture period, grafts of 12 day old embryonic femurs without an implant were retrieved after 5, 7 and 9 days of culturing on the CAM. These grafts were placed in sterile PBS and the CAM tissue away from the bone was trimmed off. The femurs were then transferred onto the CAM of a new host egg. The serial grafts were harvested after 7 days and the vitality of the bone examined under the dissecting microscope.

3.4 Results

3.4.1 MG63 and human mandibular bone cells

Twelve grafts were made with MG63 cells and twelve with mandibular bone cells. The clump of cells placed on the surface of the CAM appeared as whitish plaques no larger than 1mm across at the time of retrieval. Many were difficult to locate visually. The grafted bone cells failed to produce any bone and remained as a clump on the surface of the CAM without any overt response from this tissue. The grafts which were visible had two types of histological appearance. The first showed that the clump of cells had settled on the outer epithelium of the CAM. The CAM did not proliferate around the cells which adopted a rounded morphology with poor intercellular contacts. Many were necrotic. There was no sign of matrix formation and the CAM showed slight thickening of the ectodermal epithelium but the mesodermal layer was not infiltrated by inflammatory cells. The second type of appearance was the encapsulation of the grafted cells by the CAM. The grafted cells had a mainly fibroblastic shape and were not distinguishable from those originating from the CAM. No bone formation was observed.

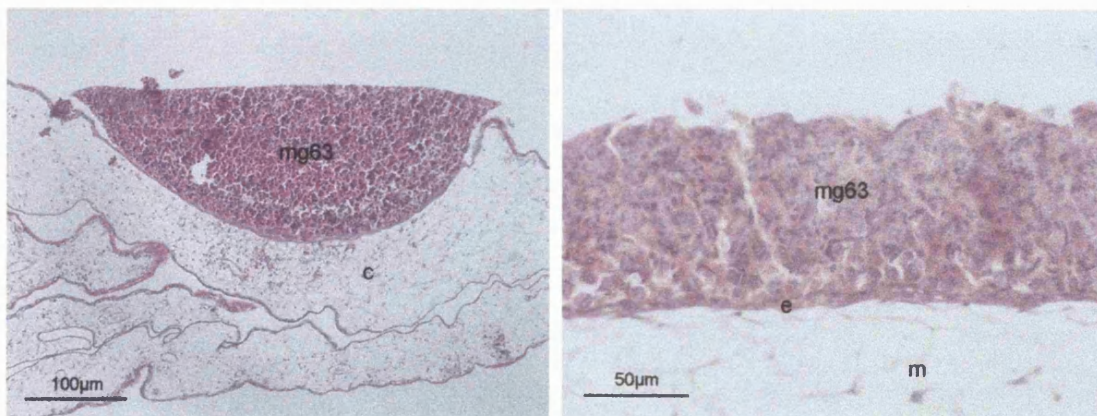


Figure 3.3 *MG63 cells grafted on the CAM (left & right). The cells remained as clumps on the surface of the CAM without being enveloped by the epithelium (e) or invaded by blood vessels within the mesenchymal tissue (m). Stain: H&E*

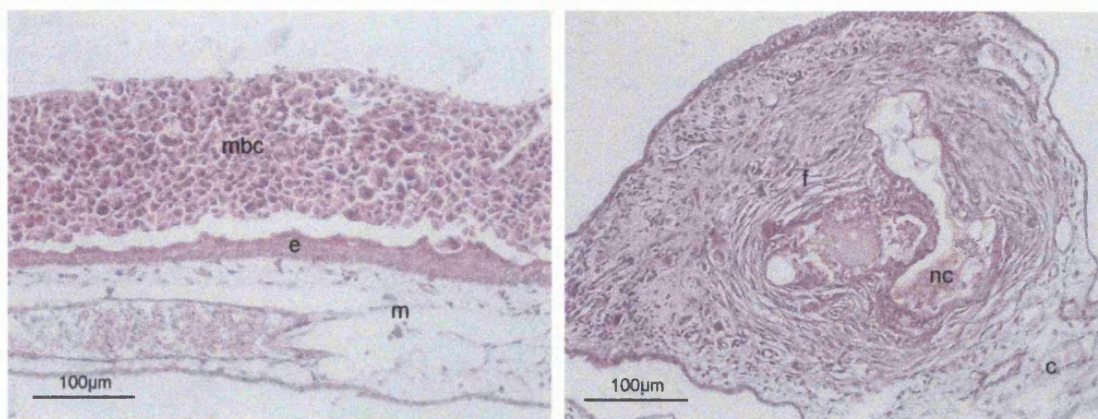


Figure 3.4 Human mandibular bone cells grafted on CAM (mbc). Left: The cells settled as a clump on the CAM (c). Right: The grafted cells enveloped by the CAM, showing fibroblast-like morphology (f). Necrotic cells were found at the centre of the graft (nc). Stain: H&E.

3.4.2 Calvaria, mandibles and femurs

The numbers of grafts made, including those containing implants but excluding the serial grafts are shown in the table below:

Site	Age of donor embryo	Duration of culture on CAM	Number of grafts
Limb rudiments	6	7	4
Mandible	6	7	2
		8	8
	8	9	4
	9	6	2
		7	12
		8	3
	12	7	4
		8	2
Calvariae	8	9	4
	9	7	13
		8	8
	10	8	3
Femur	10	7	4
	12	7	6
		8	7
		9	14
		10	5
	14	7	4
		9	4
	16	7	8
			Total: 121

Table 3.2 Number and types of grafts made

3.4.2.1 Survival rates of the bone grafts

A total of 121 grafts was made. The outcome at the time of graft retrieval is shown in Table 3.3-3.7. The macroscopic appearance of the grafts can be seen in Figs 3.5 - 3.9. At the time of graft retrieval, 13 hosts had died, giving a host survival rate of 89.2%. Out of the remaining 108 grafts, 21 were found to be completely or partially necrotic giving a graft survival rate of 80.6%.

Table 3.3 *Grafts of limb rudiments, mandibles, calvaria and femurs without implants*

Graft Number	Source of Tissue	Age of Donor	Duration of Culture	Outcome
1	Forelimb	6	7	all 4 limbs enveloped by CAM, significant growth showing normal morphology, feathers visible
2	Forelimb	6	7	
3	Hindlimb	6	7	
4	Hindlimb	6	7	
5	Mandible(1/2)	6	7	both grafts enveloped by CAM, normal morphology
6	Mandible(1/2)	6	7	
7	Femur	10	7	whole femur covered by CAM, vascularised
8	Femur	10	7	whole femur covered by CAM, vascularised
9	Femur	10	7	whole femur covered by CAM, vascularised
10	Femur	10	7	necrotic bone, connected to CAM at one end
11	Calvarium	10	8	dead host
12	Mandible	10	8	dead host
13	Mandible	10	8	mandible enveloped by CAM, became vascularised
14	Mandible	10	8	graft enveloped by CAM, blood clot at one end
15	Calvarium	10	8	graft appeared as a clump with capillary ingrowth
16	Calvarium	10	8	graft appeared as a clump with capillary ingrowth

Table 3.4 *Calvarial grafts containing implants*

Graft Number	Age of Donor	Implant	Duration of Culture	Outcome
1	8	Titanium	9	necrotic graft
2	8	Apoceram	9	dead host
3	8	Apoceram	9	necrotic graft
4	8	Titanium	9	necrotic graft
5	9	Apoceram	8	tissue stuck to egg shell
6	9	Titanium	8	tissue integrated with CAM
7	9	Titanium	7	tissue integrated with CAM
8	9	Apoceram	7	tissue integrated with CAM
9	9	Titanium	7	necrotic graft
10	9	Apoceram	7	graft went through perforation in CAM
11	9	Apoceram	7	implant separated from tissue
12	9	Titanium	7	lost, egg tipped over during incubation
13	9	Apoceram	7	tissue integrated with CAM
14	9	Titanium	7	lost, egg tipped over during incubation
15	9	Apoceram	7	graft partly necrotic
16	9	Titanium	7	necrotic graft
17	9	Apoceram	7	implant separated from tissue
18	9	Titanium	8	necrotic graft
19	9	Apoceram	8	tissue integrated with CAM (Fig. 3.5)
20	9	Apoceram	8	dead host
21	9	Titanium	8	tissue integrated with CAM
22	9	Apoceram	7	tissue integrated with CAM
23	9	Apoceram	7	tissue integrated with CAM
24	9	Titanium	8	implant separated from tissue
25	9	Apoceram	8	tissue integrated with CAM

Table 3.5 *Mandibular grafts (mandible halves) containing implants*

Graft Number	Age of Donor	Implant	Duration of Culture	Outcome
1	8	Apoceram	9	graft integrated with CAM, vascularised
2	8	Titanium	9	necrotic graft on CAM surface, not covered
3	8	Apoceram	9	necrotic graft not covered by CAM
4	8	Titanium	9	graft integrated with CAM, vascularised
5	6	Apoceram	8	graft integrated with CAM, vascularised
6	6	Titanium	8	graft integrated, fluid filled vesicle covered muscle
7	6	Titanium	8	graft integrated with CAM, vascularised
8	6	Apoceram	8	graft integrated with CAM, vascularised
9	6	Apoceram	8	necrotic graft
10	6	Titanium	8	dead host
11	6	Apoceram	8	dead host
12	6	Titanium	8	graft integrated with CAM, vascularised
13	6	Titanium	8	graft integrated with CAM, vascularised
14	9	Titanium	7	necrotic graft
15	9	Apoceram	7	graft integrated with CAM, vascularised
16	9	Titanium	7	graft integrated with CAM, vascularised
17	9	Apoceram	7	graft integrated with CAM, vascularised
18	9	Titanium	7	graft integrated with CAM, vascularised
19	9	Apoceram	7	graft integrated, fluid filled vesicle at proximal end
20	9	Apoceram	7	graft integrated with CAM, vascularised
21	9	Titanium	7	mand. damaged before grafting, graft small at retrieval
22	9	Titanium	7	necrotic mandible, enveloped by CAM
23	9	Titanium	8	graft integrated with CAM, vascularised
24	9	Apoceram	8	graft integrated with CAM, vascularised (Fig. 3.6)
25	9	Titanium	8	necrotic mandible, not covered by CAM
26	9	Apoceram	7	graft integrated with CAM, normal morphology lost
27	9	Titanium	7	dead host
28	9	Titanium	7	graft migrated to bottom of egg, ? CAM perforated
29	12	Titanium	8	dead host
30	12	Apoceram	8	graft necrotic
31	9	Apoceram	6	graft integrated with CAM, vascularised
32	9	Titanium	6	blood clot around graft, abnormal morphology
33	12	Apoceram	7	graft integrated with CAM, vascularised
34	12	Titanium	7	graft vital, curved membrane bone, cartilage separated
35	12	Titanium	7	graft integrated, pronounced curvature
36	12	Apoceram	7	graft integrated but implant separated from bone

Table 3.6 *Grafts of 12 day embryonic femur containing implants*

Graft Number	Implant	Duration of Culture	Outcome
1	Titanium	8	femur partly enveloped by CAM, half of implant outside bone
2	Apoceram	8	graft integrated, but femur morphology abnormal
3	Titanium	7	graft integrated, vascularised, >1.5cm long
4	Apoceram	7	graft integrated, vascularised, growth ++
5	Titanium	7	graft integrated, stunted growth
6	Apoceram	7	dead host
7	Titanium	7	graft integrated, distorted shape
8	Apoceram	7	graft integrated
9	Titanium	9	graft well integrated, approx. 2cm long
10	Apoceram	9	graft integrated, bone curved
11	Titanium	9	dead host
12	Apoceram	9	graft integrated
13	Titanium	9	graft integrated, approx. 2cm long
14	Apoceram	9	graft integrated, approx. 2cm long
15	Titanium	9	graft integrated
16	Apoceram	9	graft integrated
17	Titanium	9	graft integrated, approx. 2cm long
18	Apoceram	9	graft integrated, approx. 2cm long

Table 3.7 *Femoral grafts of different donor age without implants*

Graft Number	Age of Donor	Duration of Culture	Outcome
19	12	8	whole femur covered by CAM
20	12	10	whole femur covered by CAM, bone curved
21	12	8	half of femur covered by CAM, blood clot on CAM
22	12	10	whole femur covered by CAM
23	12	8	whole femur covered by CAM
24	12	10	dead host
25	12	8	whole femur covered by CAM, blood clot on CAM
26	12	10	dead host
27	12	8	whole femur covered by CAM
28	12	10	whole femur covered by CAM, blood clot on CAM
29	14	7	whole femur covered by CAM
30	14	9	whole femur covered by CAM
31	14	7	whole femur covered by CAM
32	14	9	necrotic femur, partially covered by CAM
33	14	7	whole femur covered by CAM, blood clot on CAM
34	14	9	whole femur covered by CAM
35	14	7	femur covered by CAM at epiphyseal ends only
36	14	9	whole femur covered by CAM
37	16	7	dead host
38	16	7	femur necrotic at one end
39	16	7	femur covered by CAM
40	16	7	femur necrotic at one end
41	16	7	femur necrotic at one end
41	16	7	necrotic femur
43	16	7	necrotic femur
44	16	7	femur covered by CAM

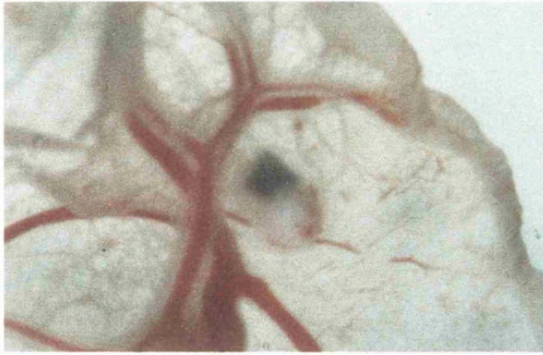


Figure 3.5 Graft of calvarium from 9-day old donor (containing an Apoceram implant) cultured for 7 days. Part of the implant was situated outside the calvarial tissue. Original magnification x16



Figure 3.6 Graft of a half mandible from 9-day old donor (containing an Apoceram implant) cultured for 7 days. Original magnification x9

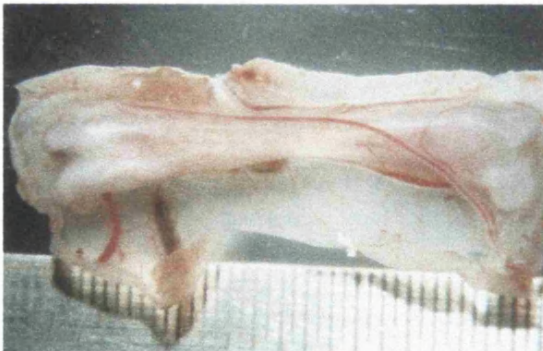


Figure 3.7 A well-integrated femur cultured for 9 days. Its length was 19mm. Original magnification x6



Figure 3.8 A femoral graft which had failed to be enveloped by the CAM. The bone appears necrotic. Original magnification x6



Figure 3.9 One epiphyseal end of this femur had become necrotic during the culture period and was enclosed in a fluid-filled vesicle. Original magnification x6

3.4.2.2 Serial grafts

Eighteen serial grafts were made. Groups of six femurs cultured for 5, 7 and 9 days were retrieved and regrafted in new host eggs. At the time when serial grafting was performed, the femurs which had already been cultured on the CAM for 5, 7 and 9 days had lengths of 13mm, 15mm and 18-19mm respectively. All the serial grafts showed signs of partial or complete necrosis at the time of retrieval after 1 week of culture in the second host.

3.4.3 Histology of grafts containing implants

During the sectioning procedure, the implant materials separated from the resin embedded tissue. Each time a titanium implant passed across the knife edge, the cut metal curled up and became partially detached from the resin as the section floated on the water surface. A light touch with a single eyelash attached to a wooden stick was all that was needed to make the metal sink to the bottom of the water-filled boat. Slices of titanium were collected from the boats of the diamond knives, allowed to dry and placed on self-adhesive carbon-coated pads on aluminium stubs. They were then coated with gold in a sputter coating unit (Polaron E5000) and examined under a scanning electron microscope (Cambridge Instruments Stereoscan 9B). Figure 3.10 shows examples of these titanium pieces. The edges which were at the interface between the implant and the bone had few tissue remnants.

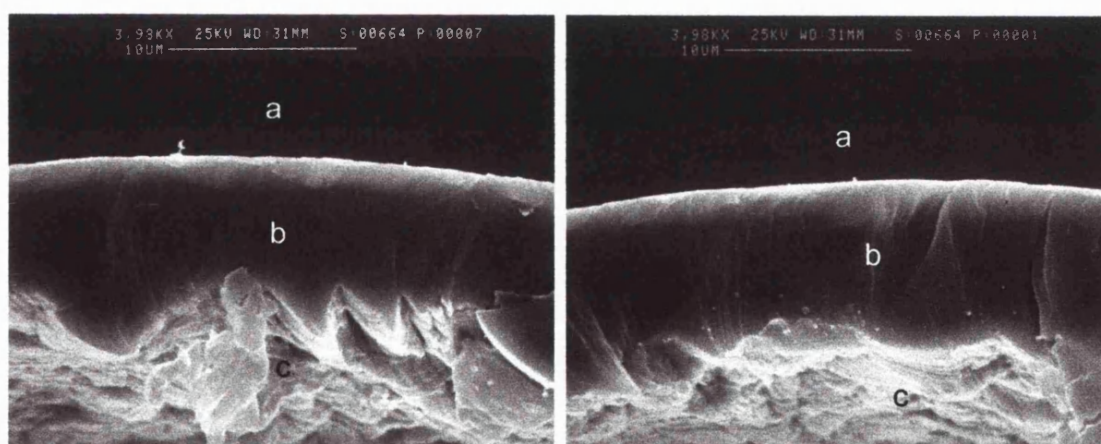


Figure 3.10 Examples of SEM images of the side view of pieces of titanium retrieved after sectioning. The surface facing (a) was produced by the 'good' diamond knife for producing 1-2 μ m sections. (b) is the edge in contact with the resin embedded tissue. (c) was produced by the old diamond knife used for rough trimming. The curvature of the titanium is evident in both pictures (original magnification $\times 4980$)

When Apoceram was sectioned, the glass ceramic remained as a film attached to the resin as the section floated on water. The film disintegrated as the section was lifted out of the boat. However, particles of the glass ceramic remained attached to the tissue along the bone-implant interface. This is evident in all light micrographs of specimens containing Apoceram. An example can be seen in Fig. 3.15.

3.4.3.1 Calvarial grafts with implants

Several implants were displaced completely from the calvarial tissue during the culture period by movement of the host embryo. They became surrounded by the mesenchymal tissue of the CAM (Fig. 3.11). The surfaces of the implants were covered by fibroblast-like cells. There was no inflammation except at the sharp corners of the implants in some specimens. In those areas, aggregations of small round leukocytes were observed. None of the implants was entirely enveloped by the calvarial tissues at the time of graft retrieval. The calvarial bone grew into a ball-like mass and the implant protruded partly outside the bone tissue. Where the membrane bone faced the implant, migration of mesenchymal cells towards the direction of the implant was observed but there was no new bone formation on the implant surface (Fig. 3.12).

3.4.3.2 Mandibular grafts with implants

Implants placed within the mesenchymal tissue between cartilage and membrane bone in the developing mandible had a layer of fibroblast-like cells on their surfaces and were surrounded by poorly differentiated connective tissue (Fig. 3.13). When the implants were inserted into the thin body of the mandibular bone, they were surrounded by marrow-like tissue with many blood vessels (Fig. 3.14). Again bone formation on the implant surfaces was not seen either with titanium or Apoceram.

3.4.3.3 Femoral grafts with implants

Some of the sites in which implants were placed into the chick embryonic femurs were invaded by the CAM tissue. This occurred when the wound created for the insertion of the implant was too large and the edges were not approximated when the femur was grafted on the CAM with the wounded side facing the membrane. When the implants were well buried within the femurs and the CAM excluded, new bone formed around the implants. Direct contact between the implant surface and osteoid and mineralised bone was observed for both titanium and Apoceram (Figs. 3.15 and 3.16).

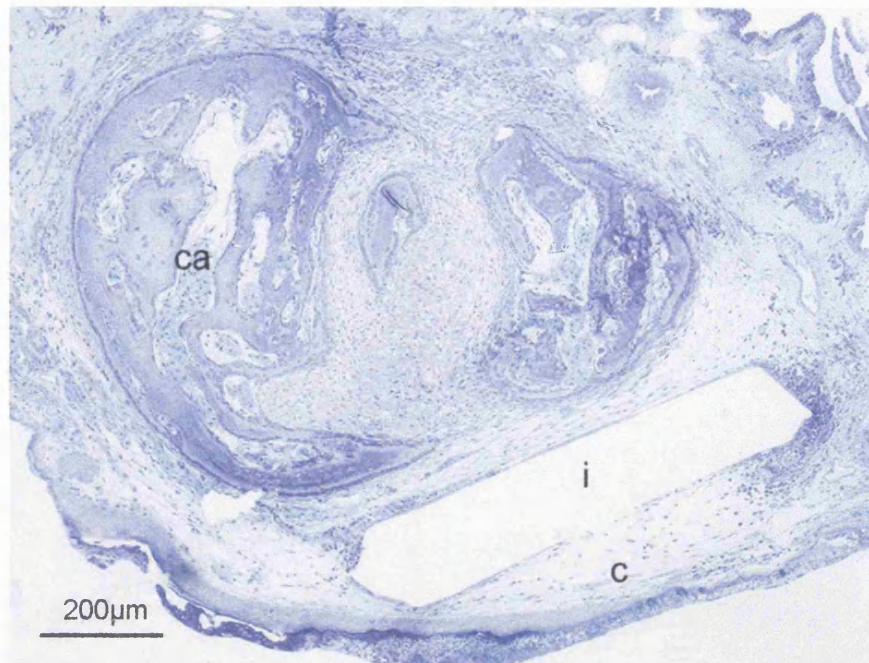


Figure 3.11 The titanium implant (i) had been displaced from the folded calvarial bone (ca) during the culture period and became located within the mesenchymal tissue of the CAM (c)

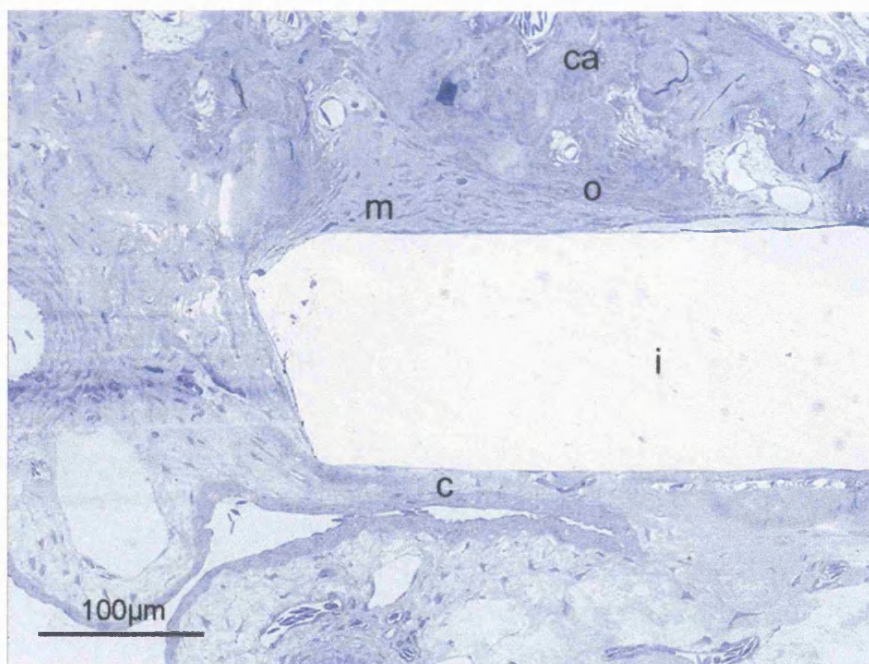


Figure 3.12 Mesenchymal cells (m) from the calvarial bone tissue (ca) migrating towards the surface of this titanium implant (i), their morphology resembles fibroblasts rather than osteoblasts (o) seen on the surface of the calvarial bone.

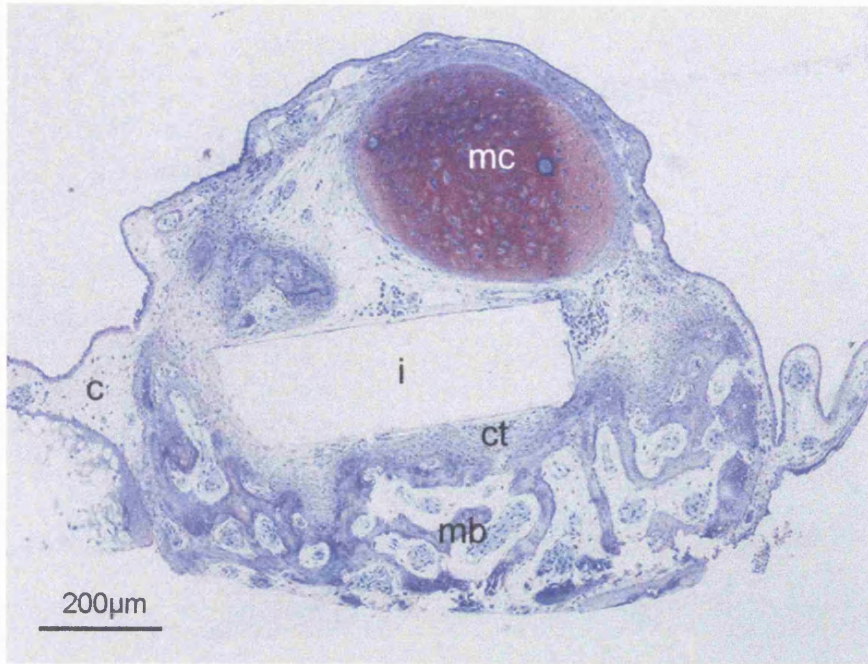


Figure 3.13 The implant (i) in this mandibular section was placed in the interstitial connective tissue (ct) between the Meckel's cartilage (mc) and the associated membrane bone (mb); it is covered by a layer of fibroblast-like cells.

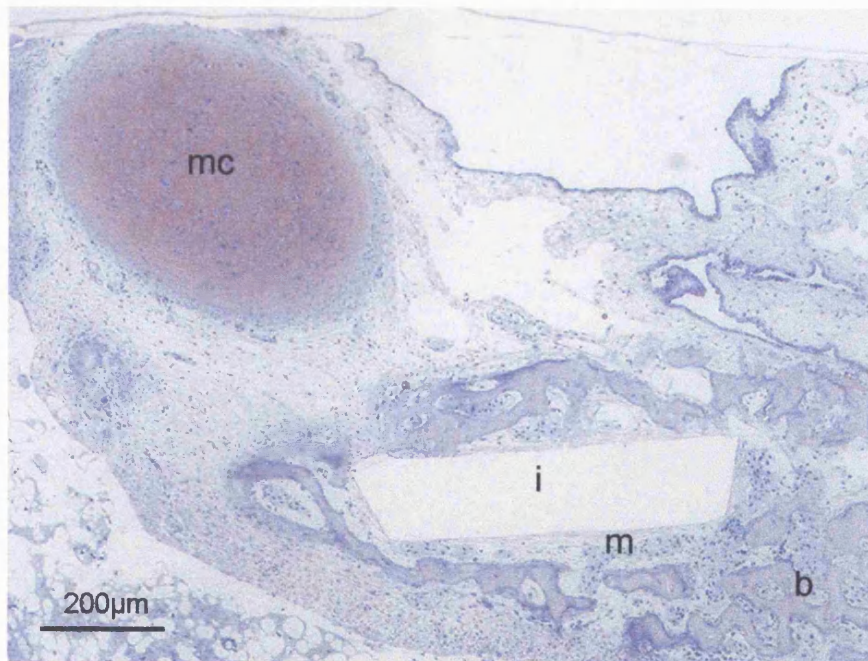


Figure 3.14 The implant (i) was inserted within the membrane bone (b) in this mandibular graft. Its is surrounded by marrow tissue with many large blood capillaries (m). The Meckel's cartilage is at the top left corner .

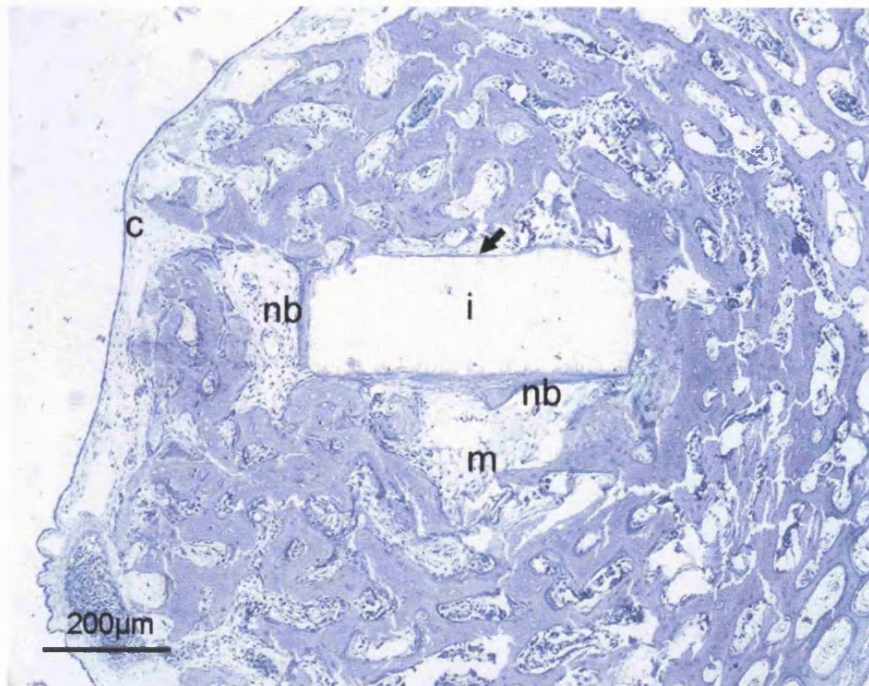


Figure 3.15 A femoral graft which received an Apoceram implant showing new bone formation on the implant surface (nb). The thickness of bone on the implant surface varies, on one side consisting of a very thin seam (arrow); implant space (i); 9 day graft.

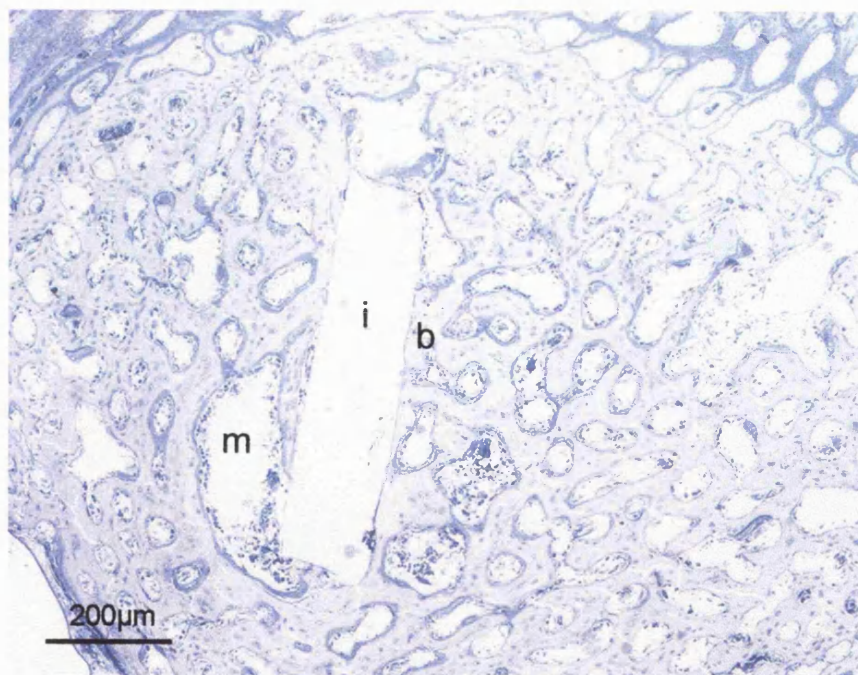


Figure 3.16 A femoral graft which received a titanium implant. Bone formation parallel to the surface of the implant within the central marrow cavity (m). Direct bone-implant contact (b); implant space (i); 9 day graft.

3.5 Discussion

3.5.1 Culture of bone cells on the CAM

The culture of pelleted bone cells on the CAM was not successful, probably for two principal reasons: a) The cells were dissociated, washed and centrifuged before they were grafted and the cell-cell association would have been disrupted by this procedure and could have failed to reestablish on the CAM before the fluids within the egg had dispersed the cells. b) In most cases where the cells had remained as clumps on the CAM, they failed to elicit the proliferation of the CAM or the invasion of blood capillaries. Most of the cell transplants thus remained avascular and had to rely on the fluids bathing the CAM for gaseous exchange and nutrients. Nijweide et al. (1982) placed cells from the calvaria of chick embryos onto the CAMs of quail embryos and reported a survival rate of only 25% for all their transplants after 6 days on the CAM. They felt that the absence of blood vessel ingrowth was one of the major reasons for the failure of many transplants.

The reason behind this attempt to culture bone cells on the CAM was that bone cells, especially those derived from human sources, do not readily form bone *in vitro*. An alternative approach might have been to allow the cells to attach and grow on substrates such as Millipore filters or even the implant materials for a short period *in vitro*, and the combination transferred to the CAM for further culture.

3.5.2 Bone organ culture on CAM

With bone tissue/organ cultures, 10% of the hosts were lost during culture. The probable causes of this include infection and inadvertent damage to the CAM during grafting. Also, not all host eggs incubated were viable at the time of window preparation for grafting. This tended to occur in clusters within certain batches of eggs. Factors such as the temperature during transport of the eggs, the duration of storage prior to incubation and the season can all affect the viability of the embryos. Even without undergoing the grafting procedure, not all fertilised eggs could be expected to develop to full term. There was variability in the stage of development of the CAM at the time of grafting and it was noted that the CAM was not vascularised to the same degree in all eggs when the

windows were made. Where there was any doubt about underdevelopment of the CAM, the eggs were not used for grafting. The same criterion was applied to the donor chicks.

Partial or total necrosis of the grafts were regarded as failures. This happened in 20.3% of the grafts retrieved in this preliminary study. The rate is based on the combined results of all donor bone sites and ages, and appeared to be lower than that reported by Takahashi et al. (1991) for their experiment on fracture healing of chick femurs in CAM culture. They found 21 out of 70 (i.e.30%) 14-day old femurs had failed to integrate completely on the CAM.

Most of the grafts which were totally necrotic at the time of retrieval were either not connected to the CAM at all or had small patches attached to the CAM. Only a few were completely covered by the membrane. Many of the larger grafts were not completely surrounded by the CAM and became partially necrotic with reduced growth. The starting lengths of the embryonic femurs were, at 12 days: 9-10mm; 14 days:12-13mm; and 16 days:14-15mm. The size of the 14 day old femur seemed to be the limit in relation to the viability of the graft. 16 day old femurs became necrotic during culture. This inverse relationship between the size of the tissue to be grafted and the subsequent viability and incorporation into the circulation of the CAM was also reflected in the results of the serial graft experiment. By the time the second stage grafting was performed, the size of the bone had become too large for complete incorporation into the vascular system of the CAM of the second host egg before bone necrosis occurred.

The grafts which were totally enveloped by the CAM and were connected to the blood supply of the host embryo showed good vitality and growth. Kirchner et al. (1996) showed in a chimera experiment where limb buds of three day old quail embryos were transferred to the CAM of chicks that such grafts were vascularised by a network of capillaries which were partially derived from sprouts of the chick CAM vasculature. Using the Feulgen reaction and an antibody to quail endothelial and haemopoietic cells, they detected numerous chimeric capillaries which consisted of host endothelial cells and graft pericytes.

The growth of successful grafts may be illustrated by the change in length of 14 day old embryonic femurs. At the time of grafting, the femurs were between 12-13mm long (measured to the nearest half mm). Where the bones became fully integrated with the host vasculature, they grew to 15-16mm long after 7 days of culturing on the CAM, and after 9 days, they measured 18.5-20.5mm. This served as a benchmark for subsequent experiments (Chapters 4 and 5) studying the bone-implant interface.

The morphology of the grafts was generally well maintained. But with increasing size of the bone at the time of grafting, there was a tendency to develop abnormal morphologies. The mandibles and long bones became curved suggesting that the direction of longitudinal growth was restricted by the surrounding CAM tissue.

3.5.3 Choice of model for studying bone-implant interactions

The outcome of the implant experiment using different types of bone tissue revealed several parameters which affected the type of interface between the implant and tissue in which it was grafted. The size of the donor tissue affects its suitability for receiving implants in two ways. The tissue must have sufficient bulk to accommodate the implant without the bone breaking up during the implantation procedure. Invasion by the CAM tissues was a risk if the wound created for insertion of the implant remained open. However, using bulkier donor tissue would increase the chance of bone necrosis during culture.

The stage of the development of the donor bone as an organ also affected the outcome. When the implant was inserted into undifferentiated mesenchyme, as was the case with some of the mandibular grafts, new bone formation did not take place on the implant surfaces within the duration of the culture experiments. Implants placed within the newly formed mandibular membrane bone in which there was an open trabecular structure and large marrow spaces became surrounded by marrow tissue. For the 8-9 day calvarial tissue, the periosteum became detached from the bone when it was lifted in order to place the implant against the endocranial surface. Folding the bone tissue over the implant was not a reliable way of maintaining contact between the donor tissue and the implant during culturing on the CAM. Disturbance by movement of the host embryo

resulted in exposure of the implant material to the cells derived from the CAM. Even for the embryonic femurs, it was important that the CAM was excluded from the healing process around the implant for bone formation to occur at the interface. As for the age of the embryonic femurs, the oldest ones used, 16 day long bones, were easiest to handle during the insertion of implants in terms of control over the size and position of the wound but the bones became necrotic during culture. The 12 day old femurs often had remnants of the central cartilage core at the mid-diaphyseal region at the time of grafting, whereas in 14 day old femurs, the formation of the central marrow cavity was complete at the site of implant insertion. On balance, amongst all the bone tissues tested, the 14 day embryonic femur was the most suitable for further investigations on the early bone healing response around implant materials.

3.5.4 Chick vs. Man

There are several fundamental differences between chick and humans in terms of tissue histology which have to be taken into account in the interpretation of the sections of the retrieved specimens in this and subsequent experiments.

Birds have evolved bones which are trabecular (less dense than human bones) to reduce body weight so that they can fly (although domestic chickens do not fly). The typical histological appearance of the embryonic chick bone grafts is the presence of many inter-trabecular channels containing marrow tissue and the lack of lamellar structure in the cancellous bone. The organisation of bone marrow of the chicken is different from that of mammals. Erythropoiesis takes place within the vascular sinusoids, rather than in the extravascular tissue. The immature red blood cells are found adjacent to the endothelium of a sinusoid. As division and maturation of these cells progress, the older ones move inward. Thus, mature erythrocytes accumulate in the centre of the vessel. As in mammals, cells of the granulocytic series (heterophils, eosinophils and basophils) develop in the extravascular spaces of the marrow. Birds have mature erythrocytes and thrombocytes (platelets) which are nucleated. The avian heterophil is equivalent to the neutrophil in other species. It is so named because its cytoplasm contains a large number of eosinophilic granules. The term neutrophil is therefore not appropriate.

4. The bone-implant interface in the femoral graft model

4.1 Introduction

On the basis of the results of the experiments described in Chapter 3, the 14 day old embryonic femur was chosen as the model in which the early stages of the development of the bone-implant interface were to be studied using the CAM as the organ culture environment. It is important to remember that the healing response around the implants took place within a background of continuing bone development and growth. The development of the mid-diaphyseal region of embryonic chick long bone has been described by Caplan & Pechak (1987) as follows:

Day 8 The first collar of mineralised bone has formed around a non-mineralised cartilaginous core and a periosteum is evident.

Day 9 Bony struts have formed which radiate from the first mineral ring or collar.

Day 10 A second mineral ring is almost complete and vasculature and perivascular elements have invaded the cartilage core.

Day 11 Most of the cartilage core has been replaced by marrow and new bone is deposited in a radial direction as the bone increases in girth.

Day 12 The marrow cavity as well as the innermost channels between trabeculae contain numerous haemopoietic cells, while the outermost channels are lined with active osteoblasts.

Day 14 The number of mineral trabeculae has increased substantially from earlier stages and each trabecula is separated by extensively anastomosing channels.

Day 18 Extensive remodelling of the innermost trabeculae has occurred, with a resultant increase in diameter of the marrow cavity. New trabeculae and channels have become more uniform in shape and are less interconnected than in earlier stages.

2 days post-hatching. Removal of the innermost trabeculae and the addition of new trabeculae to the outside of the bone increases the size of the marrow cavity and the circumference of the bony collar.

4.1.1 Aims and objectives

The aims of the main study were to:

1. To describe the healing process of bone around titanium and Apoceram in the femur CAM culture model.
2. To carry out quantitative assessment of bone-implant contact in femur grafts.
3. To perform histochemical and immunohistochemical characterisation of the peri-implant tissue in the femur graft model.
4. To examine the deposition of matrix at the bone-implant interface at the ultrastructural level.

The objectives of culturing femurs implanted with titanium or Apoceram on the CAM were to perform the following:

1. Descriptive histology using light microscopy.
2. Histomorphometry of bone-implant contact.
3. Demonstration of mineralized bone tissue using von Kossa technique.
4. Histochemical staining for alkaline phosphatase (marker for osteogenic activity).
5. Histochemical staining for tartrate resistant acid phosphatase (marker for osteoclastic activity).
6. Demonstration of new bone formation by tetracycline staining.
7. Immunohistochemical staining for bone matrix proteins: type I collagen & osteonectin.
8. Examination of the organisation of the matrix at the bone-implant interface using transmission electron microscopy.

4.2 Materials and methods

4.2.1 Histology

14 day old embryonic chick femurs were implanted with either titanium or Apoceram at the mid-diaphyseal region as described in Chapter 3. The femurs were cultured on the CAM for 1, 2, 3, 5, 7, and 9 days. The grafts were retrieved and fixed in

10% neutral buffered formalin. Only those femurs which had remained viable with no signs of necrosis were processed and embedded in LR White resin. The development of the bone-implant interface was assessed using light microscopy of toluidine blue stained sections.

4.2.2 Histomorphometric analysis

The Quantimet 520 image analysis system (Cambridge Instruments, UK) was used for assessing the percentage of implant contact with osteoid and mineralised bone in the resin-embedded sections. This system consists of an Olivetti M240 computer (Olivetti, Italy), two colour monitors, an image store and a digitab. The image of the toluidine blue stained section was produced by a video camera (JVC, Japan) attached to the optical microscope (Standard microscope 14, Carl Zeiss, Germany) and displayed in colour on the first monitor as a reference image. The video signal was also fed into a six bit analogue to digital converter to produce a 64 levels grey image on the second display unit which contained the detection and measurement frames.

By using the IMAGE SET-UP function both the contrast and the brightness of the grey image were adjusted. The microscope was set at x100 magnification and the implant space was positioned in the centre of the measurement field. Spatially, the measurement field consisted of 512x512 picture points or pixels.

Image set-up was followed by CALIBRATION. Using a micrometer slide placed under the microscope, the dimensions represented by each pixel in the image seen was computed. This dimension then remained constant every time the image was set-up and this facility was used to check that the camera and microscope settings remained constant during different measurement sessions.

Next the EDIT function was used to mark the outline of the implant and the sites of implant-bone contact. Four sections of each specimen were used for the assessment. For every section a line was traced at the perimeter of the implant space using the digitab and submitted to a new bit plane as a binary image for measurement. The length of this line was measured by recording the PERIMETER output of the

MEASURE FEATURE function (see Appendix III for discussion of feature parameters). Then, the image of the line was edited to erase parts of the line where the implant was not in contact with mineralised bone or osteoid. Mineralised bone appeared as pale pink and in the osteoid, osteoblasts were surrounded by dark bluish purple extracellular matrix. To distinguish between soft tissue and osteoid contact, the sections were reviewed through the microscope eyepiece at a higher magnification (x400) before the line on the monitor, produced at x100 magnification, was edited. The length of the portions of the implant perimeter adjacent to bone and osteoid was measured. The lines were further edited to erase the segment(s) representing contact with osteoid. A final measurement of these lines was taken to obtain the length of contact with mineralised bone. The percentages of the implant-mineralised bone contact, implant-osteoid-mineralised bone contact over the whole perimeter of the implant were calculated. The reproducibility of the measurements was assessed by selecting randomly one section from each time period and performing the measurements six times.

4.2.3 Von Kossa staining

Slides containing sections of femurs embedded in LR White resin were placed in 1% aqueous silver nitrate solution and exposed to strong light for 60 mins. The slides were washed in distilled water, treated with 2.5% sodium thiosulphate for 5 mins and washed again in distilled water. Toluidine blue was used for counterstaining.

4.2.4 Alkaline phosphatase and tartrate resistant acid phosphatase

Femur specimens containing implants were fixed in 90% ethanol and embedded in glycol-methacrylate (Agar Scientific Ltd., Stanstead, U.K.) (see Appendix II). Reagents from Sigma Kits No.86R and 387A (Sigma Diagnostics, St. Louis, U.S.A.) were used for histochemical staining of alkaline phosphatase and tartrate resistant acid phosphatase.

100µl of Fast Garnet GBC Base solution (7.0mg/ml Fast Garnet GBC base in 0.4 mol/L hydrochloric acid with stabiliser) was mixed with 100µl of sodium nitrite solution (0.1mol/L) and allowed to stand for 2 mins. 100ul of this mixture was added to two test-tubes, each containing 4.5ml of deionised water pre-warmed to 37°C. 50µl of naphthol

AS-BI phosphoric acid solution (12.5mg/ml), 200µl of acetate solution (2.5mol/L, pH5.2) were added to the first tube (Solution A). 50µl of naphthol AS-BI phosphoric acid solution, 200µl of acetate solution and of tartrate solution (0.335mol/L, pH4.9) were added to the second tube (Solution B).

100µl of FRV-Alkaline Phosphatase solution (Fast Red Violet LB Base 5mg/ml in 0.4mol/L hydrochloric acid with stabiliser) was added to 100µl of sodium nitrite solution (0.1mol/L) and allowed to stand for 2 mins. This mixture was added to 4.5ml of deionised water at 18-26°C. 100µl of naphthol AS-BI alkaline solution (4mg/ml naphthol AS-BI phosphate in 2mol/L AMPD buffer, pH9.5) was added to the diluted diazonium salt solution (Solution C).

Glycol-methacrylate embedded specimens were cut dry and placed onto drops of distilled water on slides coated with poly-L-Lysine. The slides were allowed to dry thoroughly at room temperature before 100µl of Solution A or Solution B or Solution C was placed on each slide. The slides were transferred to a light-proof box placed in a 37°C water bath and incubated for one hour (acid phosphatase) or 15mins (alkaline phosphatase). After incubation, the slides were rinsed in deionised water and counterstained with Gill No. 3 Haematoxylin solution.

4.2.5 Tetracycline labelling

Tetracycline hydrochloride in pulverised powder form was dissolved in sterile PBS (Achromycin, Lederle Laboratories, Gosport, U.K.) and administered to the host eggs twenty-four hours prior to retrieval of the grafts for intra-vital labelling of the mineralisation front. The dosage recommended for whole animal studies was 20-30 mg per kg body weight when injected peritoneally (Berry, 1985). Twelve intact unincubated eggs were weighed with and without their contents. The average weight of the egg contents was around 50g (range 47-52g). For each egg, 1mg tetracycline hydrochloride in 0.5ml PBS was placed directly on the CAM for it to be absorbed via the capillary network in the membrane. The grafts were retrieved a day later, fixed in 10% neutral buffered formalin, dehydrated and embedded in LR White resin. 2µm sections were cut and dried onto glass slides, mounted with Citifluor and examined using an Olympus BH2

microscope set up for epifluorescence microscopy with an excitation filter for 440nm wavelength and emission filter for 530nm. Images of the sections were recorded using Kodak TMAX3200 black & white film.

4.2.6 Immunohistochemistry of bone matrix proteins

Polyclonal antisera raised in rabbits, reactive against (i) human α I(1) carboxy-telopeptide in type I collagen (LF-67) which was cross-reactive with chick and (ii) osteonectin (LF-8), specific for chick and quail, (Fisher et al., 1995) were kindly donated by Dr. Larry Fisher, National Institute of Dental Research, Bethesda, U.S.A.

Femur specimens containing implants were fixed with 4% paraformaldehyde in 0.1M phosphate buffer, pH7.2, at 4°C for four hours. Dehydration was carried out in a graded series of ethanol at 4°C, followed by infiltration in increasing concentrations of cold LR White resin. The specimens were embedded in LR White resin held in gelatin capsules placed in an ice cold aluminium block. Sections were cut and placed on drops of distilled water on poly-L-lysine coated glass slides. They were allowed to dry at room temperature for at least 12 hours prior to staining. The sections were pre-treated by incubation with 0.1% trypsin (Sigma) for 30 minutes at 37°C. They were then washed in phosphate buffered saline (PBS) for 5 minutes. Endogenous peroxidase was blocked with 3% H₂O₂ in PBS for 15 minutes at room temperature. The sections were washed twice in PBS. Background blocking was carried out by incubating the sections with 1% bovine serum albumin (BSA), 10% foetal calf serum (FCS) in PBS for 30min at room temp followed by washing three times for 5 minutes with PBS. The primary anti-sera were diluted to 1:20 and kept on ice. The slides were dried carefully around the sections, taking care not to dry sections out. 100µl of primary antibody solution was placed on each slide and covered with a plastic coverslip to prevent drying out. The slides were incubated at 4 °C overnight. For negative control, pre-immune rabbit serum was used. After incubation, the coverslips were removed and the sections washed once in PBS, once in millon water, and once in Tris-buffered saline (TBS) with 1% Triton X. Biotinylated goat anti-rabbit IgG was diluted to 1:20 in PBS with 10% FCS and 1% BSA. 100µl of this secondary antibody solution was applied to each slide and incubated for 20-30 minutes. The slides were rinsed twice with TBS with 1% Triton X. 100µl

ExtrAvidin Peroxidase in buffer (1:20) was applied and left for 20-30 min. 3,3'-diaminobenzidine tetrahydrochloride (DAB) solution was made in milliRo water, vortexed to dissolve and passed through a 0.2µm filter. The slides were washed three times in milliRo water. 200-300µl DAB solution was applied to each slide and left for 5 minutes after which the slides were given three final washes in milliRo water.

4.2.7 Ultrastructure of the bone-implant interface

Femurs implanted with Apoceram or Titanium were grafted onto the CAM and retrieved after 9 days. They were fixed overnight in 3% glutaraldehyde in 0.1M sodium cacodylate buffer at 4°C. Dehydration was carried out in a graded series of ethanol, followed by infiltration in increasing concentrations of LR White resin. The specimens were embedded in LR White resin held in gelatin capsules placed in a cold aluminium block.

A fracture technique was used for preparing resin blocks containing titanium implants. First, a block face was produced, using the method employed for the preparation of sections for light microscopy, to reveal a cross-section of the femur with the implant. Two score lines were then made in the resin extending from the ends of the implant to the sides of the block. The resin was fractured along the lines using a new disposable razor blade. The implant either remained attached to the main block or to the fractured resin. The side without the implant was then re-embedded in LR White resin and a new block face prepared for sectioning. For Apoceram it was possible to produce sections suitable for transmission electron microscopy without first removing the implant from the resin-embedded tissue.

Thin sections (light gold interference colour, 90-100nm) were prepared using a diamond knife (Diatome 45°, Diatome Ltd., Bienne, Switzerland) set at a clearance angle of 3° on a Reichert-Jung Ultracut-E ultramicrotome (Reichert-Jung, Vienna, Austria). The sections were floated on water and lifted onto Formvar/carbon-coated 200mesh copper grids (Agar Scientific Ltd., Stanstead, U.K.). They were stained with uranyl acetate in absolute ethanol, washed twice in absolute ethanol for 5 minutes followed by staining in Reynold's lead citrate solution and washing in distilled water for 5 minutes.

The grids were allow to dry prior to ultrastructural examination using a JEOL CX100 transmission electron microscope set at 60kV. The TEM images were recorded on 6.5 x 9 cm format film (Estar thick base 4489 electron microscope film, Eastman Kodak Co., Rochester, U.S.A.).

4.3 Results

The number of grafts, consisting of femur with implants, placed on the CAM of host eggs and successfully retrieved at different time intervals are shown in Table 4.1

Table 4.1 *Grafts of femur with implants on CAM*

Duration of Culture	Implant	No. of grafts made	No. of grafts retrieved
1 day	Apoceram	6	6
	Titanium	6	6
2 days	Apoceram	6	6
	Titanium	6	6
3 days	Apoceram	6	6
	Titanium	9	6
5 days	Apoceram	18	16
	Titanium	18	14
7 days	Apoceram	18	14
	Titanium	18	15
9 days	Apoceram	18	15
	Titanium	18	14

4.3.1 Chronological development of the bone-implant interface

A descriptive account of the changes within the tissues surrounding the Apoceram and titanium implants at different time intervals is presented in this section, accompanied by images of the toluidine blue stained cross-sections of the diaphyseal region of femurs containing the implants (Figures 4.1 to 4.14). Since the implants separated from the tissue during sectioning, the original location of the implants will be denoted with an 'i' for orientation. The day on which grafting was performed is counted as Day 0.

At the time of grafting, the cross-section of the mid-diaphyseal region of the 14 days old chick embryonic femur consists of the periosteum with its outer proliferative layer with osteoprogenitor cells of fibroblastic morphology. Beneath this layer are the preosteoblasts followed by the secretory osteoblasts either overlying, or within the layer of osteoid on the surface of the mineralised bone trabeculae with lacunae containing osteocytes. The trabeculae are separated by interconnecting channels containing marrow cells and vascular tissue. This collar of cancellous bone surrounds the central marrow cavity which is gradually enlarging through resorption at the endosteal surface. Overall growth in the circumference of the femur arose from subperiosteal bone deposition, reflected by the higher number of secretory osteoblasts and a thicker osteoid layer on the outermost bone trabeculae. As seen in the cross-section of the femur in Figure 4.1, the implant was partly located in the central marrow cavity and partly within the trabecular bone collar. The base of the implant rested on bone fragments displaced into the marrow cavity when the implant was inserted into the femur or on the endosteal surface of the bone facing the marrow cavity.

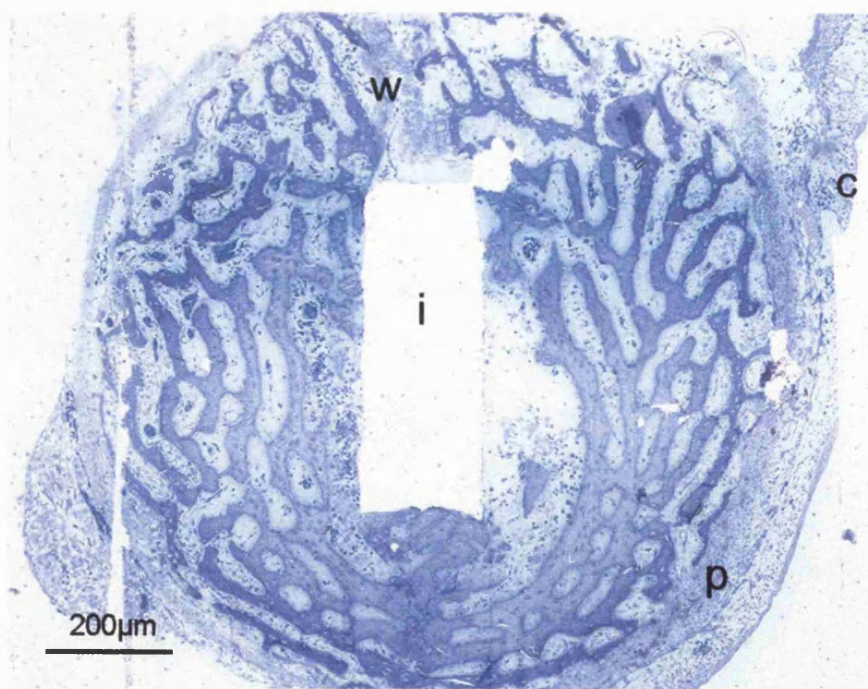


Figure 4.1 Cross section of a femur containing an Apoceram implant one day after grafting on the CAM. The implant was inserted via the wound (w) made through the thickness of the bone collar. Part of the CAM on which the graft lay is seen at the top right (c). Periosteum (p).

Day 1

Blood supply to the femur had ceased when it was removed from the host chick embryo. Despite this, there was extravasation of blood cells into the tissues at the site of implant insertion. One day after the insertion of the implant and placement of the femur on the chorioallantoic membrane, the undersurface of the graft has become attached to the CAM. Gaseous and nutritional supply for the graft came from the chorioallantoic fluid. Marrow cells as well as osteocytes and bone-lining cells at the centre of the graft had undergone necrosis while the periosteal and subperiosteal areas remained vital. There were patches of contact between the implant and the bone trabeculae within the femoral shaft. The wound through which the implant was inserted was filled with a fibrinous blood clot. Most of the implant was surrounded by marrow spaces containing large numbers of blood cells, mostly erythrocytes and thrombocytes and a small number of monocyte/macrophages and granulocytes (Figure 4.2).

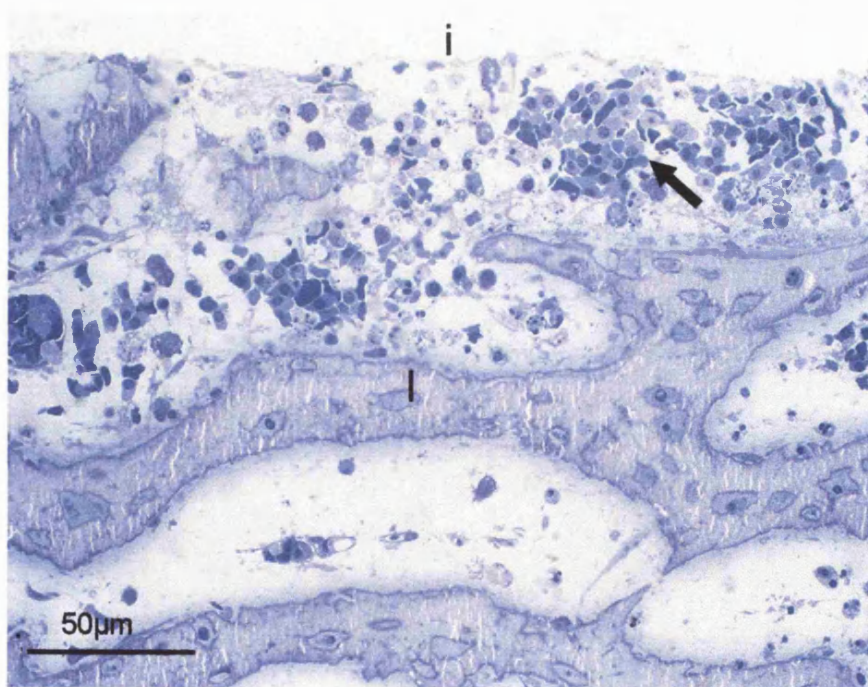


Figure 4.2 *Day 1 after grafting. Apoceram. Blood cells accumulated adjacent to the implant (arrow). Osteocytes at the centre of the graft became necrotic, some empty lacunae can be seen (l). There is degeneration of the marrow tissue between the trabeculae.*

Day 2

The CAM has proliferated to cover nearly half the circumference of the femur but a new blood supply to the centre of the graft has not yet been established. The centre of the grafts showed, typically, cell necrosis and degeneration of the marrow; whereas at the peripheral areas, capillaries containing blood cells were visible. The central marrow area adjacent to the implant was still filled with cell debris. Amongst the degenerating erythrocytes and fibrinous clot, there were some macrophages showing multiple vacuoles formed after the ingestion of the debris. There was no obvious difference at this stage between grafts containing Apoceram and titanium implants.

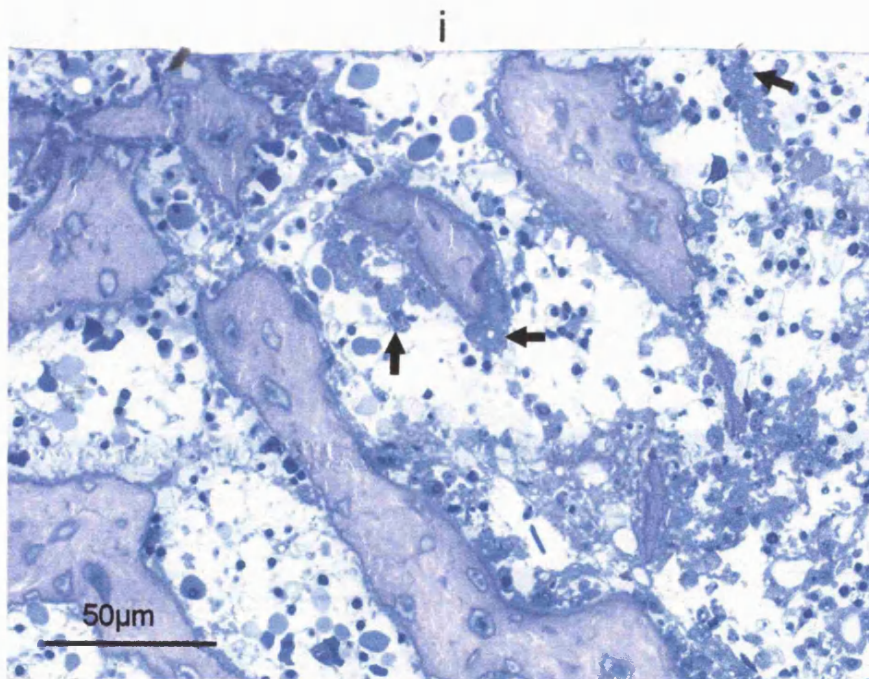


Figure 4.3 *Day 2. Titanium. The marrow spaces are filled with cell debris. There are many macrophages with cytoplasmic vacuoles (arrows)*

Day 3

Vascularity has been re-established by Day 3. The marrow tissue was regenerating. New blood vessels were found within the central marrow cavity. There were still macrophages within the marrow, distinguishable by the numerous cytoplasmic vacuoles formed after the ingestion of cell debris. In the subperiosteal area, formation of osteoid had resumed and the surface of the trabeculae near the centre of the bone collar which had been devoid of cells were being repopulated by osteoblasts. Mesenchymal cells began to accumulate adjacent to the implant surface. Cells with migratory phenotypes were observed on the surface of existing bone trabeculae which were situated close to the implant surface, in particular those at the two ends of the implant away from the central marrow space. The cells which made contact with the implant surface were of elongated shape. There was no obvious difference between specimens containing Apoceram and titanium. (Figure 4.3 Titanium, Figures 4.4, 4.5 Apoceram)

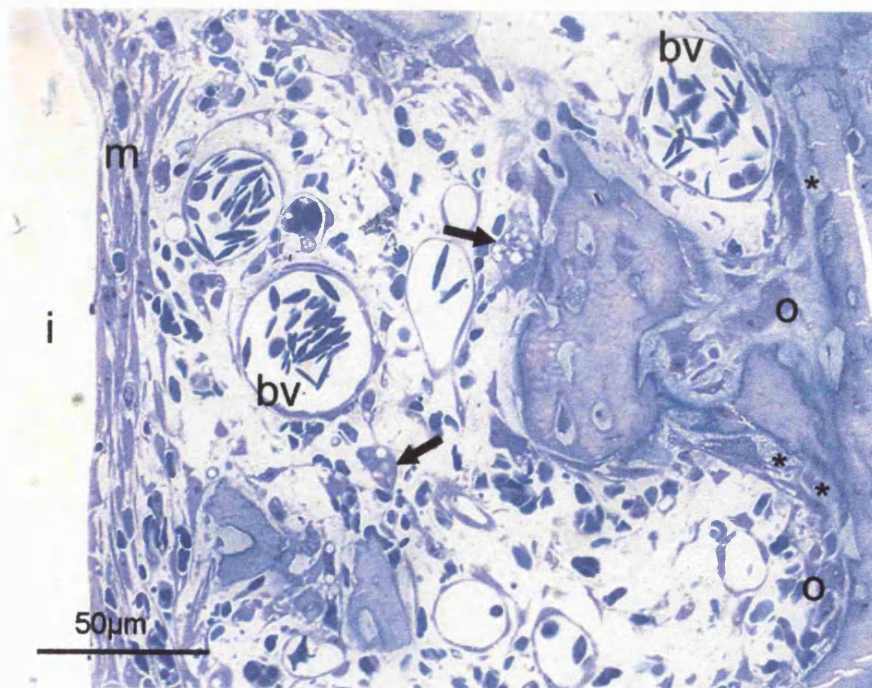


Figure 4.4 Day 3 after grafting. Titanium. *m* - mesenchymal cells, *bv* - blood vessel, *o* - osteoblasts, * - new osteoid, arrow - macrophage.

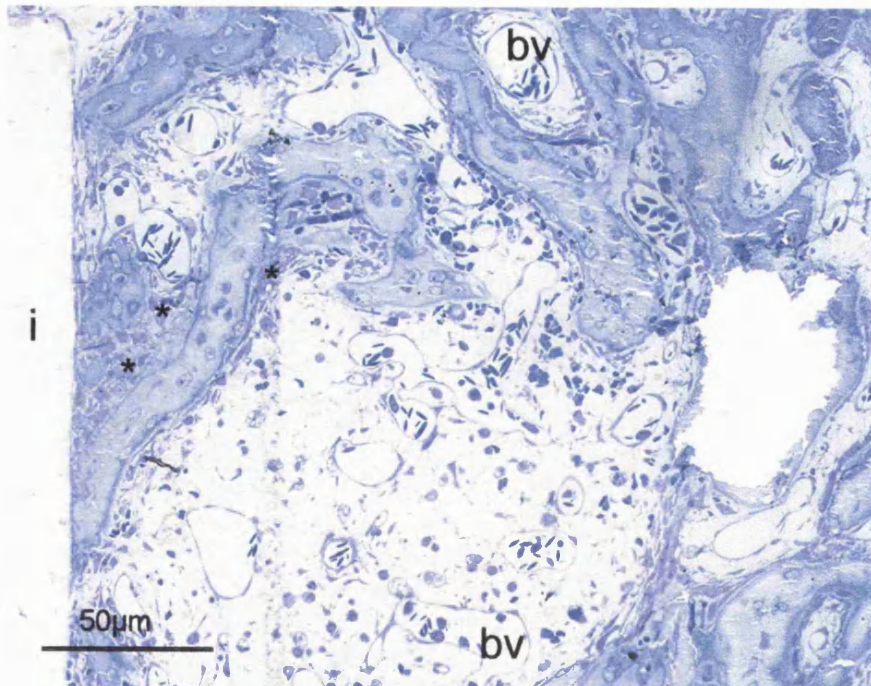


Figure 4.5 Day 3 after grafting. Apoceram. Blood vessels (bv) are clearly visible in the central marrow cavity. Osteoblasts () repopulate the surface of an existing bone trabeculum close to the implant surface and lay down new matrix.*

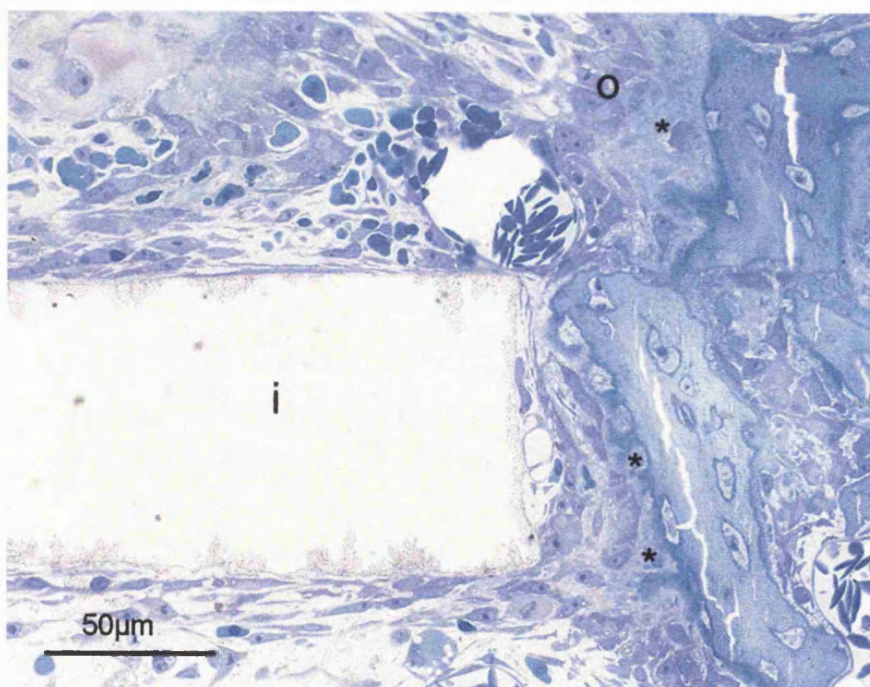


Figure 4.6 Day 3 after grafting. Apoceram. Cell proliferation and migration are the key features at regions near the end of the implant (i). Osteoid formation () has resumed at the surface of the existing bone trabeculae. o = osteoblasts.*

Day 5

New bone formation on the implant surface was evident by day 5. On Apoceram implants, new bone extended from existing trabeculae onto the surface of the implant or was laid down as a thin seam directly on the implant by osteoblasts which had migrated onto the implant surface. For titanium implants, new bone trabeculae extended along the side of the implant with the osteoid and base of the cells laying down the matrix facing the implant surface. These cells were either enclosed within the osteoid or became flattened where the osteoid made contact with the implant. In many areas, struts of osteoid lined by osteoblasts were separated from the implant by bone marrow with small capillaries.

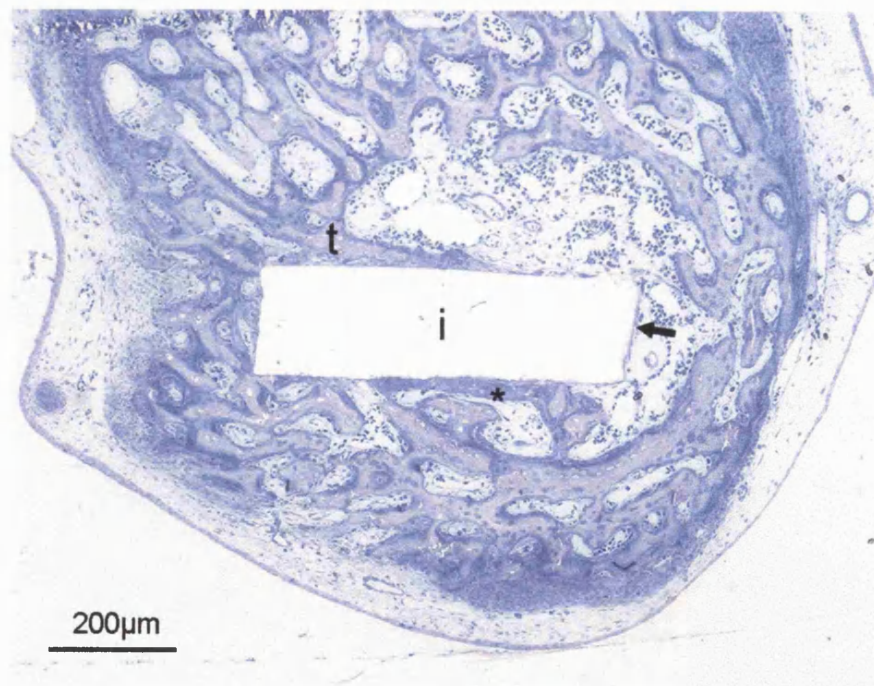


Figure 4.7 Day 5 after grafting. Apoceram. Osteoid (*) being laid down on the surface of the implant. A bone trabeculum (t) from the endosteal region extends down the side of the implant. A thin seam of new bone is formed on the marrow-facing surface of this implant (arrow).

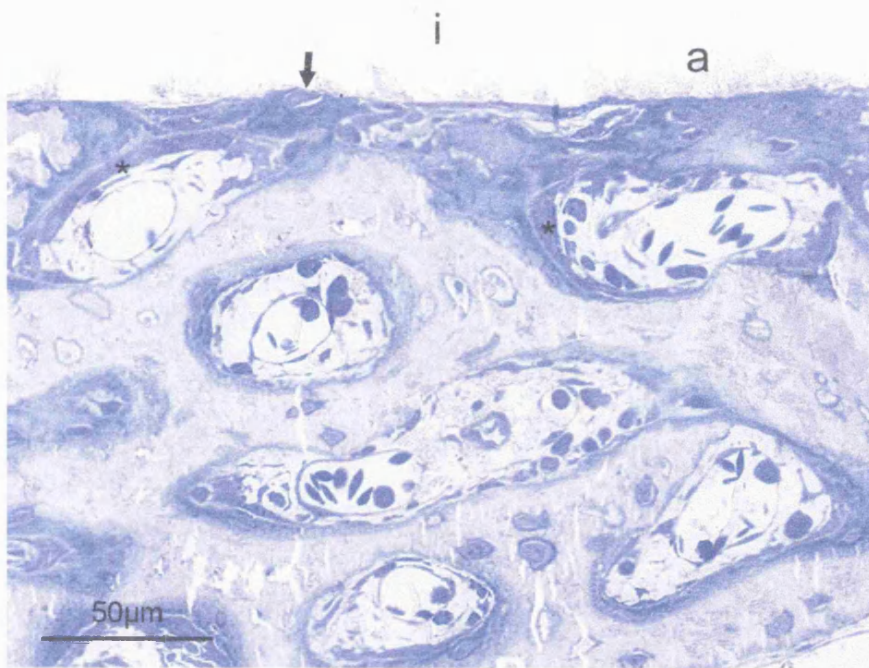


Figure 4.8 Day 5 after grafting. Particles of Apoceram (a) are attached to the newly formed osteoid (*). The osteogenic cells, some of which lie directly on the implant surface (arrow), become trapped within the matrix.

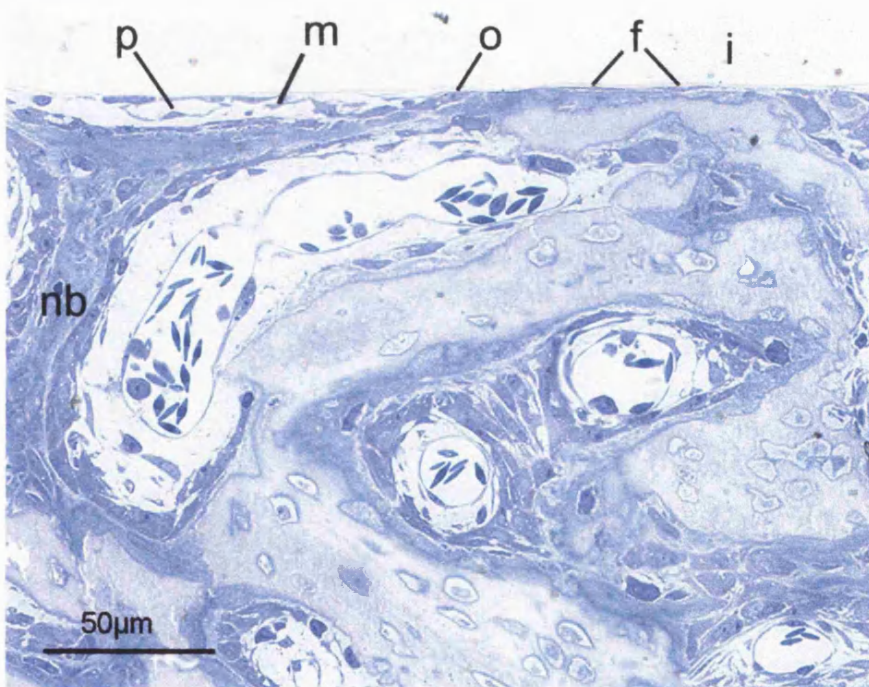


Figure 4.9 Day 5 after grafting. Titanium. A new T-shaped strut of bone is being formed (nb). Osteoblasts (o) line the surface of the new bone which is separated from the implant surface by marrow tissue (m) in which a blood vessel with a pericyte (p) can be seen. Adjacent to this pocket of marrow are flattened cells (f) trapped between the osteoid and the implant surface (i).

Day 7

New bone formation continued and the contact between osteoid and the implant surface increased. It was noted that on the Apoceram implants adjacent to the areas of osteoid and new bone formation, large multinucleated cells were present on the implant surface. These cells were not observed on titanium implants.

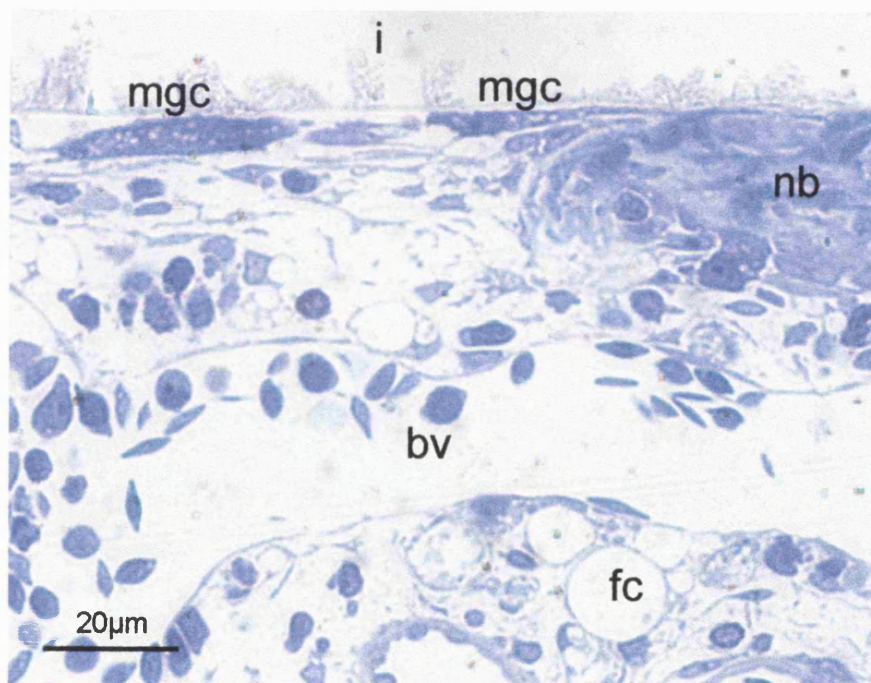


Figure 4.10 *Day 7 Apoceram. Multinucleated giant cells on the surface of the implant (i), in close proximity to a region of new bone formation (nb). bv = blood vessel. fc = fat cell.*

Day 9

By day 9, a significant proportion of the implant surface was in contact with mineralised bone. For Apoceram, such contact was found in areas where the implant passed through the pre-existing bone collar as well as in the region of the central marrow cavity. This mineralised bone usually appeared as a broad band forming an extension of trabeculae from the original bone collar, growing down the side of the implant. But within the central marrow cavity, often a continuous thin seam of mineralising matrix was produced by osteoblasts which had migrated onto the implant surface. The bone-forming cells were either trapped within the mineralised matrix or were interspersed in the osteoid further away from the implant surface. (Figures 4.11 and 4.12)

With titanium implants, contacts with mineralised bone were found mainly in the areas where the implant passed through the pre-existing bone collar. At x200 and x400 magnification, a thin dark blue line, 200-800nm thick was observed on the surface of the mineralised bone facing the implant space in the sections. Where the titanium implant extended into the central marrow cavity, there were patches of contact with mineralised bone and osteoid from trabeculae orientated parallel to the implant surface. Within pockets of marrow tissue, there were elongated, fibroblast-like cells adjacent to the implant. Occasionally, on the endosteal surface of the bone facing the central marrow cavity, and at the junction between bone, implant and marrow, isolated osteoclasts with their bases oriented towards the bone surface could be identified. (Figures 4.13 and 4.14)

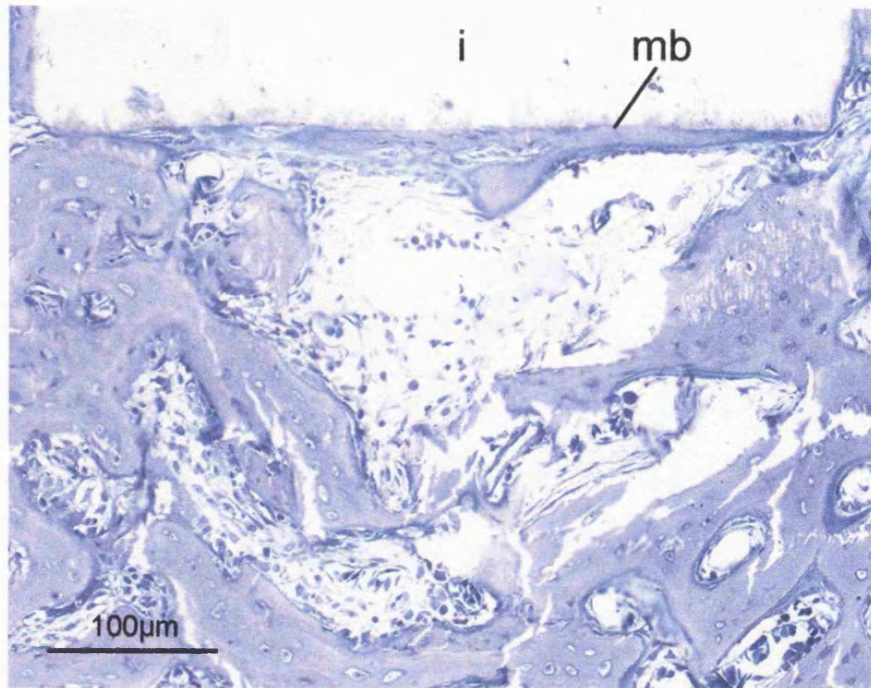


Figure 4.11 Day 9. Apoceram implant across the central marrow cavity. Mineralised bone (mb) in direct contact with implant surface.

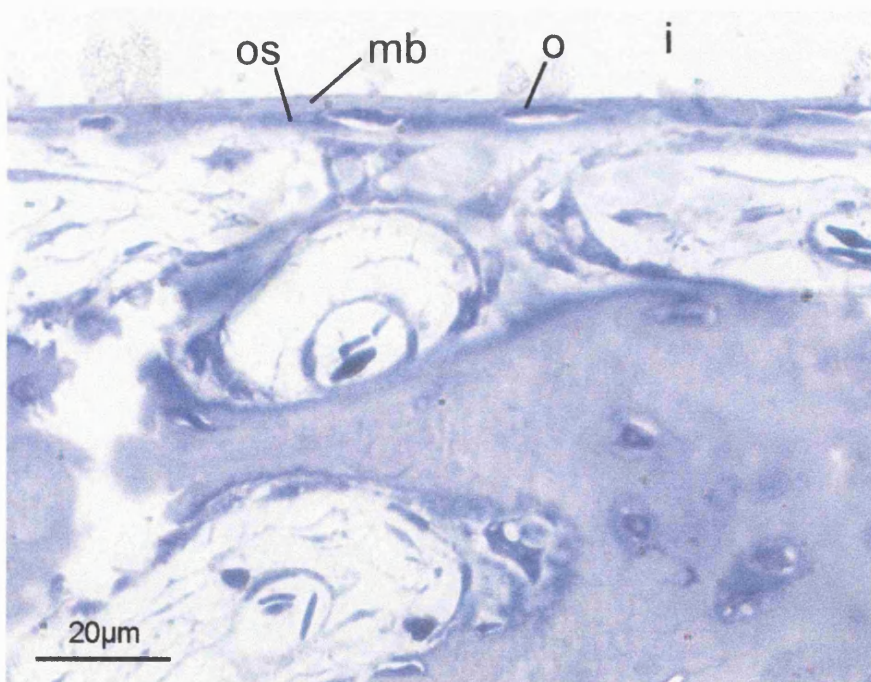


Figure 4.12 Day 9. Apoceram. A thin seam of bone has been laid down on the implant surface. The distribution of mineralised bone matrix (mb) and osteoid (os) suggests that the osteoblasts (o) secreted the matrix directly on the implant. The earlier formed matrix becomes mineralised first, new osteoid is deposited as the osteoblasts move away from the implant surface.

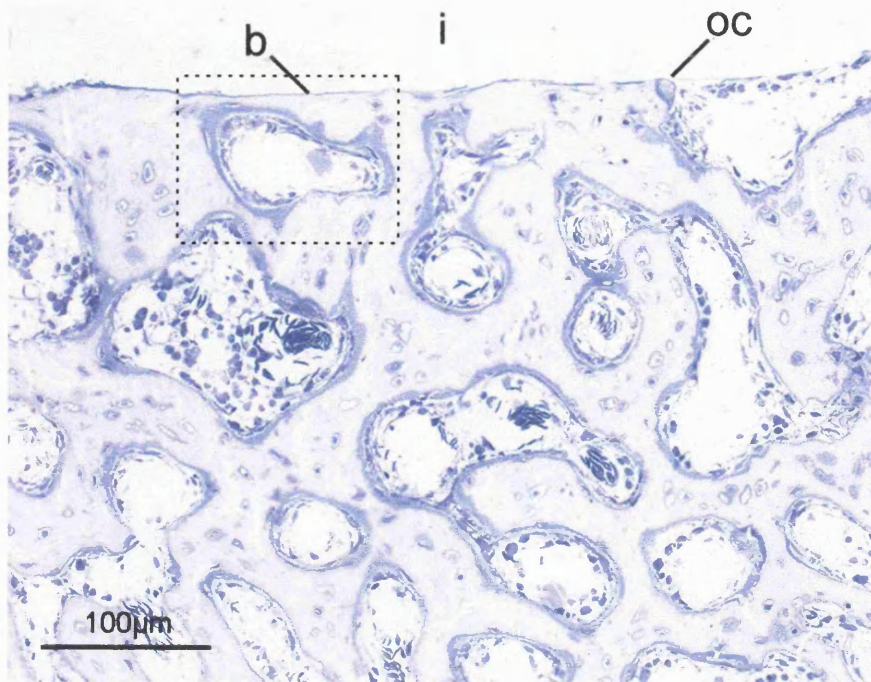


Figure 4.13 Day 9. Titanium. Mineralised bone tissue forming direct contact with the implant surface with an intervening basophilic line (b). At the junction between mineralised bone, implant and marrow, an osteoclast (oc) can be seen with its base against the bone surface.

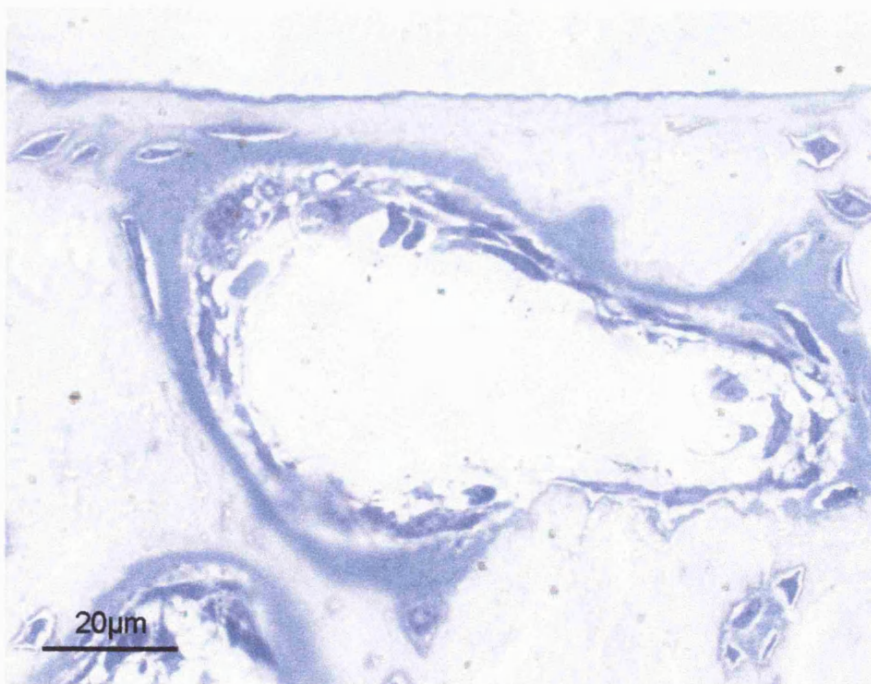


Figure 4.14 Day 9. Titanium. Magnified view of field shown in Fig. 4.13. The basophilic line can be seen clearly at a higher magnification.

Key features in the chronological development of the tissue surrounding the implant can be summarised in Figure 4.15.

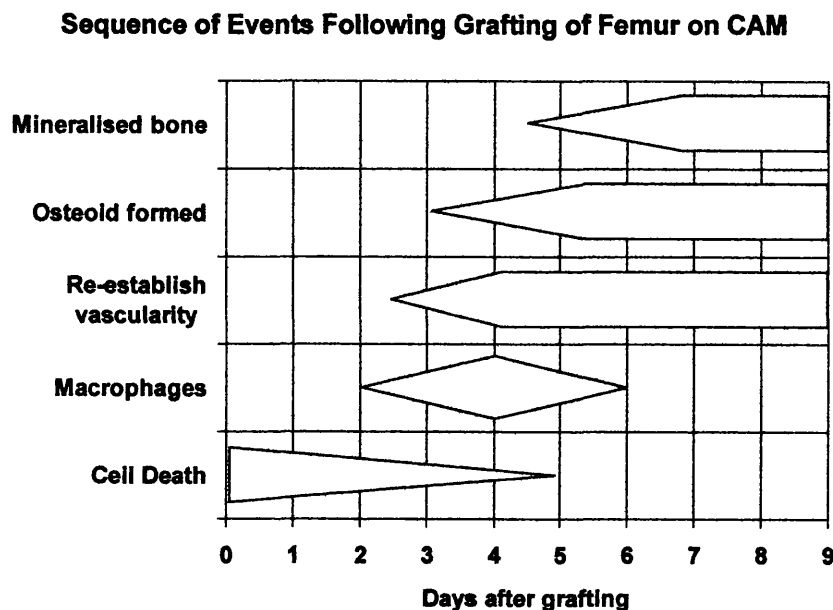


Figure 4.15 *Chronological development of the bone-implant interface*

The stages and timing of the initial phases before Day 5 are similar for grafts containing Apoceram and titanium implants. When new bone is formed within the graft following the re-establishment of the blood circulation, the pattern and amount of bone formation appeared to differ between the two materials. Results of the assessment of the percentage of implant surface in contact with bone is presented in the next section.

4.3.2 Percentage of bone-implant contact

For histomorphometric analysis, sections from six femurs containing titanium implants and six containing Apoceram implants harvested at each of the following time intervals: 1, 2, 3, 5, 7 and 9 days were assessed. The 95% confidence intervals for six measurements of the percentages of the perimeter of the implant in contact with mineralised bone and osteoid, and with mineralised bone alone in one sample section at each time period ranged from $\pm 0.8\%$ to $\pm 3.0\%$ (Appendix III)

The means and standard deviations of the percentages of the perimeter of the implant in contact with mineralised bone and osteoid, and with mineralised bone alone, measured once in four sections from each specimen, are shown in Tables 4.2 to 4.13. The group means and group standard deviations are also presented in the same tables.

The raw data for each time period were analysed using a repeated measures analysis of variance to explore the effect of the type of implant and the within-specimen effect of the sections on the percentage contact with bone & osteoid and with bone alone (Appendix IV). Each femur was treated as one case, with the section variable set as a within-subject factor.

In Tables 4.2 to 4.13, group means marked with asterisks denote that statistically significant differences ($p < 0.05$) exist between Apoceram- and titanium-containing specimens harvested at the same time period. Figure 4.16 provides an overall summary of the results for the six time periods assessed.

Table 4.2 Day 1 Titanium

Specimen	% contact with bone	
	mean	s.d.
1	3.8	2.5
2	5.4	2.3
3	7.5	3.0
4	6.4	1.6
5	2.9	1.5
6	10.3	3.4
	<i>Mean</i> 6.1	
	<i>S.D.</i> 2.7	

Table 4.3 Day 1 Apoceram

Specimen	% contact with bone	
	mean	s.d.
1	4.1	2.8
2	3.5	1.2
3	5.1	2.4
4	2.7	2.1
5	9.9	4.6
6	5.4	3.3
	<i>Mean</i> 5.1	
	<i>S.D.</i> 2.5	

Table 4.4 Day 2 Titanium

Specimen	% contact with bone	
	mean	s.d.
1	6.1	2.3
2	9.2	2.1
3	5.4	3.5
4	3.6	1.8
5	6.3	2.4
6	2.8	2.0
	<i>Mean</i> 5.6	
	<i>S.D.</i> 2.3	

Table 4.5 Day 2 Apoceram

Specimen	% contact with bone	
	mean	s.d.
1	2.4	1.9
2	7.5	2.0
3	4.9	1.8
4	6.6	2.5
5	3.4	1.3
6	3.7	3.2
	<i>Mean</i> 4.8	
	<i>S.D.</i> 2.0	

Table 4.6 Day 3 Titanium

Specimen	% contact with bone and osteoid		% contact with bone	
	mean	s.d.	mean	s.d.
1	4.1	1.4	3.0	0.7
2	7.6	3.4	6.2	3.4
3	9.4	2.7	7.4	1.3
4	6.2	2.1	5.4	1.5
5	6.3	2.7	5.7	2.5
6	8.6	2.4	7.3	2.1
	<i>Mean</i> 7.0 <i>S.D.</i> 1.9		<i>Mean</i> 5.3 <i>S.D.</i> 3.8	

Table 4.7 Day 3 Apoceram

Specimen	% contact with bone and osteoid		% contact with bone	
	mean	s.d.	mean	s.d.
1	4.3	2.4	4.3	2.4
2	7.3	2.3	5.8	3.7
3	5.8	3.9	2.5	1.6
4	11.5	4.2	7.0	2.6
5	12.0	2.3	8.4	2.5
6	11.1	2.6	7.8	1.5
	<i>Mean</i> 8.7 <i>S.D.</i> 3.3		<i>Mean</i> 6.0 <i>S.D.</i> 2.2	

Table 4.8 Day 5 Titanium

Specimen	% contact with bone and osteoid		% contact with bone	
	mean	s.d.	mean	s.d.
1	14.1	3.9	5.2	2.5
2	23.1	4.8	16.8	6.8
3	20.5	3.8	11.4	2.8
4	24.9	9.6	13.4	5.2
5	20.9	7.5	6.3	4.5
6	18.1	6.2	7.9	2.6
	<i>Mean</i> 20.3 <i>S.D.</i> 3.8	*	<i>Mean</i> 10.0 <i>S.D.</i> 4.3	

Table 4.9 Day 5 Apoceram

Specimen	% contact with bone and osteoid		% contact with bone	
	mean	s.d.	mean	s.d.
1	38.9	5.2	11.4	3.4
2	43.7	5.6	17.3	4.0
3	36.4	5.5	11.8	2.3
4	39.6	6.3	15.2	3.5
5	34.5	6.7	14.8	4.7
6	29.1	9.7	8.6	3.0
	<i>Mean</i> 37.0 <i>S.D.</i> 5.0	*	<i>Mean</i> 13.7 <i>S.D.</i> 3.2	

Table 4.10 Day 7 Titanium

Specimen	% contact with bone and osteoid		% contact with bone	
	mean	s.d.	mean	s.d.
1	35.3	5.0	22.4	6.8
2	28.0	8.4	14.0	7.8
3	29.1	4.9	17.8	5.3
4	21.8	4.7	13.4	5.4
5	26.1	9.2	16.8	4.9
6	25.7	8.7	11.6	5.2
	<i>Mean 27.7</i> *		<i>Mean 16.0</i>	
	<i>S.D. 4.5</i>		<i>S.D. 3.9</i>	

Table 4.11 Day 7 Apoceram

Specimen	% contact with bone and osteoid		% contact with bone	
	mean	s.d.	mean	s.d.
1	33.9	11.8	15.6	4.3
2	32.4	9.4	13.9	3.4
3	39.2	5.8	22.6	5.7
4	33.2	8.1	17.8	4.8
5	44.5	8.8	21.4	7.5
6	46.1	8.7	30.7	4.5
	<i>Mean 38.2</i> *		<i>Mean 20.3</i>	
	<i>S.D. 6.0</i>		<i>S.D. 6.1</i>	

Table 4.12 Day 9 Titanium

Specimen	% contact with bone and osteoid		% contact with bone	
	mean	s.d.	mean	s.d.
1	46.1	6.8	32.7	7.8
2	39.7	7.1	27.5	7.7
3	21.8	4.9	14.7	6.9
4	42.1	6.3	22.0	8.9
5	40.6	4.9	23.0	6.4
6	42.6	5.4	20.0	8.3
	<i>Mean 38.8</i> *		<i>Mean 25.0</i> *	
	<i>S.D. 8.6</i>		<i>S.D. 7.3</i>	

Table 4.13 Day 9 Apoceram

Specimen	% contact with bone and osteoid		% contact with bone	
	mean	s.d.	mean	s.d.
1	66.1	11.8	55.9	6.4
2	64.9	10.8	54.6	8.3
3	47.3	7.0	29.7	2.4
4	62.4	12.4	48.2	10.1
5	57.8	8.4	50.6	10.2
6	57.9	9.7	47.6	7.2
	<i>Mean 59.7</i> *		<i>Mean 47.8</i> *	
	<i>S.D. 6.8</i>		<i>S.D. 9.5</i>	

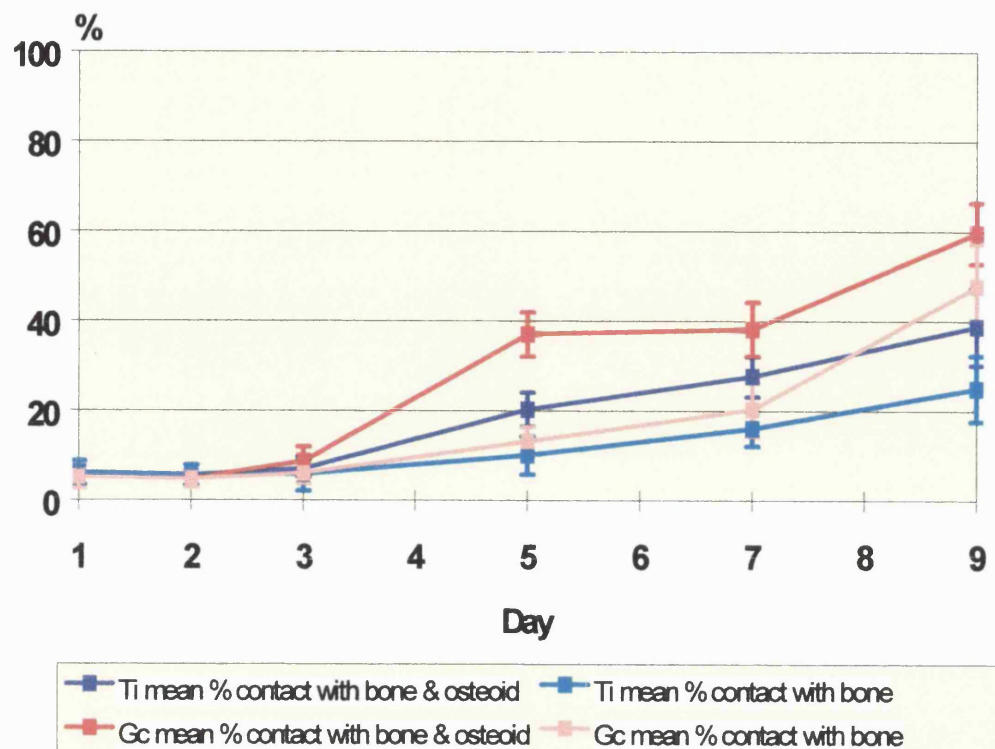


Figure 4.16 Summary of the means and standard errors of percentage of implant perimeter in contact with bone and osteoid. Titanium: Ti. Apoceram glass ceramic :Gc.

4.3.3 Histochemical and immunohistochemical staining

4.3.3.1 Von Kossa staining for mineralised bone tissue

Contact between mineralised bone and the implants was confirmed with Von Kossa staining. Mineralised bone trabeculae stained chocolate brown. Examples of sections are shown in Figures 4.17 and 4.18.

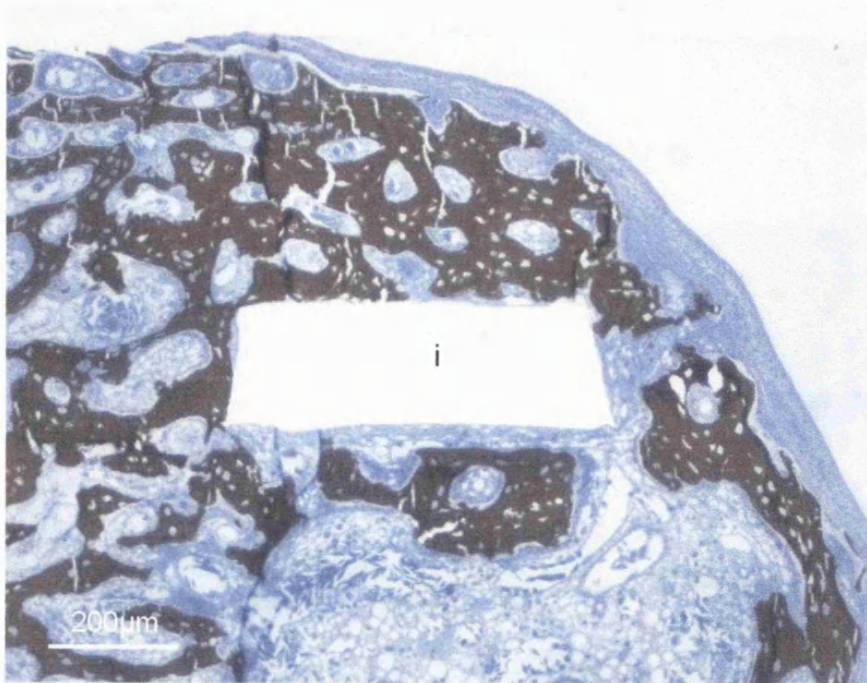


Figure 4.17 Von Kossa staining. Titanium implant. Calcified bone is stained dark brown. Toluidine blue counterstain.

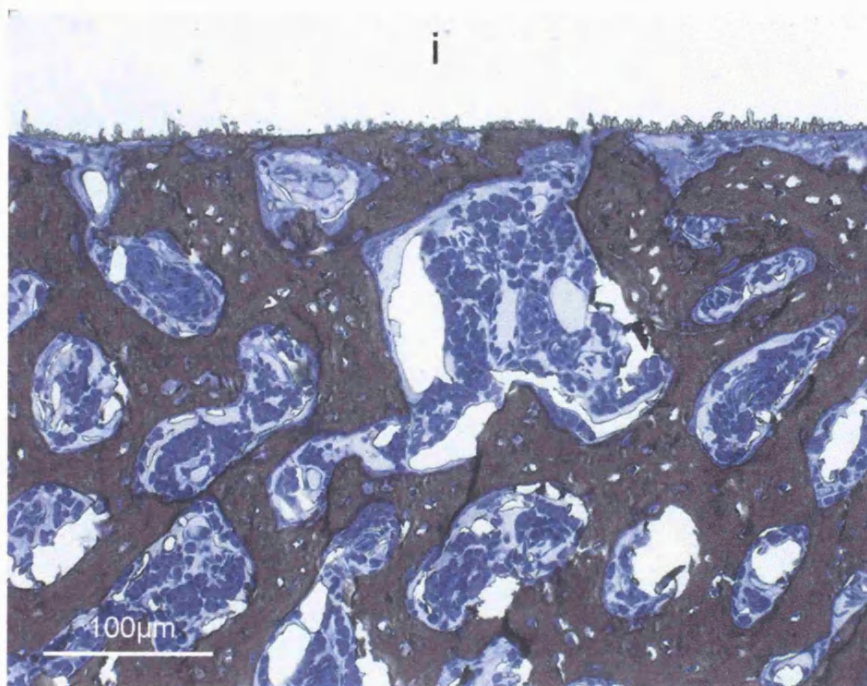


Figure 4.18 Von Kossa staining. Apoceram. Mineralised bone forming direct contact with particles of the glass ceramic attached to the interface.

4.3.3.2 Alkaline phosphatase staining

The results of alkaline phosphatase staining are illustrated in Figures 4.19 - 4.20. The enzyme appears red in the sections. Within the cross-section of the femur, the periosteal region can be seen to stain intensely positive for alkaline phosphatase, the cells lining the trabeculae also stained positive for the enzyme but the level of expression at the endosteal surface was lower than that at the periosteal region. Alkaline phosphatase staining was found directly on the implant surface where there was active new bone formation.

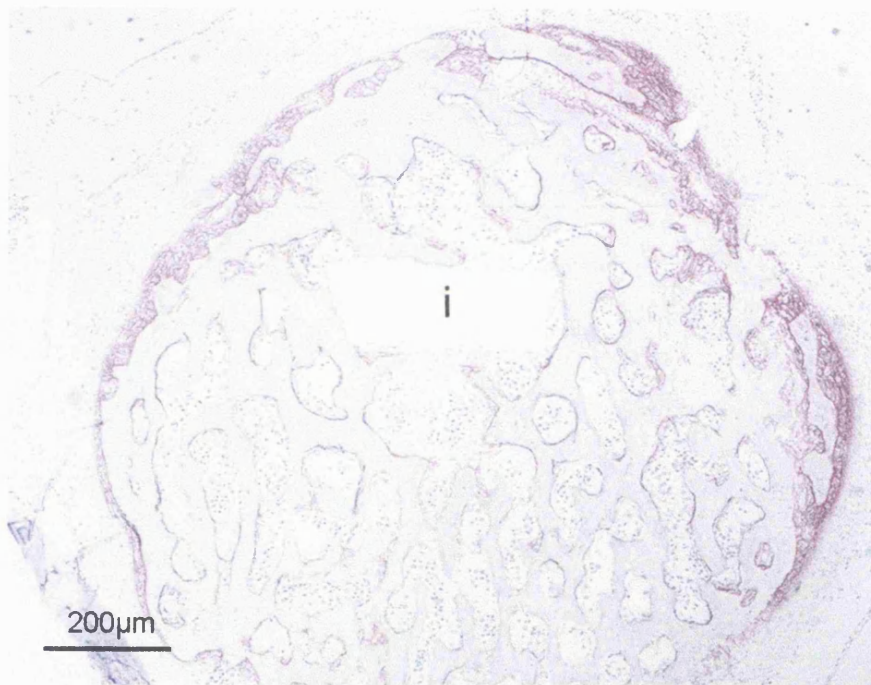


Figure 4.19 Alkaline phosphatase distribution. Titanium implant. 7 days after grafting. Haematoxylin counterstain.

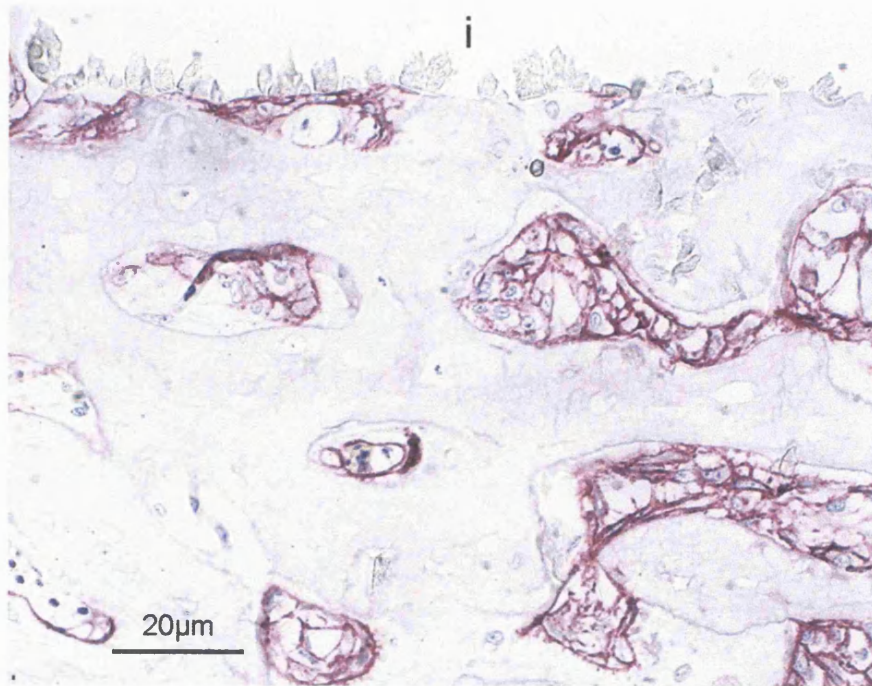


Figure 4.20 *Apoceram at 7 days after grafting. Many alkaline phosphatase positive cells are present on the surface of the implant. Haematoxylin counterstain.*

4.3.3.3 Tartrate resistant acid phosphatase

Within the cross-section of the femur, positive staining for tartrate resistant acid phosphatase (TRAP) was found along the endosteal surface around the central marrow cavity and largely absent in the periosteal tissue. Intense staining was found in large multi-nucleated cells, presumably osteoclasts and the trabecular surfaces in contact with them. When tartrate solution was omitted from the reagents for staining, the distribution of positive staining represented that of acid phosphatases. This showed a distribution similar to that of TRAP except for the additional positive staining of a small number of mononuclear cells within the bone marrow. The distribution of TRAP positive cells differed between specimens with the titanium and glass ceramic implants in that several of these large multinucleated cells could be present along the perimeter of Apoceram implants and the positive staining for TRAP extended onto the implant surface and bone surface adjacent to these cells. TRAP positive cells were not observed on the titanium surface in the specimens examined (Figures 4.21 and 4.22).

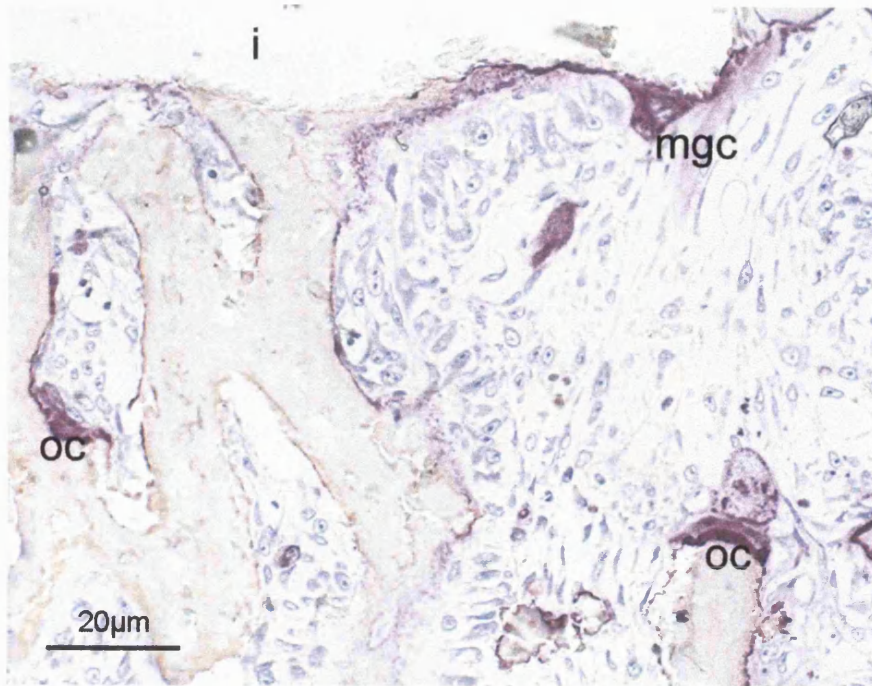


Figure 4.21 *Apoceram 5 days. Intense staining for TRAP is present in a multinucleated giant cell (mgc) on the surface of the implant and osteoclasts (oc) on the bone trabeculae. The endosteal bone surface and the implant surface also showed positive staining.*

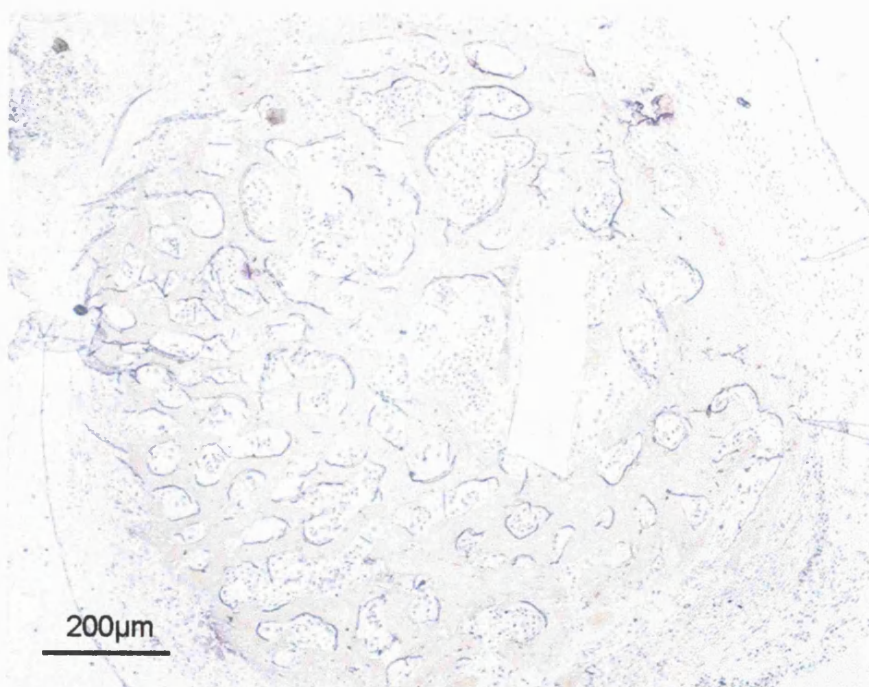


Figure 4.22 *Titanium at 5 days. Positive staining for acid phosphatase is found mostly on the endosteal surfaces and in osteoclasts and some mononuclear cells in the marrow.*

4.3.3.4 Tetracycline labelling

The dosage used for labelling of the mineralisation front was 1mg tetracycline hydrochloride in 0.5ml PBS per egg. It was not possible to produce sections much thicker than 2-3 μ m using the diamond knife without inducing excessive damage in the section and the knife-edge. Tetracycline fluorescence faded very quickly at the light intensity used for photography of the sections. The images presented in Figures 4.23 to 4.26 provide a limited amount of information. In general, the mineralisation front could be clearly seen in the subperiosteal region of the graft where new bone formation was most abundant.

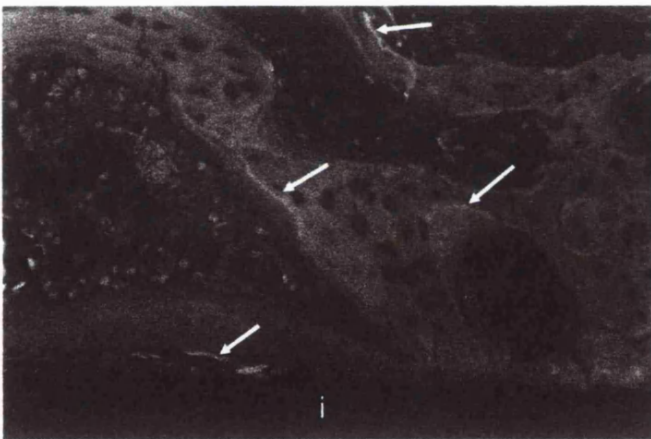


Figure 4.23 Day 7. Titanium. The mineralisation front on the bone trabeculae. Original magnification: x200

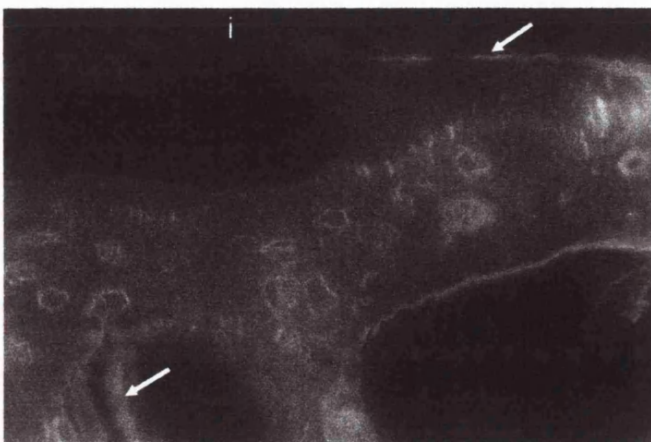


Figure 4.24 7 days after grafting. A thin line of fluorescent material lies against the surface of this Apoceram implant. Original magnification: x400

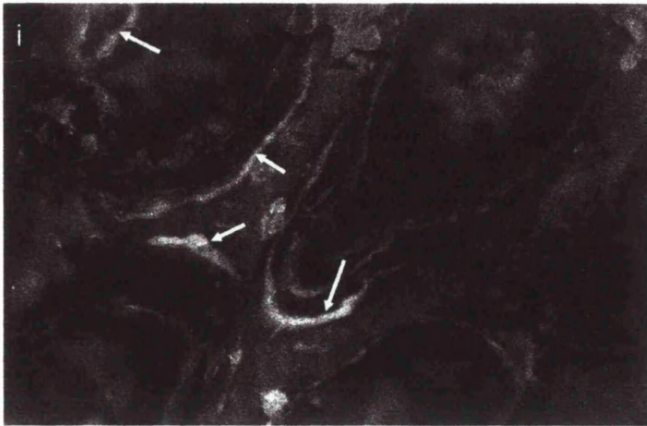


Figure 4.25 Day 9. Apoceram. Tetracycline fluorescence located between the osteoid and mineralised bone at the mineralisation front. Original magnification: x200

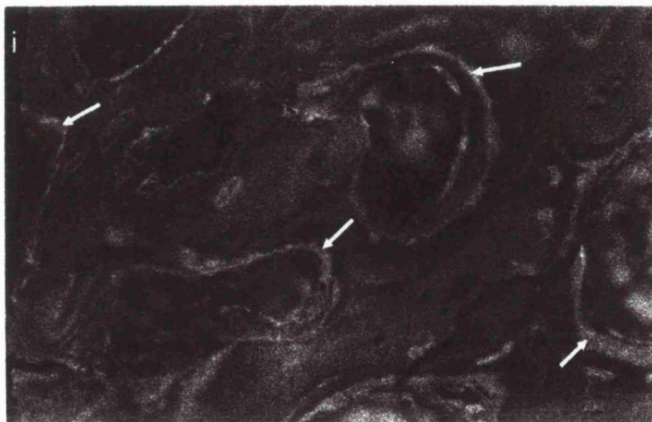


Figure 4.26 Day 9. Titanium. Tetracycline fluorescence located between the osteoid and mineralised bone at the mineralisation front. Original magnification: x200

4.3.3.5 Immunohistochemistry of bone matrix proteins

The negative control sections in which non-immune rabbit serum was used instead of the primary antibodies had no positive staining, as seen in Fig. 4.27. The long periods of immersion in aqueous solution required for the staining protocol resulted in lifting and creasing of the sections even though the slides have been precoated with poly-L-lysine. Positive staining for LF67 (type I collagen) was present in the periosteum, within the bone trabeculae and overlying osteoid and weakly in osteoblasts and some osteocytes. For titanium implants, where the surfaces contact marrow tissue, there was no staining for LF67. Positive staining for the same antigen could be detected in seams of tissue on Apoceram implants. Positive staining for LF8 (osteonectin) was found in the periosteum, the matrix of fully mineralised bone trabeculae but only weakly in the osteoid, in osteoblasts and some osteocytes. The pattern of distribution of Type I collagen (LF67) and osteonectin (LF8) are shown in Figs. 4.28- 4.29.

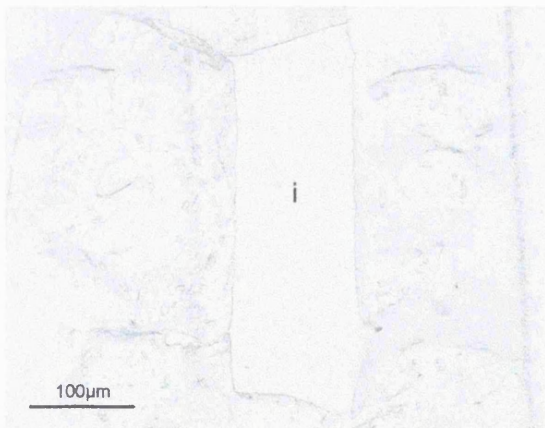


Figure 4.27 Negative control, pre-immune rabbit serum used instead of primary antibody. The section is clear at the end of the staining procedures.

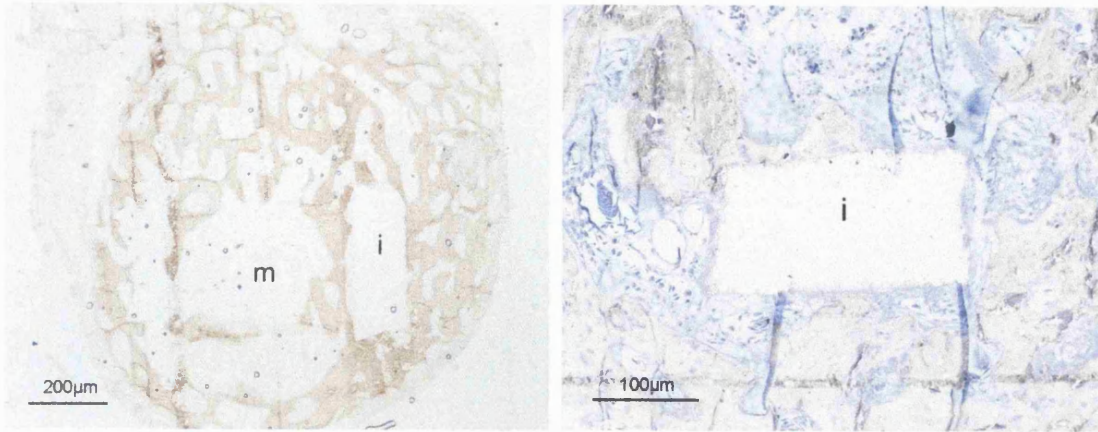


Figure 4.28 Staining for type I collagen (LF67). Left: Day 7. Titanium. No counterstaining. (m) central marrow cavity. Right: Day 7. Apoceram. Counterstained with toluidine blue.

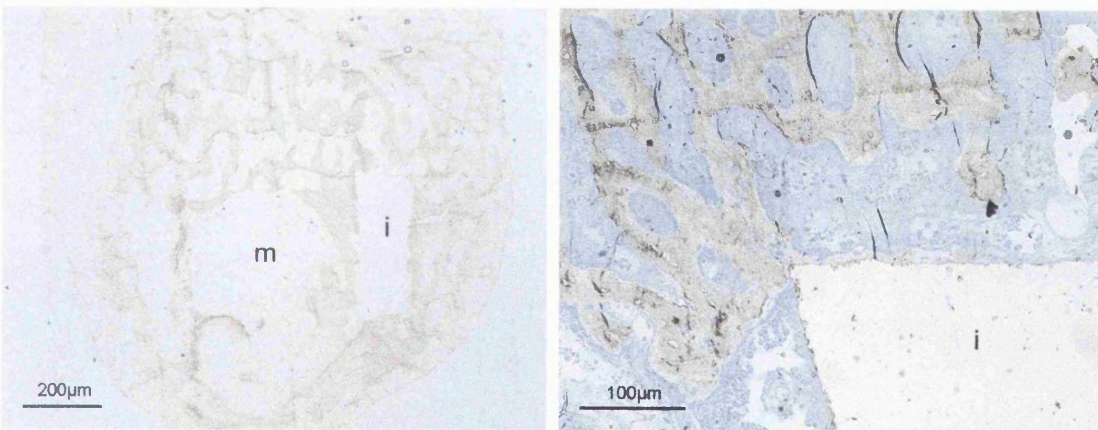


Figure 4.29 Staining for osteonectin (LF 8). Left: Day 7. Titanium. No counterstaining. Right: Day 7. Apoceram. Counterstained with toluidine blue.

4.3.4 Ultrastructure of the bone implant interface

The preservation of the tissues at the bone-implant interface during the preparation of ultra-thin sections of grafts containing the hard implants was essential to the interpretation of such sections. During sectioning, the glass ceramic material, Apoceram, fractured as the knife-edge passed through the implant. When the sections were floated in the boat, fractured particles could be seen to sink slowly to the bottom of the boat. Care was taken to prevent loose particles from floating onto the surface of the embedded bone tissue. In the electron micrographs, there is good evidence of the preservation of the interface tissue as glass ceramic particles remained attached to the embedded tissue. For specimens containing titanium implants, it was not possible to produce ultrathin sections without removal of the metal. The fracture technique used for separating the implants from the resin-embedded tissue yielded a small number of fragments of tissue cleanly separated from the metal surface but in an unpredictable fashion. When these fragments were re-embedded and sectioned, the titanium-tissue interface appears as a thin electron dense line. The images presented here are of interfaces between the implants and the bone tissue at 9 days after implantation and grafting. (Figures 4.30 to 4.44)

4.3.4.1 *Apoceram*

Areas of contact between Apoceram and bone show a variety of ultrastructural features. Figure 4.30 shows the direct attachment of an osteocyte on the surface of the glass ceramic material. The cell is well spread on the implant surface and surrounded the other side by a matrix of mineralised collagen. There is no distinct direction of orientation of collagen fibres in this region in which osteocytes with cell processes are embedded in the matrix. Also present on the implant surface are polygonal osteoblasts with matrix vesicles and secreting collagen. A zone of osteoid, in which collagen fibres are clearly distinguishable, surrounds the secretory osteoblast and more electron dense mineralised matrix appears adjacent to this, extending along the surface of the implant material (Figure 4.31). In areas where osteoid was in contact with the implant surface, collagen fibres with characteristic banding can be seen immediately adjacent to the glass ceramic remnants without an intervening afibrillar zone. (Figure 4.32)

There are also areas where the implant surface is covered by one or multiple layers of loosely packed flattened cells. These cells frequently show signs of degeneration. (Figure 4.33)

A small number of the ultrathin sections contained parts of the multinucleated giant cells attached to the surface of the Apoceram particles. Numerous lysosomal granules are present in their cytoplasm. (Figures 4.34, 4.35)

In areas where more heavily mineralised matrix was adjacent to the Apoceram implant surface, the calcified material either appears to be continuous with the glass ceramic particles (Figure 4.36) or shows several other distinctive features at the interface zone. At x40,000 magnification, there were globular calcified deposits, often fused together, which were continuous with the Apoceram particles. Needle-like mineral aggregates as well as amorphous electron dense globules were interspersed between collagen fibrils at the interface zone (Figures 4.37, 4.38). Another type of interface arrangement showed this spherical calcified material adjacent to mineralised collagen matrix which was separated from the Apoceram particles by a layer of loosely arranged fibrils (Figure 4.39).

4.3.4.2 *Titanium*

The tissue-titanium interface was represented by an electron dense line in the TEM sections presented. Some osteoblasts lie directly on this line, with osteoid laid down on the other sides of the cell (Figures 4.40 to 4.42). Mineralised bone matrix was separated from the electron dense line by a zone of collagen fibres and a band of fibrillar material around 800nm thick, with a reticular appearance (Figures 4.43 and 4.44).

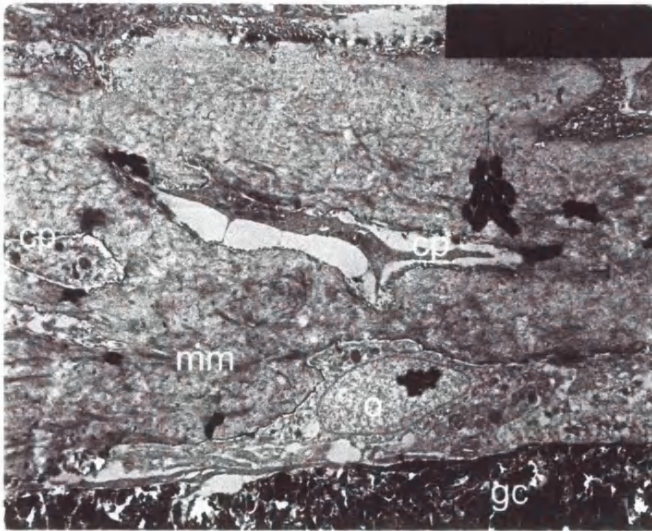


Figure 4.30 An osteoblast (o) on the surface of Apoceram (gc) is being surrounded by mineralised matrix (mm). Two osteocytes with cell processes (cp) can be seen within the bone matrix. Collagen fibres in cross-section can be seen at the top of the field. Field width: 25 μ m

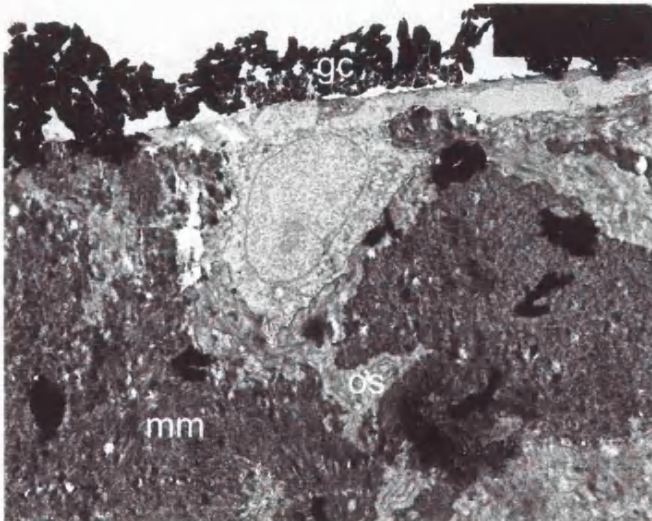
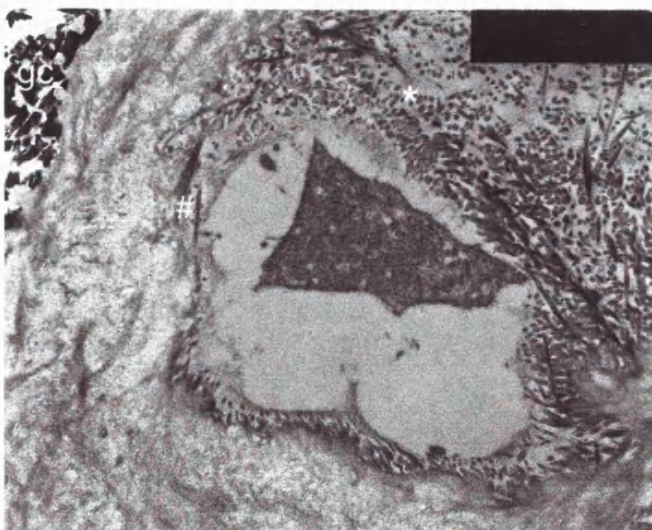


Figure 4.31 The osteoid and mineralised matrix surrounding this osteoblast on Apoceram (gc) can be differentiated by the different levels of electron density. Collagen fibres are visible within the osteoid (os) but not discernable where they are more heavily mineralised (mm). Matrix vesicles are present in the cytoplasm of this bone forming cell (arrow). Field width: 25 μ m



*Figure 4.32 Apoceram. Collagen fibres at different orientation surrounding a lacuna containing the cell process of an osteoblast. Osteoid in direct apposition against the glass ceramic (gc) particles. # collagen fibres in longitudinal section. * collagen fibres in cross-section. Field width: 14 μ m*

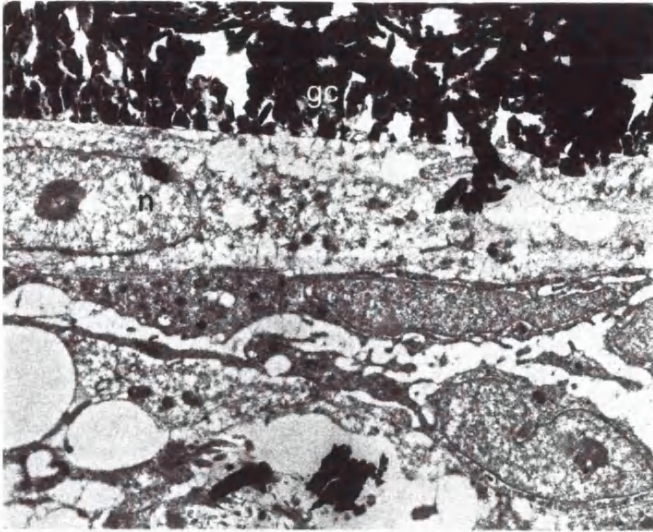


Figure 4.33 Apoceram. The presence of ceramic particles (gc) at the top of the field reflects the preservation of the interface. The implant surface is covered by several elongated cells showing signs of degeneration. Field width: 14 μ m

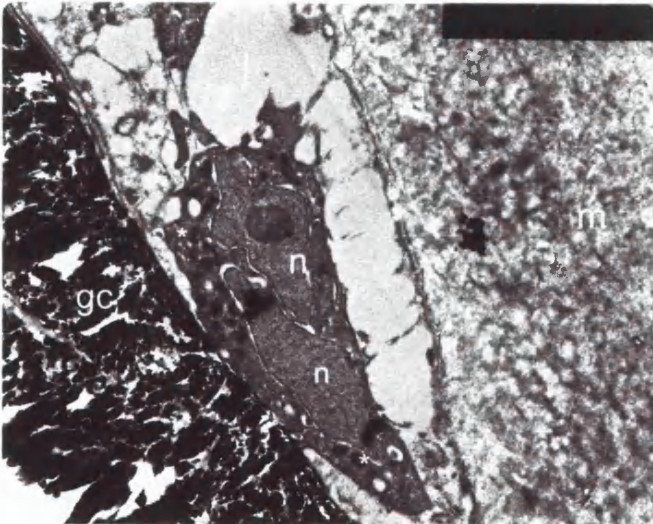


Figure 4.34 Part of a multinucleated giant cell on the surface of Apoceram (gc). Two nuclei (n) are visible with many electron dense lysosomal granules in the cytoplasm (). m - mineralised matrix. Field width: 17.5 μ m*

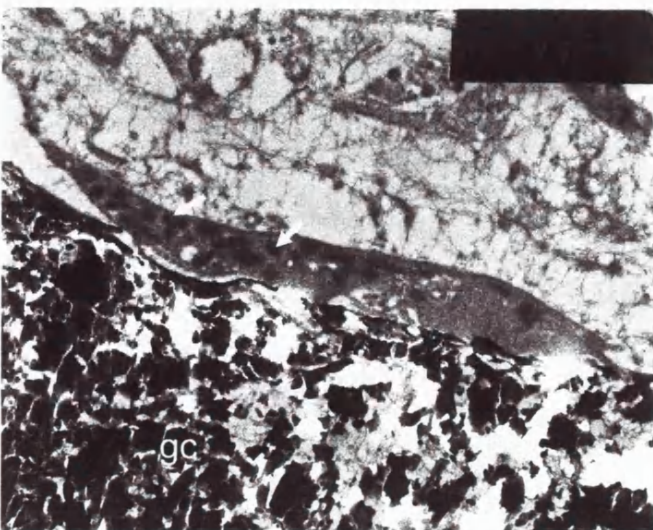


Figure 4.35 Part of a multinucleated giant cell attached to the surface of an Apoceram implant (gc). Arrows: lysosomal granules. Field width: 8.75 μ m

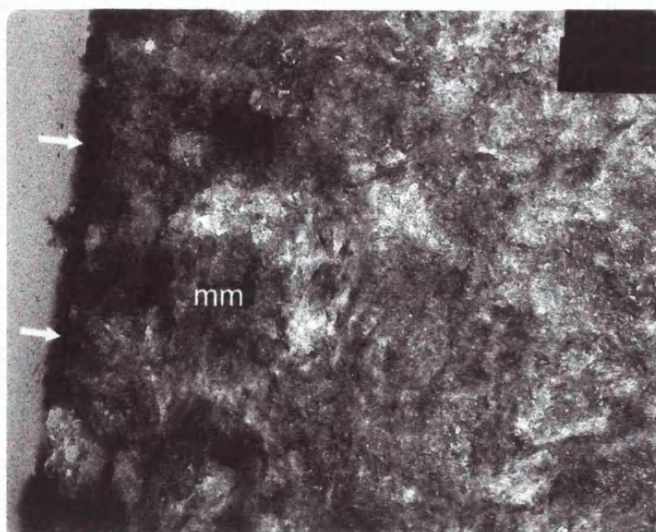


Figure 4.36 Dense mineralised matrix (mm) making direct contact with Apoceram. The arrows indicate a continuous layer of the glass ceramic remaining attached to the mineralised matrix following sectioning. Field width: 35 μ m

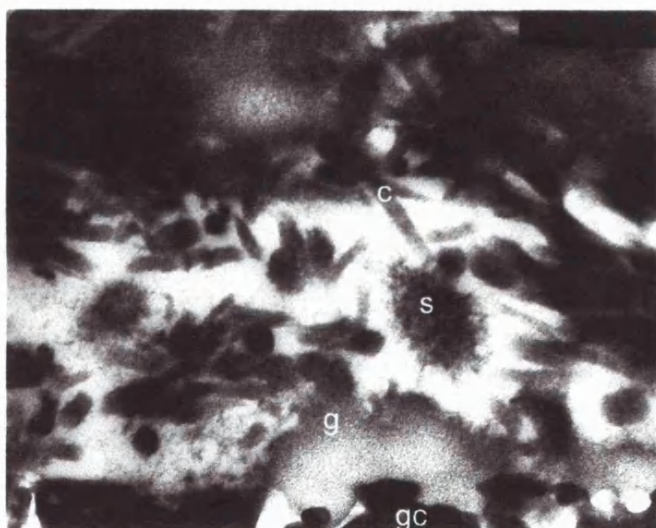


Figure 4.37 Apoceram (gc). Needle-like mineral aggregates (s) amongst the collagen fibres. The glass ceramic is continuous with amorphous globular deposits (g), collagen fibres (c) with characteristic banding intermingle with the mineral deposits. Field width: 1.75 μ m

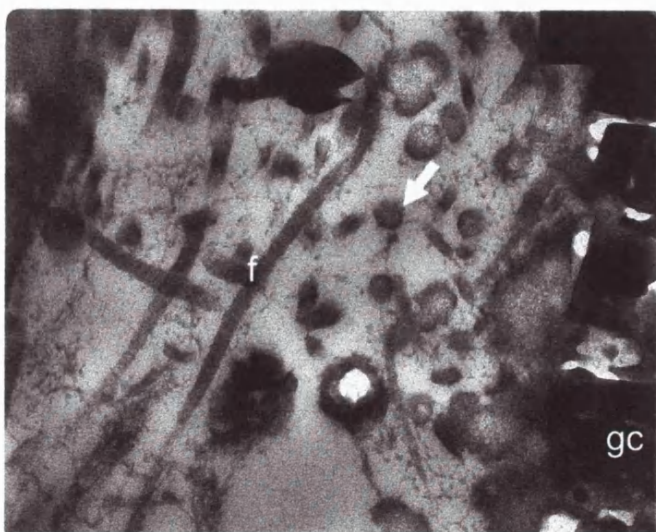


Figure 4.38 Apoceram (gc). Fused globular mineral deposits continuous with the glass ceramic particles. Isolated spheres of mineral (arrow) interspersed among banded collagen fibres (f) on a background of thin fibrillar material. Field width: 1.75 μ m

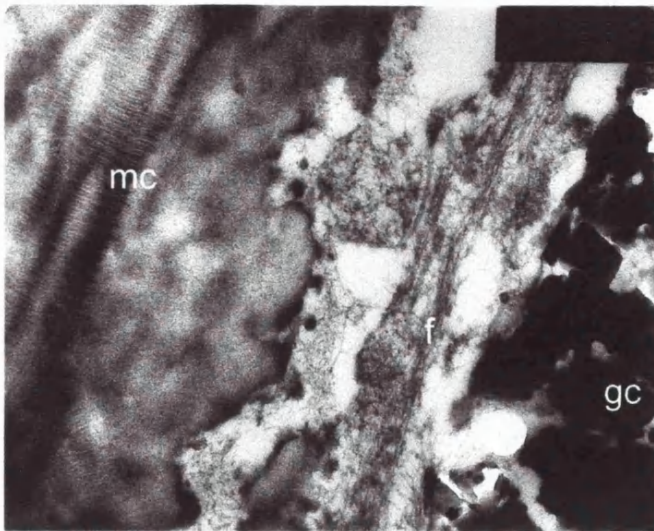


Figure 4.39 Apoceram. A less dense fibrillar zone (f) is present between the mineralised matrix and the glass ceramic particles (gc). Spherical mineral deposits are present along the edge of the calcified collagen matrix (mc). Field width: 3.5 μ m

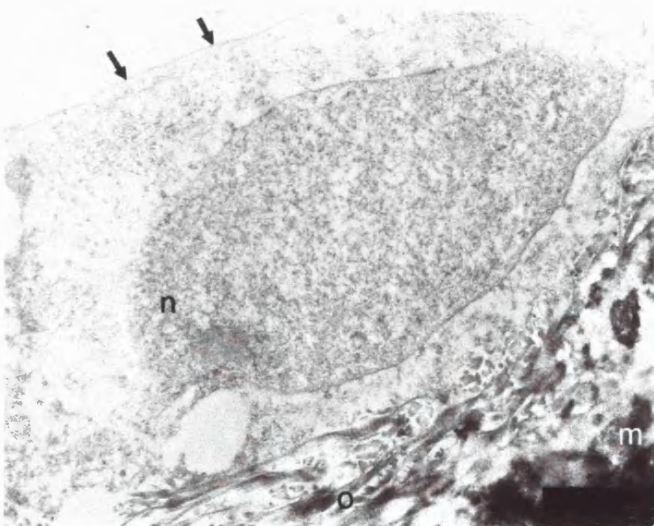


Figure 4.40 Titanium. A continuous electron dense line at the metal interface with the tissue (arrows). Collagen fibres within a band of osteoid surround the cytoplasm and part of the nucleus (n) of this osteoblast on the implant surface. A small area of mineralised matrix (m) can be seen at the bottom right of the field. Field width: 7 μ m

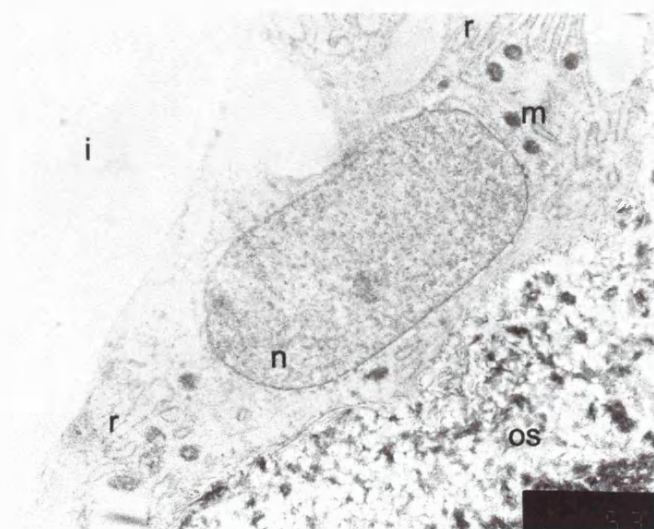


Figure 4.41 Titanium. Mitochondria (m) and rough endoplasmic reticulum (r) in the cytoplasm surrounding the nucleus (n) of this osteoblast surrounded by osteoid (os) at the interface. i - implant space. Field width: 8.75 μ m

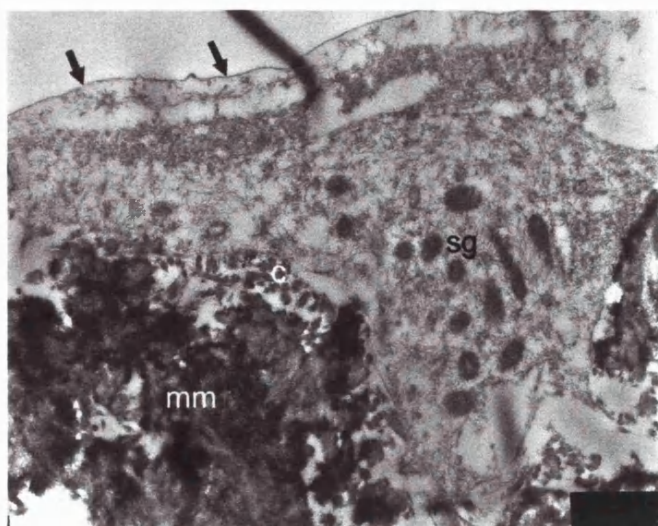


Figure 4.42 Titanium. Electron dense secretory granules (sg) within the cytoplasm of a secretory cell depositing collagen (c). mm-mineralised matrix. Arrows - interface. Field width: 7 μ m

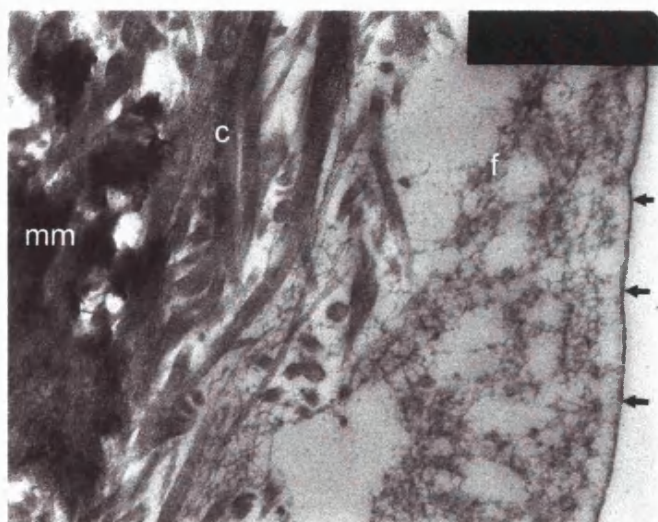


Figure 4.43 Titanium. A layer of loose fibrils with a reticular appearance (f) lies between the titanium surface and collagen fibres (c) on the surface of the mineralised matrix (mm). Arrows - electron dense line at the interface. Field width: 2.6 μ m

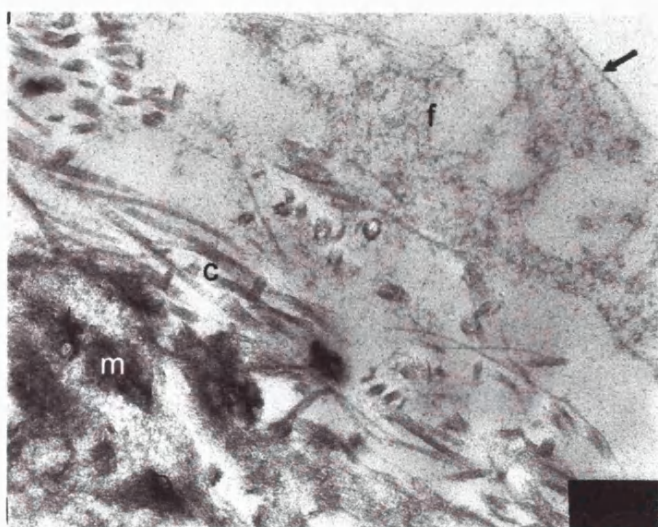


Figure 4.44 Titanium. Unmineralised layer with thin fibrils (f) between the titanium surface (arrow) and collagen fibres (c) overlying the mineralised matrix (m). Field width: 2.6 μ m

4.4 Discussion

4.4.1 The sequence of events following implantation and grafting

In the chick embryonic femur CAM graft model, the process of bone healing following implant insertion can be divided into two phases: *before* and *after* the re-establishment of the vascular supply to the graft. The first phase took place over the first three days following grafting. During day 1 and day 2 of the culture period, the key features were extravasation of blood cells into the marrow spaces and cell death within the centre of the graft. Marrow tissue, osteoblasts and osteocytes all underwent necrosis while the periosteal and subperiosteal regions remain viable since the graft was bathed in chorioallantoic fluid which formed the medium for exchange of gases, nutrients and metabolic wastes.

During this time, the CAM proliferated around the periosteum of the femur. By day 3 the whole femur was enveloped by the CAM tissue which has brought with it a new blood supply. The re-establishment of the blood circulation was evident in the formation of new blood vessels and re-organisation of the marrow tissues with large numbers of macrophages removing the dead marrow tissue. Surfaces of the bone trabeculae became repopulated by cells which go on to form osteoid.

By day 5, the wound created for the insertion of the implant had become bridged by periosteal proliferation and new osteoid joining the two sides of the bone margins. There were several patterns of osteoid deposition at the interface with Apoceram. The first was where an existing bone trabeculum was in close proximity with the implant. Following repopulation of the bone surface, osteogenic cells laid down new matrix which extended along the implant surface. The cells became enveloped in the matrix which eventually became mineralised. The second pattern was one in which the base of the osteoblasts was first attached to the implant surface and osteoid was formed towards the direction of the marrow cavity. The new bone thus formed had the mineralised region on the implant surface and the osteoid further away from it. This arrangement was most frequent at the region of the implant within the central marrow cavity. The first pattern described was also evident on titanium surfaces, but the second was predominantly found

in Apoceram. A different pattern was observed in regions where titanium crossed the central marrow cavity, where struts of new bone were formed parallel to the implant surface but not directly on its surface. Patches of marrow tissue separated the new bone from the titanium. Further deposition of matrix on these new struts of bone resulted in the bone-forming cells being trapped between the osteoid and the implant surface. The distribution of alkaline phosphatase staining in the glycol-methacrylate embedded sections further reinforced the observed difference in the pattern of bone formation between the two materials. On day 7, many of the cells on the surface of Apoceram had positive staining for alkaline phosphatase, corresponding to the regions of osteoid and bone formation directly on the implant surface. For the femoral grafts with titanium implants, alkaline phosphatase staining was found on the surface of new bone formed adjacent to titanium surface. Positive staining was present in the osteoid and the associated cell layers making contact with the implant surface.

4.4.2 Cells contributing to the healing response

The bridging of the wound created for the insertion of the implant is likely to have arisen from the periosteum within which osteoprogenitor cells proliferate and differentiate into active osteoblasts laying down new matrix across the gap. The bone cells originally on the surface of the trabeculae at the centre of the graft underwent necrosis during the first two days following grafting and were replaced by new osteoblasts when the circulation was re-established. Extensive anastomosis of the marrow spaces would allow the migration of cells from the viable areas of the graft. The newly organised marrow also provided a source of mesenchymal stem cells which differentiated into the osteoblasts that lay down new matrix on the existing bone trabeculae and on the implant surface. On day 5, many of the cells on the surface of Apoceram showed intense positive staining for alkaline phosphatase, a marker for differentiated osteoblasts.

The new osteogenic cells are likely to originate from the graft rather than the host. This is supported by observations in chimera experiments reported in the literature. Simmons and Gilliam (1981) performed an experiment in which wounds were produced in the cartilaginous epiphyses of quail femurs which were then grafted on the CAM of

chick eggs. The cell nuclei of the quail contains distinctive heterochromatic nucleoli and this feature can be used to distinguish quail cells from chicken cells by using Feulgen staining (Nijweide et al., 1982). Simons and Gilliam (1981) found that femurs in which the wound was restricted to the proliferative and hypertrophic zones of the cartilaginous epiphyses failed to repair with cartilage. But wounds which had penetrated through the cartilage into the subchondral marrow space were filled with calcified bone trabeculae. All the osteoblasts and osteocytes in the repair bone had nuclei of the quail (graft). They concluded that new bone was derived from osteoprogenitor cells in the marrow stroma which moved with capillaries into the wounded area.

Numerous macrophages were observed in the marrow spaces during the early half of the grafting period. They performed the function of clearing necrotic cell debris and were present even prior to the re-establishment of the circulation. At that stage, they would have arisen from the blood monocytes which were released into the intertrabecular spaces when the implant was inserted. Reorganisation of the marrow spaces with formation of new blood vessels from day 3 onwards would provide a new source of macrophages derived from the host blood circulation.

4.4.2.1 Multinucleated giant cells

In the femur CAM graft model, multinucleated giant cells were observed only on the surface of Apoceram but not the titanium implants. Only three to four of these cells were observed on the implant surface in any one section. These cells showed intense staining for TRAP but did not show a ruffled border where they contacted the Apoceram surface. They were found in close proximity to bands of osteoblasts laying down osteoid on the implant surface. In some of the sections involving titanium implants, at day 9, osteoclasts were occasionally found at the endosteal surface of bone facing the marrow cavity adjacent to the point where the implant traversed the marrow space.

Multinucleated giant cells have been reported in many studies involving metallic as well as ceramic implants in experimental animals. Their existence at the interface is not universal and there are sometimes contradictory findings. Piatelli et al. (1996) reported that large numbers of multinucleated giant cells were present on the surface of

plasma-sprayed titanium implants but not on machined and sandblasted titanium placed in rabbit femurs. However, Rahal et al. (1993) placed machined titanium screws in femurs of mice and observed prominent multinucleated giant cells with phagocytic inclusions on the part of screws within the marrow cavity. Sennerby (1991) has observed multinucleated cells in a similar rabbit tibia model involving machined titanium. When Johansson et al. (1990) compared tantalum, niobium, and titanium sputter-coated on to the surfaces of polycarbonate plastic implants in the rabbit tibia model, they noted differences in the presence of MGCs between the materials. Multinucleated cells could occasionally be recognized at the interface zone for tantalum. They were more numerous and more striking at the niobium interface but not observed at the titanium interface. Gross et al. (1991) also reported the presence of such multi-nucleated cells at the edge of bone trabeculae bonding to hydroxyapatite implants placed in rabbit femurs and on coral implants in rat femurs. The same group investigated glow-discharge treatment of implants and found 'osteoclast-like' cells without ruffled borders on bone-bonding glass ceramics implanted in rat femurs (Müller-Mai et al., 1992).

The exact nature of these multinucleated cells has yet to be determined. It is interesting to find that Piatelli et al. (1996) noted that the MGCs observed in their study showed a negative reaction when stained for acid phosphatase. From this, they deduced that these cells were not 'activated'. They also commented that these cells were present mostly where there was a higher quantity of newly formed bone, similar to the observations in the chick embryonic femur in this study. The multinucleated giant cells present on titanium implants were described by Sennerby (1991) as lacking a ruffled border characteristic of osteoclasts. He went on to suggest that these cells could either be osteoclasts or foreign body type giant cells and concluded that it was not possible to safely distinguish between osteoclasts and foreign body giant cells with morphological techniques and that immunocytochemical methods are required. This is only partly correct since distinguishing between foreign body giant cells and osteoclasts is difficult, even by immunocytochemistry. Kadoya et al. (1994) found that foreign body giant cells in peri-implant tissues of loosened total joint arthroplasties showed significant heterogeneity and in some cases, they were found to express markers for osteoclasts.

An experiment performed by Webber et al. (1990) may provide some insight into the potential for different types of giant cells to form within the haemopoietic system of the embryonic chick in response to implant materials. They placed different materials directly on the CAM for the purpose of examining giant cell/osteoclast formation. Multinucleated giant cells were classed as active osteoclasts by the morphological appearance of a ruffled border and immunolabelling with monoclonal antibody 121F. Giant cells formed on devitalised bone grafted on the CAM had ruffled borders and stained positive for the antigen. In contrast, those that formed on non-resorbable materials such as Sepharose beads, mica and methacrylate lacked ruffled borders and were negative for the 121F antigen. The expression of the 121F osteoclast antigen was said to correlate with the appearance and extent of ruffled membrane development. It was suggested that the presence of the 121F antigen indicated the developmental or functional state of giant cells (osteoclasts) that form on resorbable substrates. Earlier chick-quail chimeric experiments by Jotereau & LeDourain (1978) had shown that osteoclasts in bone grafted on the CAM originated from the haematopoietic system of the host.

The exact nature of the cells which participate in the repair process in the CAM graft model has not been explored in this study. It is anticipated that their identification using immunocytochemical methods will be a challenging task since the preservation of an intact implant-tissue interface precludes the use of frozen sections and paraffin embedding, methods which allow reliable maintenance of antigenicity in the tissues for immunolabelling. However, this hurdle will have to be overcome to allow precise identification of cells and macromolecules involved in the formation of the implant-tissue interface. To date, immunogold labelling coupled with low temperature resin embedding techniques have been employed in a limited number of studies on protein distribution but have yet to be used for localisation of cell-type specific markers within hard tissues surrounding implants *in vivo* (Nanci et al., 1994; Rosengren et al., 1996).

4.4.3 Immunohistochemistry and enzyme histochemistry

The results of immunohistochemical staining of bone matrix proteins highlights the specific problems presented by resin embedded hard tissues. The two matrix proteins

which were examined, type I collagen and osteonectin, were selected on the basis that they are the most abundant bone matrix proteins in foetal bone, although their presence is not restricted to bone and they are not necessarily regarded as definitive bone markers. Type I collagen makes up 85-90% of the total bone protein. Osteonectin is present in high concentrations in the newly mineralised matrix of foetal bone where it is associated with collagen fibrils. It is thought to regulate mineralisation by preventing excessive crystal growth in the mineral phase. The labelling of these proteins was performed to determine if satisfactory penetration of immunoglobulin complexes could be achieved in undecalcified sections of the embryonic bone. Bone matrix stained positively for both proteins but intracellular labelling was weak.

The methods which may be used for the histologic, histochemical and immunohistochemical examination of the hard tissue surrounding hard implants are dictated by the need to preserve: (i) cellular and tissue morphology, (ii) the implant-tissue interface, (iii) the enzymatic activity in the tissue, (iv) the integrity of antigenic sites. The demonstration of antigens and enzymes is particularly sensitive to fixation, decalcification and embedding procedures.

Infiltration and embedding of undecalcified bone tissue in methacrylate resins as used in this work are standard procedures widely used for bone histology. The polymerisation of LR White resin by heat would destroy enzyme activity and protein antigenicity in the tissues. Preliminary tests showed that 4% paraformaldehyde in 0.1M phosphate buffer or 1% glutaraldehyde at 4°C followed by embedding in LR White resin using chemical polymerisation at 4°C had failed to sufficiently preserve the activity of alkaline phosphatase and tartrate resistant acid phosphatase. Subsequent staining for the two enzymes was successful only by employing a combination of 90% ethanol for fixation and glycol methacrylate for embedding. As glycol methacrylate swelled up in water, the resin blocks had to be cut dry. This combined with the softness of the resin made the preparation of the sections a slow and difficult task. More expensive systems involving polyhydroxydimethacrylate (LR Gold) or ethylmethacrylate/2-hydroxyethyl methacrylate (Lowicryl, Technovit 7200) involving low temperature infiltration and

polymerisation of the resin by blue or U.V. light are available for overcoming such difficulties.

Very recently, Erben (1997) suggested a modified embedding protocol for methyl methacrylate which involved the addition of methylbenzoate to the methacrylate solution, infiltration and chemical polymerisation at low temperature. The technique requires deplasticization of the sections prior to staining but was found to preserve the activity of alkaline phosphatase, tartrate resistant acid phosphatase and antigenicity for a monoclonal antibody ED1 against macrophages and osteoclasts. This protocol may signal a further step towards the application of molecular biology techniques for the identification of the cell types and gene expression involved in the process of bone healing around implants.

4.4.4 Bone formation around the implant

The percentage of the implant perimeter in contact with bone in the resin-embedded sections was very low at the beginning of the grafting period. This minimal contact was with mineralised bone rather than osteoid since the implants were located in the region of the femur away from the subperiosteal region where substantial osteoid was present because of the pattern of circumferential growth. Changes to this percentage were not clearly evident until after day 3, coinciding with the re-establishment of vascularity and resumption of bone formation at the centre of the graft. With new bone formation, the percentage of contact with osteoid and mineralised bone increased progressively throughout the remaining culture period. Statistically significant differences between titanium and Apoceram was found at day 7 when the mean percentage contact with bone and osteoid was $27.7 (s.d.\pm 4.5\%)$ for titanium and $38.2 (s.d.\pm 6.0\%)$ for Apoceram. However, contact with mineralised bone did not differ significantly between the two implant materials except at day 9 of the culture period when this was higher for Apoceram than for titanium. At day 9, the mean percentage contact with bone and osteoid was $38.8\pm 8.6\%$ for titanium and $59.7 (s.d.\pm 6.8\%)$ for Apoceram, the percentage contact with mineralised bone was $25.0 (s.d.\pm 7.3\%)$ and $47.8 (s.d.\pm 9.5\%)$ for titanium and Apoceram respectively. The percentage contact length provide an indication of the extent of bone formation on the implant surface but is not

representative of the total amount of bone formed around the implants. Where the implant traversed the central marrow cavity, the contact was mostly with a very thin seam of bone formed during the later half of the grafting period following either the migration of the osteogenic cells along the implant surface or the growth of an existing bone trabeculum parallel to the implant surface.

There was variability in the results in sections from the same specimen and within each group of specimens for the two implant materials. Several factors may contribute to this: biological variations, differences in the implant insertion procedure and errors in the histomorphometric measurements. The first factor cannot be avoided. The femurs from each donor was implanted with titanium and Apoceram but pairwise comparisons have not been made since they were cultured in different hosts. Also in some cases, one of a pair of donor femurs showed incomplete integration with the CAM and had to be excluded from the histomorphometric analysis. By restricting the analysis to specimens which were completely enveloped by the CAM with no signs of necrosis on gross examination, variability in results owing to the grafting procedure was minimised. The implantation procedure was standardised to a certain extent in that the wound created for the insertion of the implant was made to penetrate only the bony collar but it was evident in the sections that there were variations in the depth of placement of the implant.

Toluidine blue stained sections were used for the measurement of bone-implant contact. This introduced both certain advantages and drawbacks. Fully mineralised bone appeared as pale pink on the sections and osteoid stained a bluish purple. Their contrast in terms of grey levels in the detected image in the Quantimet setup was excellent, whereas staining methods such as von Kossa counterstained with van Gieson or the Goldner trichrome method would have given bone and osteoid a similar level on the grey scale image. When stains such as haematoxylin and eosin, van Gieson were used on the LR White sections, only pale staining was obtained because of the limited thickness of the sections. Distinguishing between osteoid and soft tissue contact in toluidine blue stained sections was made by checking the section at x400 magnification prior to editing the implant outline at x100 magnification. Other software-related constraints contributing to the measurement error are explained in Appendix III. Overall, the observed

differences between titanium and Apoceram in the late stages of the culture period are greater than the variability in the measurement procedure. Tetracycline labelling prior to the retrieval of the grafts confirmed the location of the mineralisation fronts at sites of new bone formation. If the rate of bone formation were to be quantified using multiple fluorochrome labels, sections which are at least 10µm thick will be required to prevent fading of fluorescence (Baron et al., 1983). They would only be obtainable either by removal of the implant prior to re-embedding and sectioning or by using ground section techniques requiring greater tissue bulk.

Despite the short duration of the CAM graft experiments in this project, mean percentages of bone-implant contact of 25.0% and 47.8% were found for titanium and Apoceram respectively. The figures for Apoceram are comparable with those of bioactive glass-ceramics in reports of short-term experiments *in vivo*. In an experiment involving 200-355µm granules of apatite-wollastonite containing glass-ceramic and hydroxyapatite placed in 2.5mm diameter defects in rats, Ono et al. (1990) have reported 60% coverage of the granule surface with bone for the glass-ceramic and 20% coverage for hydroxyapatite at 2 weeks after implantation. Gross and Struntz (1985) found 5-75% glass-ceramic-bone contact at 2 weeks in the rat femur which was dependant on glass composition. Reports on titanium *in vivo* tend to focus on much later periods and show higher bone-implant contact than that found in the CAM graft model. The percentage of bone contact length with porous titanium implants was reported by Pilliar et al. (1991a) to be approximately 50%, a value also suggested by Hipp and Brunski (1987) for integrated commercially pure titanium implants. The CAM graft model is unique in the dimensions of the grafts and implants. The average thickness of each trabeculum within the embryonic chick femur is between 30-50µm. The thickness of each implant is around 150µm. Where the implant passed through the collar of bone in the mid-diaphysis, the implant surface is no more than 10µm from the existing bone trabeculae at the start of the grafting period. The gap to be bridged by new bone is quite small. Where the implant traversed the central marrow cavity, the seams of new bone formed on or near the surface of the implant were around 15µm thick at 9 days after grafting, giving an indication of the rate of new bone apposition.

There are crucial differences between different experimental studies: the type of implant, the site of implantation, the species of animal and the loading conditions. Also, details of the experimental design and measuring techniques have to be considered. The method by which bone-implant contact was determined also differed widely between studies. Most reports rely on a single section of each specimen. The thickness of the sections varied. Since the perimeter of most dental implants would be much larger than the visible field at even the lowest magnification on a light microscope, most of the measurements were carried out at very low magnification and the percentage reported may relate only to part of the whole implant perimeter, for instance, where the implant passed through cortical bone. All these factors imply that percentages of bone-implant contact cannot be taken at face value although they are useful for within experiment comparisons between materials. There is some evidence that a positive correlation exists between removal torque and the percentage of bone-implant contact, at least in screw-type metal implants (Johansson & Albrektsson, 1987).

4.4.5 Ultrastructure of the bone-implant interface

Ultrastructural studies of the bone-implant interface are rare, probably because of the complexity of specimen preparation. The results of the fracture technique used in these experiments for specimens containing titanium implants did not produce consistent clean separation between the implant and the bone tissue. In some sections of the re-embedded tissue, discontinuities of cell outlines could be seen. In all the sections included in the results section in this chapter, an electron dense line was always present. Ultrastructural examination of the bone-titanium interface revealed that mineralised matrix did not come into direct contact with the implant surface. There was a 200-800nm thick layer interposed between mineralised bone matrix and the implant. This correlates with the observation of the basophilic line at the interface at light microscopy level at x400 magnification. It has been suggested that mineralised bone can be deposited as closely as 100-500nm to endosteal dental implants (Steflik et al., 1992c). Many features have been reported in the region between the mineralised matrix and the implant: a finely fibrillar layer (Steflik et al., 1992c), amorphous material (Sennerby,

1991; Murai et al., 1996), cell debris (Nanci et al., 1994). Both fibrillar and amorphous material have been observed in the relatively immature bone-titanium interface in the CAM graft model. Steflik et al. (1994) also reported that the outer aspect of mineralised bone was coated by an electron dense deposit 20-50nm thick and at times only this deposit separate the bone and implant. This deposit has been referred to as a lamina-limitans like line by Sennerby et al. (1992) and Nanci et al. (1994). Although an electron dense line was consistent present at the interface in the CAM graft model, it is not known if this is the same as the lamina-limitans layer referred to by other authors.

The ultrastructure of the interface between Apoceram and chick embryonic bone shows a variety of features similar to those reported in studies involving other bioactive glasses. There are areas where mineralised matrix is in complete contact with the implant surface. Mineral deposits, often globular in shape, fused with the implant surface and there is a less dense region, in which similar deposits intermingle with collagen fibres, interposed between the heavily mineralised matrix and the implant surface. This has been reported both *in vivo* (Hench, 1988; Gross and Strunz, 1985) and *in vitro* (Matsuda & Davies, 1987) for bioactive glasses and glass ceramics. Hench & Andersson (1993) reviewed the mechanisms by which bioactive glasses became bonded to bone. The dissolution of alkali ions from the glass surface under physiological conditions leaves a SiO₂ rich layer which protects the bulk glass from further attack. A calcium phosphate rich layer then develops on this surface and hydroxapatite crystals are formed. It is this layer to which collagen fibres, produced by nearby osteoblasts, become attached. Further mineralisation of the matrix leads to the so called bone-bonding phenomenon.

4.4.6 Does the model mimic bone healing *in vivo*?

The femur model used in this project has features which resemble as well as differ from bone healing *in vivo*. Repair of the wound created for the insertion of the implant proceeded in the same manner as was observed by Takahashi et al. (1991) as well as Bale & Andrew (1994). Both groups had placed fractured long bones on the

CAM and followed the repair process. This was characterised by healing without an external callus and minimal inflammatory response. The wound edges were bridged by subperiosteal bone formation. The repair progressed rapidly and granulation tissue was not a significant feature. This is quite different from the way many bone fractures heal *in vivo*.

The majority of bone fractures heal by a process referred to as secondary healing, which can be divided into three stages (Simmons, 1985). The first is the inflammatory stage which involves the formation of a blood clot by blood released from vessels damaged in the fracture; vasodilation of surrounding vessels; the addition of exudate (plasma and cells) to the clot and a fall in pH. Following this, the ruptured vessels clot, bone cells whose nutrition has been disrupted, die. At this point phagocytic cells move in to remove necrotic tissue. The second, reparative stage overlaps the inflammatory stage and involves the formation of a fracture callus which bridges the break in the bone. Capillaries proliferate and invade the blood clot whilst pluripotent mesenchymal cells in the periosteum and endosteum proliferate and differentiate. Cartilage is formed within the haematoma, giving rise to the callus which is further strengthened by endochondral ossification and bone formation on existing bone surfaces, resulting in bony trabeculae bridging the fracture and continuing until all the cartilage has been replaced. The third stage is the remodelling of the fracture site until bone is restored to near normal strength, form and function.

Callus formation is clearly absent in the femur CAM graft model. In this respect, it is not a system which resembles secondary bone repair. However, we need to consider two other models of bone healing *in vivo*. The first is experimental cortical bone defect healing and the second is direct or primary fracture healing where there is close approximation of the fragment ends under stable conditions.

Drilling of small bur holes in cortical bone in experimental animals leads to activation of bone-forming cells and a scaffold of woven bone is formed quickly within the defect. The new trabeculae are randomly oriented, with numerous blood vessels in the intertrabecular compartments. A continuous layer of osteoblasts is found on the

surface of the trabecular scaffold and these cells deposit lamellar bone on the walls of the intertrabecular spaces leading to the narrowing of the holes. Subsequent remodelling of the newly formed bone completes the healing process. There are several notable features. Bone formation does not occur via endochondral ossification. Bone tissue is deposited on a solid surface which is provided either by the defect wall onto which the primary scaffold of woven bone is anchored or, later, by the surfaces of the woven bone trabeculae. Osteoclasts appear at the onset of cortical bone remodelling within the avascular cortical rim of the bur hole. There is a critical size above which complete bone infill would not occur and it varies depending on the site and the animal species. Primary bone healing across small gaps between fractured bone ends with stable fixation follows a similar process. Blood vessels and mesenchymal cells invade the gap and osteoblasts deposit bone on the surface of the fragment ends. The gap then becomes filled by lamellar bone and remodelling follows. (Schenk & Hunziker, 1994)

When we consider early bone healing around implants with stable fixation in precisely drilled and tapped holes in experimental animal models, the early post-operative situation is nearer to the last two *in vivo* bone healing models discussed above. Both of these models have minimal inflammatory response at the defect site and a cartilaginous callus is also absent. For the femurs with implants which were cultured on the CAM, there was complete disruption of blood supply during the initial period. This probably does not happen *in vivo* but the observed pattern of healing is similar to the *in vivo* primary bone healing models. It has to be acknowledged that the graft is not subject to mechanical loads in culture. The embryonic nature of the graft tissue and host is the key to the rapid rate of repair in the CAM graft model. It is known that foetal bone healing *in vivo* is characterised by its rapidity in addition to minimal soft-tissue inflammation and absence of callus formation (Longaker et al., 1992).

There are other features unique to the culture system which deserve consideration:

4.4.6.1 Immunological capacity of the host chick embryo

According to Hall (1978), rejection mechanisms within the embryonic chick develop at around 15 or 16 days of incubation. His recommendation was that non-mammalian grafts could be retrieved at up to 18 days of incubation of the host and mammalian tissues should be retrieved at 15 or 16 days of incubation of the host. The immunological activity of the chicken embryo is primarily effected by the thymus and bursa and cell-mediated immunity appears in the second week of incubation (Jankovic et al., 1975). Vainio et al. (1989) found that CD4⁺ cells (including peripheral T-cells and thymocytes) first appeared in the thymus on day 13 of embryonic life but were not present in the peripheral blood until after hatching. The implication is that the model is not suitable for studying immune responses to grafted tissue as well as any implanted materials but can also be viewed as a system in which tissue responses can be observed independent of immune reactions.

4.4.6.2 Avian vs mammalian bone

The pattern of organogenesis in avian long bones is different from that in mammalian long bones (Hall, 1987). In the chick embryo, initial mineralization of the primitive bone collar occurs without concurrent mineralisation of cartilage and unlike mammalian osteoclasts, avian osteoclasts resorb uncalcified cartilage matrix during the formation of the primitive marrow cavity (Caplan & Pechak, 1987). In addition to this the architecture of avian bone differs from mammalian bone due to different physiological requirements (see discussion in Chapter 3). However, they share similar cell and matrix components. Moreover, endochondral and membranous ossification occur during skeletal growth in both avian and mammalian bone (Hall, 1987).

4.4.7 How does the model compare with bone organ culture *in vitro*?

The CAM cultured femur maintains its viability and shows excellent bone growth compared to bone organ cultures *in vitro*. Foetal long bone of chick, rat and mouse origins has been used in many *in vitro* studies but its limitation for studying bone formation is reflected by the fact that the majority of the experiments related to bone resorption and not bone formation. In long-term organ culture of long bones, the

osteogenic precursors from the periosteum and endosteum differentiate into osteoblasts which synthesise matrix that subsequently mineralises but only at a slow rate (Roach, 1994). Gaillard et al. (1979) also commented that the formation of a marrow cavity in chick long bones is difficult to attain in culture *in vitro*. The main advantage of the CAM cultured femur over *in vitro* preparations is its unique capacity for repair, a characteristic important for the examination of healing response to implants which is not facilitated by *in vitro* culture conditions. Bone formation continues unimpaired in the CAM graft when vascularity is established, in contrast with the limited bone formation which can be obtained *in vitro*.

4.5 The main findings:

1. The events in the development of the implant-containing femoral graft on the CAM follow a consistent pattern involving cell death; revascularisation of the graft; reorganisation of the marrow; repopulation of the bone surface within the centre of the graft by viable cells.
2. There is minimal inflammation and absence of cartilaginous callus formation during the healing of the wound created for implant insertion.
3. The space adjacent to the implant was initially filled with blood cells which degenerated and were removed by macrophages between days 3 to 5. Migration of mesenchymal cells onto the implant surface was evident by day 3 after grafting.
4. The degree of bone-implant contact was greater for Apoceram than for titanium at the end of the grafting period.
5. Where the implant traversed the central marrow cavity, new bone formation originating from the implant surface was frequent for Apoceram but not titanium.
6. Multinucleated giant cells which were positive for tartrate resistant acid phosphatase were observed on Apoceram but not on Titanium.
7. The variety of features observed at the bone-implant interface at ultrastructural level in the femoral CAM graft model resemble that reported *in vivo*.

5. Bone response to local release of basic fibroblast growth factor in the CAM graft model

5.1 Introduction

The identification and purification of bone growth factors and more recently their production using recombinant technology have stimulated investigations into the *in vitro* and *in vivo* effects of these factors on bone formation and repair. Many animal experimental studies pointing to the potential clinical applications of bone growth factors have appeared in the literature during the course of this project. These include the enhancement of incorporation of bone grafts (Yaszemski et al., 1996), bone defect reconstructions using natural or artificial growth factor carriers (Meikle et al., 1994; Okuda et al., 1995; Hollinger & Leong, 1996; Busch et al., 1996), and inducing bone formation around dental implants (Jin et al., 1994). The questions asked in a clinical context are whether there is a way of accelerating the process of osseointegration and whether the quantity of new bone formation can be increased around implants?

Often conflicting results are found in *in vitro* and *in vivo* experiments. The addition of growth factors to an injured area does not always enhance tissue repair. Many animal wound models designed to assess experimental treatments are underscored by the complex relationships between biologic regulatory molecules, their temporal profile and concentrations, the interplay among cells and the local microenvironment.

5.1.1 Aim and objective

The aim of this experiment was to assess the feasibility of using the femoral graft model for studying the effects of local delivery of growth factors on bone healing. Basic fibroblast growth factor was chosen as the effector and the objective was to deliver this factor in a localised manner to embryonic chick femurs grafted on the CAM and to assess whether there was earlier or increased bone formation around the growth factor carrier in the grafts compared to a control group of grafts implanted with the carrier without the growth factor.

5.1.2 Bone growth factors implicated in bone repair

Recent studies on fracture healing suggest regulatory roles for platelet derived growth factor (PDGF), acidic fibroblast growth factor (aFGF), basic fibroblast growth factor (bFGF), transforming growth factor (TGF- β) and the bone morphogenetic proteins (BMPs) in the development of the fracture callus (Bolander, 1994). Table 5.1 lists the growth factors implicated in bone repair and some of their known biologic activities.

Table 5.1 *Growth factors implicated in bone repair*

Growth Factors	Produced by	Matrix Location	Biologic Activities
TGF- β	Platelets, inflammatory cells (monocytes, macrophages), osteoblasts, chondrocytes	Bone is the most abundant source of TGF- β in the body	Regulation of matrix calcification, stimulation of osteoblast activity, chemoattractant for macrophages, promotes angiogenesis
BMPs	Osteoprogenitor cells Chondrocytes	BMPs were originally identified in bone but are now known to be widely distributed in the body e.g. urinary bladder epithelium, brain	TGF- β -like structure, may be involved in cartilage formation, important regulator during embryogenesis
Fibroblast Growth Factors	Inflammatory cells, osteoblasts, chondrocytes	Binds heparan sulphate proteoglycans in bone and cartilage matrix	Stimulates neovascularisation, chemoattractant and mitogen for chondrocytes and most cells of mesoderm or neuroectoderm origin
Platelet-derived Growth Factors	Platelet, monocytes, activated macrophages, endothelial cells	Interactions unknown	Mitogenic for most cells of mesoderm origin
Insulin-like Growth Factors	Osteoblasts, chondrocytes, liver	Interactions unknown	Mitogenic, promotes cartilage synthesis, acts as second messenger to PTH, modulator of other growth factors

5.1.2.1 Basic fibroblast growth factor

Basic fibroblast growth factor (bFGF) is a member of the fibroblast growth factor (FGF) family, currently comprised of seven related mitogenic proteins which show 35-55% amino acid conservation. bFGF has been isolated from a number of sources, including neural tissue, pituitary, adrenal cortex, corpus luteum and placenta. It

stimulates the proliferation of all cells of mesodermal origin, and many cells of neuroectodermal, ectodermal and endodermal origin (Gospodarowicz, 1992). The cells include fibroblasts, endothelial cells, astrocytes, oligodendrocytes, neuroblasts, keratinocytes, osteoblasts, smooth muscle cells, and melanocytes. bFGF is chemotactic and mitogenic for endothelial cells *in vitro*.

Several *in vitro* studies which evaluated the effect of FGFs on bone forming cells have produced contradictory results. Rodan et al. (1987b) showed that acidic fibroblast growth factor (aFGF) extracted from bovine brain, was a potent mitogen for both osteoblastic and non-osteoblastic cell cultures derived from rat calvaria but an inhibitor of the expression of osteoblastic features. Canalis et al. (1988) found that basic fibroblast growth factor (bFGF) had similar effects. Further *in vitro* studies by Globus et al. (Globus et al., 1988; Globus et al., 1989) revealed that FGFs present in bone matrix were the product of osteoblast secretion, rather than of the endothelial cells from the local vascular network and confirmed that bFGF is more potent than aFGF as a mitogen.

Pitaru et al. (1993) treated rat bone marrow stromal cells with bFGF and found increased proliferative activity as well as increased cAMP responsiveness to PTH, alkaline phosphatase activity and osteocalcin expression. Their conclusion was that bFGF increased the osteogenic differentiation of bone marrow stromal cells in addition to being mitogenic.

Iwasaki et al. (1995) in a study of the *in vitro* effects of TGF- β and bFGF on periosteal mesenchymal cells, showed that these cells, under the stimulus of bFGF, tended to increase their replicative rate, but did not show any tendency to differentiate without the addition of TGF- β . These findings were suggestive of the existence of a synergistic effect of bFGF with TGF- β .

In vivo, FGFs have been found to promote cell proliferation, stimulate tissue regeneration and wound repair, and induce angiogenesis (Gospodarowicz et al., 1992; Eppley et al., 1988; Schweigerer, 1990). FGFs play a significant role in the early phases of embryonic development, where these factors might provide the tissues of an efficient

network of local proliferative-differentiative signals, in the absence of a well-established vascular system (Schweigerer, 1990). Frenkel and Singh (1991) studied the effect of administration of bFGF in chick embryos and found an increased number of osteoblasts in the femurs of treated embryos but a reduction of collagen synthesis compared with the control group. Nakamura et al (1995) reported that systemic administration of recombinant human bFGF in rats induced endosteal, rather than periosteal, bone formation. A series of *in vivo* studies by Wang and Aspenberg showed that local infusion of bFGF promoted bone formation in a dose and time dependant way in bone grafts placed within titanium chambers in rats (Wang & Aspenberg, 1993; Wang & Aspenberg, 1994; Aspenberg et al., 1994; Wang & Aspenberg, 1996a). Higher doses of bFGF induced fibroblastic rather than osteoblastic cell proliferation, whereas lower doses had the opposite effect. However, an earlier study by Eppley et al.(1988) showed no evidence of increased osteogenesis when bFGF was infused into bone grafts placed directly on the mandibles of skeletally mature rabbits despite increased blood vessel formation.

While most studies reported a proliferative effect of bFGF on osteoblastic cells, there are some doubts about its influence on their differentiation. The general opinion is that there is an inhibitory action of FGFs on osteoblast and chondroblast differentiation, in exchange for a longer proliferative activity, both *in vivo* and *in vitro* (Hauschka, 1990; Frenkel and Singh, 1991; Gospodarowicz, 1992; Jingushi et al, 1995). Yet, other studies revealed a different effect of bFGF, which, in some conditions, would promote differentiation rather than delaying it (Nakamura et al, 1995; Wang and Aspenberg, 1996a; Iwasaki et al, 1995). Various explanations of these differences in observations have been proposed. Pitaru et al (1993) suggested that there was a synergistic effect between FGFs and medium supplements including dexamethasone, ascorbic acid and β -glycerophosphate which lead to osteocalcin synthesis, increased ALP activity and Ca^{2+} deposition, all marks of osteoblastic differentiation. The functional interaction between bFGF and TGF- β also came under scrutiny. Early studies showed that the two factors would co-operate in promoting bone cells proliferation, but reducing the synthesis of osteocalcin (Globus et al, 1988). On the contrary, experiments by Iwasaki et al (1995) showed that TGF- β would oppose, rather than add to FGFs effects, inhibiting mitotic

event, and inducing collagen production. Further evidence of a link between the two factors was presented by Nakamura et al (1995) who found that treatment with bFGF lead to an increased immunostaining of preosteoblastic cells for TGF- β in rats. However, in an *in vivo* experiment in which alveolar bone defects in dogs were treated with a combination of bFGF, IGF-2 and TGF- β , no differences in fibroblast and collagen density were detected, and indeed, bone formation was more significant in the control than in the test group (Selvig et al, 1994).

In summary, most *in vitro* studies show that bFGF stimulates osteoblastic cells into proliferation and inhibits their phenotypic expression and *in vivo* experiments seem to show an increase in bone formation in response to its local or systemic application. The following investigation was set up to explore the effect of bFGF on bone formation within CAM grafted femurs, taking into consideration the question of how well the model fits into picture provided by *in vitro* and *in vivo* findings reported in the literature.

5.2 Materials and Methods

5.2.1 Preparation of implants loaded with bFGF

Agarose beads (Affi-Gel[®] Blue Gel, Bio-Rad Laboratories, Hercules, U.S.A.), size 100-200 mesh (wet), were washed in PBS and transferred to 100 μ l of sterile PBS in a tissue culture dish. A 2 μ l drop of PBS containing 2 μ g of bovine bFGF (R&D Systems, Abingdon, U.K) was placed in the same dish. The agarose beads were placed into the growth factor solution and allowed to soak for one hour at room temperature.

5.2.2 Insertion of implants and grafting

The carrier beads containing either bFGF or PBS as control were implanted in the mid-diaphyses of 14 day old chick embryonic femurs which were grafted on the CAM of host eggs which had been incubated for nine days.

5.2.3 Histology & histochemistry

The grafts were harvested after 6, 7 and 9 days of incubation and were fixed either in 4% paraformaldehyde, dehydrated and embedded in LR White resin, or fixed in

95% ethanol, dehydrated and embedded in glycol methacrylate resin. LR White embedded specimens were sectioned and stained with toluidine blue. Glycol methacrylate embedded specimens were stained for alkaline phosphatase using Sigma Kit No.86R.

5.3 Results

Femurs implanted with carrier beads with and without bFGF were harvested after 6, 7 and 9 days' incubation. Grafts in which the femur had not been completely covered with the CAM and showed signs of necrosis were excluded from the analysis.

Table 5.2 *Grafts of femur implanted with carrier beads*

Duration of Culture	Implant	No. of grafts made	No. of grafts analysed
6 days	control	12	8
	bFGF	12	8
7 days	control	12	12
	bFGF	12	12
9 days	control	12	10
	bFGF	12	10

A qualitative evaluation was carried out by assessing the following regions for several features:

1. The surface of the bead

Cell density	rated	■	normal appearance
		■■	moderately increased
		■■■	highly increased

Is the bead in contact with	cells?	yes = +, no = 0
	osteoid?	yes = +, no = 0
	mineralised bone?	yes = +, no = 0

2. Within one bead diameter from the bead surface

Cell density	rated		normal appearance
			moderately increased
			high increased

Is there an increase in osteoid thickness? yes = +, no = o

3. Central marrow cavity

Is there a condensation of cells into a trabecular pattern?	yes = +, no = 0
Is there formation of osteoid within the cavity?	yes = +, no = 0
Is there formation of mineralised bone within the cavity?	yes = +, no = 0

The results are presented in Tables 5.3 to 5.5.

The overall picture showed a consistent effect with the beads carrying bFGF; namely, cell proliferation on the surface and for several cell diameters from the bead and an increase in the amount of osteoid slightly further away from the bead. The effect appeared to be localised as the tissues distant to the bead appeared normal. Condensation of cells into trabeculae and subsequent bone formation was seen in the central marrow cavity in most of the grafts in the test group.

The control group, i.e. grafts with beads only soaked in PBS also showed a consistent pattern: the surfaces of the beads were surrounded by normal mineralised bone, osteoid or marrow tissue. The central marrow cavity remained clearly defined without signs of increased cell proliferation. Figures 5.1 to 5.6 show the histological appearance of the tissues surrounding the beads.

The morphology of the cells surrounding the beads with bFGF resembled osteoblasts. When sections were stained for alkaline phosphatase, a distinct difference was found between the test and the control groups (Figures 5.7 and 5.8). The five to six layers of cells immediately surrounding the bead with bFGF were negative for alkaline phosphatase. Further away, intense staining of alkaline phosphatase was present on cells overlying the bands of osteoid. In the control group, alkaline phosphatase staining was found throughout the graft, including the cells adjacent to the bead if it was not completely surrounded by mineralised bone.



Figure 5.1 Cross-section of femur from the control group at day 9. The wound created for the insertion of the agarose bead has healed completely. The bead is surrounded by mineralised bone (arrow) and marrow tissue (*). Toluidine blue stain.

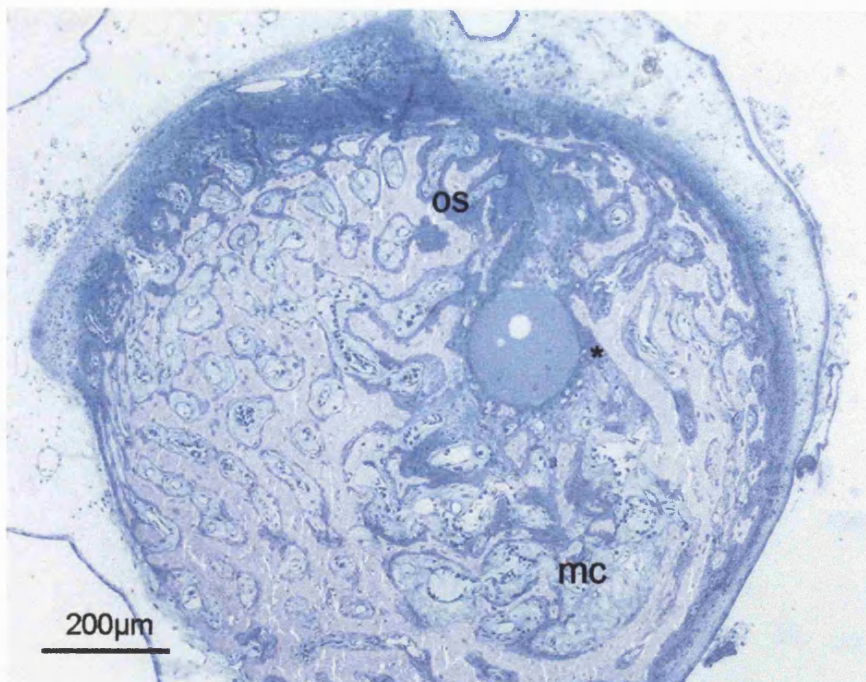


Figure 5.2 Cross-section of femur from test group at day 9. There is a localised increase in cell density around the bead (*). Further away, the thickness of the osteoid (os) layer is increased. The central marrow cavity (mc) is filled with new bone trabeculae.

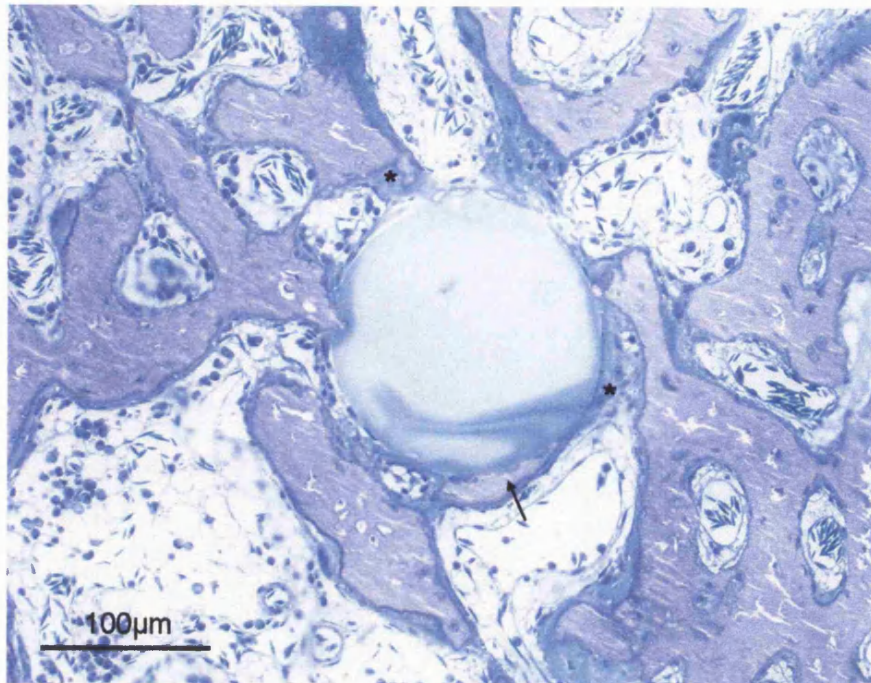


Figure 5.3 Femur from the control group at day 7. Osteoid () and new bone (arrow) formation around the agarose bead.*

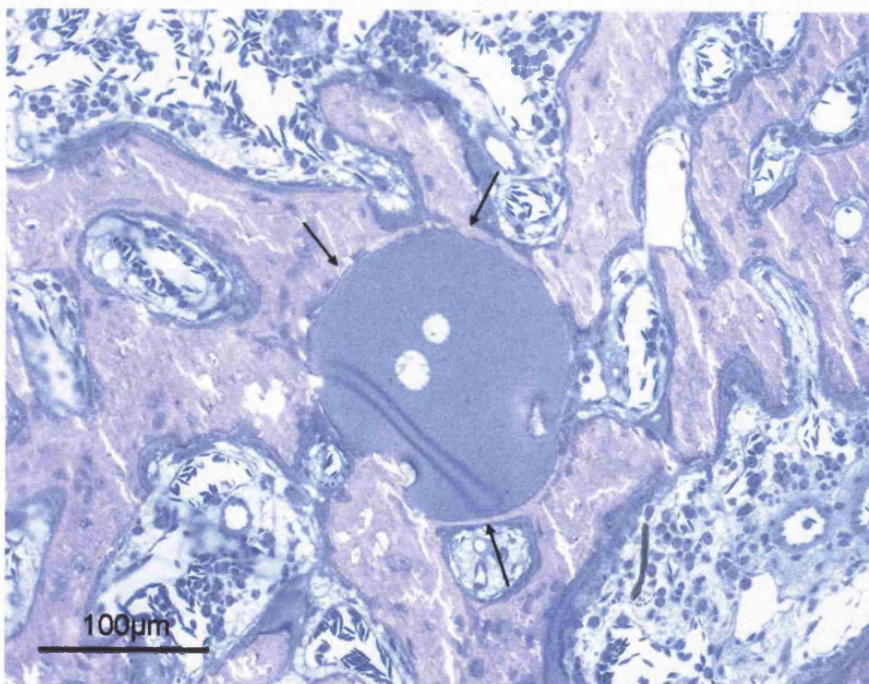


Figure 5.4 Femur from the control group at day 9. This bead is almost completely surrounded by mineralised bone (arrows).

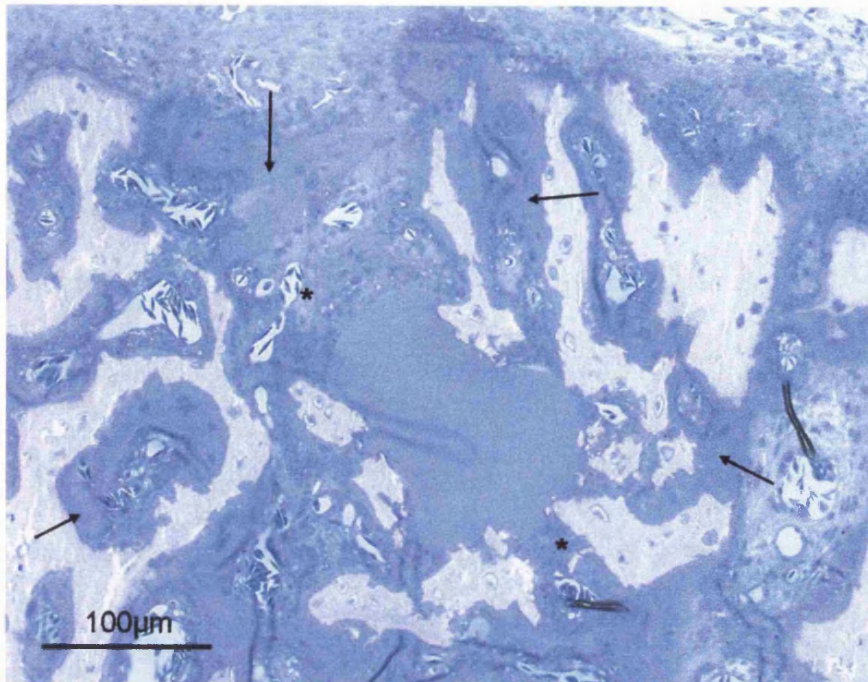


Figure 5.5 Test group at day 7, there is a massive increase in cell density() around the bead and thick layers of osteoid (arrows) further away.*

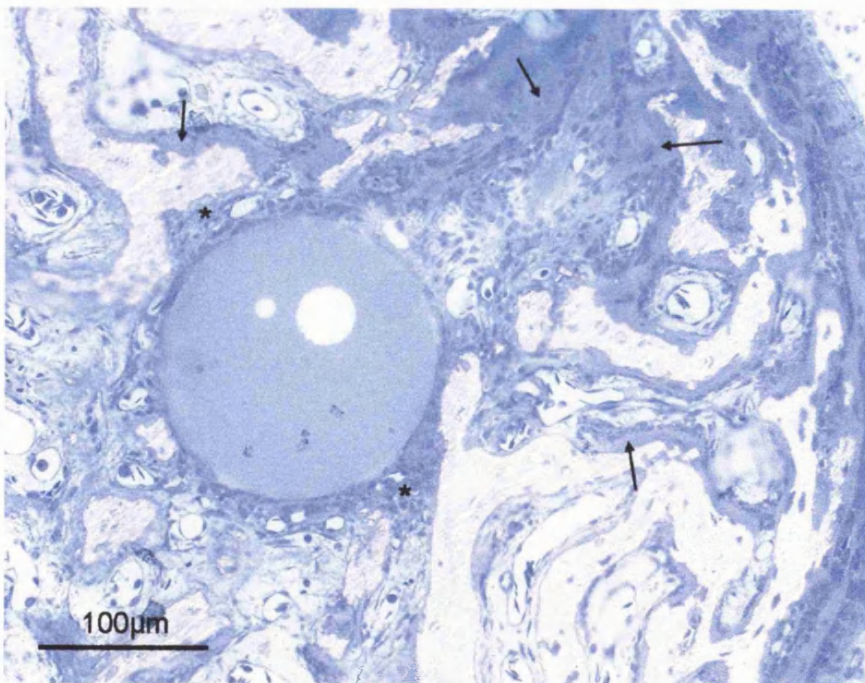


Figure 5.6 Test group at day 9, the increased cell density() and osteoid thickness (arrows) are still apparent.*

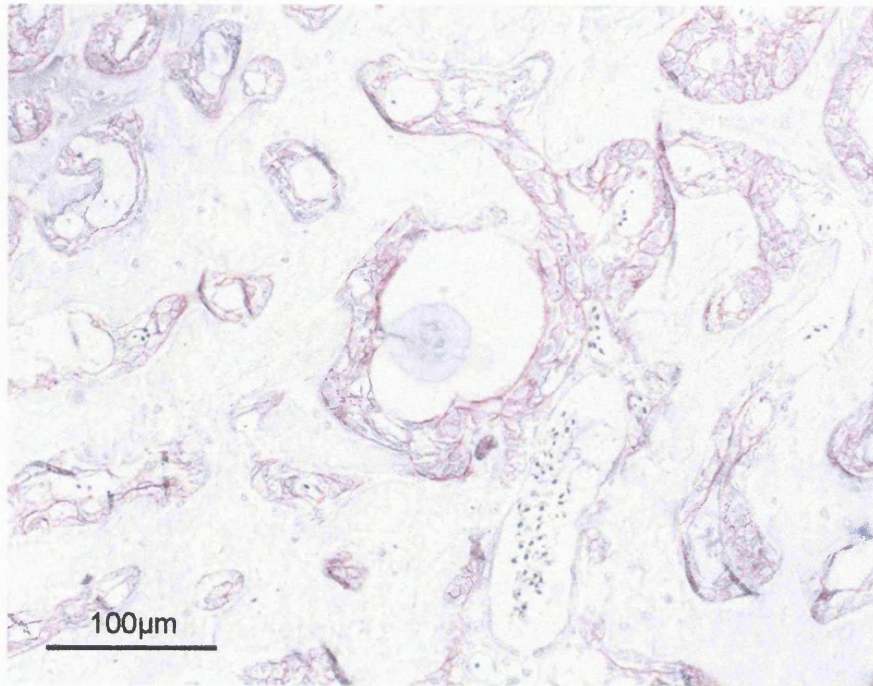


Figure 5.7 Control group at day 7. The cells surrounding this bead stain positively for alkaline phosphatase (in red). Counterstain haematoxylin.

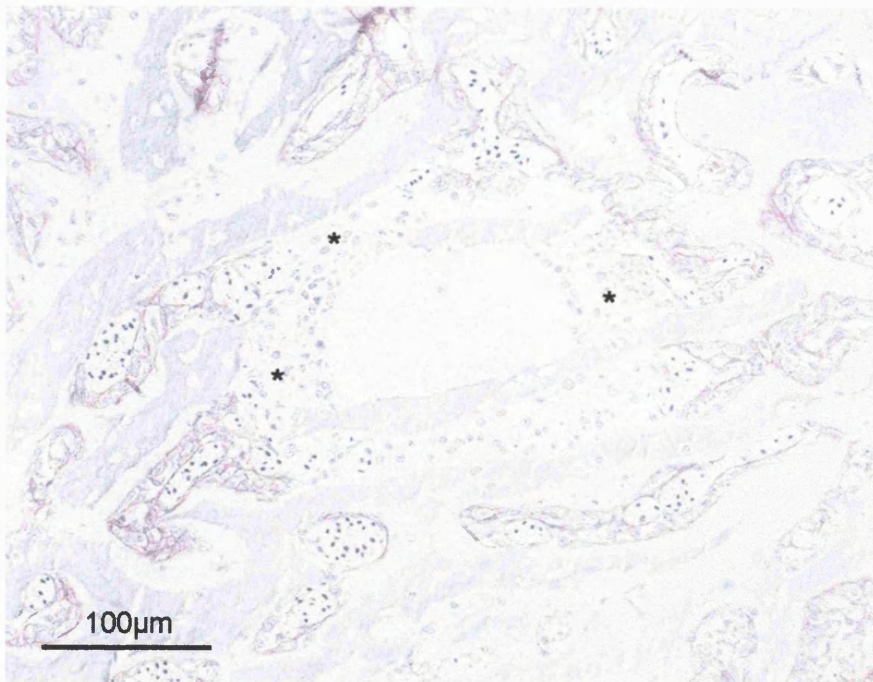


Figure 5.8 Test group at day 7. Alkaline phosphatase staining is conspicuously absent in the cells () around the bead up to 5 cell diameters away from its surface.*

	<i>bFGF</i>								<i>Control</i>							
<i>FEATURES</i>	1	2	3	4	5	6	7	8	1	2	3	4	5	6	7	8
<u><i>On surface of bead</i></u>																
Cell density	■■■	■■	■■	■■	■■■	■■■	■■	■■	■	■	■	■	■	■	■	■
Contact with cells	+	+	+	+	+	+	+	+	+	+	+	+	+	+	+	+
Contact with osteoid	+	o	o	o	o	o	o	o	+	+	+	+	+	+	+	+
Contact with mineralised bone	o	+	o	+	o	+	+	+	+	+	+	+	+	+	+	+
<u><i>One bead diameter away</i></u>																
Cell density	■■■	■■■	■■	■■	■■■	■■■	■■■	■■	■	■	■	■	■	■	■	■
Thickening of osteoid layer	+	+	+	+	+	o	o	o	o	o	o	o	o	o	o	o
<u><i>Central marrow cavity</i></u>																
Cell density	■■	■	■■	■■■	■■■	■■■	■■■	■■■	■	■	■	■	■	■	■	■
Condensation of cells into trabeculae	+	+	+	+	+	+	o	+	o	+	o	o	o	o	o	o
Presence of osteoid	+	+	+	+	+	o	o	+	o	+	o	o	o	o	o	o
Formation of mineralised bone	o	+	o	+	+	o	o	o	o	+	o	o	o	o	o	o

■ *normal appearance* ■■ *moderately increased* ■■■ *highly increased*
 + *present* o *absent*

Table 5.3 *Day 6 after grafting femurs containing agarose beads on CAM*

	<i>bFGF</i>												<i>Control</i>											
<i>FEATURES</i>	1	2	3	4	5	6	7	8	9	10	11	12	1	2	3	4	5	6	7	8	9	10	11	12
<u><i>On surface of bead</i></u>																								
Cell density	■■■	■■■	■■■	■■■	■■	■■■	■■■	■■■	■■■	■■	■■■	■■■	■	■	■	■■	■	■	■	■	■	■	■	■
Contact with cells	+	+	+	+	+	+	+	+	+	+	+	+	+	+	+	+	+	+	+	+	+	+	+	+
Contact with osteoid	o	o	o	o	+	+	+	o	+	+	+	o	o	o	+	+	+	+	o	o	o	+	o	+
Contact with mineralised bone	o	o	o	+	+	o	+	+	+	+	o	+	o	+	+	+	+	+	+	+	+	+	o	+
<u><i>One bead diameter away</i></u>																								
Cell density	■■■	■■■	■■■	■■■	■■	■■■	■■■	■■■	■■■	■■	■■■	■■■	■	■	■	■■	■	■	■	■	■	■	■	■
Thickening of osteoid layer	+	+	o	+	o	+	o	+	+	+	+	+	o	o	o	o	o	o	o	o	o	o	o	o
<u><i>Central marrow cavity</i></u>																								
Cell density	■■■	■■	■■■	■■■	■	■■	■■■	■■	■	■	■	■	■	■	■	■■	■	■	■	■	■	■	■■	■
Condensation of cells into trabeculae	+	+	+	+	+	+	+	+	+	+	+	+	o	o	o	o	o	o	o	o	o	+	o	o
Presence of osteoid	+	+	+	+	+	+	+	+	+	+	+	+	o	o	o	o	o	o	o	o	o	o	o	o
Formation of mineralised bone	+	o	+	+	+	+	+	+	+	+	+	+	o	o	o	o	o	o	o	o	o	+	o	o

■ *normal appearance* ■■ *moderately increased* ■■■ *highly increased*
 + *present* o *absent*

Table 5.4 *Day 7 after grafting femurs containing agarose beads on CAM*

	<i>bFGF</i>										<i>Control</i>									
<i>FEATURES</i>	1	2	3	4	5	6	7	8	9	10	1	2	3	4	5	6	7	8	9	10
<u><i>On surface of bead</i></u>																				
Cell density	■■■	■■■	■■■	■■■	■■■	■■	■■■	■■■	■■■	■■■	■	■	■■	■	■	■	■	■	■	■
Contact with cells	+	+	+	+	+	+	+	+	+	+	+	+	+	+	+	+	+	+	+	+
Contact with osteoid	+	o	o	+	+	+	o	+	+	o	o	o	+	+	o	+	o	o	o	o
Contact with mineralised bone	+	o	o	o	+	+	o	+	o	o	+	+	+	+	o	+	+	o	+	+
<u><i>One bead diameter away</i></u>																				
Cell density	■■■	■■	■■	■■■	■■	■	■	■■	■■	■	■	■	■	■	■	■	■	■	■	■
Thickening of osteoid layer	+	o	o	+	o	+	o	+	+	o	o	o	o	o	o	o	o	o	o	o
<u><i>Central marrow cavity</i></u>																				
Cell density	■■	■	■■	■■	■■	■	■	■■	■	■■	■	■	■■	■	■	■	■	■	■	■
Condensation of cells into trabeculae	+	+	+	+	+	+	o	+	+	+	o	o	o	o	o	+	o	o	o	o
Presence of osteoid	+	+	+	+	+	o	o	+	+	+	o	o	o	o	o	+	o	o	o	o
Formation of mineralised bone	+	+	+	+	+	+	o	+	+	+	o	o	o	o	o	+	o	o	o	o

■ *normal appearance* ■■ *moderately increased* ■■■ *highly increased*
 + *present* o *absent*

Table 5.5 *Day 9 after grafting femurs containing agarose beads on CAM*

5.4 Discussion

The findings in this experiment confirm current concepts of the effects of bFGF on bone formation. The histology of the femur sections clearly shows a different local tissue reaction in the presence of beads carrying the growth factor, compared to the control group. In a typical section from the control group, the repair of the wound created by the insertion of the carrier bead was completed by day 6. This is in keeping with the findings in the earlier implant experiments. The cross-section of the femur showed more bone-forming cells and thicker layers of non-mineralised matrix in the subperiosteal region, as expected for normal circumferential growth. The cell density and bone architecture around the bead was the same as distant areas at the same depth within the section. A well-defined central marrow cavity was present in nearly all of the control group specimens.

In the test group, the examination of the sections reveals a proliferative effect around the bead. On the surface of the bead was a large number of cells showing osteoblastic morphology without matrix formation but more abundant osteoid further away from the bead, suggestive of the presence of a strong proliferative stimulus from the locally released growth factor. The absence of alkaline phosphatase in the several cell layers on the bead surface is a clear illustration that the cells in a proliferative phase show reduced phenotypic expression.

An increase in cell density was also observed in the marrow spaces together with bone formation within the central marrow cavity. The normal growth pattern in which endosteal resorption leads to the enlargement of the marrow cavity was affected by the presence of bFGF. This is inferred from the high number of cases where the marrow cavity was markedly reduced or even obliterated by new bone trabeculae. The formation of these trabeculae within the central marrow cavity could have arisen from bone marrow stromal cells which have differentiated into osteoblasts. *In vitro* work by Pitaru et al. (1993) has demonstrated that bFGF has a strong promoting effect on osteogenesis in bone marrow stromal cell cultures.

There are several ways in which exogenous bFGF may lead to increased bone formation

1. Direct stimulation of proliferation of bone forming cells resulting in an increase in total bone formation.
2. Direct stimulation of differentiation of the bone cells.
3. A combination of 1 and 2.
4. Via synergistic effects with other bone growth factors already present in bone matrix
5. As an indirect consequence of increased angiogenesis.

This CAM graft experiment provides direct confirmation of point 1. Point 2 and 3 cannot be confirmed or excluded since the relatively higher concentration of the growth factor immediately around the bead resulted in proliferation rather than differentiation, but it is not known whether the increased bone matrix formation further away from the bead was solely due to the higher number of osteogenic cells or not. However, the deposition of new bone trabeculae within the central marrow cavity, where they were not expected to form during normal growth, may be an indication that pluripotential marrow stromal cells were stimulated into differentiation into osteoblasts by the growth factor. The mechanisms underlying possible synergism between growth factors can only be adequately explored using *in vitro* cultures where serum-free medium can be used to control precisely the amount and combination of growth factors. The embryonic femur cultured on the CAM would be subject to the growth factors released from the bone matrix during the implantation procedure, those produced by the cells and to circulating growth factors from the host, a situation more akin to *in vivo* systems. The effect of bFGF on angiogenesis has not been explored in this experiment. Even within the control group, new blood vessel formation was a prominent feature in this grafting system. Distinguishing bFGF effects above this background level of activity will require detailed histomorphometric analysis.

5.4.1 The mode of delivery of the growth factor

The agarose carrier used in this experiment was chosen instead of other carriers such as hydroxyapatite, collagen or demineralised bone matrix which are known for exerting their own effects on bone formation in addition to growth promoting substances they may carry. The growth factor in solution was absorbed into the highly hydrophilic polymer network rather than adsorbed on the surface as could be the case for other solid polymeric carriers, unless the growth factor was physically dispersed within the polymeric matrix by compression moulding. The dynamics of release of the growth factor from the agarose beads used in this set of experiments is unknown, although the system has been successfully used to evaluate the effect of FGF-4 on tooth morphogenesis (Vaahtokari et al., 1996), and to deliver bFGF blocking antibodies in CAM grafts of chick embryonic calvaria (Moore, 1997).

By administering the growth factor locally rather than systemically, a concentration gradient would be present within the cross-section of the femur. Cells close to the bead, where there was a higher concentration of growth factor, showed continued proliferation at the expense of differentiation, although cells further away from the bead at the intermediate area where the concentration of bFGF was lower expressed alkaline phosphatase and formed osteoid. Several *in vivo* studies in which bFGF was released locally have shown increased mesenchymal cells and osteoid-like tissue within bone allografts and hydroxyapatite (Wang and Aspenberg, 1994, 1996a, 1996b).

Given that many growth factors exhibit effects on multiple cell types, systemic administration of growth factors for therapeutic use may produce undesirable effects in addition to the therapeutic targets. In the case of bFGF, Mazuè et al. (1992) found that repeated intravenous administrations of high doses in monkeys and rats resulted in normochromic, normocytic anaemia. Urea, serum creatinine, total serum protein, albumin and urinary protein were affected and there were lesions in the kidney glomeruli. Hyperostosis was found only in rats in the sternae and femurs where there was proliferation of trabecular bone within the diaphyseal cavity. These changes reduced but did not disappear completely with time. Localised delivery of the growth factor should reduce undesirable side effects. The local effects of bFGF seen in this study are

encouraging in this respect. Further work is needed to study the binding of the growth factor to surfaces of metal and ceramic implant materials and their release into the peri-implant tissues. bFGF is known to have an affinity to heparin and heparan sulphate proteoglycans (HSPGs). A coating of HSPGs may be a potential vehicle for releasing the growth factor from implant surfaces.

5.4.2 The time factor

In the test group sections, the observed cell proliferation and abundance of osteoid matrix which had yet to become mineralised by the end of grafting period, would indicate a delayed expression of the osteoblast phenotype. It is likely that in a late phase, following the cessation of the effect of bFGF, full mineralisation of the matrix would result. The duration of the experiment did not allow the follow-up of the biphasic effect which has been suggested in reports of *in vivo* experiments. Nakamura et al (1995) in an *in vivo* study in rats, reported that systemic administration of bFGF daily for 7 days led to an increase of preosteoblastic cells in the first 1-3 days, then a differentiation of such cells into osteoblasts, and finally, after the fifth day, a production of new bone. In other words, the proliferative event was limited to an initial phase which, in time, is followed by the onset of phenotypic expression.

5.5 Conclusion

Basic fibroblast growth factor delivered locally in the femurs promoted cell proliferation. The cells adjacent to the carrier bead did not produce alkaline phosphatase or differentiate osteogenically, indicating that when in a proliferative mode their phenotypic expression was reduced. Compared to the control group, more immature bone matrix was present in the region beyond the zone of proliferation. The conclusion is that addition of this particular growth factor would increase bone formation but the maturation of the bone formed would take place over a longer period of time than untreated sites. The clinical implication is that the short-term local application of this factor would lead to a greater amount of bone formation but would not shorten the time for osseointegration to occur. The results of this experiment using the CAM graft model showed features similar to those observed both *in vitro* and *in vivo* in respect of bFGF

effects, providing further demonstration of the potential and limitations of the model as a short-term assay system for studying bone-biomaterial interactions.

6. General Discussion

The chorioallantoic membrane of developing chick eggs provides a completely self-contained culture environment to sustain the growth, development and repair of bone. Within this environment, the embryonic femur grafts described in the previous chapters consistently showed:

1. Good bone growth with maintenance of normal morphology and tissue architecture.
2. The relationship between the periosteal, trabecular bone, marrow and vascular elements is preserved.
3. Both osteogenic and osteoclastic cells were functional within the grafts.
4. The new bone matrix formed become mineralised.
5. The ability of the graft to repair following insertion of titanium and Apoceram implants.
6. The grafted tissue responds to local release of basic fibroblast growth factor with increased cell proliferation and bone formation.

The femoral CAM graft brings together the different elements involved in the process of bone healing and provides a model which complements *in vitro* and *in vivo* experimental work on the response of bone to implant insertion. It has been demonstrated that the model can be used to follow the development of the early bone-implant interface, to distinguish variations in the rate and pattern of bone formation between different implant materials and to study the effects of growth factors which may influence bone healing. In this chapter, a general appraisal of the model in terms of its advantages and limitations is presented together with a discussion of its role in the experimental strategies for studying bone-biomaterials interactions. Finally, some suggestions are made for the directions of future work, which stems from the development of the femoral CAM graft system.

6.1 The advantages and limitations of the CAM graft system

The CAM graft model is a truly self-sustaining culture system. Apart from an egg incubator, no specialised equipment is required. It is cheap and easy to maintain when compared to any laboratory animal systems as well as *in vitro* cell and tissue culture set-ups. The eggs cost less than twenty pence each and are available all year round. By using eggs of similar size from an identical strain at the same stage of development, size and genetic variations in the donor tissue can be kept to a minimum and the hosts can be kept in a constant environment.

The grafting and implantation procedures involve microdissection which requires good manual dexterity and care. The ability to manipulate tissues under magnification can be acquired with training by most research workers. A retrieval rate of 80% and above can be readily achieved. Within this system, the different cell types in the donor tissue are maintained in their normal relationship and can interact naturally. The tissues, specifically bone grafts, show excellent vitality compared to *in vitro* cultures.

Once integrated with the CAM, the graft is connected to the host blood circulation. This feature is crucial to the maintenance of repair capacity of the grafted bone. It also implies that the graft is exposed to systemic factors such as hormones and other substances carried in the host blood stream. It is possible to administer drugs or chemical agents either systemically or locally. With the chick egg being a fully enclosed environment, however, metabolites and excretory products also remain within the system, although becoming sequestered into the allantois. Nitrogenous wastes are also produced in an insoluble form, as uric acid and not soluble urea.

The CAM graft model has two main constraints. The first is the limit to the size of tissue which can be grafted. As reported in Chapter 3, the survival of the graft is reduced with increasing size, the upper limit of tissue thickness beyond which viability is compromised is around 2mm. The critical period is the first two days following grafting. Prior to the complete proliferation of the CAM around the bone and the re-establishment of the blood circulation to the graft, the tissues are susceptible to becoming necrotic. The

larger the graft, the longer it takes for the CAM to grow around the tissue and the more difficult it is for gases, nutrients and metabolites to infiltrate the full depth of the tissues. The size limitation also applies to the size of the implant which can be used. This factor influences to a certain extent the subsequent handling of the tissue specimens and the examination methods. The positive aspects are: the small bone specimens can be processed without decalcification; dehydration and infiltration times are relatively short compared to larger specimens obtained from *in vivo* experiments. The preparation of resin-embedded sections using diamond and glass knives rather than by sawing and grinding is also made possible by the small size of the specimens. The resolution of such sections at light microscopy level is superior to the much thicker ground sections. It is possible to obtain serial sections without the loss of tissue that occurs with ground section techniques. But the drawback is that it is a slow and laborious process when the specimens contain hard metallic or ceramic implants. Semi-automation, which is possible with currently available sawing and grinding equipment, is unfortunately not an option.

The second major constraint of the CAM graft model is the duration of the culture period. This is most evident in the experiment performed to study basic fibroblast growth factor effects, presented in Chapter 5. The eventual phenotypic expression of the alkaline phosphatase negative cells on the surface of the growth factor carrier bead remains unknown at the end of the 9-day culture period. However, this limitation of the model has been mitigated to a great extent by the inherently high growth rate and repair capacity of the donor foetal chick tissue which is facilitated by the vascular supply from the host chick. It has been clearly demonstrated that within the duration of the grafting period, significant amounts of new bone form on the surface of both the Apoceram and titanium implants (Chapter 4). The increase in percentage figures for bone-implant contact during the grafting period reflects the level of activity within the graft and these figures were almost comparable to those reported in much longer term *in vivo* experiments. This can be attributed to the fact that the embryonic femur is highly cellular with a large population of mesenchymal cells, providing a rich source of osteogenic cells for new bone formation. The contribution of the scale and proportions of the implant and graft have been discussed in Chapter 4. The model can

almost be regarded as a miniaturised, ‘fast-forward’ system in which bone formation and repair progress under near *in vivo* conditions.

Nevertheless, the time factor, as well as the absence of mechanical loads, makes the CAM grafted femur inappropriate for examination of longer term events such as bone remodelling and degradation of the implant surface after the development of the early interface.

6.2 *In vitro* vs. *in vivo* approaches to implant testing: where does the CAM graft model fit in?

By understanding of the capabilities and limitations of the CAM graft system, we can put the model into perspective amongst the experimental strategies available for studying bone-implant interactions. When an intra-oral site is prepared for a dental implant, there is injury to the mucosa, the periosteum, cortical and cancellous bone, bone marrow, muscle, nerve and blood supply. The contributions of each of the tissues to the overall healing process will dictate the clinical outcome. This is further influenced by the physical, chemical and mechanical characteristics of the implant. Determining how each of these components affects the potential for and rate of healing requires not only the characterisation of the implant materials but also understanding of the mechanisms of tissue repair.

It is true to say that the ultimate test of the performance of an implant material is by clinical usage. No assay system, *in vitro* or *in vivo*, can faithfully reproduce the complete range of anatomy, physiology and biochemistry of the human tissues which will be host to the artificial substrata. The purpose of experimental investigations is to establish the biological safety of new materials prior to their clinical application, to distinguish the stages and components in biological reactions to various implant materials and to elucidate the underlying control mechanisms. The outcome of such work will ultimately help to expand clinical application of implants, improve clinical outcomes and reduce failures. The choice of experimental system depends on the hypotheses to be tested. Evaluation of biological responses can be performed at the organism, organ, tissue, cellular and molecular levels. The salient features of *in vitro* and

in vivo approaches to biological testing have been reviewed in Chapter 1 and are summarised in the table below:

<i>In vitro</i>	<i>In vivo</i>
<ul style="list-style-type: none"> • cell culture <ul style="list-style-type: none"> – usually single cell types • tissue culture <ul style="list-style-type: none"> – retain histological and biochemical differentiation – cannot be propagated – variation • organ culture <ul style="list-style-type: none"> – preserve parenchymal and stromal components – non-growing – variation • advantages <ul style="list-style-type: none"> – controlled environment – quantitative measurements – quick results at relatively low cost • disadvantages <ul style="list-style-type: none"> – unsuitable for complex tissue responses where the integrity of the blood supply is required • applications <ul style="list-style-type: none"> – cytotoxicity – cell attachment – cell spreading – cell/tissue growth – differentiation (molecular and gene expression) 	<ul style="list-style-type: none"> • diffusion chamber <ul style="list-style-type: none"> – isolated from host cells but receives nutrients and growth factors • implantation in whole animal <ul style="list-style-type: none"> – mainly for tissue histology and biomechanical testing • advantages <ul style="list-style-type: none"> – physiological environment • disadvantages <ul style="list-style-type: none"> – variation – cost – ethical considerations • applications <ul style="list-style-type: none"> – systemic toxicity – immune reactions – tissue histology – molecular and gene expression

In the context of evaluation of bone-biomaterials interactions, there is a clear dichotomy in the nature of *in vivo* and *in vitro* methods. The nature of the CAM graft model is closer to the *in vivo* situation and can be used to overcome some of the shortcomings of, as well as complement, both approaches. *In vivo* experimentation mainly provides information on tissue histology at the bone-biomaterials interface and is used for biomechanical testing. It is the only way in which medium to long term tissue responses can be studied. For assessment of short-term cell or tissue toxicity, we can use

in vitro culture systems to evaluate cell death or damage caused by contact with novel implant materials. If overt cell toxicity is absent in such tests, the CAM graft model can be applied as a simple and economical way of assessing the early stages of healing of bone around implants. The model should produce consistent results among laboratories and is less expensive for screening newly developed materials. It seems reasonable to discriminate between the early effects of an implant material on the processes during wound healing which affect the development of immature tissue and the late effects which modify the turnover of a more mature tissue, as, in the case of bone, the remodelling. For instance, if one wishes to examine a large range of compositions of a new glass-ceramic material, by studying the early effects with the CAM graft model, one can determine whether an implant material should also be studied in more clinically analogous implant sites in large animals to look at loading, implant design in long-term trials. This will reduce the unnecessary sacrifice of laboratory animals.

In terms of elucidating the biology of bone healing around implants, the complexity of the *in vivo* environment does make the task of defining the cascades of biological, material and interfacial responses difficult. The premise of using *in vitro* systems is to reconstitute the events which takes place during the healing period, whether one at a time or as many as possible, with isolated cells, cytokines, growth factors and other molecules presumed to be important to the development of the bone-implant interface. The biomaterials literature over the last few years shows a definite trend of placing isolated bone-forming cells on implant materials to observe their attachment, growth, phenotypic as well as gene expression. Techniques developed in the field of fundamental cell biology are applied to bone cells grown on artificial implant substrata in place of tissue culture polystyrene. By using isolated cells and controlling the environment in which they are cultured, details of cell behaviour, down to molecular level can be readily quantified. However, the complex nature of bone as an organ or tissue means that the study of each cell and its functions as isolated systems may not accurately depict the *in vivo* biology of bone healing. An implant site *in vivo* contains a heterogeneous population of cells whose distribution changes with time. Interactions between different cells types seem to be neglected in many *in vitro* experiments purporting to explore bone-implant interactions. The commitment and differentiation of

osteogenic cells are dependent on and influenced by signals emanating from other cells, from the matrix and the general environment of the organism (systemic factors). In this respect, the CAM graft model mimics aspects of the known *in vivo* responses and is well placed for the examination of the early stages in the formation of the bone-implant interface. The role of the CAM graft model can be perceived as a stepping stone for further elucidation of the significant biological events in order to devise appropriate *in vitro* simulation. The relative contributions of periosteum, bone cortex, marrow, and vasculature to the healing process can be evaluated experimentally by ablation of specific compartments by surgical manipulation, use of barriers or pharmacological treatments. One of the tasks ahead is to identify individual cell populations at the wound site, not just the osteoblastic and osteoclastic phenotypes, but more importantly the identity of cells involved in the organisation of wound repair as well as those attaching to the implant surface. The temporal and spatial expression of cytokines, growth factors, and inflammatory mediators which contribute to the cascade of repair is another area to be explored. The mechanisms of interaction may then be explained by further studies employing cell and molecular biologic methods.

Some of the observations in the CAM graft experiments raise questions which I would like to explore *in vitro*: Do macrophages in the bone wound provide signals for the osteoprogenitor cells to migrate into the wound and attach to the implant? Is the recruitment and formation of the multinucleated giant cells influenced by the type of implant material and are they osteoclasts? Perhaps the use of co-culture systems or incorporating medium conditioned by one cell type exposed to the implant in the culture of bone cells on the same material would help address the issue of interactions between different cell types? The contribution of individual cells to bone repair and how they modulate each other's action requires elucidation by the integrated use of both *in vivo* and *in vitro* models. Given the complexity of skeletal repair and the large number of factors involved in the regulation of these processes, the question of 'what is the most useful type of assay?' is less important than 'what is one attempting to test?'.



Acknowledgements

I am deeply grateful to my supervisors, Professor John Hobkirk, head of Dept. of Prosthetic Dentistry, Eastman Dental Institute and Professor Peter Thorogood, head of Developmental Biology Unit, Institute of Child Health, for their guidance and constant support throughout this project.

I would like to express my gratitude to all who helped me during the course of my work, in particular:

Ms. Nicola Mordan and Mrs. Pauline Barber
Electron Microscopy Unit, Eastman Dental Institute

Prof. Paul Speight, Dr. Jonathan Bennett, Mr. Paul Darkins, Mrs. Bushra Ahmed and Miss Anousheh Alavi
Oral Pathology Department, Eastman Dental Institute

Dr. Sajeda Meghji
Oral and Maxillofacial Surgery Department, Eastman Dental Institute

Miss Rachael Moore, Miss Sanjukta Sarkar and Dr. Jo Chan
Developmental Biology Unit, Institute of Child Health

Prof. Rees Rawlings, Dr. Belinda Taylor and Dr. Hasan Alanyali
Dept. of Materials, Imperial College, London

Dr. Larry Fisher
National Institute of Dental Research, U.S.A

Finally, I thank Eric for his patience and understanding.

References

- ABERCROMBIE, M., HEAYSMAN, J. E. M., and PEGRUM, S. M. (1970). The locomotion of fibroblasts in culture. II. 'Ruffling'. *Exp. Cell Res.* **60**, 437-444.
- ABIKO, Y., BRUNETTE, D. M., JENSEN, J. A., NANJI, A., TODESCAN, R., and HEATH, J. P. (1993). Immunohistochemical investigation of tracks left by the migration of fibroblasts on titanium surfaces. *Cells & Materials* **3**, 161-170.
- ADELL, R., ERIKSSON, B., LEKHOLM, U., BRÄNEMARK, P. I., and JEMT, T. (1990). A long-term follow-up study of osseointegrated implants in the treatment of the totally edentulous jaws. *Int. J. Oral Maxillofac. Implants* **5**, 347-359.
- AKAGAWA, Y., HASHIMOTO, M., KONDO, N., SATOMI, K., TAKATA, T., and TSURU, H. (1986). Initial bone-implant interfaces of submergible and supramergible endosseous single-crystal sapphire implants. *J. Prosthet. Dent.* **55**, 96-100.
- AKAGAWA, Y., SATOMI, K., NIKAI, H., and TSURU, H. (1990). Initial interface between submerged hydroxyapatite-coated titanium alloy implant and mandibular bone after non-tapping and tapping insertions in monkeys. *J. Prosthet. Dent.* **63**, 559-564.
- ALBERTS, B., BRAY, D., LEWIS, J., RAFF, M., ROBERTS, K., and WATSON, J. D. (1989). The extracellular matrix. In "Molecular Biology of the Cell", 2nd Ed., pp. 802-823. Garland Publishing Inc., New York.
- ALBREKTSSON, T. (1984a). Osseous penetration rate into implants pretreated with bone cement. *Arch. Orthop. Trauma Surg.* **102**, 141-147.
- ALBREKTSSON, T. (1984b). The response of bone to titanium implants. In "CRC Critical Reviews in Biocompatibility" (D. F. Williams, Ed.), Vol. 1, pp. 53-84. CRC Press, Boca Raton, Florida.
- ALBREKTSSON, T. (1988). A multi-center report on osseointegrated oral implants. *J. Prosthet. Dent.* **60**, 75-84.
- ALBREKTSSON, T., and HANSSON, H. A. (1986). An ultra-structural characterization of the interface between bone and sputtered titanium or stainless steel surfaces. *Biomaterials* **7**, 201-205.
- ALBREKTSSON, T., and SENNERBY, L. (1991). State of the art in oral implants. *J. Clin. Periodontol.* **18**, 474-481.
- ALBREKTSSON, T., HANSSON, H. A., and IVARSSON, B. (1985). Interface analysis of titanium and zirconium bone implants. *Biomaterials* **6**, 97-101.
- ALLIOT-LICHT, B., GREGOIRE, M., ORLY, I., and MENANTEAU, J. (1991). Cellular activity of osteoblasts in the presence of hydroxyapatite: an in vitro experiment. *Biomaterials* **12**, 752-756.
- AMIR, D., MÜLLER-MAI, C., WENDLAND, H., GROSS, U., and SELA, J. (1989). Effect of glass-ceramic implants on primary calcification in rat tibial bone after injury. *Biomaterials* **10**, 585-589.
- ANNEROTH, G., HEDSTROM, K. G., KJELLMAN, O., KONDELL, P. A., and NORDENRAM, A. (1985). Endosseous titanium implants in extraction sockets. An experimental study in monkeys. *Int. J. Oral Surg.* **14**, 50-54.

ANSELME, K., LANEL, B., GENTIL, C., HARDOUIN, P., MARIE, P. J., and SIGOTLUIZARD, M. F. (1994). Bone organotypic culture method - a model for cytocompatibility testing of biomaterials. *Cells & Materials* **4**, 113-123.

ARONOW, M. A., GERSTENFELD, L. C., OWEN, T. A., TASSINARI, M. S., STEIN, G. S., and LIAN, J. B. (1990). Factors that promote progressive development of the osteoblast phenotype in cultured fetal rat calvarial cells. *J. Cell Physiol.* **143**, 213-221.

ARVIDSON, K., FARTASH, B., MOBERG, L. E., GRAFSTROM, R., and ERICSSON, I. (1991). In vitro and in vivo experimental studies on single crystal sapphire dental implants. *Clin. Oral Implants Res.* **2**, 47-55.

ASHTON, B. A., ALLEN, T. D., HOWLETT, C. R., EAGLESOM, C. C., HATTORI, A., and OWEN, M. (1980). Formation of bone and cartilage by marrow stromal cells in diffusion chambers in vivo. *Clin. Orthop.* **151**, 294-307.

ASHTON, B., CAVE, F., WILLIAMSON, M., SKYES, B., COUCH, M., and POSER, J. (1985). Characterization of cells with high alkaline phosphatase activity derived from human bone and marrow: preliminary assessment of their osteogenicity. *Bone* **6**, 313-319.

ASPENBERG, P., WANG, J. S., CHOONG, P., and THORNGREN, K. G. (1994). No effect of growth hormone on bone graft incorporation. Titanium chamber study in the normal rat. *Acta. Orthop. Scand.* **65**, 456-461.

ATTAWIA, M. A., DEVIN, J. E., and LAURENCIN, C. T. (1995). Immunofluorescence and confocal laser scanning microscopy studies of osteoblast growth and phenotypic expression in three-dimensional degradable synthetic matrices. *J. Biomed. Mater. Res.* **29**, 843-848.

AUBIN, J. E., and TURKSEN, K. (1996). Monoclonal antibodies as tools for studying the osteoblast lineage. *Microsc. Res. Tech.* **33**, 128-140.

AUBIN, J. E., TURKSEN, K., and HEERSCHKE, J. N. M. (1993). Osteoblastic cell lineage. In "Cellular and molecular biology of bone" (M. Noda, Ed.), pp. 1-29. Academic Press Inc., San Diego, California.

BAB, I., PASSI-EVEN, L., GAZIT, D., SEKELES, E., ASHTON, B., PEYLAN-RAMU, N., ZIV, I., and ULAMANSKY, M. (1988). Osteogenesis in in vivo diffusion chamber cultures of human marrow cells. *Bone Miner.* **4**, 373-386.

BAGAMBISA, F. B., and JOOS, U. (1990). Preliminary studies on the phenomenological behaviour of osteoblasts cultured on hydroxyapatite ceramics. *Biomaterials* **11**, 50-56.

BAGAMBISA, F. B., JOOS, U., and SCHILLI, W. (1993). Mechanisms and structure of the bond between bone and hydroxyapatite ceramics. *J. Biomed. Mater. Res.* **27**, 1047-1055.

BAIER, R. E., MEYER, A. E., NATIELLA, J. R., NATIELLA, R. R., and CARTER, J. M. (1984). Surface properties determine bioadhesive outcomes: methods and results. *J. Biomed. Mater. Res.* **18**, 327-355.

BALE, R. S., and ANDREW, J. G. (1994). Characterisation of fracture healing using a chorioallantoic membrane model. *Bone* **15**, 732 (Abstract P4).

BARON, R., VIGNERY, A., NEFF, L., SILVERGATE, A., SANTA MARIA, A. (1983). Processing of undecalcified bone specimens for bone histomorphometry. In "Bone histomorphometry: techniques and interpretation" (R. R. Recker, Ed.), pp. 13-35. CRC Press, Boca Raton, Florida.

BARZILAY, I., GRASER, G. N., IRANPOUR, B., NATIELLA, J. R., and PROSKIN, H. M. (1996). Immediate implantation of pure titanium implants into extraction sockets of Macaca Fascicularis. Part II: histologic observations. *Int. J. Oral Maxillofac. Implants* **11**, 489-497.

BEGLEY, C. T., DOHERTY, M. J., HANKEY, D. P., and WILSON, D. J. (1993). The culture of human osteoblasts upon bone graft substitutes. *Bone* **14**, 661-666.

BELL, P. B. (1978). Contact inhibition of movement in transformed and non-transformed cells. *Birth Defects* **14**, 177-194.

BELLOWS, C. C., and AUBIN, J. E. (1989). Determination of numbers of osteoprogenitors present in foetal rat calvaria cells in vitro. *Dev. Biol.* **133**, 8-13.

BELLOWS, C. G., AUBIN, J. E., HEERSCHE, J. M. N., and ANTOSZ, M. E. (1986). Mineralized bone nodules formed in vitro from enzymatically released rat calvaria cell populations. *Calcif. Tissue Int.* **38**, 143-154.

BELLOWS, C. G., AUBIN, J. E., and HEERSCHE, J. N. M. (1987). Physiological concentrations of glucocorticoids stimulate formation of bone nodules isolated from rat calvaria cells in vitro. *Endocrinology* **121**, 1987-1992.

BENBASSAT, H., KLEIN, B. Y., LERNER, E., AZOURY, R., RAHAMIM, E., SHLOMAI, Z., and SARIG, S. (1994). An in vitro biocompatibility study of a new hydroxyapatite ceramic ha-sall - comparison to bioactive bone substitute ceramics. *Cells & Materials* **4**, 37-50.

BENTLEY, K. L., and KLEBE, R. J. (1985). Fibronectin binding properties of bacteriologic petri plates and tissue culture dishes. *J. Biomed. Mater. Res.* **19**, 757-769.

BERESFORD, J. N., GALLAGHER, J. A., GOWEN, M., MCGUIRE, M. K. B., POSER, J., and RUSSELL, R. G. G. (1983). Human bone cells in culture. A novel system for the investigation of bone cell metabolism. *Clin. Sci* **64**, 38-39.

BERESFORD, J. N., GALLAGHER, J. A., POSEN, J. W., and RUSSELL, R. G. G. (1984). Production of osteocalcin by human cells in vitro. Effects of 1,25(OH)₂D₃; 24,25(OH)₂D₃; parathyroid hormone and glucocorticoids. *Metab. Bone Dis. Rel. Res.* **5**, 229-234.

BERESFORD, J. N., GRAVES, S. E., and SMOOTHY, C. A. (1993). Formation of mineralized nodules by bone derived cells in vitro: A model of bone formation? *Am. J. Med. Genet.* **45**, 163-178.

BERESFORD, J. N., JOYNER, C. J., DEVLIN, C., and TRIFFIT, J. T. (1994). The effects of dexamethasone and 1,25 dihydroxyvitamin D₃ on osteogenic differentiation of human bone marrow stromal cells in vitro. *Arch. Oral Biol.* **39**, 941-947.

BERRY, J. L. (1985). A method to prepare bone-implant specimens for laboratory analysis. *Calcif. Tissue Int.* **37**, 572-574.

BERSTEIN, A., BERNAUER, I., MARX, R., and GEURTSSEN, W. (1992). Human cell culture studies with dental metallic materials. *Biomaterials* **13**, 98-100.

BERTOLINI, D. R., and STRASSMANN, G. (1991). Differential activity of granulocyte-macrophage and macrophage colony stimulating factors on bone resorption in fetal rat long bone organ cultures. *Cytokine* **3**, 421-427.

BERTOLINI, D. R., VOTTA, B., HOFFMAN, S., and STRASSMANN, G. (1994). Interleukin 6 production in fetal rat long bone cultures is correlated with PGE₂ release and does not correlate with the extent of bone resorption. *Cytokine* **6**, 368-375.

BHARGAVA, U., BAR-LEV, M., BELLOWS, C. G., and AUBIN, J. E. (1988). Ultrastructural analysis of bone nodules formed in vitro by isolated fetal rat calvarial cells. *Bone* **9**, 155-163.

- BJURSTEN, L. M., EMANUELSSON, L., ERICSON, L. E., THOMSON, P., LAUSMAA, J., MATTSSON, L., ROLANDER, U., and KASEMO, B. (1990). Method for ultrastructural studies of the intact tissue-metal interface. *Biomaterials* 11, 596-601.
- BLOTTIERE, H. M., DACULSI, G., ANEGON, I., POUZAT, J. A., NELSON, P. N., and PASSUTI, N. (1995). Utilization of activated u937 monocytic cells as a model to evaluate biocompatibility and biodegradation of synthetic calcium phosphate. *Biomaterials* 16, 497-503.
- BOLANDER, M. E. (1994). Regulation of fracture repair and synthesis of matrix macromolecules. In "Bone formation and repair" (C. T. Brighton, M. D. Friedlaender, and J. M. Lane, Eds.), pp. 185-196. American Academy of Orthopaedic Surgeons, Rosemont, Illinois.
- BOUVIER, M., MARTIN, J. M., EXBRAYAT, P., RIGOLLET, E., LE MOGNE, T., TREHEUX, D., and MAGLOIRE, H. (1994). Ultrastructural study of calvaria-released osteoblasts cultured in contact with titanium-based substrates. *Cells & Materials* 4, 135-142.
- BOWERS, K. T., KELLER, J. C., RANDOLPH, B. A., WICK, D. G., and MICHAELS, C. M. (1992). Optimization of surface micromorphology for enhanced osteoblast responses in vitro. *Int. J. Oral Maxillofac. Implants* 7, 302-310.
- BOYAN, B. D., HUMMERT, T. W., DEAN, D. D., and SCHWARTZ, Z. (1996). Role of material surfaces in regulating bone and cartilage cell response. *Biomaterials* 17, 137-146.
- BOYDE, A. (1991). Scanning microscopies of bone cells and bone matrix. *Calcif. Tissue Int.* 48(A43), Abstr.4.
- BRÅNEMARK, P. I. (1983). Osseointegration and its experimental background. *J. Prosthet. Dent.* 50, 399-410.
- BROOK, I. M., CRAIG, G. T., and LAMB, D. J. (1991). In vitro interaction between primary bone organ cultures, glass-ionomer cements and hydroxyapatite/tricalcium phosphate ceramics. *Biomaterials* 12, 179-186.
- BROOK, I. M., CRAIG, G. T., HATTON, P. V., and JONCK, L. M. (1992). Bone cell interactions with a granular glass-ionomer bone substitute material: in vivo and in vitro culture models. *Biomaterials* 13, 721-725.
- BRUNETTE, D. M. (1986a). Fibroblasts on micromachined substrata orient hierarchically to grooves of different dimensions. *Exp. Cell Res.* 164, 11-26.
- BRUNETTE, D. M. (1986b). Spreading and orientation of epithelial cells on grooved substrata. *Exp. Cell Res.* 167, 203-217.
- BRUNETTE, D. M., KENNER, G. S., and GOULD, T. R. (1983). Grooved titanium surfaces orient growth and migration of cells from human gingival explants. *J. Dent. Res.* 62, 1045-1048.
- BURCHARD, W. B., COBB, C. M., DRISKO, C. L., and KILLOY, W. J. (1991). The effects of chlorhexidine and stannous fluoride on fibroblast attachment to different implant surfaces. *Int. J. Oral Maxillofac. Implants* 6, 418-426.
- BURGER, E. H., KLEIN-NULEND, J., and VELDHUIJZEN, J. P. (1991). Modulation of osteogenesis in fetal bone rudiments by mechanical stress in vitro. [Review]. *J. Biomech.* 24 Suppl 1, 101-109.
- BURR, D. B., MORI, S., BOYD, R. D., SUN, T. C., BLAHA, J. D., LANE, L., and PARR, J. (1993). Histomorphometric assessment of the mechanisms for rapid ingrowth of bone to HA/TCP coated implants. *J. Biomed. Mater. Res.* 27, 645-653.

- BUSCH, O., SOLHEIM, E., BANG, G., and TORNES, K. (1996). Guided tissue regeneration and local delivery of insulinlike growth factor I by bioerodible polyorthoester membranes in rat calvarial defects. *Int. J. Oral Maxillofac. Implants* **11**, 498-505.
- BUSHINSKY, D. A., LAM, B. C., NESPECA, R., SESSLER, N. E., and GRYPNAPAS, M. D. (1993). Decreased bone carbonate content in response to metabolic, but not respiratory, acidosis. *Am. J. Physiol.* **265**(4 Pt 2), F530-F536.
- CABRINI, R. L., GUGLIELMOTTI, M. B., and ALMAGRO, J. C. (1993). Histomorphometry of initial bone healing around zirconium implants in rats. *Implant Dent* **2**, 264-267.
- CANALIS, E., CENTRELLA, M., and MCCARTHY, T. (1988). Effects of basic fibroblast growth factor on bone formation in vitro. *J. Clin. Invest.* **81**, 1572-1577.
- CANALIS, E., CENTRELLA, M., and MCCARTHY, T. L. (1991). Regulation of insulin-like growth factor-II production in bone cultures. *Endocrinology* **129**, 2457-2462.
- CAPLAN, A. I., and PECHAK, D. G. (1987). The cellular and molecular embryology of bone formation. In "Bone and mineral research" (W. A. Peck, Ed.), Vol. 5, pp. 117-183. Elsevier, Amsterdam.
- CARLSSON, L., ROSTLUND, T., ALBREKTSSON, B., and ALBREKTSSON, T. (1988). Implant fixation improved by close fit. Cylindrical implant-bone interface. *Acta. Orthop. Scand.* **59**, 272-275.
- CASSER-BETTE, M., MURRAY, A. B., CLOSS, E. I., ERFLE, V., and SCHMIDT, J. (1990). Bone formation by osteoblast-like cells in a 3-D cell culture. *Calcif. Tissue Int.* **46**, 46-56.
- CHEHROUDI, B., GOULD, T. R., and BRUNETTE, D. M. (1989). Effects of a grooved titanium-coated implant surface on epithelial cell behaviour in vitro and in vivo. *J. Biomed. Mater. Res.* **23**, 1067-1085.
- CHEHROUDI, B., GOULD, T. R. L., and BRUNETTE, D. M. (1990). Titanium-coated micromachined grooves of different dimensions affect epithelial and connective-tissue cells differently in vivo. *J. Biomed. Mater. Res.* **24**, 1203-1219.
- CHEHROUDI, B., RATKAY, J., and BRUNETTE, D. M. (1992). The role of implant surface geometry on mineralization in vivo and in vitro: a transmission and scanning electron microscopic study. *Cells & Materials* **2**, 89-104.
- CHENU, C., VALENTIN-OPRAN, A., CHAVASSIEUX, P., SAEZ, S., MUNIEN, P. J., and DELMAS, P. D. (1990). Insulin like growth factor: hormonal regulation by growth hormone and by 1,25(OH)D3 and activity on human osteoblast-like cells in short term cultures. *Bone* **11**, 81-86.
- CHESMEL, K. D., CLARK, C. C., BRIGHTON, C. T., and BLACK, J. (1995). Cellular responses to chemical and morphologic aspects of biomaterial surfaces .2. the biosynthetic and migratory response of bone cell populations. *J. Biomed. Mater. Res.* **29**, 1101-1110.
- CHEUNG, H. S., and HAAK, M. H. (1989). Growth of osteoblasts on porous calcium phosphate ceramic: an in vitro model for biocompatibility. *Biomaterials* **10**, 63-67.
- CLOKIE, C. M. L., and WARSHAWSKY, H. (1995). Morphologic and radiographic studies of bone formation in relation to titanium implants using the rat tibia as a model. *Int. J. Oral Maxillofac. Implants* **10**, 155-165.
- COOK, S. D., KAY, J. F., THOMAS, K. A., and JARCHO, M. (1987). Interface mechanics and histology of titanium and hydroxylapatite-coated titanium for dental implant applications. *Int. J. Oral Maxillofac. Implants* **2**, 15-22.

COOPER, L. F., HANDELMAN, B., MCCORMACK, S. M., and GUCKES, A. D. (1993). Binding of murine osteoblastic cells to titanium disks and collagen I gels: implications for alternative interpretations of osseointegration. *Int. J. Oral Maxillofac. Implants* **3**, 264-272.

COURTENNEY-HARRIS, R. G., KAYSER, M. V., and DOWNES, S. (1995). Comparison of the early production of extracellular matrix on dense hydroxyapatite and hydroxyapatite-coated titanium in cell and organ culture. *Biomaterials* **16**, 489-495.

DALTON, J. E., and COOK, S. D. (1995). In vivo mechanical and histological characteristics of ha-coated implants vary with coating vendor. *J. Biomed. Mater. Res.* **29**, 239-245.

DAVIES, J. E. (1987). Human bone marrow cells synthesize collagen, in diffusion chambers, implanted into the normal rat. *Cell Biol. Int. Rep.* **11**, 125-130.

DAVIES, J. E. (1990). The use of cell and tissue culture to investigate bone cell reactions to bioactive materials. In "Handbook of Bioactive Ceramics Vol.1 Bioactive Glasses and Glass-Ceramics" (T. Yamamuro, L. L. Hench, and J. Wilson, Eds.), pp. 195-225. CRC Press, Boca Raton, Florida.

DAVIES, J. E., TARRANT, S. F., and MATSUDA, T. (1987). Interaction between primary bone cell cultures and biomaterials. Part 1: Method; the in vitro and in vivo stages. In "Biomaterials and Clinical Applications" (A. Pizzoferrato, P. G. Marchetti, A. Ravaglioli, and A. J. C. Lee, Eds.), pp. 579-584. Elsevier, Amsterdam.

DAVIES, J. E., LOWENBERG, B., and SHIGA, A. (1990). The bone-titanium interface in vitro. *J. Biomed. Mater. Res.* **24**, 1289-1306.

DAVIES, J. E., SHAPIRO, G., and LOWENBERG, B. F. (1993). Osteoclastic resorption of calcium phosphate ceramic thin films. *Cells & Materials* **3**, 245-256.

DE BRUIJN, J. D., KLEIN, C. P., DE GROOT, K., and VAN BLITTERSWIJK, C. A. (1992). The ultrastructure of the bone-hydroxyapatite interface in vitro. *J. Biomed. Mater. Res.* **26**, 1365-1382.

DE BRUIJN, J. D., FLACH, J. S., DEGROOT, K., VAN BLITTERSWIJK, C. A., DAVIES, J. E., JONES, D. B., DOTY, S. B., DACULSI, G., and MCKEE, M. D. (1993). Analysis of the bony interface with various types of hydroxyapatite invitro. *Cells & Materials* **3**, 115-127.

DE BRUIJN, J. D., BOVELL, Y. P., DAVIES, J. E., and VAN BLITTERSWIJK, C. A. (1994). Osteoclastic resorption of calcium phosphates is potentiated in postosteogenic culture conditions. *J. Biomed. Mater. Res.* **28**, 105-112.

DE BRUIJN, J. D., VAN BLITTERSWIJK, C. A., and DAVIES, J. E. (1995). Initial bone matrix formation at the hydroxyapatite interface in vivo. *J. Biomed. Mater. Res.* **29**, 89-99.

DE LANGE, G. L., and DONATH, K. (1989). Interface between bone tissue and implants of solid hydroxyapatite or hydroxyapatite-coated titanium implants. *Biomaterials* **10**, 121-125.

DE LA PIEDRA, C., TRABA, M. L., MUNICIO, M. J., and TORRES, R. (1993). Parathyroid hormone related peptide (1-34) and 1,25-dihydroxyvitamin D, have no additive effects on bone tartrate resistant acid phosphatase activity in fetal rat calvaria cultures. *Horm. Metab. Res.* **25**, 417-420.

DOGLIOLI, P., and SCORTECCI, G. (1991). Characterization of endosteal osteoblasts isolated from human maxilla and mandible: an experimental system for biocompatibility tests. *Cytotechnology* **7**, 39-48.

DOHERTY, M. J., SCHLAG, G., SCHWARZ, N., MOLLAN, R. A., NOLAN, P. C., and WILSON, D. J. (1994). Biocompatibility of xenogeneic bone, commercially available coral, a bioceramic and tissue sealant for human osteoblasts. *Biomaterials* **15**, 601-608.

- DOILLON, C. J., and CAMERON, K. (1990). New approaches for biocompatibility testing using cell culture. *Int. J. Artif. Organs* **13**, 517-520.
- DONATH, K., and BREUNER, G. A. (1982). A method for the study of undecalcified bones and teeth with attached soft tissue. *J. Oral Pathol.* **11**, 318-325.
- DOWD, J. E., SCHWENDEMAN, L. J., MACAULAY, W., DOYLE, J. S., SHANBHAG, A. S., WILSON, S., HERNDON, J. H., and RUBASH, H. E. (1995). Aseptic loosening in uncemented total hip arthroplasty in a canine model. *Clin. Orthop.* **319**, 106-121.
- DUNN, G. A. (1982). Contact guidance of cultured tissue cells: a survey of potentially relevant properties of the substratum. In "Cell Behaviour" (R. Bellairs, A. S. G. Curtis, and G. A. Dunn, Eds.), pp. 247-280. Cambridge University Press, Cambridge.
- ECAROT-CHARRIER, B., GLORIEUX, F. H., VAN DER REST, M., and PEREIRA, G. (1983). Osteoblasts isolated from mouse calvaria initiate matrix mineralization. *J. Cell Biol.* **96**, 639-643.
- ECAROT-CHARRIER, B., SHEPARD, N., CHARETTE, G., GRYPNAS, M., and GLORIEUX, F. (1988). Mineralization in osteoblast cultures: a light and electron microscope study. *Bone* **9**, 147-154.
- EPPLEY, B. L., DOUCET, M., CONNOLLY, D. T., and FEDER, J. (1988). Enhancement of angiogenesis by bFGF in mandibular bone graft healing in the rabbit. *J. Oral Maxillofac. Surg.* **46**, 391-398.
- ERBEN, R. G. (1997). Embedding of bone samples in methylmethacrylate: an improved method suitable for bone histomorphometry, histochemistry and immunohistochemistry. *J. Histochem. Cytochem.* **45**, 307-313.
- ERICSON, L. E., JOHANSSON, B. R., ROSENGREN, A., SENNERBY, L., and THOMSEN, P. (1991). Ultrastructural investigation and analysis of the interface of retrieved metal implants. In "The Bone-Biomaterial Interface" (J. E. Davies, Ed.), pp. 425-437. University of Toronto Press, Toronto.
- ERNSTS, M., HEATH, J. K., SCHMID, C., FROESCH, R. E., and RODAN, G. A. (1989). Evidence for a direct effect of oestrogen on bone cells in vitro. *J. Steroid. Biochem.* **34**, 279-284.
- EVANS, G. H., MENDEZ, A. J., and CAUDILL, R. F. (1996). Loaded and nonloaded titanium versus hydroxyapatite-coated threaded implants in the canine mandible. *Int. J. Oral Maxillofac. Implants* **11**, 360-371.
- FEDARKO, N. F., BIANCO, P., VETTER, U., and GERHON-ROBEY, P. (1990). Human bone cell enzyme expression and cellular heterogeneity: correlation of alkaline phosphatase enzyme activity with cell cycle. *J. Cell Physiol.* **144**, 115-121.
- FELL, H. B. (1928). Experiments on the differentiation in vitro of cartilage and bone. *Arch. Exptl. Zellforsch.* **7**, 360-410.
- FELL, H. B. (1932). The osteogenic capacity in vitro of periosteum and endosteum isolated from the limb skeleton of fowl embryos and young chicks. *Journal of Anatomy* **66**, 157-191.
- FERGUSON, M. M., HUNTER, K. M., BUCKINGHAM, D. A., LORIMER, A. M., KARDOS, T. B., and METSON, J. B. (1991). Analysis of factors regulating osteoblast attachment to titanium. In "Fundamentals of Bone Growth: Methodology and Applications" (A. D. Dixon, B. G. Sarnat, and D. A. N. Hoyte, Eds.), Proceedings of the Third International Conference, pp. 313-328. CRC Press, Boca Raton, Florida.
- FISHER, L. W., STUBBS, J. T., and YOUNG, M. F. (1995). Antisera and cDNA probes to human and certain animal model bone matrix noncollagenous proteins. *Acta. Orthop. Scand. Suppl.* **66**, 61-65.

FOGH, J., and TREMPPE, G. (1975). New human tumor cell lines. In "Human Cell Lines in vitro" (J. Fogh, Ed.), pp. 115-159. Plenum, New York.

FRENKEL, S., and SINGH, I. J. (1991). The effects of fibroblast growth factor on osteogenesis in the chick embryo. In "Fundamentals of bone growth. Methodology and applications" (A. D. Dixon, B. G. Sarnat, and D. A. N. Hoyte, Eds.), pp. 245-259. CRC Press, Boca Raton.

FRESHNEY, R. I., Ed. (1987). "Culture of Animal Cells - A Manual of Basic Techniques", 2nd Ed. Wiley-Liss, New York.

FROMDEL, J. L., Jr., FUNK, G. F., CAPPER, D. T., FRIDRICH, K. L., BLUMER, J. R., HALLER, J. R., and HOFFMAN, H. T. (1993). Osseointegrated implants: a comparative study of bone thickness in four vascularized bone flaps. *Plast. Reconstr. Surg.* **92**, 449-455. (discussion 456-8)

GAILLARD, P. J., HERRMANN-ERLEE, M. P. M., HEKKELMAN, J. W., BURGEREH, and NIJWEIDE, P. J. (1979). Skeletal tissue in culture. *Clin. Orthop.* **142**, 196-241.

GALLAGHER, J. A., BERESFORD, J. N., SHARRARD, M., GOWAN, M., POSER, J., MACDONALD, B. R., MCGUIRE, M. J. B., and RUSSELL, R. G. G. (1983). Human bone cells in culture - A novel system for the investigation of osteoblast function. *Calcif. Tissue Int.* **35**, A24.

GARVEY, B. T., and BIZIOS, R. (1994). A method for transmission electron microscopy investigation of the osteoblast/hydroxyapatite interface. *J. Appl. Biomater.* **5**, 39-45.

GARVEY, B. T., and BIZIOS, R. (1995). A transmission electron microscopy examination of the interface between osteoblasts and metal biomaterials. *J. Biomed. Mater. Res.* **29**, 987-992.

GERSTENFELD, L. C., CHIPMAN, S. D., GLOWACKI, J., and LIAN, J. B. (1987). Expression of differentiated function by mineralizing cultures of chicken osteoblasts. *Dev. Biol.* **122**, 49-60.

GERSTENFELD, L. C., CHIPMAN, S. D., KELLY, C. M., HODGENS, K. J., and LEE, D. D. (1988). Collagen expression, ultrastructural assembly, and mineralization in cultures of chicken embryo osteoblasts. *J. Cell Biol.* **106**, 979-989.

GLANT, T. T., and JACOBS, J. J. (1994). Response of three murine macrophage populations to particulate debris: bone resorption in organ cultures. *J. Orthop. Res.* **12**, 720-731.

GLOBUS, R. K., PATTERSON-BUCKENDAHL, P., and GODSPODAROWICZ, D. (1988). Regulation of bovine bone cell proliferation by fibroblast growth factor and transforming growth factor b. *Endocrinology* **123**, 98-105.

GLOBUS, R. K., PLOUET, J., and GOSPODAROWICZ, D. (1989). Cultured bovine bone cells synthesize basic fibroblast growth factor and store it in their extracellular matrix. *Endocrinology* **124**, 1539-1547.

GOLDBERG, V. M., STEVENSON, S., FEIGHAN, J., and DAVY, D. (1995). Biology of grit-blasted titanium alloy implants. *Clin. Orthop.* **319**, 122-129.

GOMI, K., LOWENBERG, B., SHAPIRO, G., and DAVIES, J. E. (1993). Resorption of sintered synthetic hydroxyapatite by osteoclasts in vitro. *Biomaterials* **14**, 91-96.

GOSPODAROWICZ, D. (1992). Fibroblast growth factors. In "Human cytokines - Handbook for basic research" (B. Aggarwal, and J. Guterman, Eds.), pp. 329-352. Blackwell Scientific Publications, Boston.

GOTTLANDER, M., and ALBREKTSSON, T. (1991). Histomorphometric studies of hydroxyapatite-coated and uncoated cp titanium threaded implants in bone. *Int. J. Oral Maxillofac. Implants* **6**, 399-404.

- GOWEN, M., CHAPMAN, K., LITTLEWOOD, A., HUGHES, D., EVANS, D., and RUSSELL, G. (1990). Production of tumour necrosis factor by human osteoblasts in modulated by other cytokines but not by osteotrophic hormones. *Endocrinology* **126**, 1250-1255.
- GRANCHI, D., STEA, S., CIAPETTI, G., SAVARINO, L., CAVEDAGNA, D., and PIZZOFERRATO, A. (1995). In vitro effects of bone cements on the cell cycle of osteoblast-like cells. *Biomaterials* **16**, 1187-1192.
- GREGOIRE, M., ORLY, I., and MENATEAU, J. (1990). The influence of calcium phosphate biomaterials on human bone cell activities. An in vitro approach. *J. Biomed. Mater. Res.* **24**, 165-177.
- GRINNELL, F., and FELD, M. K. (1981). Adsorption characteristics of fibronectin in relationship to biological activity. *J. Biomed. Mater. Res.* **15**, 363-381.
- GROESSNER-SCHREIBER, B., and TUAN, R. S. (1992). Enhanced extracellular matrix production and mineralization by osteoblasts cultured on titanium in vitro. *J. Cell Sci.* **101**, 209-217.
- GROESSNER-SCHREIBER, B., KRUKOWSKI, M., LYONS, C., and OSDOBY, P. (1992). Osteoclast recruitment in response to human bone matrix is age related. *Mech. Ageing Dev.* **62**, 143-154.
- GRONOWICZ, G., and MCCARTHY, M. B. (1996). Response of human osteoblasts to implant materials: integrin-mediated adhesion. *J. Orthop. Res.* **14**, 878-887.
- GROSS, U., and STRUNZ, V. (1985). The interface of various glasses and glass ceramics with a bony implantation bed. *J. Biomed. Mater. Res.* **19**, 251-271.
- GROSS, U., ROGGENDORF, W., SCHMITZ, H. J., and STRUNZ, V. (1986). Testing procedures for surface reactive biomaterials. In "Biological and biomechanical performance of biomaterials" (P. Christel, A. Meunier, and A. J. C. Lee, Eds.), pp. 367-373. Elsevier, Amsterdam.
- GROSS, U. M., KINNE, R., SCHMITZ, H. J., and STRUNZ, V. (1988). The response of bone to surface-active glasses/glass ceramics. *Crit. Rev. Biocompat.* **4**, 155-179.
- GROSS, U. M., MÜLLER-MAI, C., and VOIGT, C. (1991). Comparative morphology of the bone interface. In "The Bone-biomaterial Interface" (J. E. Davies, Ed.), pp. 302-320. University of Toronto Press, Toronto.
- GRUNDEL, R. E., CHAPMAN, M. W., YEE, T., and MOORE, D. C. (1991). Autogeneic bone marrow and porous biphasic calcium phosphate ceramic for segmental bone defects in the canine ulna. *Clin. Orthop.* **266**, 244-258.
- GRZESIK, W. J., and ROBEY, P. G. (1994). Bone matrix RGD glycoproteins: immunolocalization and interaction with human primary osteoblastic bone cells in vitro. *J. Bone Miner. Res.* **9**, 487-496.
- GUILLEMIN, G., HUNTER, S. J., and GAY, C. V. (1995). Resorption of natural calcium carbonate by avian osteoclasts in vitro. *Cells & Materials* **5**, 157-165.
- GUNDLE, R., JOYNER, C. J., and TRIFFITT, J. T. (1995). Human bone tissue formation in diffusion chamber culture in vivo by bone-derived cells and marrow stromal fibroblastic cells. *Bone* **16**, 597-601.
- GUY, S. C., MCQUADE, M. J., SCHEIDT, M. J., MCPHERSON, J. C., 3d., ROSSMANN, J. A., and VAN DYKE, T. E. (1993). In vitro attachment of human gingival fibroblasts to endosseous implant materials. *J. Periodontol.* **64**, 542-546.
- HAIDER, R., WATZEK, G., and PLENK, H. (1993). Effects of drill cooling and bone structure on IMZ implant fixation. *Int. J. Oral Maxillofac. Implants* **8**, 83-91.

HALE, T. M., BORETSKY, B. B., SCHEIDT, M. J., MCQUADE, M. J., STRONG, S. L., and VAN DYKE, T. E. (1991). Evaluation of titanium dental implant osseointegration in posterior edentulous areas of micro swine. *J. Oral Implantol.* **17**, 118-124.

HALL, B. K. (1972). Immobilization and cartilage transformation into bone in the embryonic chick. *Anat. Rec.* **173**, 391-404.

HALL, B. K. (1978). Grafting of organs and tissues to the chorioallantoic membrane of the embryonic chick. *Tissue Culture Association Manual* **4**, 881-884.

HALL, B. K. (1987). Earliest evidence of cartilage and bone development in embryonic life. *Clin. Orthop.* **225**, 255-272.

HAMBURGER, V., Ed. (1973). "A Manual of Experimental Embryology". University of Chicago Press, Chicago.

HANKS, C. T., WATAHA, J. C., and SUN, Z. (1996). In vitro models of biocompatibility: a review. *Dent. Mater.* **12**, 186-193.

HANSSON, H. A., ALBREKTSSON, T., and BRÅNEMARK, P. I. (1983). Structural aspects of the interface between tissue and titanium implants. *J. Prosthet. Dent.* **50**, 108-113.

HARMAND, M. F., BORDENAVE, L., DUPHIL, R., JEANDOT, R., and DUCASSOU, D. (1986). Human differentiated cell cultures: in vitro models for characterization of cell/biomaterial interface. In "Biological and biomechanical performance of biomaterials" (P. Christel, A. Meunier, and A. J. C. Lee, Eds.), pp. 361-366. Elsevier, Amsterdam.

HARRISON, A., HUGGETT, R., WATSON, C. J., and BECK, C. B. (1992). A survey of complete denture prosthetics for the elderly, the handicapped and difficult patients. *Br. Dent. J.* **172**, 51-56.

HAUSCHKA, P. V. (1990). Growth factor effects in bone-forming cells. In "Bone" (B. K. Hall, Ed.), Vol. 1 The osteoblast and osteocyte, pp. 103-170. The Telford Press, Caldwell, New Jersey.

HAUSER, S. P., WALDRON, J. A., UPUDA, K. B., and LIPSCHITZ, D. A. (1995). Morphological characterization of stromal cell types in hematopoietically active long-term murine bone marrow cultures. *J. Histochem. Cytochem.* **43**, 371-379.

HAUSTVEIT, G., TORHEIM, B., FYSTRO, D., EIDEM, T., and SANDVIK, M. (1984). Toxicity testing of medical device materials tested in human tissue cultures. *Biomaterials* **5**, 75-80.

HAYNES, D. R., ROGERS, S. D., HAY, S., PEARCY, M. J., and HOWIE, D. W. (1993). The differences in toxicity and release of bone-resorbing mediators induced by titanium and cobalt-chromium-alloy wear particles [see comments]. *J. Bone Joint Surg. Am.* **75**, 825-834.

HAYNESWORTH, S. E., GOSHIMA, J., GOLDBERG, V. M., and CAPLAN, A. I. (1992). Characterization of cells with osteogenic potential from human marrow. *Bone* **13**, 81-88.

HEALY, K. E., THOMAS, C. H., REZANIA, A., KIM, J. E., MCKEOWN, P. J., LOM, B., and HOCKBERGER, P. E. (1996). Kinetics of bone cell organization and mineralization on materials with patterned surface chemistry. *Biomaterials* **17**, 195-208.

HEERSCHE, J. H. M., and AUBIN, J. E. (1990). Regulation of cellular activity of bone-forming cells. In "Bone" (B. K. Hall, Ed.), Vol. 1 The osteoblast and osteocyte, pp. 327-350. The Telford Press, Caldwell, New Jersey.

HEIKKILA, J. T., AHO, A. J., YLI-URPO, A., ANDERSSON, O. H., AHO, H. J., and HAPPONEN, R. P. (1993). Bioactive glass versus hydroxylapatite in reconstruction of osteochondral defects in the rabbit. *Acta. Orthop. Scand.* **64**, 678-682.

HENCH, L. L. (1988). Bioactive ceramics. *Ann. N. Y. Acad. Sci.* **523**, 54-71.

HENCH, L. L., and ANDERSSON, Ö. (1993). Bioactive glasses. In "An introduction to bioceramics" (L. L. Hench, and J. Wilson, Eds.), Vol. Advanced series in ceramics Vol.1, pp. 41-62. World Scientific Publishing Co., London.

HENCH, L. L., and ETHRIDGE, E. C., Eds. (1982). "Biomaterials - an interfacial approach". Academic Press, New York.

HETHERINGTON, V. J., LORD, C. E., and BROWN, S. A. (1995). Mechanical and histological fixation of hydroxylapatite-coated pyrolytic carbon and titanium alloy implants: a report of short-term results. *J. Appl. Biomater.* **6**, 243-248.

HILLMANN, G., HILLMAN, B., and DONATH, K. (1991). Enzyme, lectin and immunohistochemistry of plastic embedded undecalcified bone and other hard tissues for light microscopic investigations. *Biotech. Histochem.* **66**, 185-193.

HIPP, J. A., and BRUNSKI, J. B. (1987). Investigation of 'osseointegration' by histomorphometric analyses of fixture-bone interface. *J. Dent. Res.* **66**, 186 (Abs637).

HOBKIRK, J. A. (1981). Patterns of cortical bone growth around alumina implants. *J. Oral Rehabil.* **8**, 143-154.

HOLGERS, K. M., THOMSEN, P., TJELLSTROM, A., and ERICSON, L. E. (1995). Electron microscopic observations on the soft tissue around clinical long-term percutaneous titanium implants. *Biomaterials* **16**, 83-96.

HOLLINGER, J. O., and LEONG, K. (1996). Poly(a-hydroxy acids): carriers for bone morphogenetic proteins. *Biomaterials* **17**, 187-194.

HOLLINGER, J. O., and SCHMITZ, J. P. (1987). Restoration of bone discontinuities in dogs using a biodegradable implant. *J. Oral Maxillofac. Surg.* **45**, 594-600.

HORMIA, M., and KONONEN, M. (1994). Immunolocalization of fibronectin and vitronectin receptors in human gingival fibroblasts spreading on titanium surfaces. *J. Periodontal Res.* **29**, 146-152.

HORMIA, M., KONONEN, M., KIVILAHTI, J., and VIRTANEN, I. (1991). Immunolocalization of proteins specific for adherens junctions in human gingival epithelial cells grown on differently processed titanium surfaces. *J. Periodontal Res.* **26**, 491-497.

HOSNY, M., and SHARAWY, M. (1985). Osteoinduction in young and old rats using demineralized bone powder allografts. *J. Oral Maxillofac. Surg.* **43**, 925-931.

HOWLETT, C. R., EVANS, M. D., WALSH, W. R., JOHNSON, G., and STEELE, J. G. (1994). Mechanism of initial attachment of cells derived from human bone to commonly used prosthetic materials during cell culture. *Biomaterials* **15**, 213-222.

HULSHOFF, J. E. G., VANDIJK, K., VANDERWAERDEN, J. P. C. M., WOLKE, J. G. C., GINSEL, L. A., and JANSEN, J. A. (1995). Biological evaluation of the effect of magnetron sputtered ca/p coatings on osteoblast-like cells in vitro. *J. Biomed. Mater. Res.* **29**, 967-975.

HUNTER, A., ARCHER, C. W., WALKER, P. S., and BLUNN, G. W. (1995). Attachment and proliferation of osteoblasts and fibroblasts on biomaterials for orthopaedic use. *Biomaterials* **16**, 287-295.

HURÉ, G., DONATH, K., LESOURD, M., CHAPPARD, D., and BASLÉ, M. F. (1996). Does titanium surface treatment influence the bone-implant interface? SEM and histomorphometry in a 6-month sheep study. *Int. J. Oral Maxillofac. Implants* **11**, 506-511.

IBARAKI, K., TERMINE, J. D., WHITSON, S. W., and YOUNG, M. F. (1992). Bone matrix mRNA expression in differentiating fetal bovine osteoblasts. *J. Bone Miner. Res.* **7**, 743-754.

INTERNATIONAL STANDARDS ORGANISATION Technical Report ISO/TR 9966: Implants for surgery - Biocompatibility - Selection of biological test methods for materials and devices.

INTERNATIONAL STANDARDS ORGANISATION ISO 10933-1 Biological testing of medical devices - Part 1: Guidance on selection of tests.

IRELAND, G. W., DOPPING-HEPENSTAL, P., JORDAN, P., and O'NEILL, C. (1987). Effect of patterned surfaces of adhesive islands on the shape, cytoskeleton, adhesion and behaviour of swiss mouse 3T3 fibroblasts. *J. Cell Sci.* **8**, 19-33.

ITAKURA, Y., KOSUGI, A., SUDO, H., YAMAMOTO, S., and KUMEGAWA, M. (1988). Development of a new system for evaluating the biocompatibility of implant materials using an osteogenic cell line (Mc3T3-E1). *J. Biomed. Mater. Res.* **22**, 613-622.

ITAKURA, Y., TAJIMA, T., OHOKI, S., MATSUZAWA, J., SUDO, H., and YAMAMOTO, S. (1989). Osteocompatibility of platinum-plated titanium assessed in vitro. *Biomaterials* **10**, 489-493.

IVANOFF, C. J., SENNERBY, L., JOHANSSON, C., RANGERT, B., and LEKHOLM, U. (1997). Influence of implant diameters on the integration of screw implants. An experimental study in rabbits. *Int. J. Oral Maxillofac. Surg.* **26**, 141-148.

IWASAKI, M., NAKAHARA, H., NAKATA, K., NAKASE, T., KIMURA, T., and ONO, K. (1995). Regulation of proliferation and osteochondrogenic differentiation of periosteum-derived cells by transforming growth factor-beta and basic fibroblast growth factor. *J. Bone Joint Surg. Am.* **77**, 543-554.

JANKOVIC, B. D., ISAKOVIC, K., LUKIC, M. L., VUJANOVIC, N. L., PETROVIC, S., and MARKOVIC, B. M. (1975). Immunological capacity of the chicken embryo. I. Relationship between the maturation of lymphoid tissues and the occurrence of cell-mediated immunity in the developing chicken embryo. *Immunology* **29**, 497-508.

JANSEN, J. A., VAN DER WAERDEN, J. P., and DE GROOT, K. (1989). Epithelial reaction to percutaneous implant materials: in vitro and in vivo experiments. *J. Invest. Surg.* **2**, 29-49.

JANSEN, J. A., VAN DER WAERDEN, J. C. P. M., and DE GROOT, K. (1991a). Fibroblast and epithelial cell interactions with surface-treated implant materials. *Biomaterials* **12**, 25-31.

JANSEN, J. A., VAN DER WAERDEN, J. P. C. M., WOLKE, J. G. C., and DE GROOT, K. (1991b). Histologic evaluation of the osseous adaptation to titanium and hydroxyapatite-coated titanium implants. *J. Biomed. Mater. Res.* **25**, 973-989.

JIN, Y., WANG, X., LIU, B., and WHITE, F. H. (1994). Early histologic response to titanium implants complexed with bovine bone morphogenetic protein. *J. Prosthet. Dent.* **71**, 289-294.

JINGUSHI, S., SCULLY, S. P., JOYCE, M. E., SUGIOKA, Y., and BOLANDER, M. E. (1995). Transforming growth factor-beta 1 and fibroblast growth factors in rat growth plate. *J. Orthop. Res.* **13**, 761-768.

JOHANSSON, C., and ALBREKTSSON, T. (1987). Integration of screw implants in the rabbit: a 1-year follow-up of removal torque of titanium implants. *Int. J. Oral Maxillofac. Implants* **2**, 69-75.

JOHANSSON, C. B., and MORBERG, P. (1995a). Cutting directions of bone with biomaterials in situ does influence the outcome of histomorphometrical quantifications. *Biomaterials* **16**, 1037-1039.

JOHANSSON, C. B., and MORBERG, P. (1995b). Importance of ground section thickness for reliable histomorphometrical results. *Biomaterials* **16**, 91-95.

- JOHANSSON, C. B., HANSSON, H. A., and ALBREKTSSON, T. (1990). Qualitative interfacial study between bone and tantalum, niobium or commercially pure titanium. *Biomaterials* **11**, 277-280.
- JOHNSON, H. J., NORTHUP, S. J., SEAGRAVES, P. A., ATALLAH, M., GARVIN, P. J., LIN, L., and DARBY, T. D. (1985). Biocompatibility test procedures for materials evaluation in vitro. II. Objective methods of toxicity assessment. *J. Biomed. Mater. Res.* **19**, 489-508.
- JONES, S. A., and BOYDE, A. (1979). Colonization of various natural substrates by osteoblasts in vitro. *Scan. Electron Microsc.* **2**, 529-538.
- JOTEREAU, F. V., and LEDOURAIN, N. M. (1978). The developmental relationship between osteocytes and osteoclasts. A study using quail-chick nuclear marker in endochondral ossification. *Dev. Biol.* **63**, 253-265.
- KADOYA, Y., ALSAFFAR, N., KOBAYASHI, A., and REVELL, P. A. (1994). The expression of osteoclast markers on foreign body giant cells. *Bone Miner.* **27**, 85-96.
- KALEBO, P., and JACOBSSON, M. (1988). Recurrent bone regeneration in titanium implants. Experimental model for determining the healing capacity of bone using quantitative microradiography. *Biomaterials* **9**, 295-301.
- KASEMO, B., and LAUSMAA, J. (1988). Biomaterial and implant surfaces: on the role of cleanliness, contamination, and preparation procedures. *J. Biomed. Mater. Res.* **22**(Applied Biomaterials. Suppl. A2), 145-158.
- KELLER, J. C., YOUND, F. A., and NATIELLA, J. R. (1987). Quantitative bone remodelling resulting from the use of porous dental implants. *J. Biomed. Mater. Res.* **21**, 305-319.
- KIM, K. J., CHIBA, J., and RUBASH, H. E. (1994). In vivo and in vitro analysis of membranes from hip prostheses inserted without cement. *J. Bone Joint Surg. Am.* **76A**, 172-180.
- KIRCHNER, L. M., SCHMIDT, S. P., and GRUBER, B. S. (1996). Quantitation of angiogenesis in the chick chorioallantoic membrane model using fractal analysis. *Microvasc. Res.* **51**, 2-14.
- KITSUGI, T., NAKAMURA, T., OKA, M., CHO, S. B., and MIYAJI, F. (1995). Bone-bonding behavior of three heat-treated silica gels implanted in mature rabbit bone. *Calcif. Tissue Int.* **57**, 155-160.
- KLEIN-NULEND, J., SEMEINS, C. M., VELDHUIJZEN, J. P., and BURGER, E. H. (1993). Effect of mechanical stimulation on the production of soluble bone factors in cultured fetal mouse calvariae. *Cell Tissue Res.* **271**, 513-517.
- KLEINSCHMIDT, J. C., MARDEN, L. J., KENT, D., QUIGLEY, N., and HOLLINGER, J. O. (1993). A multiphase system bone implant for regenerating the calvaria. *Plast. Reconstr. Surg.* **91**, 581-588.
- KLEMENT, B. J., and SPOONER, B. S. (1993). Utilization of microgravity bioreactors for differentiation of mammalian skeletal tissue. *J. Cell Biochem.* **51**, 252-256.
- KÖNÖNEN, M., HORMIA, M., KIVILAHTI, J., HAUTANIEMI, J., and THESLEFF, I. (1992). Effect of surface processing on the attachment, orientation, and proliferation of human gingival fibroblasts on titanium. *J. Biomed. Mater. Res.* **26**, 1325-1341.
- LABAT, B., CHAMSON, A., and FREY, J. (1995). Effects of gamma-alumina and hydroxyapatite coatings on the growth and metabolism of human osteoblasts. *J. Biomed. Mater. Res.* **29**, 1397-1401.
- LAKATOS, P., and STERN, P. H. (1992). Effects of cyclosporins and transforming growth factor beta 1 on thyroid hormone action in cultured fetal rat limb bones. *Calcif. Tissue Int.* **50**, 123-128.

LALOR, P. A., and REVELL, P. A. (1993). The presence of a synovial layer at the bone-implant interface: an immunohistological study demonstrating the close similarity to true synovium. *Clinical Materials* **14**, 91-100.

LARSSON, C., THOMSEN, P., ARONSSON, B. O., RODAHL, M., LAUSMAA, J., KASEMO, B., and ERICSON, L. E. (1996). Bone response to surface-modified titanium implants: studies on the early tissue response to machined and electropolished implants with different oxide thicknesses. *Biomaterials* **17**, 605-616.

LAWRENCE, R. S., GROOM, M. H., ACKROYD, D. M., and PARISH, W. E. (1986). The chorioallantoic membrane in irritation testing. *Food & Chemical Toxicology* **24**, 497-502.

LEW, D., MARINO, A. A., STARTZELL, J. M., and KELLER, J. C. (1994). A comparative study of osseointegration of titanium implants in corticocancellous block and corticocancellous chip grafts in canine ilium. *J. Oral Maxillofac. Surg.* **52**, 952-958. (discussion 959)

LI, J. (1993). Behaviour of titanium and titania-based ceramics in vitro and in vivo. *Biomaterials* **14**, 229-232.

LIAN, J. B., and STEIN, G. (1992). Concepts of osteoblast growth and differentiation: basis for modulation of bone cell development and tissue formation. *Crit. Rev. Oral Biol. Med.* **3**, 269-305.

LIN, H., VAN'T VEEN, S. J., and KLEIN, C. P. (1992). Permucosal implantation pilot study with HA-coated dental implant in dogs. *Biomaterials* **13**, 825-831.

LINDER, L., ALBREKTSSON, T., BRÄNEMARK, P. I., HANSSON, H. A., IVARSSON, B., JÖNSSON, U., and LUNDSTRÖM, I. (1983). Electron microscopic analysis of the bone-titanium interface. *Acta Orthop. Scand.* **54**, 45-52.

LISTGARTEN, M. A., BUSER, D., STEINEMANN, S. G., DONATH, K., LANG, N. P., and WEBER, H. P. (1992). Light and transmission electron microscopy of the intact interfaces between non-submerged titanium-coated epoxy resin implants and bone or gingiva. *J. Dent. Res.* **71**, 364-371.

LIU, F., MALAVAL, L., GUPTA, A. K., and AUBIN, J. E. (1994). Simultaneous detection of multiple bone-related mrnas and protein expression during osteoblast differentiation - polymerase chain reaction and immunocytochemical studies at the single cell level. *Dev. Biol.* **166**, 220-234.

LOCKLIN, R. M., WILLIAMSON, M. C., BERESFORD, J. N., TRIFFITT, J. T., and OWEN, M. E. (1995). In vitro effects of growth factors and dexamethasone on rat marrow stromal cells. *Clin. Orthop.* **313**, 27-35.

LONGAKER, M. T., MOELLEKEN, B. R., CHENG, J. C., JENNINGS, R. W., ADZICK, N. S., MINTOROVICH, J., LEVINSOHN, D. G., GORDON, L., HARRISON, M. R., and SIMMONS, D. J. (1992). Fetal fracture healing in a lamb model. *Plast. Reconstr. Surg.* **90**, 161-171. (discussion 172-3)

LOWENBERG, B., CHERNECKY, R., SHIGA, A., and DAVIES, J. E. (1991). Mineralized matrix production by osteoblasts on solid titanium in vitro. *Cells & Materials* **1**, 177-187.

LOZUPONE, E., FAVIA, A., CAFAGNA, B., and CANTATORE, F. P. (1993). [The concentration of osteocalcin in the culture media of bone cultured in vitro subjected to intermittent mechanical load with the addition of 1,25(OH)2D3]. *Boll. Soc. Ital. Biol. Sper.* **69**, 281-285.

LUM, L. B., and BEIRNE, O. R. (1986). Viability of the retained bone core in the core-vent dental implant. *J. Oral Maxillofac. Surg.* **44**, 341-345.

LUM, L. B., BEIRNE, O. R., DILLINGES, M., and CURTIS, T. A. (1988). Osseointegration of two types of implants in nonhuman primates. *J. Prosthet. Dent.* **60**, 700-705.

LUNDGREN, S., MOY, P., JOHANSSON, C., and NILSSON, H. (1996). Augmentation of the maxillary sinus floor with particulated mandible: a histologic and histomorphometric study. *Int. J. Oral Maxillofac. Implants* **11**, 760-766.

MALIK, M. A., PULEO, D. A., BIZIOS, R., and DOREMUS, R. H. (1992). Osteoblasts on hydroxyapatite, alumina and bone surfaces in vitro: morphology during the first 2 h of attachment. *Biomaterials* **13**, 123-128.

MANIATOPOULOS, C., SODEK, J., and MELCHER, A. H. (1988). Bone formation in vitro by stromal cells obtained from bone marrow of young adult rats. *Cell Tissue Res.* **254**, 317-330.

MARTIN, J. Y., SCHWARTZ, Z., HUMMERT, T. W., SCHRAUB, D. M., SIMPSON, J., LANKFORD, J., DEAN, D. D., COCHRAN, D. L., and BOYAN, B. D. (1995). Effect of titanium surface roughness on proliferation, differentiation, and protein synthesis of human osteoblast-like cells (mg63). *J. Biomed. Mater. Res.* **29**, 389-401.

MARTIN, T. J., INGLETON, P. M., UNDERWOOD, J. C. E., MELICK, R. A., MICHELANGELI, V. P., and HUNT, N. H. (1976). Parathyroid hormone response adenylate cyclase in an induced transplantable osteogenic osteosarcoma in the rat. *Nature* **260**, 436-438.

MATSUDA, T., and DAVIES, J. E. (1987). The in vitro response of osteoblasts to bioactive glass. *Biomaterials* **8**, 275-284.

MAXIAN, S. H., ZAWADSKY, J. P., and DUNN, M. G. (1994). Effect of ca/p coating resorption and surgical fit on the bone/implant interface. *J. Biomed. Mater. Res.* **28**, 1311-1319.

MAZUÉ, G., BERTOLERO, F., GAROFANO, L., BRUGHERA, M., and CARMINATI, P. (1992). Experience with the preclinical assessment of basic fibroblast growth factor (bFGF). *Toxicol. Letters* **64/65**, 329-338.

MCCORMICK, J. F., NASSAUER, J., BIELUNAS, J., and LEIGHTON, J. (1984). Anatomy of the chick chorioallantoic membrane relevant to its use as a substrate in bioassay systems. *Scan. Electron Microsc.*, 2023-2030.

MEIKLE, M. C., PAPAIOANNOU, S., RATLEDGE, T. J., SPEIGHT, P. M., WATT-SMITH, S. R., HILL, P. A., and REYNOLDS, J. J. (1994). Effect of poly DL-lactide-co-glycolide implants and xenogeneic bone matrix-derived growth factors on calvarial bone repair in the rabbit. *Biomaterials* **15**, 513-521.

MEYER, U., SZULCZEWSKI, D. H., MOLLER, K., HEIDE, H., JONES, D. B., GROSS, U., VANWACHEM, P. B., BAGAMDISA, F. B., DEKKER, A., and DAVIES, J. E. (1993). Attachment kinetics and differentiation of osteoblasts on different biomaterials. *Cells & Materials* **3**, 129-140.

MEYLE, J., GULTIG, K., and NISCH, W. (1995). Variation in contact guidance by human cells on a microstructured surface. *J. Biomed. Mater. Res.* **29**, 81-88.

MICHAELS, C. M., KELLER, J. C., and STANFORD, C. M. (1991). In vitro periodontal ligament fibroblast attachment to plasma-cleaned titanium surfaces. *J. Oral Implantol.* **17**, 132-139.

MONRO, P. P. (1988). "The growth of the chick femur in ovo and its growth and repair in vitro and on the chorioallantoic membrane" [Ph.D. Thesis]. (University of Southampton).

MOORE, R. (1997) Personal communication.

MORRISON, C., MACNAIR, R., MACDONALD, C., WYKMAN, A., GOLDIE, I., and GRANT, M. H. (1995). In vitro biocompatibility testing of polymers for orthopaedic implants using cultured fibroblasts and osteoblasts. *Biomaterials* **16**, 987-992.

- MOY, P. K., LUNDGREN, S., and HOLMES, R. E. (1993). Maxillary sinus augmentation: histomorphometric analysis of graft materials for maxillary sinus floor augmentation. *J. Oral Maxillofac. Surg.* **51**, 857-862.
- MUDA, A. O., RIMINUCCI, M., and BIANCO, P. (1992). Freeze-drying of bone tissue: immunocytochemistry and enzyme histochemistry on paraffin embedded and low-temperature resin embedded specimens. *Histochemistry* **98**, 283-288.
- MÜLLER-MAI, C. M., VOIGT, C., BAIER, R. E., and GROSS, U. M. (1992). The incorporation of glass-ceramic implants in bone after surface conditioning glow-discharge treatment. *Cells & Materials* **2**, 309-327.
- MURAI, K., TAKESHITA, F., AYUKAWA, Y., KIYOSHIMA, T., SUETSUGU, T., and TANAKA, T. (1996). Light and electron microscopic studies of bone-titanium interface in the tibiae of young and mature rats. *J. Biomed. Mater. Res.* **30**, 523-533.
- MURRAY, D. W., and RUSHTON, N. (1992). Mediators of bone resorption around implants. *Clin. Orthop.* **281**, 295-304.
- MURRAY, P. D. F., Ed. (1936). "Bones". Cambridge University Press, Cambridge.
- NAJI, A., and HARMAND, M. F. (1990). Study of the effect of the surface state on the cytocompatibility of a Co-Cr alloy using human osteoblasts and fibroblasts. *J. Biomed. Mater. Res.* **24**, 861-871.
- NAJI, A., and HARMAND, M. F. (1991). Cytocompatibility of two coating materials, amorphous alumina and silicon carbide, using human differentiated cell cultures. *Biomaterials* **12**, 690-694.
- NAKAMURA, T., HANADA, K., TAMURA, M., SHIBANUSHI, T., NIGI, H., TAGAWA, M., FUKUMOTO, S., and MATSUMOTO, T. (1995). Stimulation of endosteal bone formation by systemic injections of recombinant basic fibroblast growth factor in rats. *Endocrinology* **136**, 1276-1284.
- NANCI, A., MCCARTHY, G. F., ZALZAL, S., CLOKIE, C. M. L., WARSHAWSKY, H., and MCKEE, M. D. (1994). Tissue response to titanium implants in the rat tibia -ultrastructural, immunocytochemical and lectin-cytochemical characterization of the bone-titanium interface [Review]. *Cells & Materials* **4**, 1-30.
- NELSON, S. R., WOLFORD, L. M., LAGOW, R. J., CAPANO, P. J., and DAVIS, W. L. (1993). Evaluation of new high-performance calcium polyphosphate bioceramics as bone graft materials. *J. Oral Maxillofac. Surg.* **51**, 1363-1371.
- NEW, D. A. T., Ed. (1966). "The culture of vertebrate embryos". Logos Press, London.
- NIEDERAUER, G. G., MCGEE, T. D., KELLER, J. C., and ZAHARIAS, R. S. (1994). Attachment of epithelial cells and fibroblasts to ceramic materials. *Biomaterials* **15**, 342-352.
- NIJWEIDE, P. J. (1975). Embryonic chicken periosteum in tissue culture, osteoid formation and calcium uptake. *Proc. K. Ned. Akad. Wet. C* **78**, 410-417.
- NIJWEIDE, P. J., and BURGER, E. H. (1990). Mechanisms of bone formation in vitro. In "Bone" (B. K. Hall, Ed.), Vol. 1 The osteoblast and osteocyte, pp. 303-326. The Telford Press, Caldwell, New Jersey.
- NIJWEIDE, P. J., VAN IPEREN-VAN GENT, A. S., KAWILARANG-DE HAAS, E. W. M., VAN DER PLAS, A., and WASSENAAR, A. M. (1982). Bone formation and calcification by isolated osteoblastlike cells. *J. Cell Biol.* **93**, 318-323.
- NIMB, L., JENSEN, J. S., and GOTFREDSEN, K. (1995). Interface mechanics and histomorphometric analysis of hydroxyapatite-coated and porous glass-ceramic implants in canine bone. *J. Biomed. Mater. Res.* **29**, 1477-1482.

OAKLEY, C., and BRUNETTE, D. M. (1993). The sequence of alignment of microtubules, focal contacts and actin filaments in fibroblasts spreading on smooth and grooved titanium substrata. *J. Cell Sci.* **106**(Sep (Pt 1)), 343-354.

OFFICE OF POPULATION CENSUSES AND SURVEYS Adult Dental Health 1988 UK. (HMSO London)

OHGUSHI, H., DOHI, Y., TAMAI, S., and TABATA, S. (1993). Osteogenic differentiation of marrow stromal stem cells in porous hydroxyapatite ceramics. *J. Biomed. Mater. Res.* **27**, 1401-1407.

OHNO, K., SUGIMOTO, A., SHIROTA, T., MICHI, K., OHTANI, S., YAMAGATA, K., and DONATH, K. (1991). Histologic findings of apatite-titanium complex dental implants in the jaws of dogs. *Oral Surgery, Oral Medicine, Oral Pathology* **71**, 426-429.

OHTA, Y. (1993). Comparative changes in microvasculature and bone during healing of implant and extraction sites. *J. Oral Implantol.* **19**, 184-198.

OKUDA, K., NAKAJIMA, Y., IRIE, K., SUGIMOTO, M., KABASAWA, Y., YOSHIE, H., HARA, K., and OZAWA, H. (1995). Transforming growth factor-b1 coated b-tricalcium phosphate pellets stimulate healing of experimental bone defects of rat calvariae. *Oral Dis.* **1**, 92-97.

ONG, J. L., PRINCE, C. W., and LUCAS, L. C. (1995). Cellular response to well-characterized calcium phosphate coatings and titanium surfaces in vitro. *J. Biomed. Mater. Res.* **29**, 165-172.

ONO, K., YAMAMURO, T., NAKAMURA, T., and KOKUBO, T. (1990). Quantitative study on osteoconduction of apatite-wollastonite containing glass ceramic granules, hydroxyapatite granules, and alumina granules. *Biomaterials* **11**, 265-271.

ORR, R. D., DE BRUJIN, J. D., and DAVIES, J. E. (1992). Scanning electron microscopy of the bone interface with titanium, titanium alloy and hydroxyapatite. *Cells & Materials* **2**, 241-251.

OWEN, M. (1970). The origin of bone cells. *Int. Rev. Cytol.* **28**, 213-238.

OWEN, T. A., ARONOW, M., SHALHOUB, V., BARONE, L. M., WILMING, L., TASSINARI, M. S., KENNEDY, M. B., POCKWINSE, S., LIAN, J. B., and STEIN, G. S. (1990). Progressive development of the rat osteoblast phenotype in vitro: reciprocal relationships in expression of genes associated with osteoblast proliferation and differentiation during formation of the bone extracellular matrix. *J. Cell Physiol.* **143**, 420-430.

OZAWA, S., and KASUGAI, S. (1996). Evaluation of implant materials (hydroxyapatite, glass-ceramics, titanium) in rat bone marrow stromal cell culture. *Biomaterials* **17**, 23-29.

PAPAGELOPOULOS, P. J., GIANNARAKOS, D. G., and LYRITIS, G. P. (1993). Suitability of biodegradable polydioxanone materials for the internal fixation of fractures. *Orthop Rev* **22**, 585-593.

PAPE, W. J., and HOPPE, U. (1991). In vitro methods for the assessment of primary local effects of topically applied preparations. *Skin Pharmacol.* **4**, 205-212.

PARR, G. R., GARDNER, L. K., STEFLIK, D. E., and SISK, A. L. (1992). Comparative implant research in dogs: a prosthodontic model. *J. Prosthet. Dent.* **68**, 509-514.

PECK, W. A., BIRGE, S. J., and FEDAK, S. A. (1964). Bone cells: biochemical and biological studies after enzymatic isolation. *Science* **146**, 1476-1477.

PIATELLI, A., SCARANO, A., and PIATELLI, M. (1995). Detection of alkaline and acid phosphatases around titanium implants: a light microscopical and histochemical study in rabbits. *Biomaterials* **16**, 1333-1338.

- PIATELLI, A., SCARANO, A., CORIGLIANO, M., and PIATELLI, M. (1996). Presence of multinucleated giant cells around machined, sandblasted and plasma-sprayed titanium implants: a histological and histochemical time-course study in rabbit. *Biomaterials* **17**, 2053-2058.
- PILBEAM, C. C., ALANDER, C. B., SIMMONS, H. A., and RAISZ, L. G. (1993). Comparison of the effects of various lengths of synthetic human parathyroid hormone-related peptide (hPTHrP) of malignancy on bone resorption and formation in organ culture. *Bone* **14**, 717-720.
- PILLIAR, R. M., DEPORTER, D. A., WATSON, P. A., PHAROAH, M., CHAPMAN, M., VALIQUETTE, N., et al. (1991a). The effect of partial coating with hydroxyapatite on bone remodelling in relation to porous coated titanium alloy dental implants in the dog. *J. Dent. Res.* **70**, 1338-1345.
- PILLIAR, R. M., DEPORTER, D. A., WATSON, P. A., and VALIQUETTE, N. (1991b). Dental implant design--effect on bone remodeling. *J. Biomed. Mater. Res.* **25**, 467-483.
- PITARU, S., KOTEVEMETH, S., NOFF, D., KAFFULER, S., and SAVION, N. (1993). Effect of basic fibroblast growth factor on the growth and differentiation of adult stromal bone marrow cells - enhanced development of mineralized bone-like tissue in culture. *J. Bone Miner. Res.* **8**, 919-929.
- PIZZOFERRATO, A., CIAPETTI, G., STEA, S., CENNI, E., ARCIOLA, C. R., GRANCHI, D., and SAVARINO, L. (1994). Cell culture methods for testing biocompatibility. *Clinical Materials* **15**, 173-190.
- PULEO, D. A., and BIZIOS, R. (1992). Formation of focal contacts by osteoblasts cultured on orthopedic materials. *J. Biomed. Mater. Res.* **26**, 291-301.
- PULEO, D. A., HOLLERAN, L. A., BIZIOS, R., and DOREMUS, R. H. (1991). Osteoblasts responses to orthopedic implant materials in vitro. *J. Biomed. Mater. Res.* **25**, 711-723.
- PULEO, D. A., PRESTON, K. E., SHAFFER, J. B., and BIZIOS, R. (1993). Examination of osteoblast orthopaedic biomaterial interactions using molecular techniques. *Biomaterials* **14**, 111-114.
- QU, J., CHEHROUDI, B., and BRUNETTE, D. M. (1996). The use of micromachined surfaces to investigate the cell behavioural factors essential to osseointegration. *Oral Dis.* **2**, 102-115.
- RAE, T. (1986). Tissue culture techniques in biocompatibility testing. In "Techniques of Biocompatibility Testing" (D. F. Williams, Ed.), Vol. 2, pp. 81-94. CRC Press, Boca Raton, Florida.
- RAHAL, M. D., BRÅNEMARK, P. I., and OSMOND, D. G. (1993). Response of bone marrow to titanium implants: osseointegration and the establishment of a bone marrow-titanium interface in mice. *Int. J. Oral Maxillofac. Implants* **8**, 573-579.
- RAWLINGS, R. D. (1993). Bioactive glasses and glass-ceramics. *Clinical Materials* **14**, 155-180.
- REMES, A., and WILLIAMS, D. F. (1992). Immune response in biocompatibility. *Biomaterials* **13**, 731-743.
- REVEL, J. P. (1973). Electronmicroscopic investigation of the underside of cells in culture. *Exp. Cell Res.* **78**, 1-14.
- REVEL, J. P., HOCH, P., and HO, D. (1974). Adhesion of cultured cells to their substratum. *Exp. Cell Res.* **84**, 207-218.
- REVELL, P. A. (1983). Histomorphometry of bone. *J. Clin. Pathol.* **36**, 1323-1331.
- RICCIO, V., DELLA-RAGIONE, F., MARRONE, G., PALUMBO, R., GUIDA, G., and OLIVA, A. (1994). Cultures of human embryonic osteoblasts. A new in vitro model for biocompatibility studies. *Clin. Orthop.* **308**, 73-78.

ROACH, H. I. (1992). Trans-differentiation of hypertrophic chondrocytes into cells capable of producing a mineralized bone matrix. *Bone Miner.* **19**, 1-20.

ROACH, H. I. (1994). Why does bone matrix contain non-collagenous proteins? The possible roles of osteocalcin, osteonectin, osteopontin and bone sialoprotein in bone mineralisation and resorption. *Cell Biol. Int.* **18**, 617-628.

ROBEY, P. G., and TERMINE, J. D. (1985). Human bone cells in vitro. *Calcif. Tissue Int.* **37**, 453-460.

RODAN, G. A., and NODA, M. (1991). Gene expression in osteoblastic cells. *Crit. Rev. Eukaryot. Gene Expr.* **1**, 85-98.

RODAN, S. B., IMAI, Y., THIEDE, M. A., WESOLOWSKI, G., THOMPSON, D., BAR-SHAVIT, K., SHULL, S., MANN, K., and RODAN, G. A. (1987a). Characterization of a human osteosarcoma cell line SAOS-2 with osteoblastic properties. *Cancer Res.*, 4961-4966.

RODAN, S. B., WESOLOWSKI, G., THOMAS, K., and RODAN, G. A. (1987b). Growth stimulation of rat calvarian osteoblastic cells by acidic Fibroblast Growth Factor. *Endocrinology* **121**, 1917-1923.

ROODMAN, G. D., IBBOTSON, K. J., MACDONALD, B. R., KUEHL, T. J., and MUNDY, G. R. (1985). 1,23(OH)₂ vitamin D₃ causes formation of multinucleated cells with osteoclast characteristics in cultures of primate marrow. *Proc. Natl. Acad. Sci. USA* **82**, 8213-8217.

ROSENGREN, A., JOHANSSON, B. R., DANIELSEN, N., THOMSEN, P., and ERICSON, L. E. (1996). Immunohistochemical studies on the distribution of albumin, fibrinogen, fibronectin, IgG and collagen around PTFE and titanium implants. *Biomaterials* **17**, 1779-1786.

SAMMONS, R. L., EL HAJ, A. J., and MARQUIS, P. M. (1994). Novel culture procedure permitting the synthesis of proteins by rat calvarial cells cultured on hydroxyapatite particles to be quantified. *Biomaterials* **15**, 536-542.

SATO, K., NISHII, Y., WOODIEL, F. N., and RAISZ, L. G. (1993). Effects of two new vitamin D₃ derivatives, 22-oxa-1 alpha-25-dihydroxyvitamin D₃ (OCT) and 2 beta-(3-hydroxypropoxy)-1 alpha, 25-dihydroxyvitamin D₃ (ED-71), on bone metabolism in organ culture. *Bone* **14**, 47-51.

SAUK, J. J., VAN KAMPEN, C. L., and SOMERMAN, M. J. (1991). Role of adhesive proteins and integrins in bone and ligament cell behaviour at the material surface. In "The Bone Biomaterial Interface" (J. E. Davies, Ed.), pp. 111-119. University of Toronto Press, Toronto.

SAUTIER, J. M., KOKUBO, T., OHTSUKI, T., NEFUSSI, J. R., BOULEKBACHE, H., OBOEUF, M., LOTY, S., LOTY, C., and FOREST, N. (1994a). Bioactive glass-ceramic containing crystalline apatite and wollastonite initiates biomineralization in bone cell cultures. *Calcif. Tissue Int.* **55**, 458-466.

SAUTIER, J. M., SEPTIER, D., CUISINIER, F. J. G., NEFUSSI, J. R., OBOEUF, M., VOEGEL, J. C., FOREST, N., and GOLDBERG, M. (1994b). Ultrastructural characterization of the interface between cytodex-3 microcarrier and bone formed in vitro using high-resolution electron microscopy, histochemistry and immunohistochemistry. *Cells & Materials* **4**, 357-369.

SCHENK, R. K., and HUNZIKER, E. B. (1994). Histologic and ultrastructural features of fracture healing. In "Bone formation and repair" (C. T. Brighton, G. E. Freidlaender, and J. M. Lane, Eds.), pp. 117-148. American Academy of Orthopaedic Surgeons, Rosemont, Illinois.

SCHNEIDER, G., and BURRIDGE, K. (1994). Formation of focal adhesions by osteoblasts adhering to different substrata. *Exp. Cell Res.* **214**, 264-269.

SCHROEDER, A., VAN DER ZYPEN, E., STICH, H., and SUTTER, F. (1981). The reaction of bone, connective tissue and epithelium to endosteal implants with titanium-sprayed surfaces. *J. Maxillofac. Surg.* **9**, 15-25.

- SCHWARTZ, Z., and BOYAN, B. D. (1994). Underlying mechanisms at the bone biomaterial interface. *J. Cell Biochem.* **56**, 340-347.
- SCHWEIGERER, L. (1990). Basic fibroblast growth factor: properties and clinical implications. In "Growth factors, differentiation factors, and cytokines" (A. Habenicht, Ed.), pp. 42-55. Springer-Verlag, Berlin.
- SCOTT, D. M., KENT, G. M., and COHN, D. V. (1980). Collagen synthesis in cultured osteoblast-like cells. *Arch. Biochem. Biophys.* **201**, 384-391.
- SEITZ, T. L., NOONAN, K. D., HENCH, L. L., and NOONAN, N. E. (1982). Effect of fibronectin on the adhesion of an established cell line to a surface-reactive biomaterial. *J. Biomed. Mater. Res.* **16**, 195-207.
- SELVIG, K. A., VIKESJO, U. M. E., BOGLE, G. C., and FINKELMAN, R. D. (1994). Impaired early bone formation in periodontal fenestration defects in dogs, following application of insulin-like growth factor (II), basic fibroblast growth factor and transforming growth factor b1. *J. Clin. Periodontol.* **21**, 380-385.
- SENNERBY, L. (1991). "On the tissue response to titanium implants" [Ph.D. Dissertation]. (University of Gothenburg).
- SENNERBY, L., THOMSEN, P., and ERICSON, L. E. (1992). Ultrastructure of the bone-titanium interface in rabbits. *J. Mater. Sci. Mater. Med.* **3**, 262-271.
- SHAREFKIN, J. B., and WATKINS, M. T. (1986). Methods for the measurement of cell attachment to bioprosthetic surfaces. In "Techniques of Biocompatibility Testing" (D. F. Williams, Ed.), Vol. 2, pp. 95-108. CRC Press, Boca Raton, Florida.
- SHELTON, R. M., RASMUSSEN, A. C., and DAVIES, J. E. (1988). Protein adsorption at the interface between charged polymer substrata and migrating osteoblasts. *Biomaterials* **9**, 24-29.
- SHIMAZAKI, K., and MOONEY, V. (1985). Comparative study of porous hydroxyapatite and tricalcium phosphate as bone substitute. *J. Orthop. Res.* **3**, 301-310.
- SIDQUI, M., COLLIN, P., VITTE, C., and FOREST, N. (1995). Osteoblast adherence and resorption activity of isolated calcium sulphate hemihydrate. *Biomaterials* **16**, 1327-1332.
- SIMMONS, D. J. (1985). Fracture healing perspectives. *Clin. Orthop.* **200**, 100-113.
- SIMMONS, D. J., and GRYNPAS, M. C. (1990). Mechanisms of bone formation in vivo. In "Bone" (B. K. Hall, Ed.), Vol. 1 The osteoblast and osteocyte, pp. 193-302. The Telford Press, Caldwell, New Jersey.
- SIMMONS, H. A., and RAISZ, L. G. (1991). Effects of acid and basic fibroblast growth factor and heparin on resorption of cultured fetal rat long bones. *J. Bone Miner. Res.* **6**, 1301-1305.
- SIMONS, D. J., and GILLIAM, J. (1981). Articular cartilage repair in the avian quail-chick chimera model. *Clin. Orthop.* **161**, 315-325.
- SINHA, R. K., and TUAN, R. S. (1996). Regulation of human osteoblast integrin expression by orthopedic implant materials. *Bone* **18**, 451-457.
- SINHA, R. K., MORRIS, F., SHAH, S. A., and TUAN, R. S. (1994). Surface composition of orthopaedic implant metals regulates cell attachment, spreading, and cytoskeletal organization of primary human osteoblasts in vitro. *Clin. Orthop.* **305**, 258-272.
- SISK, A. L., STEFLIK, D. E., PARR, G. R., and HANES, P. J. (1992). A light and electron microscopic comparison of osseointegration of six implant types. *J. Oral Maxillofac. Surg.* **50**, 709-716.

SOBALLE, K., HANSEN, E. S., BROCKSTEDT-RASMUSSEN, H., HJORTDAL, V. E., JUHL, G. I., PEDERSEN, C. M., HVID, I., and BUNGER, C. (1991). Gap healing enhanced by hydroxyapatite coating in dogs. *Clin. Orthop.* **272**, 300-307.

SOUEIDAN, A., GAN, O. I., BOULER, J. M., GOUIN, F., and DACULSI, G. (1995). Biodegradation of synthetic biphasic calcium phosphate and biological calcified substratum by cells of hemopoietic origin. *Cells & Materials* **5**, 31-44.

SPIVAK, J. M., RICCI, J. L., BLUMENTHAL, N. C., and ALEXANDER, H. (1990). A new canine model to evaluate the biological response of intramedullary bone to implant materials and surfaces. *J. Biomed. Mater. Res.* **24**, 1121-1149.

STANFORD, C. M., and KELLER, J. C. (1991). The concept of osseointegration and bone matrix expression. *Crit. Rev. Oral Biol. Med.* **2**, 83-101.

STANFORD, C. M., KELLER, J. C., and SOLURSH, M. (1994). Bone cell expression on titanium surfaces is altered by sterilization treatments. *J. Dent. Res.* **73**, 1061-1071.

STEFLIK, D. E., HANES, P. J., SISK, A. L., PARR, G. R., SONG, M. J., LAKE, F. T., and MCKINNEY, R. V. (1992a). Transmission electron microscopic and high voltage electron microscopic observations of the bone and osteocyte activity adjacent to unloaded dental implants placed in dogs. *J. Periodontol.* **63**, 443-452.

STEFLIK, D. E., SISK, A. L., PARR, G. R., HANES, P. J., LAKE, F. T., BREWER, P., et al. (1992b). Correlative transmission electron microscopic and scanning electron microscopic observations of the tissues supporting endosteal blade implants. *J. Oral Implantol.* **18**, 110-120.

STEFLIK, D. E., SISK, A. L., PARR, G. R., HANES, P. J., LAKE, F., SONG, M. J., BREWER, P., and MCKINNEY, R. V. (1992c). High-voltage electron microscopy and conventional transmission electron microscopy of the interface zone between bone and endosteal dental implants. *J. Biomed. Mater. Res.* **26**, 529-546.

STEFLIK, D. E., PARR, G. R., SISK, A. L., LAKE, F. T., HANES, P. J., BERKERY, D. J., and BREWER, P. (1994). Osteoblast activity at the dental implant-bone interface: transmission electron microscopic and high voltage electron microscopic observations. *J. Periodontol.* **65**, 404-413.

STEFLIK, D. E., LAKE, F. T., SISK, A. L., PARR, G. R., HANES, P. J., DAVIS, H. C., ADAMS, B. O., and YAVARI, J. (1996). A comparative investigation in dogs: 2-year morphometric results of the dental implant-bone interface. *Int. J. Oral Maxillofac. Implants* **11**, 15-25.

SEITZ, T. L., NOONAN, K. D., HENCH, L. L., NOONAN, N. E. (1982). Effect of fibronectin on the adhesion of an established cell line to a surface-reactive biomaterial. *J. Biomed. Mater. Res.* **16**, 195-207.

STEVENSON, S., CUNNINGHAM, N., TOTH, J., DAVY, D., and REDDI, A. H. (1994). The effect of osteogenin (a bone morphogenetic protein) on the formation of bone in orthotopic segmental defects in rats. *J. Bone Joint Surg. Am.* **76**, 1676-1687.

SUDO, H., KODOMA, H. A., AMAGAI, Y., YAMAMOTO, S., and KASAI, S. (1983). In vitro differentiation and calcification in a new clonal osteogenic cell line derived from newborn mouse calvaria. *J. Cell Biol.* **96**, 191-198.

SUN, J., XUE, M., KIKUCHI, M., AKAO, M., and AOKI, H. (1994). Effects of Sr-hydroxyapatite microcrystal on cultured cell. *Bio-Medical Materials & Engineering* **4**, 503-512.

SZIVEK, J. A., KERSEY, R. C., DEYOUNG, D. W., and RUTH, J. T. (1994). Load transfer through a hydroxyapatite-coated canine hip implant. *J. Appl. Biomater.* **5**, 293-306.

SZULCZEWSKI, D. H., MEYER, U., MOLLER, K., STRATMANN, U., DOTY, S. B., and JONES, D. B. (1993). Characterisation of bovine osteoclasts on an ionomeric cement invitro. *Cells & Materials* 3, 83-92.

TAKAHASHI, K., SHANAHAN, M. D., COULTON, L. A., and DUCKWORTH, T. (1991). Fracture healing of chick femurs in tissue culture. *Acta. Orthop. Scand.* 62, 352-355.

TARRANT, S. F., and DAVIES, J. E. (1987). Interactions between primary bone cell cultures and biomaterials: Part 2: osteoblast behaviour. In "Biomaterials and Clinical Applications" (A. Pizzoferrato, P. G. Marchetti, A. Ravaglioli, and A. J. C. Lee, Eds.), pp. 585-590. Elsevier, Amsterdam.

TAYLOR, A. C. (1961). Attachment and spreading of cells in culture. *Exp. Cell Res.*(Suppl. 8), 154-173.

TENENBAUM, H. C., and HEERSCHE, J. N. M. (1982). Differentiation of osteoblasts and formation of mineralized bone nodules in vitro. *Calcif. Tissue Int.* 34, 76-79.

TENENBAUM, H. C., and HEERSCHE, J. N. M. (1986). Differentiation of osteoid-producing cells in vitro: possible evidence for the requirement of a microenvironment. *Calcif. Tissue Int.* 38, 262-267.

TISDEL, C. L., GOLDBERG, V. M., PARR, J. A., BENSUSAN, J. S., STAIKOFF, L. S., and STEVENSON, S. (1994). The influence of a hydroxyapatite and tricalcium-phosphate coating on bone growth into titanium fiber-metal implants. *J. Bone Joint Surg. Am.* 76, 159-171.

TORIUMI, D. M., EAST, C. A., ROSEN, D. M., CHU, G., LIU, C. C., and LARRABEE, W. F. (1991). Bone-inducing implants in head and neck surgery: an experimental study. *Laryngoscope* 101(4 Pt 1), 395-404.

TROWELL, O. A. (1954). A modified technique for organ culture in vitro. *Exp. Cell Res.* 6, 1954.

TURNER, R. T., FRANCIS, R., BROWN, D., GARAND, J., HANNON, K. S., and BELL, N. H. (1989). The effects of fluoride on bone and implant histomorphometry in growing rats. *J. Bone Miner. Res.* 4, 477-484.

VAAHTOKARI, A., ÅVERG, T., and THESLEFF, I. (1996). Apoptosis in the developing tooth: association with an embryonic signalling center and suppression by EGF and FGF-4. *Development* 122, 121-129.

VAINIO, O., RIWAR, B., and LASSILA, O. (1989). Characterization of chicken CD4-expressing cells. In "Recent Advances in Avian Immunology Research" (B. S. Bhoghal, and G. Koch, Eds.), pp. 45-56. Alan R Liss Inc., New York.

VAN DEN BOS, T., OOSTING, J., EVERTS, V., and BEERTSEN, W. (1995). Mineralization of alkaline phosphatase-complexed collagen implants in the rat in relation to serum inorganic phosphate. *J. Bone Miner. Res.* 10, 616-624.

VILAMITJANAAMEDEE, J., BAREILLE, R., ROUAIS, F., CAPLAN, A. I., and HARMAND, M. F. (1993). Human bone marrow stromal cells express an osteoblastic phenotype in culture. *In Vitro Cell. Dev. Biol.* 29, 699-707.

VOGLER, E. A., and BUSSIAN, R. W. (1987). Short-term cell-attachment rates: a surface-sensitive test of cell-substrate compatibility. *J. Biomed. Mater. Res.* 21, 1197-1211.

VROUWENVELDER, W. C., GROOT, C. G., and DE GROOT, K. (1992). Behaviour of fetal rat osteoblasts cultured in vitro on bioactive glass and nonreactive glasses. *Biomaterials* 13, 382-392.

VROUWENVELDER, W. C., GROOT, C. G., and DE GROOT, K. (1993). Histological and biochemical evaluation of osteoblasts cultured on bioactive glass, hydroxylapatite, titanium alloy, and stainless steel. *J. Biomed. Mater. Res.* 27, 465-475.

- VROUWENVELDER, W. C., GROOT, C. G., and DE GROOT, K. (1994). Better histology and biochemistry for osteoblasts cultured on titanium-doped bioactive glass: bioglass 45S5 compared with iron-, titanium-, fluorine- and boron-containing bioactive glasses. *Biomaterials* **15**, 97-106.
- VU, M. T., SMITH, P. C., BURGER, P. C., and KLINTWORTH, G. K. (1985). An evaluation of methods to quantitate the chick chorioallantoic membrane assay in angiogenesis. *Lab. Invest.* **53**, 499-508.
- WANG, J. S., and ASPENBERG, P. (1993). Basic fibroblast growth factor and bone induction in rats. *Acta. Orthop. Scand.* **64**, 557-561.
- WANG, J. S., and ASPENBERG, P. (1994). Basic fibroblast growth factor increases allograft incorporation. Bone chamber study in rats. *Acta. Orthop. Scand.* **65**, 27-31.
- WANG, J. S., and ASPENBERG, P. (1996a). Basic fibroblast growth factor enhances bone-graft incorporation: dose and time dependence in rats. *J. Orthop. Res.* **14**, 316-323.
- WANG, J. S., and ASPENBERG, P. (1996b). Basic fibroblast growth factor promotes bone ingrowth in porous hydroxyapatite. *Clin. Orthop.* **333**, 252-260.
- WANG, J. S., GOODMAN, S., and ASPENBERG, P. (1994). Bone formation in the presence of phagocytosable hydroxyapatite particles. *Clin. Orthop.* **304**, 272-279.
- WAROCQUIERCLEROUT, R., HACHOMNITCHEU, G. C., and SIGOT LUIZARD, M. F. (1995). Reliability of human fresh and frozen gingiva explant culture in assessing dental materials cytocompatibility. *Cells & Materials* **5**, 1-14.
- WATAHA, J. C. (1996). Materials for endosseous dental implants. *J. Oral Rehabil.* **23**, 79-90.
- WEBBER, D., OSDOBY, P., HAUSCHKA, P., and KRUKOWSKI, M. (1990). Correlation of an osteoclast antigen and ruffled border on giant cells formed in response to resorbable substrates. *J. Bone Miner. Res.* **5**, 401-410.
- WEINLAENDER, M., KENNEY, E. B., LEKOVIC, V., BEUMER, J., 3d., MOY, P. K., and LEWIS, S. (1992). Histomorphometry of bone apposition around three types of endosseous dental implants. *Int. J. Oral Maxillofac. Implants* **7**, 491-496.
- WEISS, L., and BLUMENSON, L. E. (1967). Dynamic adhesion and separation of cells with hydrophilic and hydrophobic surfaces. *J. Cell Physiol.* **70**, 23-32.
- WENNERBERG, A., ALBREKTSSON, T., and ANDERSSON, B. (1996a). Bone tissue response to commercially pure titanium implants blasted with fine and coarse particles of aluminum oxide. *Int. J. Oral Maxillofac. Implants* **11**, 38-45.
- WENNERBERG, A., ALBREKTSSON, T., JOHANSSON, C., and ANDERSSON, B. (1996b). Experimental study of turned and grit-blasted screw-shaped implants with special emphasis on effects of blasting material and surface topography. *Biomaterials* **17**, 15-22.
- WENNERBERG, A., ALBREKTSSON, T., and LAUSMAA, J. (1996c). Torque and histomorphometric evaluation of c.p. titanium screws blasted with 25- and 75-microns-sized particles of Al₂O₃. *J. Biomed. Mater. Res.* **30**, 251-260.
- WHITSON, S. W., HARRISON, W., DUNLAP, M. K., BOWERS, D. E., FISHER, L. W., ROBEY, P. G., and JERMINE, J. D. (1984). Fetal bovine cells synthesize bone specific matrix proteins. *J. Cell Biol.* **88**, 607-614.
- WILLIAMS, D. F. (1987). Review: tissue-biomaterial interactions. *J. Mater. Sci.* **22**, 3421.

- WINDELER, A. S., BONEWALD, L., KHARE, A. G., BOYAN, B., and MUNDY, G. R. (1991). The influence of sputtered bone substitutes on cell growth and phenotypic expression. In "The Bone-Biomaterial Interface" (J. E. Davies, Ed.), pp. 205-213. University of Toronto Press, Toronto.
- WOLFE, L. A. (1990). Comparison of the interfacial bonding strength of a bioactive ceramic and titanium. *J. Dent. Res.* **69**, 958 Abstr.30.
- WONG, G. L., and COHN, D. N. (1974). Separation of parathyroid hormone and calcitonin-sensitive cells from non-responsive bone cells. *Nature* **252**, 713-715.
- WOOD, A. T., and THOROGOOD, P. (1987). An ultrastructural and morphometric analysis of an in vivo contact guidance system. *Development* **101**, 363-381.
- YAMADA, K. M., AKIYAMA, S. K., HASEGAWA, T., KENNEDY, D. W., and HUMPHRIES, M. J. (1985). Recent advances in research on fibronectin and other cell attachment proteins. *J. Cell Biochem.* **28**, 79-97.
- YAMAGUCHI, M., SAKURAI, T., OHTAKI, J., and HOSHI, T. (1991). Simulated weightlessness and bone metabolism: evidence for direct gravitational effect and its related insulin action. *Res. Exp. Med.* **191**, 273-280.
- YASZEMSKI, M. J., PAYNE, R. G., HAYES, W. C., LANGER, R., and MIKOS, A. G. (1996). Evolution of bone transplantation: molecular, cellular and tissue strategies to engineer human bone. *Biomaterials* **17**, 175-185.
- YLIHEIKKILÄ, P. K., FELTON, D. A., WHITSON, S. W., AMBROSE, A. A., UOSHIMA, K., and COOPER, L. F. (1995). Correlative microscopic investigation of the interface between titanium alloy and the osteoblast-osteoblast matrix using mineralizing cultures of primary fetal bovine mandibular osteoblasts. *Int. J. Oral Maxillofac. Implants* **10**, 655-665.
- YLIHEIKKILÄ, P. K., MASUDA, T., AMBROSE, W. W., SUGGS, C. A., FELTON, D. A., and COOPER, L. F. (1996). Preliminary comparison of mineralizing multilayer cultures formed by primary fetal bovine mandibular osteoblasts grown on titanium, hydroxyapatite and glass substitutes. *Int. J. Oral Maxillofac. Implants* **11**, 456-465.
- ZAMBONIN, G., and GRANO, M. (1995). Biomaterials in orthopaedic surgery: effects of different hydroxyapatites and demineralized bone matrix on proliferation rate and bone matrix synthesis by human osteoblasts. *Biomaterials* **16**, 397-402.
- ZAMBONIN ZALLONE, A., TETI, A., and PRIMERVERA, M. V. (1982). Isolated osteoclasts in primary culture: First observations on structure and survival in cultured media. *Anat. Embryol.* **165**, 405-413.
- ZHOU, H., CHOONG, P., MCCARTHY, R., CHOU, S. T., MARTIN, T. J., and NG, K. W. (1994). In situ hybridization to show sequential expression of osteoblast gene markers during bone formation in vivo. *J. Bone Miner. Res.* **9**, 1489-1499.
- ZIMMERMANN, B., WACHTEL, H. C., and NOPPE, C. (1991). Patterns of mineralization in vitro. *Cell Tissue Res.* **263**, 483-493.

Appendix I

Behaviour of fibroblasts during initial attachment to a glass-ceramic implant material *in vitro*: a time-lapse video-micrographic study

T. Leung*, A. Kakar*, J.A. Hobkirk* and P. Thorogood†

*Department of Prosthetic Dentistry, Eastman Dental Institute, 256, Gray's Inn Road, London WC1X 8LD, UK;

†Developmental Biology Unit, Institute of Child Health, 30, Guilford Street, London WC1N 1EH, UK

The *in vitro* behaviour of 3T3 fibroblasts plated on a glass-ceramic implant material, Apoceram, and on tissue culture polystyrene (TCP) was monitored using phase-contrast, time-lapse video microscopy and scanning electron microscopy. Significant differences were observed in the short-term cellular response to TCP and Apoceram in the timing of the fibroblasts' morphological changes, with earlier spreading and stabilization of the cells occurring on TCP. Cell surface ruffling activity was greater on the glass-ceramic, reflecting weaker adhesions to the substratum. The experimental method used facilitates direct analysis of the dynamic activity of cells attaching to artificial substrata.

Biomaterials (1994) **15**, (12) 1001–1007

Keywords: Dental materials, glass ceramics, cell behaviour, implants

Received 3 August 1993; accepted 20 November 1993

Biocompatibility testing *in vitro* often involves the detection of cell damage and death, i.e. cytotoxicity^{1–4}. Indeed, the International Standards Organization (ISO)'s recommendation on test methods to assess biocompatibility of implants for bone and joint surgery includes cytotoxicity and mutagenicity tests⁵. Whilst such screening is useful to detect overt adverse effects of a test material, other less dramatic expressions of incompatibility may be overlooked. For instance, the rate of growth, proliferation and differentiation of cells on a material may be dependent on successful initial attachment and spreading of the cells on the surface of the substratum. In this respect, the initial and short-term responses of cells to an implant material *in vitro* may provide valuable indicators of the long-term biocompatibility *in vivo*.

Although *in vitro* morphological responses of various cell types to different implant materials have been widely reported, such analyses are based almost without exception on fixed specimens examined by various combinations of light microscopy, scanning and transmission electron microscopy^{6–10}. This report describes, for the first time, a dynamic analysis of early behaviour of fibroblasts cultured on a glass-ceramic material using time-lapse video microscopy (TLV). Time-lapse video recording offers a number of advantages over analysis of fixed preparations. Firstly, it permits the continuous observation of a population of living cells exposed to the substratum, in contrast to observation of a fixed and stained preparation which

at best is simply a 'freeze-frame' record. Secondly, it allows qualitative assessment of changes in the morphology and behaviour of individual cells. Thirdly, quantitative assessment of such changes in relation to time and the total population under observation can be made. This method of analysis can provide unique insights into the initial and dynamic interactions between connective tissue cells and a potential implant material and, as such, provides a valuable means of assessing biocompatibility before embarking on longer and more expensive testing strategies.

In this study we have used a common murine fibroblastic cell line and, using a combination of TLV and scanning electron microscopy, monitored the behaviour of dispersed cells upon initial contact and attachment to a substratum consisting of a potential implant material. This has been facilitated by the inherent semi-transparency of the material selected, which permits visualization of the living cells. A sequence of cell phenotypes can be distinguished, each reflecting the behavioural activity of the cell at that time. Morphometric analysis of cell populations as they pass through this sequence has been used to assess the short-term cellular response to the substratum.

MATERIALS AND METHODS

Substratum preparation

The substratum employed for this study was Apoceram¹¹ (CP31 composition, phase proportions:

Correspondence to Ms T. Leung.

apatite 44.3%, wollastonite 39.9%, residual glass 15.8%), an apatite-containing glass-ceramic material developed at Imperial College, University of London, for bioengineering applications. Transcortical implantation of Apoceram in rabbit tibiae produced interfacial shear strengths in push-out tests comparable to those of commercially pure titanium¹².

Sections of Apoceram (0.5 mm thick) were cut from a cast block using a precision wire saw (Laser Technology, CA, USA). These were then serially ground with four grades of silicon carbide-coated paper (P240, 400, 800, 1200) and polished with 5 µm and then 1 µm diamond compound (Hyprez 5 star; Engis Ltd., Kent, UK) on a Metaserv rotary polishing machine (Buehler Ltd., Coventry, UK). The samples were soaked overnight in a 1:10 aqueous dilution of 7X detergent (ICN Flow, Irvine, Scotland) and rinsed in running tap water for 2 h. This was followed by ultrasonic cleaning for 3–5 min in deionized water and a 30 min wash in 70% ethanol, after which the samples were heat-sterilized in an autoclave.

Cell culture

3T3 fibroblasts were maintained in alpha modification of Eagle's minimal essential medium (αMEM, ICN Flow) + 10% fetal bovine serum (FBS; ICN Flow) + penicillin (50 U/ml)/streptomycin (50 µg/ml) (Gibco Ltd., Paisley, UK). When confluence was reached, the cells were dissociated from the culture flask by incubation with 0.05% (w/v) trypsin–0.02% (w/v) EDTA (Gibco Ltd.) at 37°C for 4 min. The dissociated cells were washed, centrifuged and resuspended in αMEM + 10% FBS. Concentration of the cell suspension was calculated using a haemocytometer (Improved Neubauer) and adjusted to 1.5×10^5 /ml. The suspension (5 ml) was added to a 25 cm² standard treated polystyrene tissue culture flask (Grenier Labortechnik, Germany) containing the glass-ceramic specimen. The cell suspension (5 ml) was put in a separate, empty flask. Tissue culture polystyrene (TCP), the material of the flask, acted as a control substratum.

Video microscopy

The cell cultures were viewed using an Olympus IMT-2 inverted phase contrast microscope fitted with a high resolution (330 TV Lines) charge-coupled device (CCD) colour video camera (JVC model TK-870U). Time-lapse video recordings were made at 2 s intervals using a VHS recorder (JVC model BR-9000 UEK). Three-hour recordings of cells plated onto the glass-ceramic material and the control tissue culture polystyrene, maintained at 37°C, were taken separately and repeated twice. The size of each field examined was 57 µm by 45 µm. The average cell number per field analysed was 15 (range 10–20).

Scanning electron microscopy

Specimens for scanning electron microscopy (SEM) were fixed in 2% glutaraldehyde in 0.1 M sodium cacodylate buffer, pH 7.2, followed by 1% osmium tetroxide in 0.1 M cacodylate buffer. The specimens were then dehydrated through a graded series of

acetone and water, critical point dried with CO₂ and gold sputter-coated for examination in an Hitachi S800 field emission scanning electron microscope.

RESULTS

Attachment and cell morphology

From the TLV recordings, a highly invariant sequence of events can be defined. On sedimentation onto the substratum from suspension, cells exhibited many bleb-like protrusions which were constantly in motion (the intensity of blebbing varied from cell to cell). At the point at which attachment to the substratum occurred, blebbing largely ceased and, upon withdrawal of the blebs, the cell acquired a 'smoother' profile. Initial attachment was followed by a spreading stage, during which extension of the cytoplasm along the substratum proceeded with a concomitant flattening of the central mass. The margin of the spreading cell was invariably active. It was characterized by filopodia and lamellipodia being extended and withdrawn, giving rise to the appearance of ruffles. Typically, spreading took place in a radially symmetrical fashion, but where a distinct leading edge became established, then the cell became polarized, both in its spreading and in its subsequent locomotion. Upon polarization, the degree and rate of ruffling became reduced at non-motile regions of the cell margin. This general pattern of cell behaviour was observable in cell populations cultured on both Apoceram and TCP, although with important quantitative differences.

Changes in cell phenotypes

A number of behavioural phenotypes were defined which, in sequence, exemplify the changes in morphology displayed by a cell as it attaches and adheres to a substratum. High resolution images of key phenotypes, generated by SEM, are shown in *Figures 1–4*. The major phenotypes are:

1. The onset of visible activity.
2. Blebbing of the cell surface (*Figure 1*).
3. Border ruffling (*Figure 2*).
4. Polarization, defined as the cell being 50% longer in its longest dimension than in its broadest dimension (*Figure 3*).
5. Onset of crawling (*Figure 3a*).
6. Cell appearing well-spread and stable (*Figure 4*).

From the TLV recordings, the position of every cell within a recording field was mapped. Each cell was followed through the duration of the recording in order to categorize the state of the cell, according to phenotype, at 15 min intervals. The collated results for each of the cell populations (i.e. on Apoceram and on TCP) are presented in *Figures 5* and *6*. Even within the relatively short time window employed in this study a progression in behaviour can be seen. *Figure 7* shows examples of tracings of cells obtained from individual frames on the video recordings at 15, 30 min, 1, 2 and 3 h. *Figures 5* and *6* reveal that on both substrata at 15 min post-plating, the majority of the cells are just contacting the substratum having sedimented out of

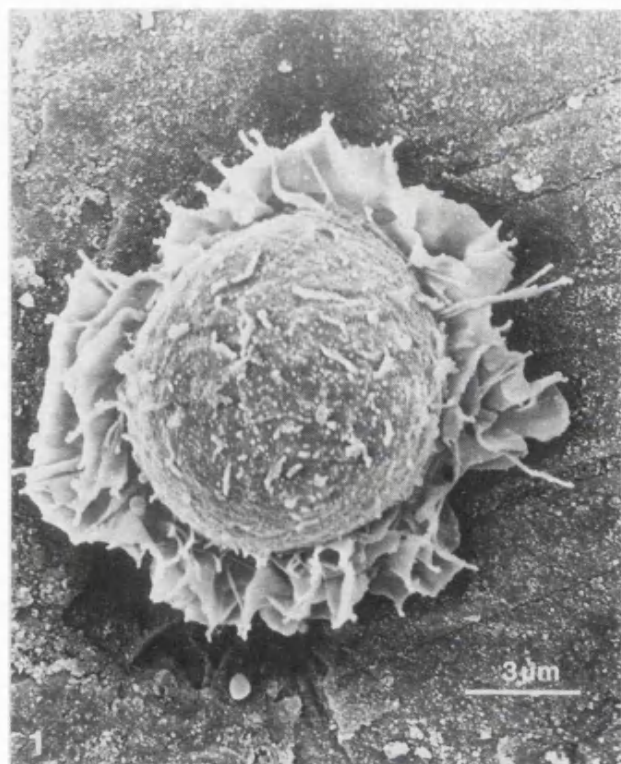


Figure 1 SEM of a round 3T3 fibroblast on Apoceram. Surface blebs can be seen. Cytoplasmic extensions appear on the periphery as the cell begins to spread.

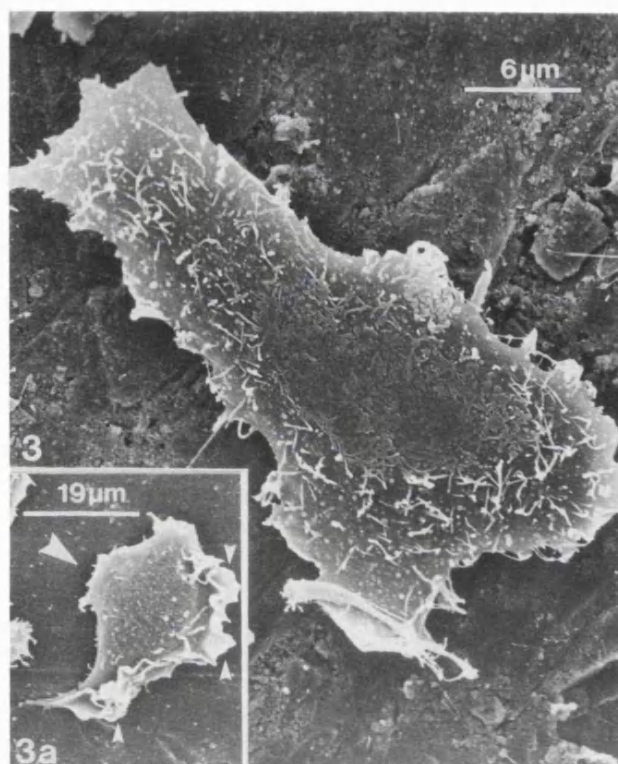


Figure 3 SEM of a polarized and flattened 3T3 fibroblast. **Inset**, The large arrow indicates the most likely direction of migration of this fibroblast. Lamellipodia are seen extending from its leading edge (small arrows).

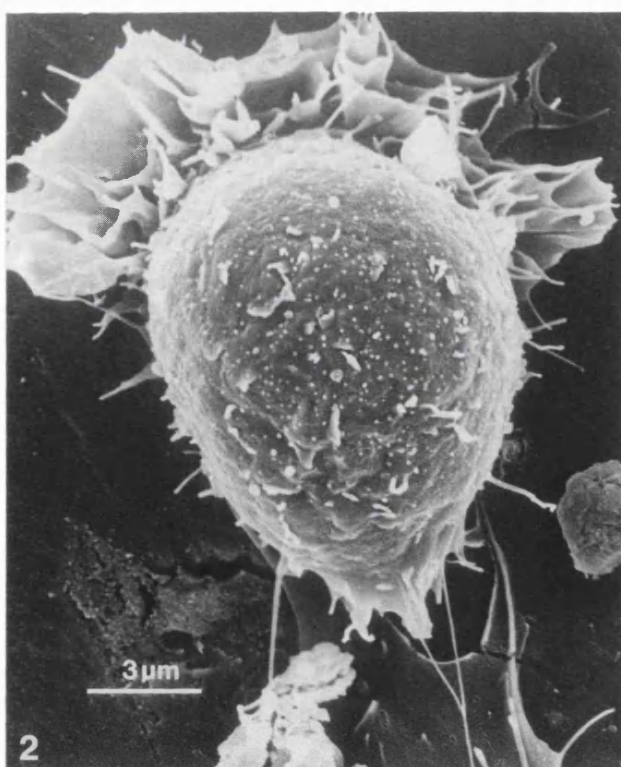


Figure 2 The leading edge of this apparently elongating cell shows layers of ruffling lamellipodia.

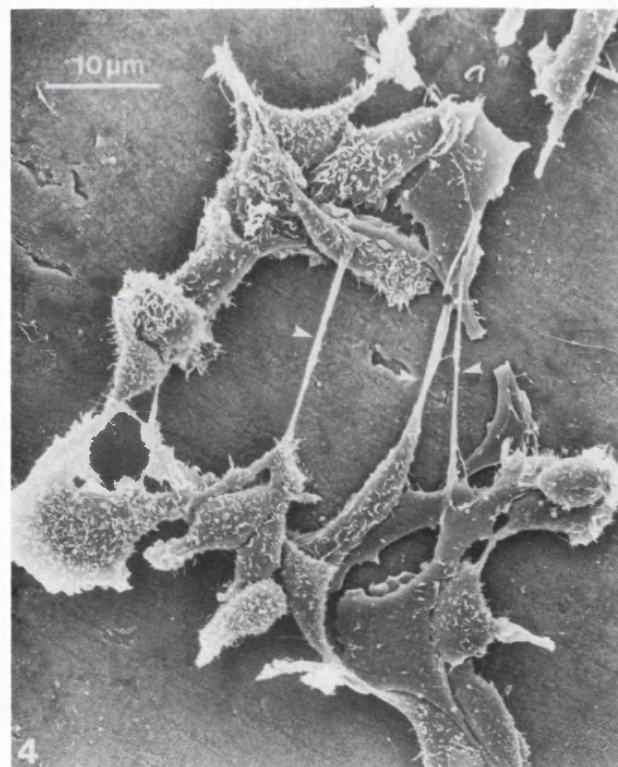


Figure 4 The fibroblasts are well spread. Long thin filopodia appear to bridge some cells.

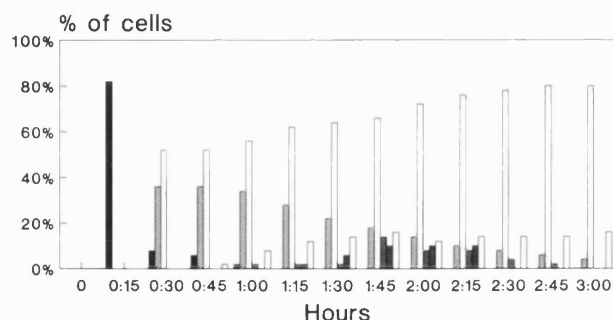


Figure 5 Distribution of behavioural phenotypes with time on Apoceram. ■, Onset of activity; ▨, blebbing; ▩, border ruffling; ▪, start crawling; ▫, polarization; □, spread and stable.

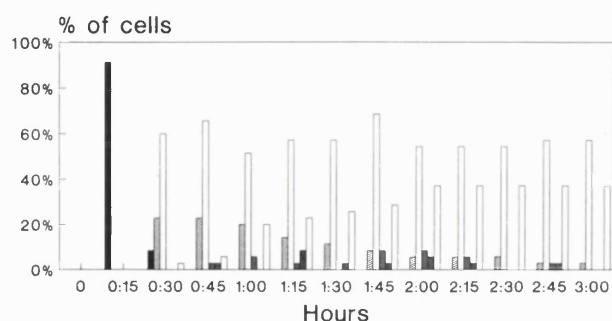


Figure 6 Distribution of behavioural phenotypes with time on tissue culture polystyrene. ■, Onset of activity; ▨, blebbing; ▩, border ruffling; ▪, start crawling; ▫, polarization; □, spread and stable.

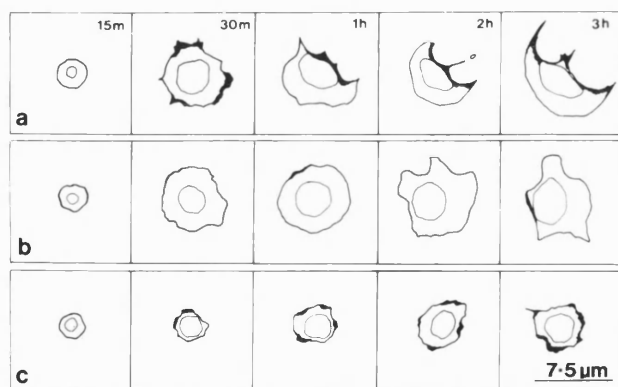


Figure 7 Tracings of cells seen through the phase-contrast microscope, recorded by the time-lapse video at 15, 30 min, 1, 2 and 3 h. **a**, Progression from a rounded morphology to a spread cell which later exhibited crawling. **b**, This cell has been spread and remained stationary with little ruffling activity. **c**, Constant ruffling of a large proportion of the cell margin was observed on this cell throughout the recording period.

suspension. In marked contrast, in both populations at 30 min, the majority of cells either display surface blebbing or have moved on to display ruffling. Subsequently, although both populations show the same progression, they do so at different rates. Thus, on TCP, the first spread and stable cells are seen at 30 min and both polarized and locomotory phenotypes

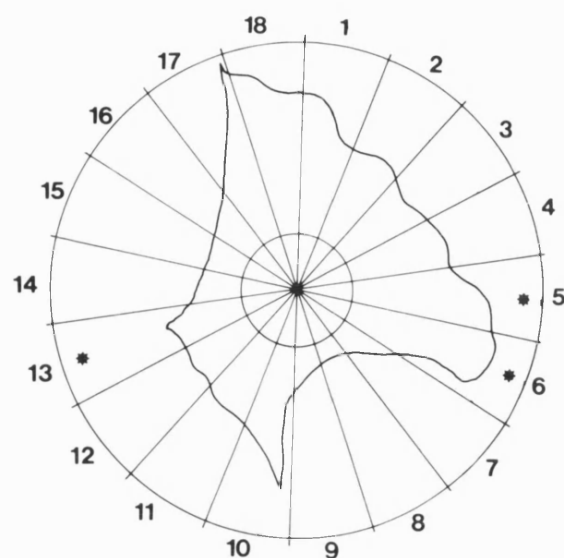


Figure 8 Method of scoring the proportion of ruffling cell margin. A cell was divided into 18 sectors using a transparent overlay placed on the video monitor. Border ruffling was observed in sectors 5, 6 and 13. This cell scored three out of 18.

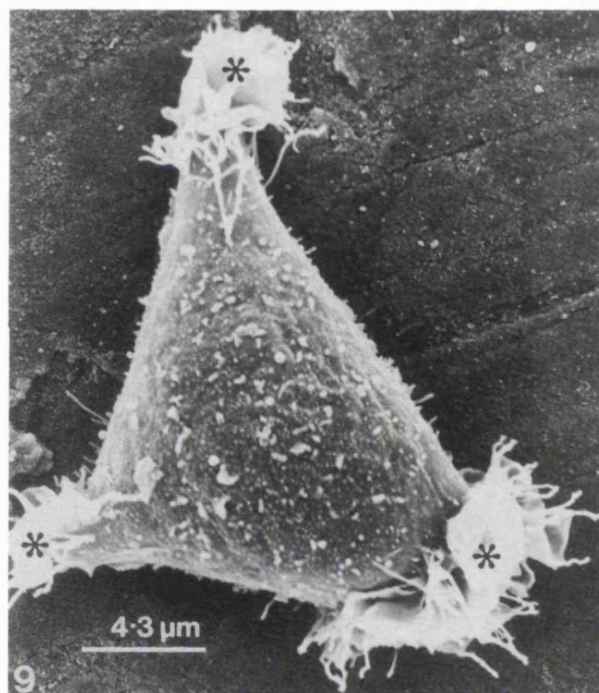


Figure 9 The margin of this fibroblast has three ruffling sites (asterisks); the remainder of the cell margin appears quiescent.

are first observed at 45 min. On Apoceram, blebbing continues for longer, such that even at 1 h 45 min, almost 20% of the cells display this phenotype (TCP controls, less than 10%). On the glass-ceramic, the first 'spread and stable' cells are only distinguishable at 45 min, the first locomotory cells at 1 h and the first polarized cells at 1 h 45 min. Clearly, there is a relative

retardation of the behaviour pattern of the cells upon the glass-ceramic substratum. A further picture emerges from detailed analysis of the activity of the cell margin.

Cell ruffling activity

The activity of the cell margin will reflect the functional state of the cytoplasm at that point, in terms of adherence to the substratum. Well-spread and flattened margins reflect stable cell-substratum adhesions, whereas ruffled margins indicate unstable cell-substratum adhesions and reflect motile cytoplasm at that point on the margin (N.B. not to be confused with whole-scale cell locomotion; see Discussion). Marginal ruffling can therefore be a sensitive indicator of cell-substratum interactions. To investigate this further, from the TLV recordings, cells were analysed individually for margin activity at 1, 2 and 3 h post-plating¹³. The margins of selected cells were proportionately scored as being 'ruffled' (i.e. non-adherent and motile) or 'quiescent' (i.e. adherent, non-motile) according to the diagram shown in Figure 8. Using a transparent overlay on the monitor screen, the margin of a cell was divided into 18 sectors, each of which was individually scored and then summed on a per cell basis. Ruffled and quiescent states are typically illustrated, in high resolution, in Figure 9. The resultant data were plotted as scatter diagrams (Figures 10 and 11).

It emerges from this analysis that for all three time intervals studied the control cells on Apoceram display, on a per cell basis, a higher number of ruffling sites with means of 1.69, 2.09 and 2.00 at 1, 2 and 3 h, respectively (Figure 10). In contrast, the cells on TCP display a significantly lower number of ruffling sites, with means of 1.59, 1.49 and 1.38 at the equivalent time intervals, and with smaller upper limits to the distribution ranges (Figure 11). The average numbers of segments of ruffling cell margin, out of 18 segments per cell at 1, 2 and 3 h, were 3.17, 4.16 and 4.26 for Apoceram and 3.32, 2.89 and 3.05 for TCP. In other words, over the period analysed, cells on the glass-ceramic are likely to be less adherent and less capable of locomotion (through an inability to maintain tractional purchase) than their counterparts on TCP.

DISCUSSION

The results of this study show that 3T3 fibroblasts plated onto TCP and the glass-ceramic material, Apoceram, exhibited similar morphological changes but with differences in the timing of the typical behavioural response to contact and adhesion to the substratum in question. A higher proportion of cells on TCP appeared well-spread and flattened at the end of the recording, indicating the formation of stable adhesive contacts. The border ruffling represents the activity of lamellipodia and cell processes extending from the spreading cells. Those lamellipodia that fail to attach firmly to the substratum, because of weak cell-to-substratum adhesions, would be pulled backwards by the cortical tension to produce a

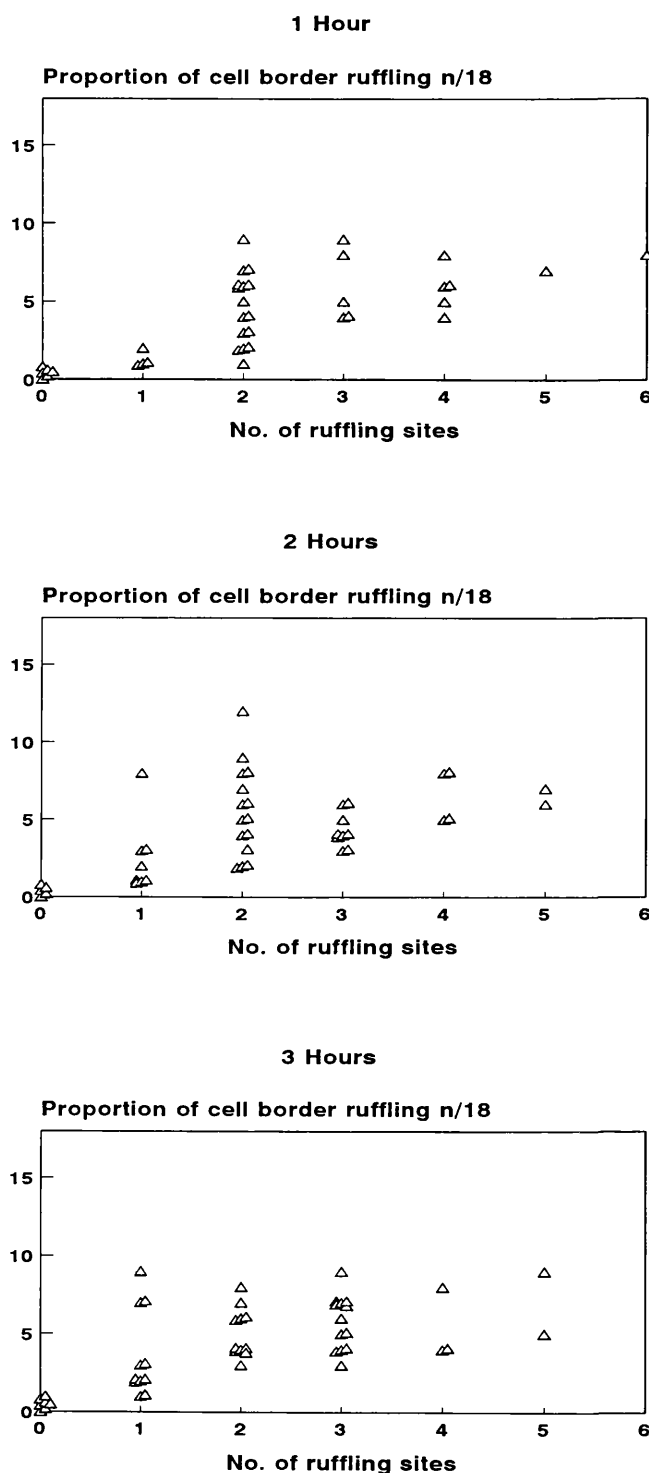


Figure 10 Proportion of cell margin ruffling ($n/18$) versus number of ruffling sites for cells cultured on Apoceram.

'ruffle'¹⁴. Ruffling activity was significantly more widespread on the Apoceram and this is interpreted as poor or weak cell-to-substratum adhesion as compared to that displayed by cells on the TCP.

The adhesion of cells in suspension to an artificial substratum involves the adsorption of serum proteins to the substratum¹⁵, contact of rounded cells with the substratum followed by attachment and spreading of the cells. Three morphological stages have been described by Taylor¹⁶:

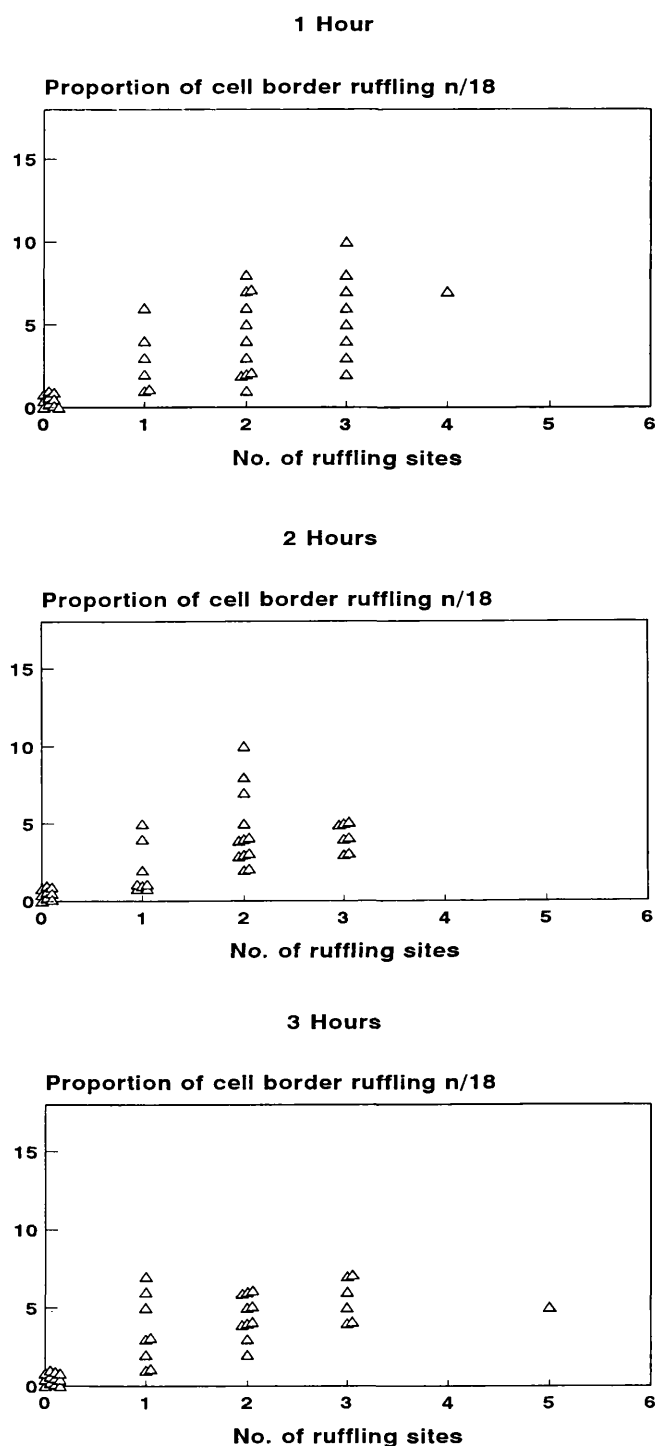


Figure 11 Proportion of cell margin ruffling ($n/18$) versus number of ruffling sites for cells cultured on tissue culture polystyrene.

- Stage 1. Spherical or irregular cells with no processes attached to the substratum.
- Stage 2. Flattening cells with attached processes, retaining an elevated cytoplasmic mass.
- Stage 3. Spread cells, nuclei flattened.

A similar progression from rounded to spread morphologies has been observed in this study. However, assessment of the rate of progression through the sequence of behavioural phenotypes, and of

marginal activity, provides a more sensitive view of cell response during the process of attachment and spreading on the substratum. Such activity can be influenced by a range of factors such as surface energy, surface charge and wettability, in a protein-free medium^{17,18}. Moreover, in the presence of serum, similar factors would affect the affinity of the substratum for adhesion proteins such as fibronectin, and thereby modify the rate of attachment¹⁹. The conformation of these proteins when they are adsorbed to the substratum may also influence their binding activity with cell surface receptors²⁰. Additionally, surface preparation during either manufacturing or sterilization can produce different adsorption properties on the same material²¹. Seitz *et al.*²² reported that in serum-free culture, coating of Bioglass (University of Florida, Gainesville, USA) with fibronectin had no apparent effect on the initial adhesion of rounded fibroblasts, but the rate of spreading was more rapid and the final morphology of the cells was more flattened. TCP is known to have enhanced fibronectin binding properties²³ and, although we have not yet explored these variables within this system, we anticipate that fibronectin from the serum will have been similarly bound in our assays.

It is our contention that procedures such as that described in this report, whereby analysis of the dynamic train of events following initial cell-substratum interactions can be carried out, provide a very sensitive means of exploring the short-term biocompatibility of artificial materials with implantation potential. Phenomena emerge from such analyses that are not recognizable in the assessment of fixed and stained preparations on *in vitro* assays. Consequently, we suggest that, whereas *in vitro* techniques are a valuable adjunct to the long-term results generated by whole animal implantation studies, they can be made more powerful and more revealing by an increased emphasis on cell behaviour.

ACKNOWLEDGEMENTS

The authors wish to acknowledge the assistance of Mrs P. Barber and Ms N. Morden of the Electron Microscopy Unit, Eastman Dental Institute, London. Dr R.D. Rawlings of the Materials Department, Imperial College, University of London kindly provided Apoceram for the study.

REFERENCES

- 1 Doillon CJ, Cameron K. New approaches for biocompatibility testing using cell culture. *Int J Artif Organs* 1990; **13**(8): 517–520.
- 2 Haustveit G, Torheim B, Fystro D, Eidem T, Sandvik M. Toxicity testing of medical device materials tested in human tissue cultures. *Biomaterials* 1984; **5**(2): 75–80.
- 3 Johnson HJ, Northup SJ, Seagraves PA *et al.* Biocompatibility test procedures for materials evaluation *in vitro*. II. Objective methods of toxicity assessment. *J Biomed Mater Res* 1985; **19**(5): 489–508.
- 4 Rae T. Tissue culture techniques in biocompatibility testing. In: Williams DF, ed. *Techniques of Biocompat-*

- ibility Testing, Vol. 2. Boca Raton, FL: CRC Press, 1986: 81–94.
- 5 International Standards Organisation. Technical Report ISO/TR 9966: Implants for surgery—biocompatibility—selection of biological test methods for materials and devices, 1989.
 - 6 Sharefkin JB, Watkins MT. Methods for the measurement of cell attachment to bioprosthetic surfaces. In: Williams DF, ed. *Techniques of Biocompatibility Testing*, Vol. 2. Boca Raton, FL: CRC Press, 1986: 95–108.
 - 7 Naji A, Harmand MF. Cytocompatibility of two coating materials, amorphous alumina and silicon carbide, using human differentiated cell cultures. *Biomaterials* 1991; **12**(7): 690–694.
 - 8 Jansen JA, van der Waerden JCPM, de Groot K. Fibroblast and epithelial cell interactions with surface-treated implant materials. *Biomaterials* 1991; **12**: 25–31.
 - 9 Könönen M, Hormia M, Kivilahti J, Hautaniemi J, Thesleff I. Effect of surface processing on the attachment, orientation, and proliferation of human gingival fibroblasts on titanium. *J Biomed Mater Res* 1992; **26**: 1325–1341.
 - 10 Revel JP, Hoch P, Ho D. Adhesion of cultured cells to their substratum. *Exp Cell Res* 1974; **84**: 207–218.
 - 11 Rawlings RD. Bioactive glasses and glass-ceramics. *Clin Mater* 1993; **14**: 155–179.
 - 12 Wolfe LA. Comparison of the interfacial bonding strength of a bioactive ceramic and titanium. *J Dent Res* 1990; **69**: 958 (Abstr. 30).
 - 13 Bell PB. Contact inhibition of movement in transformed and non-transformed cells. *Birth Defects: Original Article Series* 1978; **14**: 177–194.
 - 14 Abercrombie M, Heaysman JEM, Pegrum SM. The locomotion of fibroblasts in culture. II. 'Ruffling'. *Exp Cell Res* 1970; **60**: 437–444.
 - 15 Revel JP. Electron microscopic investigation of the underside of cells in culture. *Exp Cell Res* 1973; **78**: 1–14.
 - 16 Taylor AC. Attachment and spreading of cells in culture. *Exp Cell Res* 1961; Suppl. 8: 154–173.
 - 17 Baier RE, Meyer AE, Natiella JR, Natiella RR, Carter JM. Surface properties determine bioadhesive outcomes: methods and results. *J Biomed Mater Res* 1984; **18** (4): 327–355.
 - 18 Weiss L, Blumenson LE. Dynamic adhesion and separation of cells with hydrophilic and hydrophobic surfaces. *J Cell Physiol* 1967; **70**: 23–32.
 - 19 Grinnell F, Feld MK. Adsorption characteristics of fibronectin in relationship to biological activity. *J Biomed Mater Res* 1981; **15**: 363–381.
 - 20 Yamada KM, Akiyama SK, Hasegawa T, Kennedy DW, Humphries MJ. Recent advances in research on fibronectin and other cell attachment proteins. *J Cell Biochem* 1985; **28**: 79–97.
 - 21 Kasemo B, Lausmaa J. Biomaterial and implant surfaces: on the role of cleanliness, contamination, and preparation procedures. *J Biomed Mater Res* 1988; **22** (Applied Biomaterials, Suppl. A2): 145–158.
 - 22 Seitz TL, Noonan KD, Hench LL, Noonan NE. Effect of fibronectin on the adhesion of an established cell line to a surface-reactive biomaterial. *J Biomed Mater Res* 1982; **16**: 195–207.
 - 23 Bentley KL, Klebe RJ. Fibronectin binding properties of bacteriologic petri plates and tissue culture dishes. *J Biomed Mater Res* 1985; **19**: 757–769.

Announcement

Relocation of Journal Publishing Office

As from 1st October 1994, the publishing, editorial, production and reprint offices are moving to:

Elsevier Science Ltd
The Boulevard, Langford Lane,
Kidlington, Oxford, OX5 1GB, UK
Main switchboard:
Tel: +44 (0)1865 843000
Fax: +44 (0)1865 843010

All correspondence and queries relating to the journal should be sent to this address

Newly submitted manuscripts should be mailed to the Editor

Zinc phosphate cements: an evaluation of some factors influencing the lactic acid jet test erosion

J.A. Williams, R.W. Billington and G.J. Pearson

Department of Biomaterials, Institute of Dental Surgery, 256 Gray's Inn Road, London, WC1X 8LD, UK

The lactic acid jet test was used to measure erosion rates of eight commercial zinc phosphate cements at 23 and 37°C after 24 h and 2 months. Rates exceeded the ISO 9917 published limit of 0.1 mm/h when tested according to this specification (23°C, 24 h), suggesting the limit should be increased. Erosion was measured by both weight loss and depth change. At 24 h erosion decreased as temperature increased, whereas after 2 months temperature had no significant effect. No trend was seen with increasing specimen maturity. Stannous fluoride may increase erosion resistance.

Biomaterials (1994) **15**, (12) 1008–1012

Keywords: Dental materials, zinc phosphate cement, lactic acid jet test, ISO 9917, erosion

Received 13 September 1993; accepted 5 December 1993

The lactic acid jet test has been the subject of a number of studies indicating that erosion measured by the jet test is superior to the method of measuring water leachable content in the prediction of clinical performance^{1–3}. Studies of glass ionomer cement erosion rates *in vitro* by Setchell *et al.*⁴ and *in vivo* by Ibbetson *et al.*⁵ showed these to be related. A similar relationship was also noted for zinc phosphate and zinc polycarboxylate cements^{6–8}.

The most recent ISO specification for dental cements⁹, ISO 9917–1991, which covers all water-based dental cements—glass polyalkenoate (ionomer), zinc phosphate, zinc polycarboxylate, silicate and silicophosphate cements—includes the lactic acid jet test in preference to the water leachable content measurement formerly specified in ISO 7489–1986¹⁰. Different erosion rate limits are set for each general group of cements, but that of 0.1 mm/h given for zinc phosphate cements appears surprisingly low since Wilson *et al.*¹ found zinc phosphate cements to erode at 0.2–0.4 mm/h.

Significantly, some test parameters have been changed from those used in the initial evaluations¹¹.

Most importantly, the solution temperature selected is 23°C rather than 37°C. Wilson *et al.*¹¹ found that, for one material in each general class of dental cements, erosion increased with temperature. The extent varied from material to material and it was concluded that 37°C should be used to approximate the oral cavity. This also enables a comparison of *in vivo* and *in vitro* results to be made. Additionally, although 23°C appears appropriate from the experimental point of

view as it approximates ambient temperatures, difficulties may occur in maintaining this temperature. Many pumps introduce heat into a circulating system, such as exists in the jet test, which may cause the temperature to rise above 23°C in a relatively short space of time. Furthermore, the rate of increase is unpredictable, being dependent on the ambient conditions.

A further variation is introduced by measuring erosion by taking five depth measurements using a specially obtained dial gauge rather than the more common method of measuring weight loss, even though Wilson *et al.*¹ demonstrated that the two methods could give equivalent results.

A study of the effects of maturation time on dental materials by the present authors¹² showed that the one zinc cement included had an erosion rate which increased, although not significantly so, with time. This was in contrast to glass ionomers, all of which had rates which decreased with time. It was not known whether this zinc phosphate cement was atypical. Wilson *et al.*¹¹ did not include zinc phosphate cements in their study of the effects of maturation. Swartz *et al.*¹³ showed that the water leachable content of zinc phosphate and silicophosphate cements decreased with time, but this may not be the case when erosion is measured. It was considered that the effect of maturation would be an appropriate and clinically relevant factor to consider.

The aim of this study, therefore, was to investigate whether zinc cements would fulfill the jet test requirements as specified by ISO 9917 and to assess the effect of temperature and maturation time on erosion rate. A comparison of the two methods of measuring erosion would be made. Commercially available materials were selected since these should have passed the

Correspondence to Mrs J.A. Williams

Appendix II

PROCESSING OF CAM GRAFT SPECIMENS

All the following processes MUST be carried out in the fume cupboard

A. For embedding in LR White resin

- 1 Fix tissue
Histology: overnight at 4°C in 10% formal saline
Immunohistochemistry: for 2 hours at 4°C in 4% paraformaldehyde in 0.1M phosphate buffer
TEM: overnight at 4°C in 3% glutaraldehyde in 0.1M sodium cacodylate buffer
- 2 Dehydrate in a graded series of ethanol preferably at 4°C;

50%	ethanol	30 mins
70%	ethanol	30 mins
90%	ethanol	30 mins
100%	ethanol	30 mins
100%	ethanol	30 mins
100%	ethanol	30 mins
- 3 Infiltrate at 4°C as follows:

1:1 LR White resin : ethanol	30 mins
2:1 LR White resin : ethanol	30 mins
Pure LR White resin	30 mins
Pure LR White resin	overnight
Pure LR White resin	30 mins
Pure LR White resin	30 mins
- 4 Embedding procedures must be carried in the cold aluminium sinks from the 0°C fridge compartment.
Add 15µl of accelerator to 10mls of pre-cooled LR White in a foil dish and stir with an orange stick for 30 secs.
Dispense mixture into gelatin capsules and immerse the specimens in the resin.
Great care must be taken to exclude air from the resin or it will not set. Do this by filling the capsules to the top and cutting a piece of parafilm to cover the surface of the resin.
- 5 Polymerise the LR White resin in the 0°C compartment for 24 hrs.

B. For embedding in glycol methacrylate resin (enzyme histochemistry)

- 1 Fix tissue in 90% ethanol at 4°C
- 2 Dehydrate in absolute ethanol at 4°C;
100% ethanol 30 mins
100% ethanol 30 mins
100% ethanol 30 mins
- 3 Following dehydration give three changes of 45 mins each in Solution A

Solution A

16ml 2-hydroxyethyl methacrylate

3ml 2-butoxyethanol

0.1g benzoyl peroxide

Dissolve using a magnetic stirrer, but no heat.

- 4 Embed in 50 parts of Solution A to one part of Solution B

Solution B

2ml Polyethylene glycol 400

0.2ml N,N-dimethylaniline

Use the cold aluminium sinks from the 0°C fridge compartment.

Dispense mixture into gelatin capsules and immerse the specimens in the resin. Great care must be taken to exclude air from the resin or it will not set. Do this by cutting a piece of parafilm to exactly fit on the surface of the resin in the gelatin capsules.

- 5 Polymerise the resin in the 4°C compartment for 24 hrs.

Appendix III

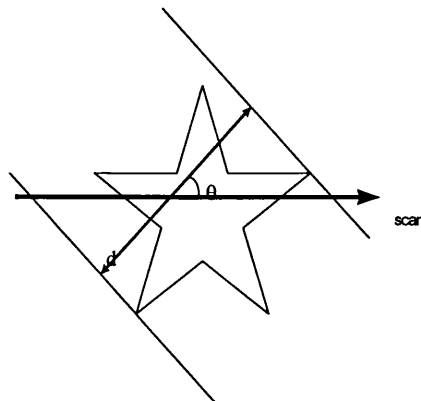
Principles of feature measurement in the Quantimet 520 Image Analysis system relevant to measurement of percentages of bone to implant contact:

Perimeter

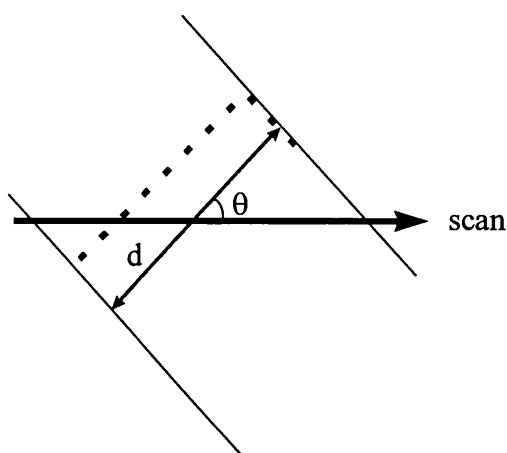
The PERIMETER or boundary of the detected feature is an orientation independent measurement. In a normal context, perimeter refers to the length of the outside boundary of an object. When the perimeter of a hollow object is assessed by the image analysis system, the inner boundary will also contribute to the measurement. For the outline of the implant space measured in the experiments reported in Chapter 4, the PERIMETER returned by the software is approximately twice the actual perimeter of the object since the breadth of the outline was very small compared to its length.

Length

The LENGTH function on the image analyser is also different from length in the conventional sense. LENGTH is defined as the largest of eight Feret measurements made at 0° , 22.5° , 45° , 67.5° , 90° , 112.5° , 135° and 157.5° to the scan line. A Feret measurement is the distance between two parallel tangents on opposite sides of an object. Using the star-shaped object below as an example, at angle θ to the scan direction, d is the Feret distance.



The LENGTH parameter is dependant on object orientation although with eight Feret measurements to determine the parameter, the error is relatively small for solid objects. However, for line objects, LENGTH does not represent the true length of the object except for straight lines. If the dotted line below represented a portion of an implant in contact with bone, the LENGTH reported by the image analysis software would be d , if the Feret measurement at angle θ was the largest out of the eight measurements made.



Measuring the PERIMETER instead of LENGTH would give a result that is approximately twice the true length of the line. The percentages of implant contact with bone and osteoid could therefore be calculated by dividing the sum of the PERIMETER of the lines marking such contacts by the PERIMETER of the complete outline of the implant. It has to be acknowledged that measurement error increases as the length of the line decreases relative to its breadth with the PERIMETER being $2l+2b$ where l is the length and b is the breadth of the line. The breadth of the lines traced was typically 2 pixels, the PERIMETER of the whole outline of the implant was in the region of 3000 pixels and the smallest value of PERIMETER recorded at the sites of bone-implant contact was in the region of 50 pixels. The assumed length of such a site would therefore be 25 pixels whilst the true length would be 23 pixels, giving an overestimation of 8.7%! However, the percentage of bone-implant contact would be increased by only 0.13% as a consequence of this overestimation. This error would increase when several short contact sites were present within one section and formed a systematic error (a difference

formed a systematic error (a difference between the expected result of a measurement and the conventional true value) quite separate from the observer errors.

The results of six repeated measurements of the percentages of the perimeter of the implant in contact with mineralised bone and osteoid, and with mineralised bone alone in one sample section at each time period is presented below:

Days after grafting	9		7		5		3		2		1
% contact with	bone & osteoid	bone	bone & osteoid	bone	bone & osteoid	bone	bone & osteoid	bone	bone	bone	bone
	59.6	47.9	33.8	25.4	27.6	15.4	6.9	6.4	5.1	2.5	
	59.0	45.8	35.9	22.2	29.2	14.9	5.3	4.8	6.1	4.8	
	64.1	56.6	31.2	23.5	26.3	17.0	6.7	4.2	7.3	3.5	
	57.9	53.2	30.0	24.9	26.1	12.3	7.2	6.8	6.5	2.9	
	55.8	48.6	28.8	27.0	32.6	13.4	5.7	5.3	4.8	3.1	
	58.0	49.2	34.8	21.5	29.6	14.8	8.8	3.1	3.9	3.4	
mean	59.1	50.2	32.4	24.1	28.6	14.6	6.8	5.1	5.6	3.4	
standard deviation	2.8	4.0	2.8	2.1	2.4	1.6	1.2	1.4	1.2	0.8	
Confidence interval (95.0%)	2.9	2.7	3.0	2.2	2.6	1.7	1.3	1.4	1.3	0.8	
Coefficient of reproducibility (s.d./mean) x 100	5	8	9	9	9	11	18	27	22	23	

Appendix IV

* * * * * A n a l y s i s o f V a r i a n c e * * * * *

DAY 1 % contact with bone(B)

Tests of Between-Subjects Effects.

Tests of Significance for T1 using UNIQUE sums of squares

Source of Variation	SS	DF	MS	F	Sig of F
WITHIN+RESIDUAL	269.36	10	26.94		
IMPLANT	10.08	1	10.08	.37	.554

Tests involving 'SECTION' Within-Subject Effect.

AVERAGED Tests of Significance for B using UNIQUE sums of squares

Source of Variation	SS	DF	MS	F	Sig of F
WITHIN+RESIDUAL	245.51	30	8.18		
SECTION	13.05	3	4.35	.53	.664
IMPLANT BY SECTION	3.76	3	1.25	.15	.927

DAY 2 % contact with bone (B)

Tests of Between-Subjects Effects.

Tests of Significance for T1 using UNIQUE sums of squares

Source of Variation	SS	DF	MS	F	Sig of F
WITHIN+RESIDUAL	180.66	10	18.07		
IMPLANT	8.68	1	8.68	.48	.504

Tests involving 'SECTION' Within-Subject Effect.

AVERAGED Tests of Significance for B using UNIQUE sums of squares

Source of Variation	SS	DF	MS	F	Sig of F
WITHIN+RESIDUAL	156.37	30	5.21		
SECTION	38.81	3	12.94	2.48	.080
IMPLANT BY SECTION	10.15	3	3.38	.65	.590

DAY 3 % contact with bone + osteoid (A)

Tests of Between-Subjects Effects.

Tests of Significance for T1 using UNIQUE sums of squares

Source of Variation	SS	DF	MS	F	Sig of F
WITHIN+RESIDUAL	289.93	10	28.99		
IMPLANT	31.20	1	31.20	1.08	.324

Tests involving 'SECTION' Within-Subject Effect.

AVERAGED Tests of Significance for A using UNIQUE sums of squares

Source of Variation	SS	DF	MS	F	Sig of F
WITHIN+RESIDUAL	222.86	30	7.43		
SECTION	4.47	3	1.49	.20	.895
IMPLANT BY SECTION	53.85	3	17.95	2.42	.086

DAY 3 % contact with bone (B)

Tests of Between-Subjects Effects.

Tests of Significance for T1 using UNIQUE sums of squares

Source of Variation	SS	DF	MS	F	Sig of F
WITHIN+RESIDUAL	147.81	10	14.78		
IMPLANT	.14	1	.18	.01	.915

Tests involving 'SECTION' Within-Subject Effect.

AVERAGED Tests of Significance for B using UNIQUE sums of squares

Source of Variation	SS	DF	MS	F	Sig of F
WITHIN+RESIDUAL	148.70	30	4.96		
SECTION	8.44	3	2.81	.57	.641
IMPLANT BY SECTION	34.60	3	11.53	2.33	.095

DAY 5 % contact with bone + osteoid (A)

Tests of Between-Subjects Effects.

Tests of Significance for T1 using UNIQUE sums of squares

Source of Variation	SS	DF	MS	F	Sig of F
WITHIN+RESIDUAL	783.79	10	78.28		
IMPLANT	3366.75	1	3366.75	43.01	.000*

Tests involving 'SECTION' Within-Subject Effect.

AVERAGED Tests of Significance for A using UNIQUE sums of squares

Source of Variation	SS	DF	MS	F	Sig of F
WITHIN+RESIDUAL	1047.23	30	34.91		
SECTION	10.12	3	3.37	.10	.931
IMPLANT BY SECTION	129.62	3	43.21	1.24	.313

- - - - -

DAY 5 % contact with bone (B)

Tests of Between-Subjects Effects.

Tests of Significance for T1 using UNIQUE sums of squares

Source of Variation	SS	DF	MS	F	Sig of F
WITHIN+RESIDUAL	562.63	10	56.26		
IMPLANT	118.44	1	118.44	2.11	.177

Tests involving 'SECTION' Within-Subject Effect.

AVERAGED Tests of Significance for B using UNIQUE sums of squares

Source of Variation	SS	DF	MS	F	Sig of F
WITHIN+RESIDUAL	453.37	30	14.51		
SECTION	43.44	3	14.48	1.00	.407
IMPLANT BY SECTION	35.13	3	11.71	.81	.500

DAY 7 % contact with bone + osteoid (A)

Tests of Between-Subjects Effects.

Tests of Significance for T1 using UNIQUE sums of squares

Source of Variation	SS	DF	MS	F	Sig of F
WITHIN+RESIDUAL	1230.68	10	123.07		
IMPLANT	988.27	1	988.27	8.03	.018*

Tests involving 'SECTION' Within-Subject Effect.

AVERAGED Tests of Significance for A using UNIQUE sums of squares

Source of Variation	SS	DF	MS	F	Sig of F
WITHIN+RESIDUAL	1910.70	30	63.69		
SECTION	251.93	3	83.98	1.32	.287
IMPLANT BY SECTION	327.47	3	109.16	1.71	.185

DAY 7 % contact with bone (B)

Tests of Between-Subjects Effects.

Tests of Significance for T1 using UNIQUE sums of squares

Source of Variation	SS	DF	MS	F	Sig of F
WITHIN+RESIDUAL	658.06	10	65.81		
IMPLANT	23.66	1	23.99	.36	.562

Tests involving 'SECTION' Within-Subject Effect.

AVERAGED Tests of Significance for B using UNIQUE sums of squares

Source of Variation	SS	DF	MS	F	Sig of F
WITHIN+RESIDUAL	914.17	30	30.47		
SECTION	38.84	3	12.95	.42	.737
IMPLANT BY SECTION	84.65	3	28.22	.93	.440

DAY 9 % contact with bone + osteoid (A)

Tests of Between-Subjects Effects.

Tests of Significance for T1 using UNIQUE sums of squares

Source of Variation	SS	DF	MS	F	Sig of F
WITHIN+RESIDUAL	2409.40	10	240.94		
IMPLANT	5287.80	1	5287.80	21.95	.001*

Tests involving 'SECTION' Within-Subject Effect.

AVERAGED Tests of Significance for A using UNIQUE sums of squares

Source of Variation	SS	DF	MS	F	Sig of F
WITHIN+RESIDUAL	2361.38	30	78.71		
SECTION	328.08	3	109.36	1.39	.265
IMPLANT BY SECTION	20.99	3	7.00	.09	.966

DAY 9 % contact with bone (B)

Tests of Between-Subjects Effects.

Tests of Significance for T1 using UNIQUE sums of squares

Source of Variation	SS	DF	MS	F	Sig of F
WITHIN+RESIDUAL	2573.33	10	257.33		
IMPLANT	6936.02	1	6936.02	26.95	.000*

Tests involving 'SECTION' Within-Subject Effect.

AVERAGED Tests of Significance for B using UNIQUE sums of squares

Source of Variation	SS	DF	MS	F	Sig of F
WITHIN+RESIDUAL	2086.09	30	69.54		
SECTION	41.70	3	13.90	.20	.896
IMPLANT BY SECTION	10.39	3	3.46	.05	.985

